STRUCTURE ELUCIDATION OF PORPHYRINS BY TANDEM MASS SPECTROMETRY: FUNDAMENTAL STUDIES, NEW STRATEGIES, AND GEOCHEMICAL APPLICATIONS

By

BRIAN DAVID BEATO

A DISSERTATION PRESENTED TO THE GRADUATE SCHOOL
OF THE UNIVERSITY OF FLORIDA IN PARTIAL FULFILLMENT
OF THE REQUIREMENTS FOR THE DEGREE OF
DOCTOR OF PHILOSOPHY

UNIVERSITY OF FLORIDA

1989

To my mom, dad, Oma, and Aunt Helen, but not my brother.
(Kevin should write his own!)

ACKNOWLEDGEMENTS

There are a great number of people I need to thank for assistance in completing this dissertation, yet I would probably leave some people out inadvertently. I have no wish to attempt an all-inclusive list, but there are certain individuals who have contributed way above and beyond the call of duty and friendship to this work. These people have much more of my appreciation than my writing can convey, yet I attempt to recognize them nevertheless.

I am certainly indebted to Professor Richard A. Yost for providing me with the tools to perform this research and with the opportunity to become an independent scientist. I also wish to thank current and former members of the Yost group, who have all taught me many things and have been very good friends. Ms. Cecilia Basic deserves special notice for spending countless hours setting up the necessary fonts I needed to print this dissertation. I am very grateful for the infinite patience of Ms. Jody Freeman, who on countless occasions saved me from impending doom. Regardless of how busy she is, she is always willing to stop what she is doing to help a fellow student. I have learned a lot from Jody, both scientifically and in dealing with people. I also wish to thank Ms. Stacy-Ann Rossi for her patience, generosity, and understanding. She has routinely bent over backwards to help me out of jams, expecting (and typically getting) nothing in return. Her creativity and

curiosity have been a boon to many of the projects discussed in this dissertation. I have relied on her common sense on many occasions when mine was absent. Above all, she has made this past year of graduate school a lot of fun.

I would also like to express my sincere gratitude to Professor J. Martin E. Quirke of Florida International University for his tireless collaboration on this research. Without his hard work and dedication, this dissertation would never have been possible. Martin has proven to be far more than an invaluable resource in the area of geoporphyrin chemistry. He has served as an energetic fountain of ideas, has provided counsel in both scientific and personal matters, and has been generous with time and accommodations when needs arose, regardless of the inconvenience. I have benefitted immeasurably from his friendship.

I am forever grateful to my family for their love and support throughout all my years of schooling. I wish to thank my brother, Kevin, for regularly keeping me up all night on the phone so I could talk with another person not afraid of being labeled with the "L" word. I also want to extend heart-felt thanks to Oma and Aunt Helen, for their faith in me has always been a source of great encouragement. Of course, I owe everything to my having raised two of the best parents someone could ever have. My mom and dad have always provided me with every opportunity to pursue my dreams. The appreciation I have for what they have done for me could comprise another entire dissertation. In lieu of that, I offer them this one as a small token of their success. I am sure they realize, however, that this does not constitute forgiveness for making me take piano lessons when I was young and defenseless!

TABLE OF CONTENTS

page

ACKNOWLEDGEMENTS.......... iii

ABSTRACT.......... x

CHAPTER

1 INTRODUCTION.......... 1

Structure Elucidation of Porphyrins.......... 1
Tandem Mass Spectrometry Applied to Porphyrins.......... 5
Scope of Dissertation.......... 16

PART 1: APPLICATIONS OF EI/MS/MS TO GEOPORPHYRINS

2 OVERVIEW OF MASS SPECTROMETRIC ANALYSIS OF GEOPORPHYRINS.......... 26

Geoporphyrin Biomarkers.......... 26
Bitumen and Kerogen.......... 31
Sample Preparation and Porphyrin Isolation.......... 34
EI/MS and EI/MS/MS Analyses of Geoporphyrins.......... 42

3 TANDEM MASS SPECTROMETRIC ANALYSES OF GEOPORPHYRINS FROM THE BITUMEN AND KEROGEN FROM SHALE.......... 43

Introduction.......... 43
Experimental.......... 44
The Ni(II) and O=V(IV) Geoporphyrins from New Albany Shale.......... 45

EI/MS/MS Analyses of the Ni(II) Geoporphyrins from the Bitumen and the Kerogen Pyrolysate.......... 52
EI/MS/MS Analyses of the O=V(IV) Geoporphyrins from the Bitumen and the Kerogen Pyrolysate.......... 55
Comparison of the Ni(II) and O=V(IV) Geoporphyrins from the Bitumen and the Kerogen Pyrolysate.......... 56
Conclusions.......... 67

4 TANDEM MASS SPECTROMETRIC ANALYSES OF GEOPORPHYRINS FROM THE BITUMEN OF DEMINERALIZED SHALE.......... 69

Introduction.......... 69
Experimental.......... 70
The Ni(II) and O=V(IV) Geoporphyrins from New Albany Bitumen-II.......... 71
EI/MS/MS Analyses of the Ni(II) Geoporphyrins from the Bitumen-II.......... 78
Comparison of the EI/MS/MS Daughter Ion Mass Spectra of Ni(II) Geoporphyrins from Bitumen-II, Bitumen-I, and the 300 °C Kerogen Pyrolysate.......... 84
EI/MS/MS Analyses of the O=V(IV) Geoporphyrins from the Bitumen-II.......... 84
Comparison of the Ni(II) and O=V(IV) Geoporphyrins from the Bitumen-II.......... 91
Conclusions.......... 91

PART 2: NEW STRATEGIES FOR AND FUNDAMENTAL STUDIES OF PORPHYRIN STRUCTURE ELUCIDATION BY MS AND MS/MS

5 DOUBLY CHARGED PORPHYRIN IONS: IMPLICATIONS FOR ENHANCED STRUCTURE ELUCIDATION BY EI/MS/MS.......... 95

Introduction.......... 95
Experimental.......... 99
The Effect of the Metal Ion on Electron Ionization of Metalloporphyrins.......... 101

Enhanced CAD Fragmentation of Doubly Charged Porphyrin Ions......118
Conclusions......136

6 POSITIVE CHEMICAL IONIZATION OF PORPHYRINS: THE CASE FOR SURFACE-INDUCED DECOMPOSITION......137

Introduction......137
Experimental......146
Surface-induced Decomposition......146
The Effect of the Metal on Positive CI of Metalloporphyrins......165
Conclusions......176

7 ELECTRON CAPTURE NEGATIVE CHEMICAL IONIZATION OF PORPHYRINS......178

Introduction......178
Experimental......181
Structural Information from ECNCI......182
Hydrogenated Negative Ions......186
Relative Sensitivities of ECNCI Toward Free-base and Metalated Porphyrins......199
Conclusions......215

8 THREE TYPES OF STRUCTURAL INFORMATION FROM THE SAME EXPERIMENT......217

Introduction......217
Experimental......218
Traditional Mass Spectrometric Methods of Porphyrin Structure Elucidation......220
MS/MS of Porphyrins and MS of Decomposition Products......229
MS/MS of Porphyrins and Porphyrinogens......234
Conclusions......241

9 SUMMARY AND FUTURE WORK......244

Summary......244

Suggested Future Work with Geoporphyrin Biomarkers.....250
Suggested Future Work with Chemical Ionization of Porphyrins.....251

APPENDIX.....257

LITERATURE CITED.....266

BIOGRAPHICAL SKETCH.....274

Abstract of Dissertation Presented to the Graduate School
of the University of Florida in Partial Fulfillment of the
Requirements for the Degree of Doctor of Philosophy

STRUCTURE ELUCIDATION OF PORPHYRINS BY TANDEM MASS SPECTROMETRY: FUNDAMENTAL STUDIES, NEW STRATEGIES, AND GEOCHEMICAL APPLICATIONS

By

Brian David Beato

August, 1989

Chairman: Richard A. Yost
Major Department: Chemistry

This work describes novel methods of enhancing structure elucidation of porphyrins by tandem mass spectrometry (MS/MS), including fundamental studies of ionization and fragmentation of porphyrins under various conditions. MS/MS analyses of geoporphyrins are also discussed.

Various nickel and vanadyl geoporphyrins from both the bitumen and the kerogen of shale were analyzed by electron ionization (EI) MS/MS. The results indicate that geoporphyrins of the same carbon-number from the same shale have very similar structures, regardless of the metal or whether they were obtained from bitumen, from demineralized bitumen, or from kerogen.

Under EI conditions, porphyrins yield relatively abundant doubly charged molecular and fragment ions, which provide structural information about peripheral substituents. These doubly charged ions fragment to a much greater extent than do singly charged ions in the source and also upon collisionally activated dissociation (CAD).

Positive chemical ionization (CI) of porphyrins can result in pyrrolic ions, useful in sequencing the pyrroles around the macrocycle. Pyrroles are shown to arise from surface-induced decomposition reactions when the porphyrins condense on the source surface. Metalloporphyrins hydrogenate extensively on this surface, and the negative ions from these hydrogenated products are shown to fragment quite easily upon CAD compared to negative metalloporphyrin ions. The nature of the source surface is shown to be a variable that can be used to optimize certain CI mass spectra.

This work presents two methods which provide structural information about the peripheral substituents and about the sequence of pyrroles around a porphyrin in a single experiment. The first is a combined experiment involving MS/MS of the porphyrin ion as it initially vaporizes from a probe filament, and then subsequent MS of pyrrolic ions vaporizing off the ion volume surface as the probe continues to heat. The other method involves MS/MS of both the porphyrin ion and its corresponding porphyrinogen ion.

The new analytical strategies presented are not unique to porphyrin analysis. Many are equally applicable to structure elucidation of other large, nonvolatile organic compounds, and future work in these areas is suggested.

CHAPTER 1

INTRODUCTION

Structure Elucidation of Porphyrins

Porphyrins are cyclic tetrapyrroles in which the four pyrrole rings are linked by sp^2 hybridized carbon bridges. Porphyrins are able to form chelates with a number of metals. Example structures of both a free-base (metal-free) porphyrin and a metalloporphyrin are shown in Figure 1-1. The specific free-base porphyrin in this case is 2,3,7,8,12,13,17,18-octaethyl-21H,23H-porphine (OEP). The metalloporphyrin depicted in Figure 1-1 is the cobalt(II) derivative of OEP, known as Co(II)OEP. Porphyrinic structures are very common in living systems, with plant chlorophyll a being one of the most important to life on earth. Metalloporphyrins are found in petroleum samples, and are believed to originate predominantly from the chlorophylls of ancient plants (Treibs, 1936). These petroporphyrins, or geoporphyrins, are useful as biological marker compounds, or biomarkers (Philp, 1986). The structures of geoporphyrins from a particular petroleum sample are indicative of its maturity and depositional environment. Structure elucidation of geoporphyrins can also provide information on oil-source rock correlation and source identification. Presumably, petroleum samples having different geochemical

Figure 1-1.

Structures of free-base 2,3,7,8,12,13,17,18-octaethyl-21H,23H-porphine, labeled OEP, and its cobalt(II) derivative, labeled Co(II) OEP

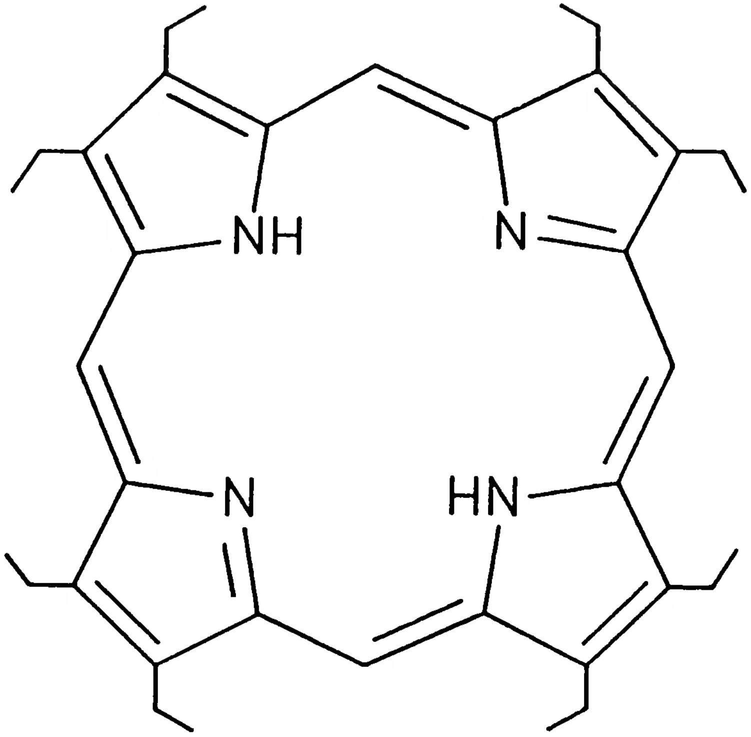

OEP

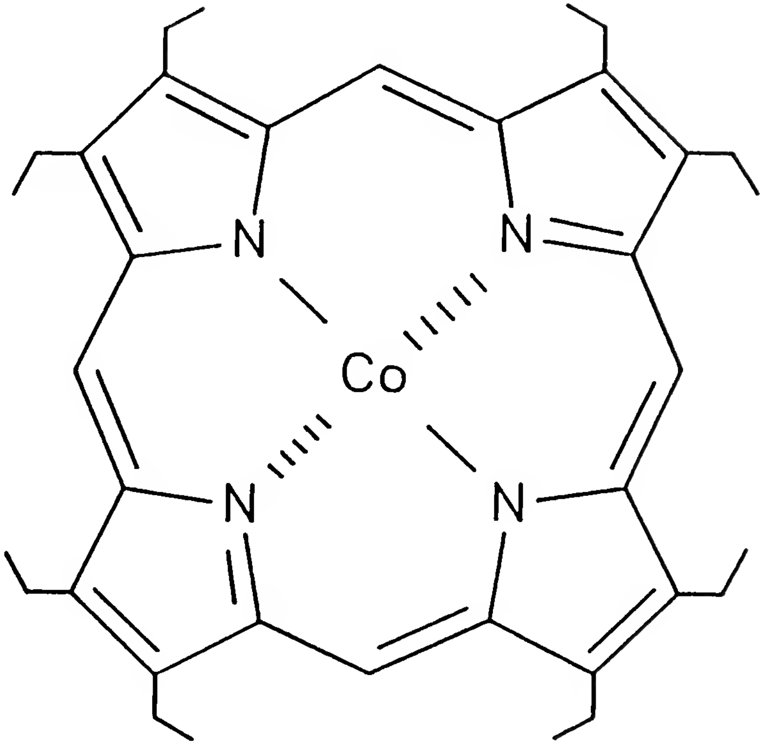

Co(II) OEP

histories will yield dissimilar biomarker fingerprints. Porphyrins are also employed in the detection and treatment of cancer (van den Bergh, 1986; Baum, 1988). Current research is also aimed at obtaining structural information from these types of porphyrins so that improved porphyrin cancer therapy drugs can be produced (Musselman et al., 1988).

Although structure elucidation of geoporphyrins may offer a significant amount of valuable information, this information can be difficult to obtain. Geoporphyrins are present in complex mixtures, and often in only trace amounts (ppm or less). They are nonvolatile, and therefore not amenable to separation by gas chromatography (GC). They can be separated by other methods such as thin layer chromatography (TLC), high performance liquid chromatography (HPLC), or supercritical fluid chromatography (SFC). These methods, however, do not offer much in the way of structural information. Structural information may be obtained from infrared (IR) spectroscopy or from ^{1}H nuclear magnetic resonance spectrometry (NMR), but these methods have strict purity requirements, and are not useful, therefore, for direct analysis of geoporphyrin mixtures. Tandem mass spectrometry (MS/MS) (McLafferty, 1983) provides a very useful way in which to obtain structural information from trace amounts of analytes in a complex mixture. This technique has been successfully applied to geoporphyrins (Britton, 1985; Brodbelt et al., 1986) and has become the analytical method of choice in biomarker research.

Tandem Mass Spectrometry Applied to Porphyrins

The triple quadrupole mass spectrometer (Yost and Enke, 1979) (Figure 1-2) is a tandem mass spectrometer consisting of an ion source, three quadrupoles (Q1, Q2, and Q3) arranged linearly, and an electron multiplier detector. One of the most useful MS/MS experiments in terms of geoporphyrin analysis is the daughter ion scan depicted in Figure 1-3. In this experiment Q1 is programmed to select ions of the mass-to-charge (m/z) ratio of interest produced in the ion source. All ions not having this m/z are prevented from passing into Q2. The collision cell, Q2, is pressurized with 1-3 mtorr of an inert gas such as nitrogen or argon. The second quadrupole is operated in the radio frequency (RF)-only mode, passing ions of essentially all m/z values. The selected ions from Q1, called parent ions, undergo collisionally activated dissociation (CAD) upon colliding with target gas molecules, yielding daughter ions. These are detected by scanning Q3, which yields a daughter ion mass spectrum of the parent ion selected in Q1. The daughter ions are indicative of the structure of the parent ion.

There are three types of structural information required from porphyrins. These are the molecular weight or carbon-number, the nature of the peripheral substituents, and the sequence of the pyrrole rings around the macrocycle. To obtain the three types of structural information from porphyrins, various ionization methods are typically employed.

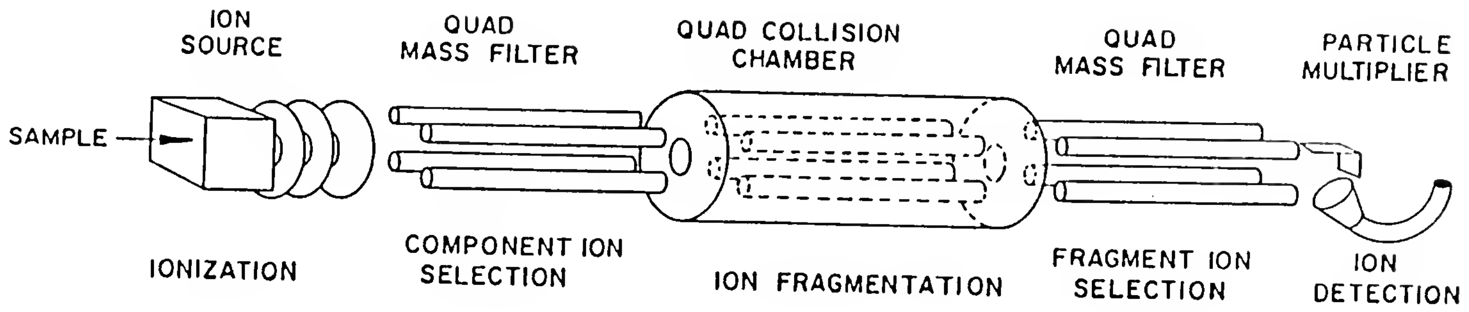
ION
SOURCE
QUAD
MASS FILTER
QUAD COLLISION
CHAMBER
QUAD
MASS FILTER
PARTICLE
MULTIPLIER
SAMPLE
IONIZATION
COMPONENT ION
SELECTION
ION FRAGMENTATION
FRAGMENT ION
SELECTION
ION
DETECTION

Figure 1-2.

The triple quadrupole mass spectrometer

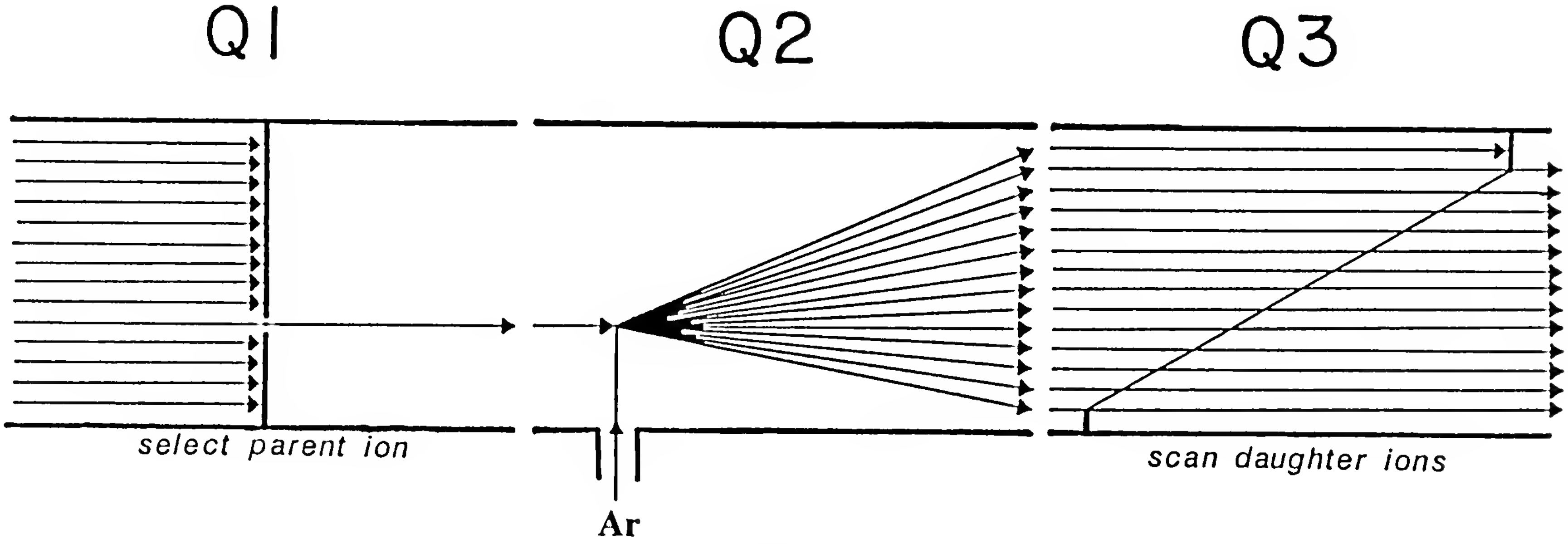
Q1
Q2
Q3
select parent ion
Ar
scan daughter ions

Figure 1-3.

Representation of the MS/MS daughter ion scan mode

The ion source of the triple quadrupole mass spectrometer includes removable ion volumes designed to provide appropriate pressures for either electron ionization (EI) or chemical ionization (CI). In each case, the porphyrin is introduced into the ion source as a solid and vaporized by heating. Introduction via solids probe involves placing a 1-5 μL porphyrin solution containing about 2 μg of porphyrin into a glass vial. After the solvent evaporates, the vial is inserted into the tip of the solids probe which is then inserted into the ion source. The solids probe can be heated as fast as 2 °C per second to a maximum of 500 °C. The porphyrins in this study all vaporize below 375°C in the high vacuum of the ion source. A direct exposure probe (DEP) consists of a rhenium filament which can be resistively heated up to a maximum temperature of 1350 °C as fast as 1000 °C per second. The DEP requires less than 1 μg of porphyrin in solution deposited directly onto the filament. The solvent is evaporated prior to insertion of the DEP into the ion source.

Electron ionization occurs when high energy (70 eV) electrons bombard gaseous neutral analyte molecules, stripping them of one or more electrons (Figure 1-4). The ions produced by EI can be left in a high energy excited state, whereby they can fragment yielding fragment ions. The EI fragmentation pathways for OEP are shown in Figure 1-5. Upon electron ionization, the porphyrin macrocycle remains intact, but the peripheral substituents tend to fragment by cleavage of bonds β to the macrocycle. Examples of the EI mass spectra from OEP and two

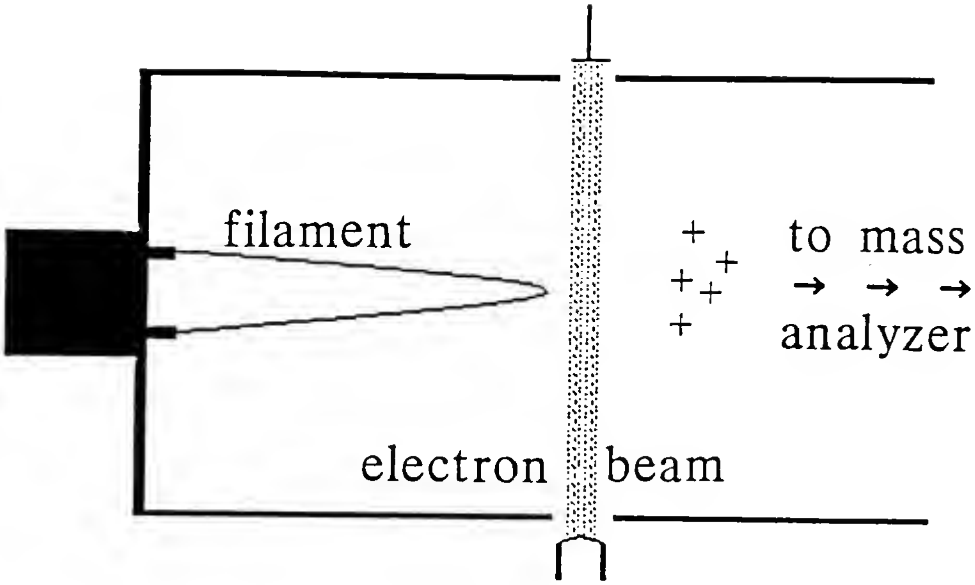
filament
to mass
→ → →
analyzer
electron beam
+
+
++
+

Figure 1-4.

Electron ionization in an EI ion volume

Figure 1-5.

Fragmentation pathways for porphyrins in an EI source

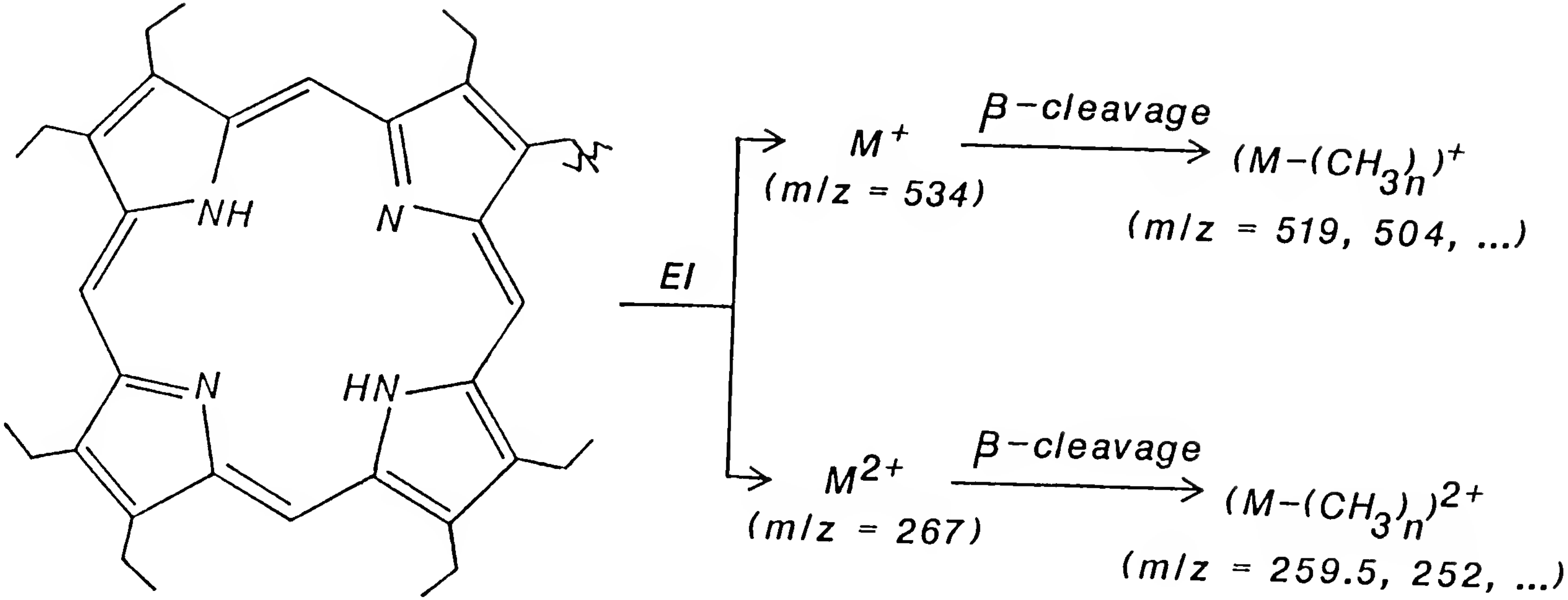
NH
N
N
HN
EI
M⁺
(m/z = 534)
β-cleavage
(M-(CH3)n)+
(m/z = 519, 504, ...)
M2+
(m/z = 267)
β-cleavage
(M-(CH3)n)2+
(m/z = 259.5, 252, ...)

Metal-Free OEP

metalated OEP derivatives are shown in Figure 1-6. These mass spectra, obtained for pure standards, show losses of methyl groups from the eight ethyl peripheral substituents in each porphyrin. Thus, EI/MS is useful in obtaining molecular weight and peripheral substituent information, but does not yield information about the sequence of the pyrroles around the porphyrin macrocycle. Although EI/MS is often used to get carbon-number ranges for geoporphyrins in petroleum samples, it is important to note that ions appearing at lower m/z values may not actually be molecular ions. Instead, they may be fragment ions from higher m/z molecular ions. It is also nearly impossible to obtain information about the peripheral substituents of individual geoporphyrins by EI/MS, because geoporphyrins are typically present as homologous series, each homolog differing from the next by one carbon-number. Thus, EI/MS has some limitations in terms of structure elucidation, especially of complex mixtures of porphyrins.

Chemical ionization occurs in a CI ion volume which is pressurized with up to 1 torr of a reagent gas such as methane, ammonia, or hydrogen. The reagent gas is ionized by the electron beam; the resulting reagent ions then react with the gaseous neutral analyte molecules (Figure 1-7). The analyte molecules are either protonated by the reagent ions, or ionized by charge exchange reactions with reagent ions in the reagent gas plasma. In the case of porphyrins under NH_3CI or H_2CI conditions, pyrrolic ions also result. Each of the mono-, di-, and tri-pyrrolic ions formed in the source are useful in determining the sequence of the

Figure 1-6.

Electron ionization mass spectrum of OEP, molecular weight M = 534

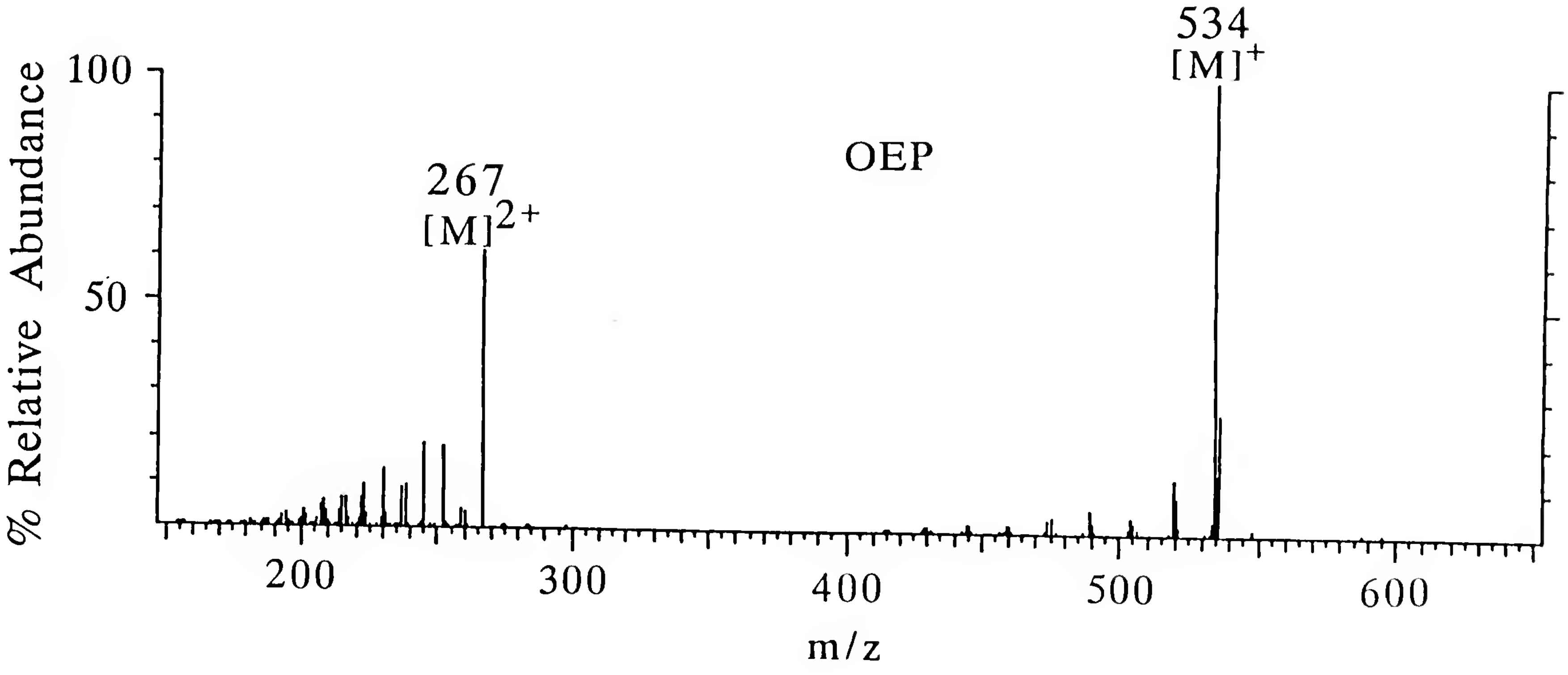
534
[M]$^+$
267
[M]$^{2+}$
OEP
% Relative Abundance
100
50
200
300
400
500
600
m/z

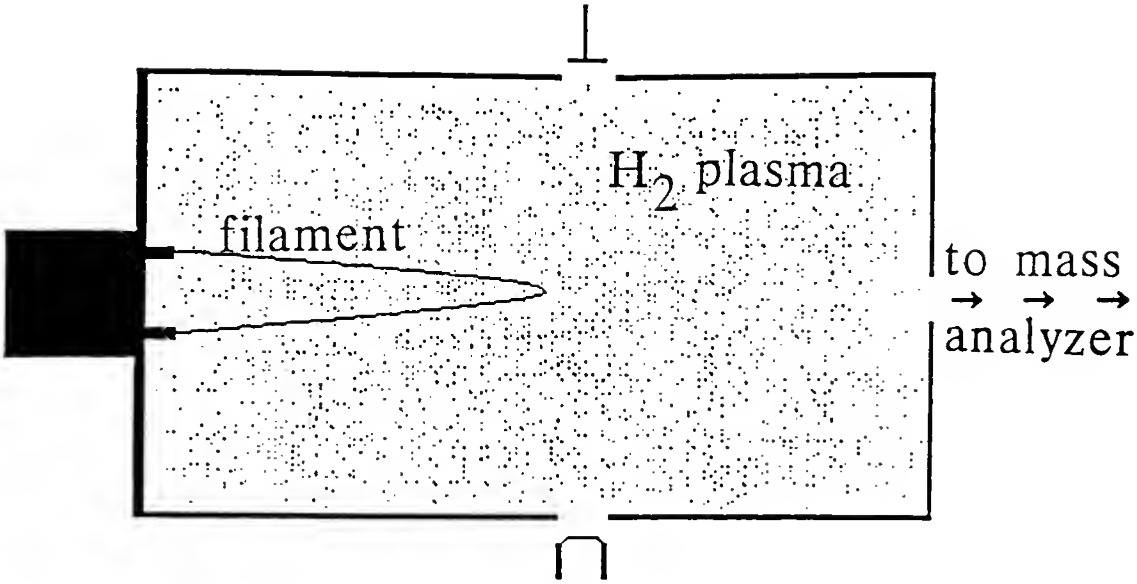
filament
H_2 plasma
to mass
→ → →
analyzer

Figure 1-7.

Hydrogen chemical ionization in a CI ion volume pyrrole rings around the porphyrin macrocycle. Data presented in this dissertation suggest that pyrroles arise from a thermal decomposition process (Figure 1-8). An example of an H_2CI mass spectrum is shown for OEP in Figure 1-9. This spectrum displays monopyrrolic ions (e.g. m/z 136), dipyrrolic ions (e.g. m/z 271), and tripyrrolic ions (e.g. m/z 406). The molecular ion appears at m/z 534, with the protonated molecular ion appearing at m/z 535. The reduced molecular ion at m/z 540 is discussed in Chapter 6. The type of structural information available from H_2CI/MS indicates that this technique may not be useful for complex mixtures of porphyrins. Regardless of whether porphyrins fragment or thermally decompose, there is no way to distinguish which pyrroles originate as part of which porphyrin structures in a complex mixture.

Tandem mass spectrometry seems well suited for analyzing complex mixtures of porphyrins. Under both EI and CI conditions, porphyrin molecular and protonated molecular ions fragment via β-cleavage of peripheral substituents upon CAD (Figure 1-10). This is very useful in determining the structures of the peripheral substituents from specific m/z porphyrins in a mixture. Unfortunately, CAD of porphyrin ions does not yield information about the sequence of the pyrroles around the macrocycle.

Scope of Dissertation

Clearly, MS/MS analyses of porphyrins are valuable, but new strategies of mass spectrometric analysis are needed to enhance structure elucidation of porphyrins

Figure 1-8.

Fragmentation pathways for porphyrins in an NH_3CI source

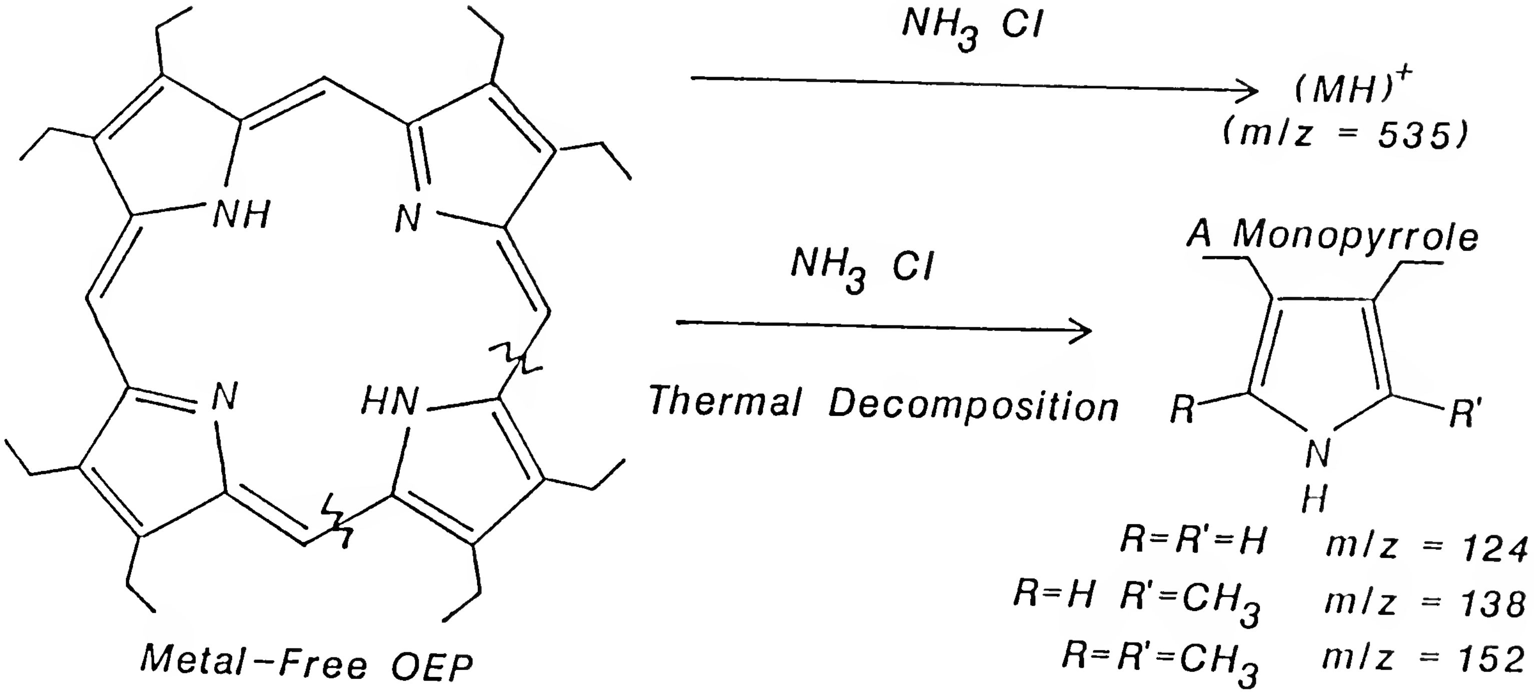
NH
N
N
HN
Metal-Free OEP
NH3 CI
(MH)+
(m/z = 535)
NH3 CI
Thermal Decomposition
A Monopyrrole
R
R'
N
H
R=R'=H m/z = 124
R=H R'=CH3 m/z = 138
R=R'=CH3 m/z = 152

Figure 1-9.

Positive hydrogen chemical ionization mass spectrum of OEP, molecular weight M=534

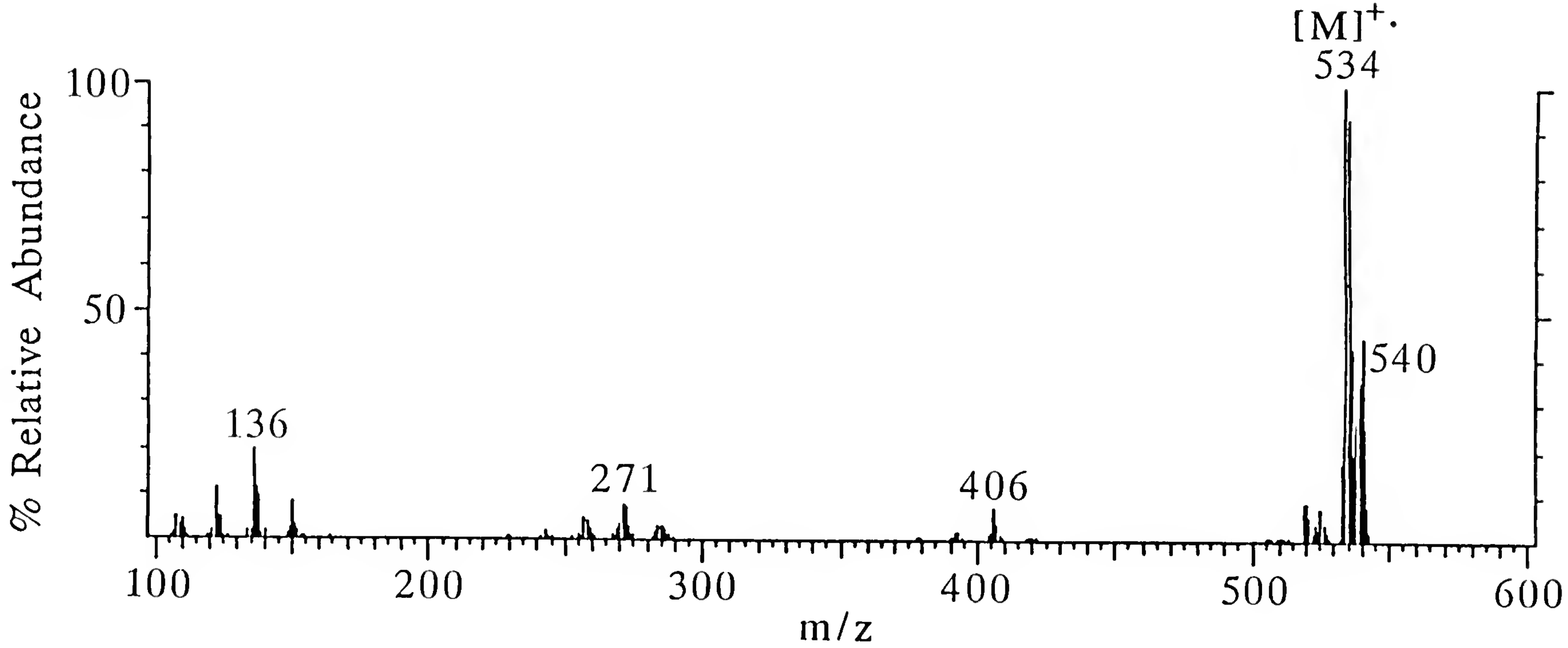
% Relative Abundance
100
50
[M]$^{+\cdot}$
534
540
136
271
406
100
200
300
400
500
600
m/z

Figure 1-10.

β-cleavage fragmentation pathway for porphyrins upon collisionally activated dissociation

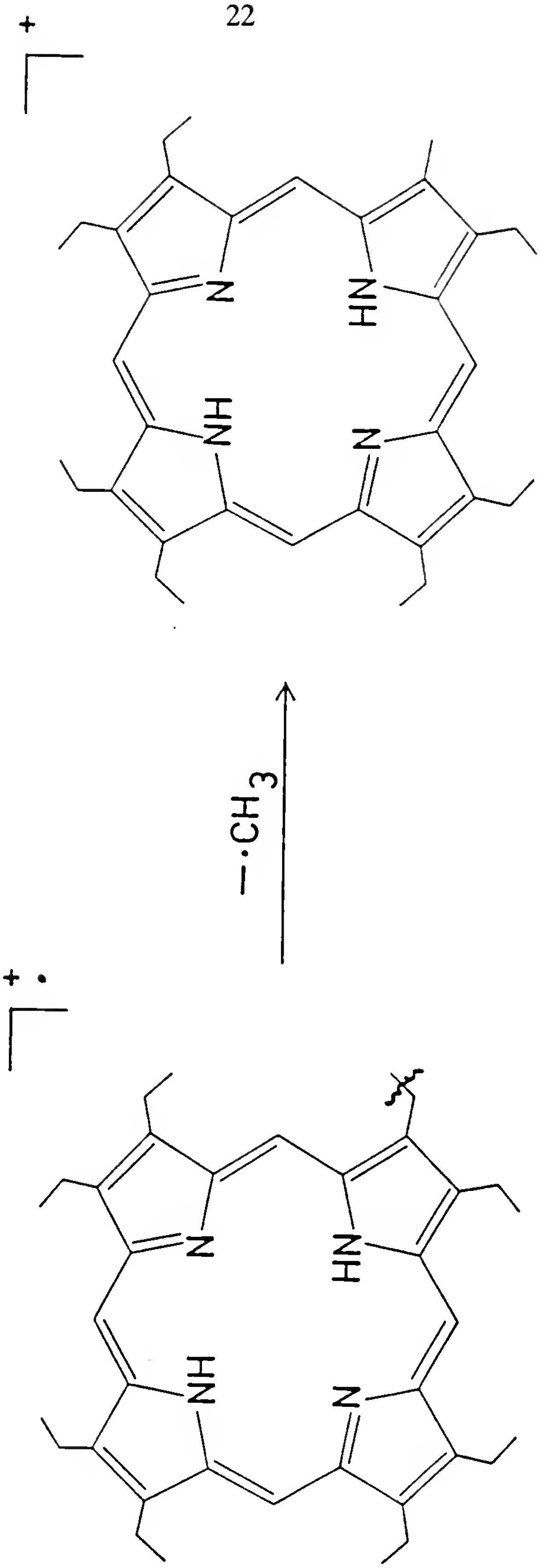
+
N
HN
NH
N
$-\cdot CH_3$
+•
N
HN
NH
N

over those methods described above. This dissertation addresses tandem mass spectrometry of porphyrins in two parts. The first part, Chapters 2-4, reports specific applications of EI/MS/MS to answer geochemical questions concerning geoporphyrins in shale. The second part, Chapters 5-8 describes novel mass spectrometric methods of enhancing structure elucidation of porphyrins, and fundamental studies of the various parameters involved.

Chapter 2 presents a detailed and specific introduction to geoporphyrin analysis and the types of geochemical questions addressed by EI/MS/MS in Part 1. Chapters 3 and 4 report the first comparisons of the nickel and vanadyl geoporphyrin structures from the kerogen, bitumen, and demineralized bitumen from the same sample of shale. These studies provide insight into the nature of kerogen, about which very little is known even though it is the earth's most abundant form of carbon. They also provide a data base for future comparisons with geoporphyrins from other geological samples.

Porphyrins yield unusually high abundances of doubly charged molecular and fragment ions upon electron ionization. In Chapter 5, the analytical utility of these doubly charged ions is presented in terms of how they can be used for structure elucidation. For instance, doubly charged porphyrin ions fragment to a greater extent, and often via different pathways, than do singly charged porphyrin ions, both in the ion source and upon CAD. The extent of fragmentation of doubly charged porphyrin ions in the ion source is also shown to depend on a stability index of its chelated metal.

In Chapters 6 and 7, decomposition on the surface of the ion volume is shown to have a major role in the CI mass spectra of porphyrins. Chapter 6 addresses positive chemical ionization of porphyrins with respect to the mechanisms by which they fragment and decompose. The pyrroles which arise in the ion source are shown to result from surface-induced decomposition on the walls of the ion volume. Electron capture negative chemical ionization (ECNCI) is discussed in Chapter 7. Free-base porphyrins are shown to metalate on the stainless steel walls of the ion volume under these conditions, while metalloporphyrins are hydrogenated on these surfaces. Electron capture negative chemical ionization is also shown to be much more sensitive toward metalloporphyrins than it is toward free-base porphyrins. The capabilities and limitations of each of these techniques with respect to structure elucidation of porphyrins is discussed in each of these chapters.

Two new H_2CI/MS/MS techniques for analyzing porphyrins are presented in Chapter 8. They yield all three types of structural information in the same experiment, rather than requiring separate EI and CI experiments. The first one involves MS/MS analysis of the porphyrin and then MS analysis of the pyrrolic decomposition products. The second one involves MS/MS analyses of porphyrin ions and their corresponding porphyrinogen ions (products of porphyrin reduction).

These two methods are compared to the more traditional EI and CI mass spectrometric techniques.

The final chapter summarizes the work presented in this dissertation. In addition, suggestions for future work in the area of mass spectrometric analyses of porphyrins are presented. These included geochemical applications such as comparing high carbon-number geoporphyrins from shale and from Boscan oil. Further studies on the effects of the ion volume surface on mass spectra of other nonvolatile compounds are also recommended. Questions raised about the ECNCI analysis of porphyrins must also be addressed. Hopefully, this dissertation will serve as a springboard for further study in an area of much importance.

PART 1: APPLICATIONS OF EI/MS/MS TO GEOPORPHYRINS

CHAPTER 2

OVERVIEW OF MASS SPECTROMETRIC ANALYSIS OF GEOPORPHYRINS

Geoporphyrin Biomarkers

Geoporphyrins were the first class of compounds identified as biomarkers, and are potentially the most valuable of all biomarkers that have been identified. This is because geoporphyrins are both ubiquitous in petroleum samples and structurally complex. The more pervasive a biomarker, the greater its potential for application to diverse samples. The more structurally complex a biomarker is, the more potential structural changes which can occur over time and upon exposure to various conditions. Alkyl porphyrins are present in a wide range of geological environments as complex mixtures of at least ten skeletal types (Figure 2-1).

The two major types of geoporphyrins found in petroleum samples are the etioporphyrins and the deoxyphylloerythroetioporphyrins (DPEP). Examples of each of these are shown in Figure 2-2. The term cycloalkanoporphyrin (CAP) will be used to describe all the porphyrins which bear a single isocyclic ring, including the DPEP's, as these species cannot be distinguished by electron ionization mass spectrometry (EI/MS). In the geosphere, geoporphyrins occur mainly as derivatives

Figure 2-1.

Skeletal structures of known geoporphyrin types, with R groups denoting peripheral substituents and M denoting the chelated metal.

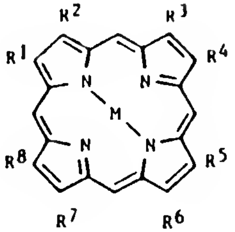
R1
R2
R3
R4
R5
R6
R7
R8
N
M

(1)

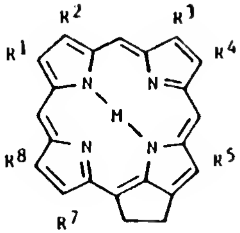
R1
R2
R3
R4
R5
R7
R8
N
M

(2)

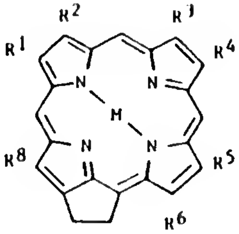
R1
R2
R3
R4
R5
R6
R8
N
M

(3)

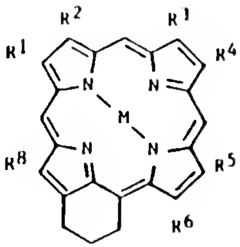
R1
R2
R3
R4
R5
R6
R8
N
M

(4)

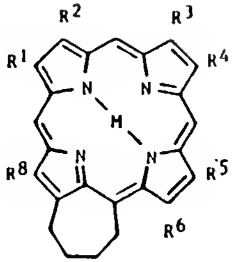
R1
R2
R3
R4
R5
R6
R8
N
M

(5)

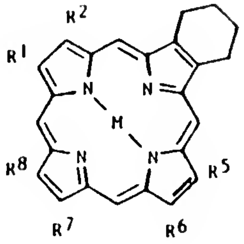
R1
R2
R5
R6
R7
R8
N
M

(6)

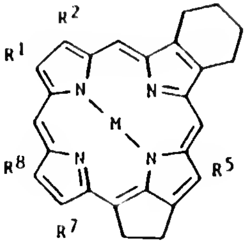
R1
R2
R5
R7
R8
N
M

(7)

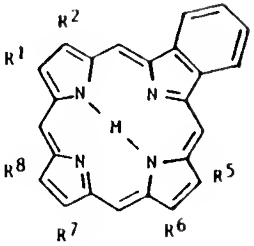
R1
R2
R5
R6
R7
R8
N
M

(8)

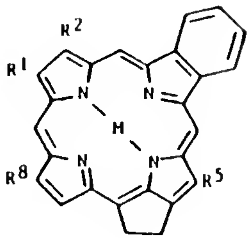
R1
R2
R5
R8
N
M

(9)

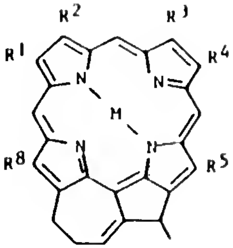
R1
R2
R3
R4
R5
R8
N
M

(10)

$R^1, R^2, R^3, R^4, R^5, R^6, R^7, R^8$ = H or Alkyl; M = H_2, Ni or VO

Figure 2-2.

Examples of an etioporphyrin having 28 carbons and a DPEP, or cycloalkanoporphyrin (CAP), with 31 carbons.

The metal ion, M, is typically Ni(II) or O=V(IV).

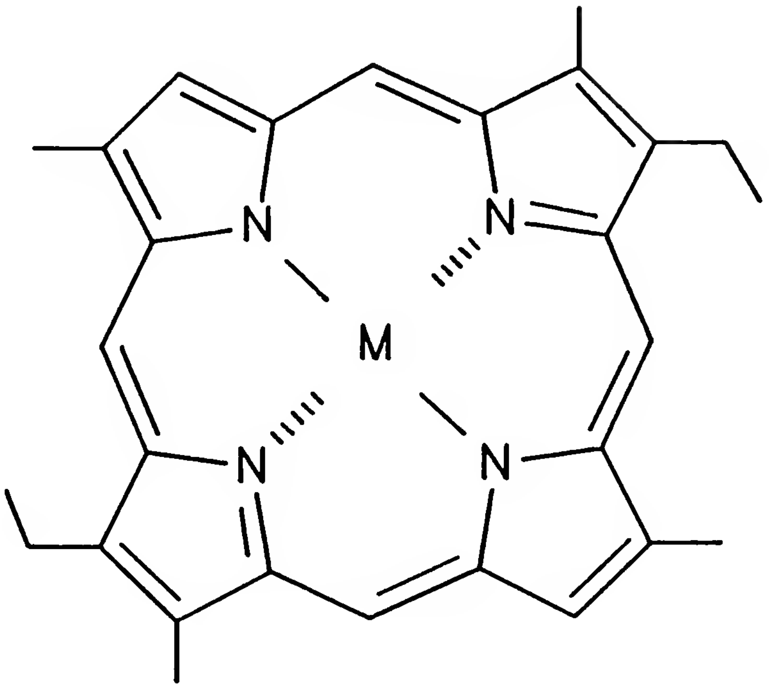

C_{28} Etioporphyrin

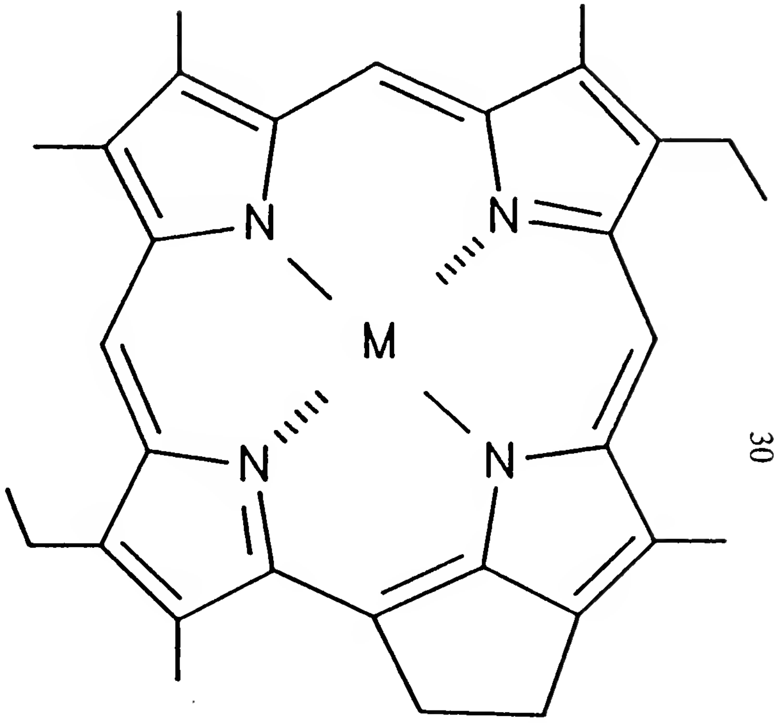

C_{31} Cycloalkanoporphyrin

of nickel or vanadyl [Ni(II) or O=V(IV), respectively] (Baker and Palmer, 1978; Quirke et al., 1982; Baker and Louda, 1983 and 1986; Van Berkel and Filby, 1987). Metal-free geoporphyrins have also been detected (Verne-Mismer et al., 1989) as have Cu(II), Fe(III), Ga(III), and Mn(III) geoporphyrin complexes (Palmer and Baker, 1978; Eckardt and Maxwell, 1989; Bonnett and Czechowski, 1981; Bonnett, 1989). Recent developments in the methods of porphyrin isolation (Sundararaman, 1985; Barwise et al., 1986; Quirke, 1987; Freeman et al., 1988) coupled with the determination of the structure of over 35 geoporphyrins (Chicarelli et al., 1987; Ocampo et al., 1987; Prowse et al., 1987; Verne-Mismer et al., 1987 and 1989; Quirke et al., 1989) have provided much information on the origin and evolution of the geoporphyrins. Nevertheless, there are still many aspects of the chemistry of the geoporphyrins which remain unresolved.

Bitumen and Kerogen

The two geoporphyrin-containing components of shale are the bitumen and the kerogen. Bitumen is organically extractable and fairly well characterized. The geoporphyrins from bitumen are relatively easy to obtain compared to those from kerogen. Kerogen is not soluble in organic solvents or in acid, and as such, very little is known about its structure or chemistry. The role of kerogen in geoporphyrin evolution has been the subject of much speculation (Baker and Louda 1983 and 1986; Mackenzie et al., 1980; Barwise and Roberts, 1984; Barwise, 1987). Baker and Louda (1983 and 1986) proposed that Ni(II) porphyrins form primarily from cyclic tetrapyrroles in bitumen, but O=V(IV) porphyrins were formed in association with kerogen and were released into the evolving bitumen by thermal cracking of the kerogen during catagenesis. This proposal was formulated on the basis of detailed analyses of geoporphyrin distributions from many Deep Sea Drilling Project cores. Mackenzie et al. (1980) proposed that O=V(IV) geoporphyrins, with an increased CAP/etioporphyrin ratio and with extended alkyl substituents, were generated from the kerogen at the zone of oil generation in sediments of the Paris Basin. Barwise and Roberts (1984) observed that the O=V(IV) geoporphyrin content of the El Lajjun shale (Upper Cretaceous, Jordan) increased in the oil generation window, and that the concentration of etioporphyrins reached a higher level than the initial porphyrin concentration, which was primarily CAP. Barwise (1987) concluded from these observations, and from studies of a suite of samples from the Gulf of Suez, that substantial quantities of etioporphyrins were generated from kerogen during catagenesis.

Although other biomarkers have been generated in vitro from the pyrolyses of kerogens (Eglinton and Douglas, 1988), there are no reports of the generation of geoporphyrins from such studies. Thus, the above hypotheses remained only speculative. The lack of data on the generation of geoporphyrins from kerogen is largely the result of a lack of samples suitable for such a pyrolysis study. An ideal sample should yield bitumen containing high concentrations of both Ni(II) and O=V(IV) porphyrins as well as being a bountiful source of kerogen. These features are essential in order to determine whether the Ni(II) and O=V(IV) porphyrins are produced via different geochemical pathways. An ample supply of kerogen is necessary to test the proposals on the generation of porphyrins from kerogen outlined above.

Recently, both Ni(II) and O=V(IV) porphyrins were generated from kerogens from the New Albany and Woodford shales by sequential pyrolyses from 110 to 450 °C of single aliquots (Van Berkel and Filby, 1987). Van Berkel and Filby (1987) reported the relative abundances of the O=V(IV) C_{28} and C_{29} etio and O=V(IV) C_{31} and C_{32} DPEP porphyrins in the New Albany kerogen pyrolysate and the bitumen. These data were only of limited value as the abundances of the entire O=V(IV) porphyrin array and the abundances of the Ni(II) porphyrins were not reported. This original study was extended by analyzing the Ni(II) and O=V(IV) geoporphyrin mixtures isolated from the bitumen and from each of the kerogen pyrolysates by EI/MS. Comparison of the mass spectra revealed that the Ni(II) and O=V(IV) geoporphyrins generated by kerogen pyrolysis at temperatures below 450 °C resembled the Ni(II) and O=V(IV) porphyrins isolated from the bitumen in both skeletal type (primarily etio and CAP) and carbon number range (Van Berkel et al., in press b and c). These data support the idea that the porphyrins in the bitumen are generated, at least in part, by release from the kerogen and solubilization in the evolving bitumen/pyrolyzing solvent. The Ni(II) and O=V(IV) porphyrin mixtures from both the bitumen and the pyrolysate were very complex. Thus, it was not possible to compare the fragment ions of the individual carbon number Ni(II) and O=V(IV) porphyrins in the pyrolysates with those of the corresponding compounds in the bitumen using conventional EI/MS. For this reason, it was not possible to obtain detailed information on the nature of the substituents of the individual carbon number Ni(II) or O=V(IV) porphyrins from either the bitumen or the pyrolysate.

Tandem mass spectrometry provides access to structural information on individual carbon number geoporphyrins without the need to isolate the individual porphyrin components of the mixture. A triple quadrupole mass spectrometer is employed to compare both Ni(II) and O=V(IV) geoporphyrins from both bitumen and kerogen from the same sample in Chapter 3. The results provide insight into the nature of kerogen in terms of how it binds geoporphyrins. The data also yield information about the geochemical histories of the Ni(II) and O=V(IV) complexes. In Chapter 4, EI/MS/MS daughter ion experiments are performed on geoporphyrins from demineralized bitumen, because very little is known about the effects of close association of inorganic mineral material with geoporphyrins. Geoporphyrins from all three media (bitumen, demineralized bitumen, and kerogen) from the same sample are compared for the first time in Part 1 of this dissertation.

Sample Preparation and Porphyrin Isolation

The bitumen extraction, kerogen isolation, and kerogen pyrolysis procedures are outlined in Figure 2-3, and are discussed in detail elsewhere (Van Berkel and

Figure 2-3.

Shale sample treatment: extraction of bitumen, isolation of kerogen, and sequential pyrolysis of kerogen

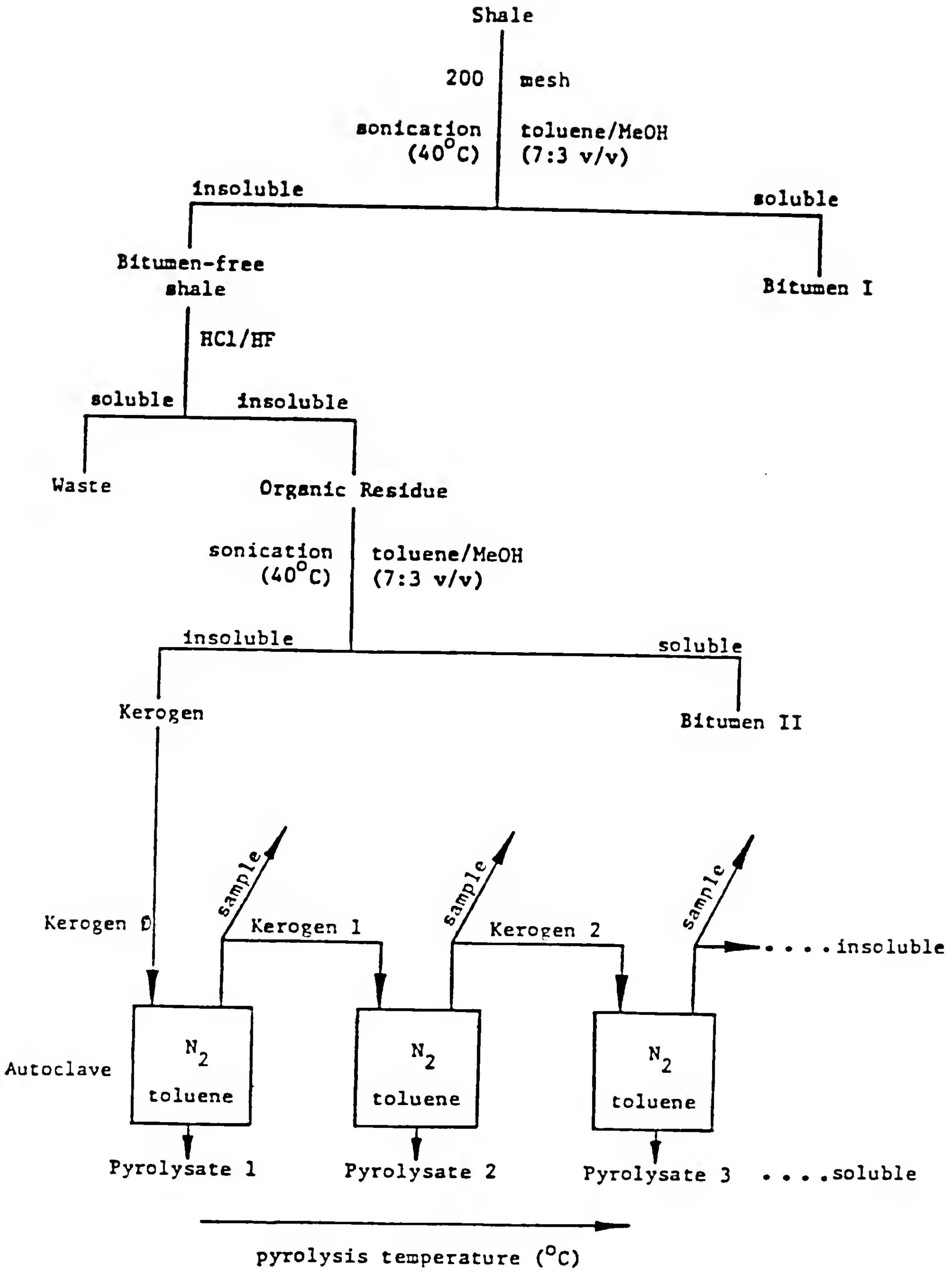
Shale
200 mesh
sonication (40°C)
toluene/MeOH (7:3 v/v)
insoluble
soluble
Bitumen-free shale
Bitumen I
HCl/HF
soluble
insoluble
Waste
Organic Residue
sonication (40°C)
toluene/MeOH (7:3 v/v)
insoluble
soluble
Kerogen
Bitumen II
Kerogen 0
sample
Kerogen 1
sample
Kerogen 2
sample
....insoluble
Autoclave
N_2
toluene
N_2
toluene
N_2
toluene
Pyrolysate 1
Pyrolysate 2
Pyrolysate 3
....soluble
pyrolysis temperature (°C)

Filby, 1987; Van Berkel et al., in press c). The procedure for the isolation and purification of the Ni(II) and O=V(IV) porphyrins from the New Albany bitumen and from the kerogen pyrolysates is described elsewhere and is summarized in Figure 2-4 (Van Berkel et al., in press b and c). The total Ni(II) and O=V(IV) geoporphyrin fractions isolated from any matrix in these studies were each separated further by TLC prior to mass spectrometric analysis. This was because the sample matrix was very complex in each case, and purifying the samples by TLC not only helped keep the mass spectrometer clean, but also avoided the possibility of nonporphyrinic material of the same m/z as the geoporphyrins of interest causing interferences. The EI mass spectrum of a total Ni(II) porphyrin chromatographed fraction (prior to TLC) is compared to the EI mass spectrum of one of the bands resulting from the same Ni(II) porphyrin chromatographed fraction after TLC in Figure 2-5. Geoporphyrins from the TLC plate are obtained by scraping off the stationary phase containing the band, and extracting it with methylene chloride. The fraction which was separated by TLC contained much less low molecular weight (less than 400 u) nonporphyrinic material than the total fraction which was not cleaned up by TLC. These spectra indicate that separation by TLC can provide a good indication as to which mass spectral peaks correspond to molecular porphyrin ions.

Figure 2-4.

Schemes for the isolation of Ni(II) and O=V(IV) porphyrins
from bitumen and from kerogen pyrolysate

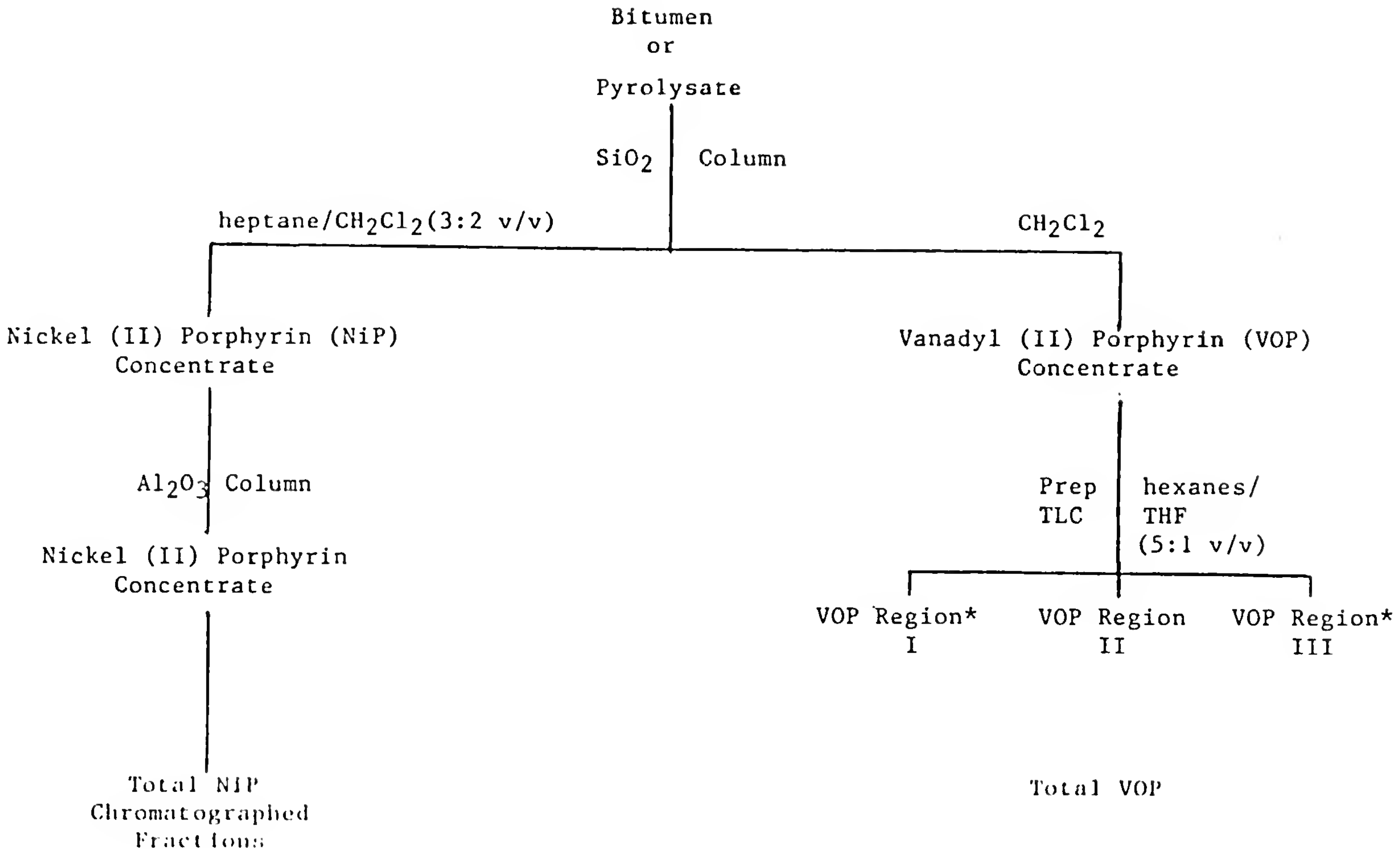
Bitumen
or
Pyrolysate
SiO2
Column
heptane/CH2Cl2(3:2 v/v)
CH2Cl2
Nickel (II) Porphyrin (NiP) Concentrate
Vanadyl (II) Porphyrin (VOP) Concentrate
Al2O3
Column
Nickel (II) Porphyrin Concentrate
Prep TLC
hexanes/ THF (5:1 v/v)
VOP Region* I
VOP Region II
VOP Region* III
Total NiP Chromatographed Fractions
Total VOP

* Trace quantities only.

Figure 2-5.

Electron ionization mass spectra of Ni(II) porphyrins:
A. of purified concentrate
B. of one chromatographed fraction

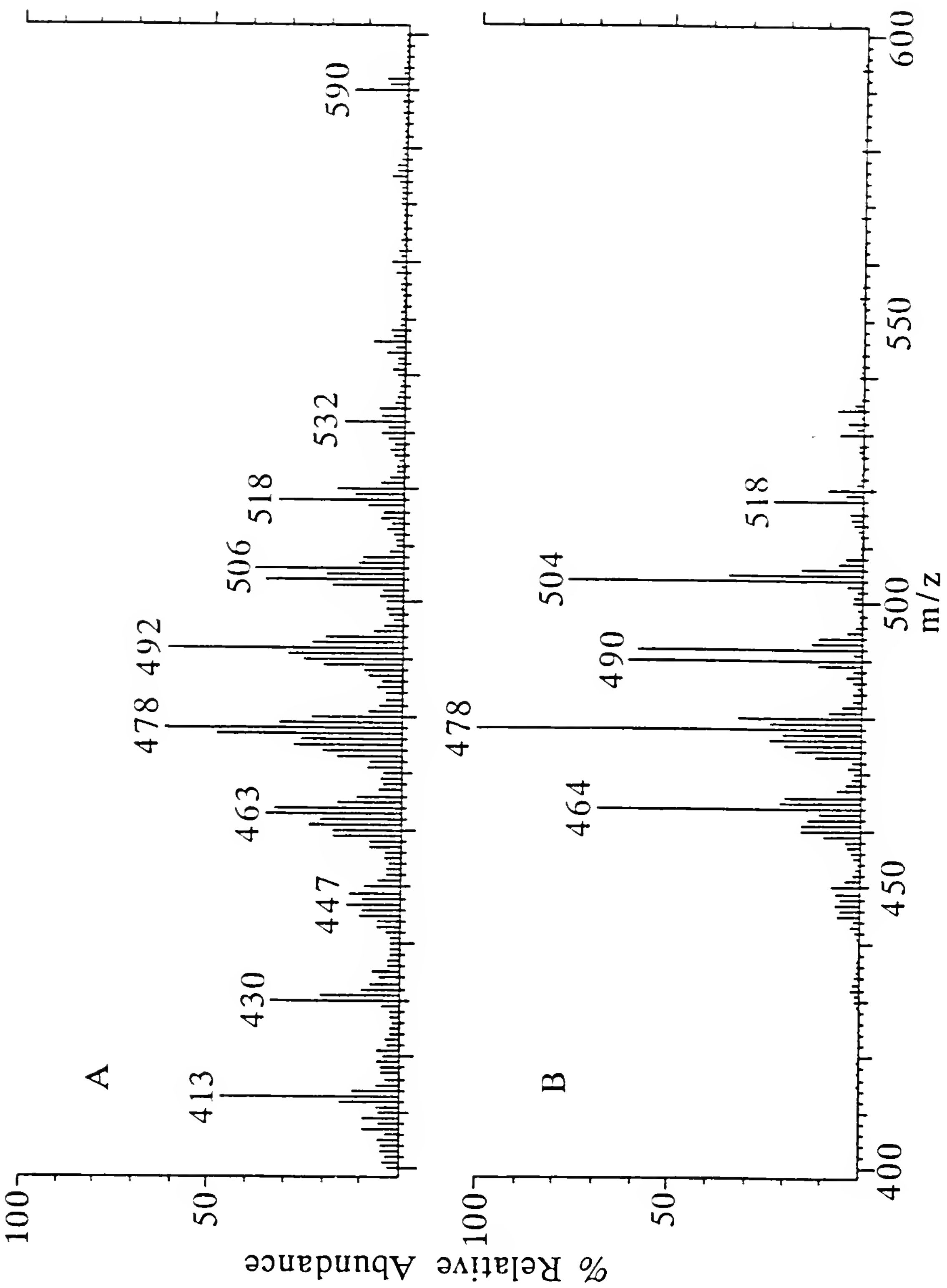
A
413
430
447
463
478
492
506
518
532
590
B
464
478
490
504
518
% Relative Abundance
100
50
400
450
500
550
600
m/z

EI/MS and EI/MS/MS Analyses of Geoporphyrins

The EI mass spectra of alkyl porphyrins, and their Ni(II) and O=V(IV) complexes, are characterized by relatively abundant molecular ions together with lesser relative abundances of fragment ions. The predominant fragmentation pathway is cleavage of alkyl groups ß to the porphyrin macrocycle (Smith, 1975; Budzikiewicz, 1978). For example, the presence of a $[M-15]^+$ fragment (i.e. loss of $\cdot CH_3$) in the mass spectrum indicates that the porphyrin contains at least one ethyl group. In Part 1 of this dissertation, discussions of EI spectra will omit the use of the unpaired electron symbol to identify radicals. This is to avoid ambiguity in terms of metal complexes, as some metals have an odd number of electrons. In EI/MS/MS daughter ion experiments, the daughter ions of porphyrin molecular ions are generated by a similar β-cleavage fragmentation process, as described in Chapter 1 (Johnson et al., 1986; Quirke, 1987). Each different type of alkyl substituent on the parent ion is expected to result in a different daughter ion. The attenuation of the molecular ions in the primary beam is variable, depending on the collision gas pressure. Thus, the intensities of the daughter ion fragments relative to the intensity of the remaining parent molecular ion in EI/MS/MS spectra can vary between analyses, but the relative abundances of the daughter ions is fairly constant. The intensities of the daughter ion fragments relative to the intensity of the parent ion in EI/MS/MS spectra may also be substantially different from the intensities of fragment ions relative to the molecular ion in conventional EI/MS spectra.

CHAPTER 3

TANDEM MASS SPECTROMETRIC ANALYSES OF GEOPORPHYRINS FROM THE BITUMEN AND KEROGEN FROM SHALE

Introduction

Daughter ion mass spectra of molecular ions of both the Ni(II) and O=V(IV) geoporphyrins from both the bitumen and the kerogen have been obtained from the same sample of New Albany shale. In this chapter, the previous studies on the New Albany shale (Van Berkel and Filby, 1987; Van Berkel et al., in press b and c) are extended by reporting MS/MS spectra of the geoporphyrins from the bitumen and the (300 °C) kerogen pyrolysate. The daughter ion mass spectra of the geoporphyrins from the bitumen are compared to those from the kerogen pyrolysate, yielding information about how geoporphyrins are bound to kerogen. The daughter ion mass spectra of various Ni(II) and O=V(IV) geoporphyrins having the same carbon number are also compared, and provide information about the geochemical histories of these two types of geoporphyrins.

Experimental

Sample

A sample from the Henryville bed of the New Albany shale (Mississippian-Devonian, Clark County, Indiana) was used in this study. A detailed description of the sample type and location is presented elsewhere (Van Berkel et al., in press b). The vitrinite reflectance value for the Henryville bed (R_0 = 0.5-0.6%) is just above the oil generation window for the source rocks in the region (Barrows and Cluff, 1984). The Ni (II) and O=V(IV) porphyrin concentrations in the New Albany bitumen are very high (9900 μg/g and 9100 μg/g, respectively). The CAP/etio ratios for the O=V(IV) and Ni(II) porphyrins are 1.4 and 0.9, respectively (Van Berkel et al., in press b).

Sample Preparation and Porphyrin Isolation

The bitumen extraction, kerogen isolation and kerogen pyrolysis procedures are summarized in Chapter 2, and are discussed in detail elsewhere (Van Berkel and Filby, 1987; Van Berkel et al., in press c). The procedure for the isolation and purification of the Ni(II) and O=V(IV) porphyrins from the New Albany bitumen and from the kerogen pyrolysates is also summarized in Chapter 2, and discussed in detail elsewhere (Van Berkel et al., in press b and c).

Tandem Mass Spectrometry

All MS/MS daughter ion mass spectra were obtained in the positive ion mode on a Finnigan MAT TSQ45 triple quadrupole mass spectrometer equipped with an INCOS data system. The samples were placed in glass vials and introduced via a solids probe in which samples were heated from ambient to 400 °C at 99 °C/min. The samples were ionized with an electron energy of 70 eV and an emission current of 0.3 mA. Daughter ion mass spectra were obtained using nitrogen (1.9 mtorr) for collisionally activated dissociation in the second quadrupole with a collision energy of 20 eV.

The Ni(II) and O=V(IV) Geoporphyrins from New Albany Shale

The porphyrins from the 300 °C kerogen pyrolysate were selected for EI/MS/MS analyses because the large amounts of Ni(II) and O=V(IV) geoporphyrins present in the pyrolysate allowed a thorough analysis. In addition, the porphyrin macrocycle would not undergo substantial thermal degradation at this temperature during the 5 hours of pyrolysis (Van Berkel et al., in press c).

The carbon number distributions of the total Ni(II) and O=V(IV) etio and CAP geoporphyrin mixtures from both the bitumen and the kerogen pyrolysate are shown in Figure 3-1 (Van Berkel et al., in press c). The O=V(IV) porphyrin mixtures from the pyrolysate and the bitumen were sufficiently clean to be used without further purification. It was necessary to separate the total Ni(II) porphyrin mixtures into fractions by thin layer chromatography (TLC) for two reasons: (a) the

Figure 3-1.

Distributions of the CAP porphyrins (shaded blocks) and the etioporphyrins (open blocks) from New Albany shale:
A. Ni(II) porphyrins from the bitumen
B. Ni(II) porphyrins from the 300 °C pyrolysate
C. O=V(IV) porphyrins from the bitumen
D. O=V(IV) porphyrins from the 300 °C pyrolysate

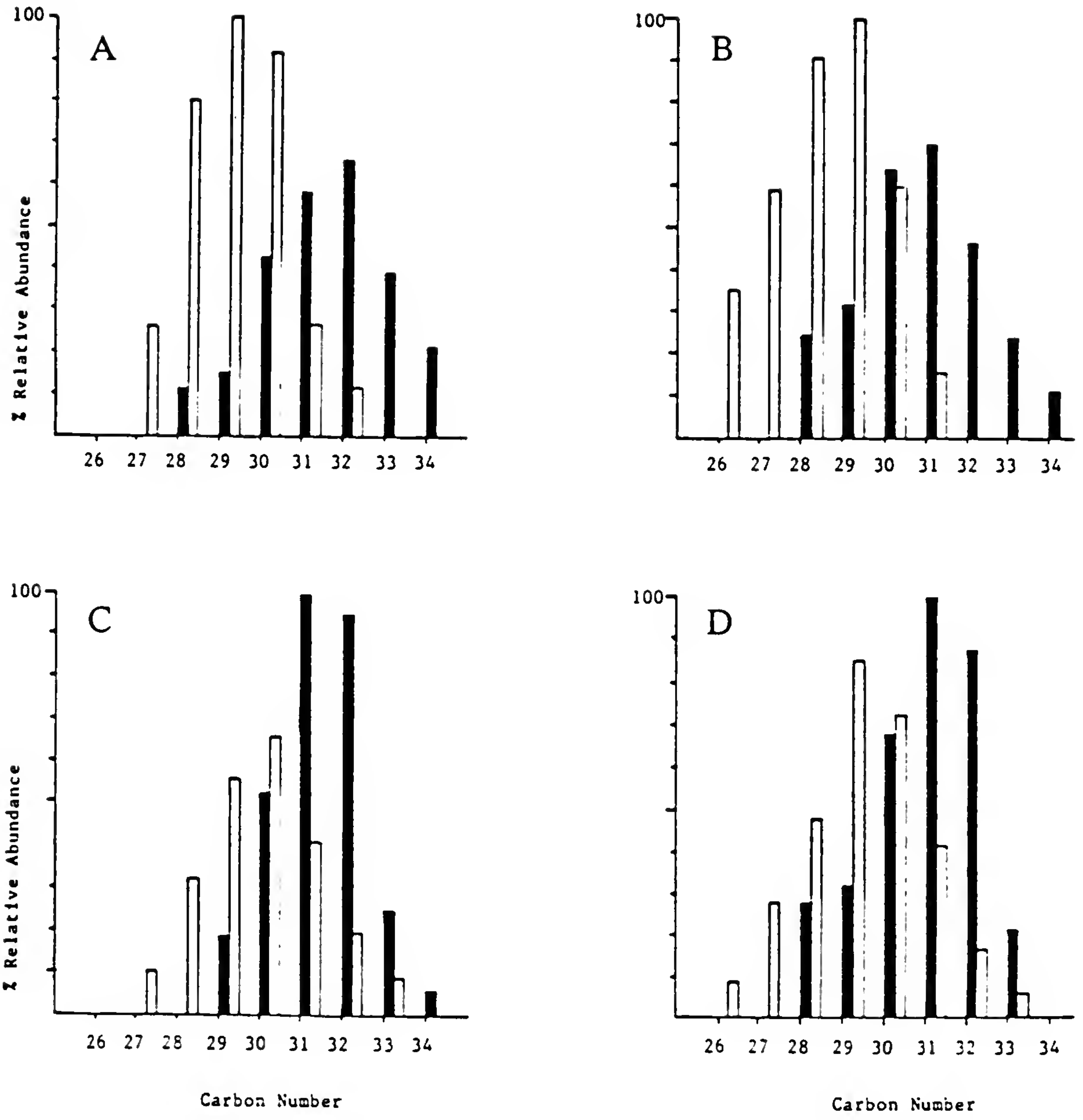
100
A
% Relative Abundance
26 27 28 29 30 31 32 33 34
100
B
26 27 28 29 30 31 32 33 34
100
C
% Relative Abundance
26 27 28 29 30 31 32 33 34
Carbon Number
100
D
26 27 28 29 30 31 32 33 34
Carbon Number

total Ni(II) geoporphyrin mixtures from both the pyrolysate and the bitumen contained nonporphyrinic impurities which interfered with the EI/MS/MS analyses; and (b) more importantly, it was necessary to separate the Ni(II) CAP and etio porphyrins of the same carbon number because of the coincidence of ^{60}Ni CAP and ^{58}Ni etio porphyrin molecular ions. Otherwise, the daughter ion mass spectra of the Ni(II) etio porphyrins might be misinterpreted. In most cases the Ni(II) etio and CAP porphyrins of the same carbon number could be separated into different fractions; however, the C_{32} CAP porphyrin(s) occurred as a minor component in the same fractions as the C_{32} etio porphyrin(s) (Van Berkel et al., in press b and c). Thus the daughter ions of the molecular ions of the ^{58}Ni(II) C_{32} etio porphyrins may include small contributions from ^{60}Ni(II) C_{32} CAP porphyrin molecular ions.

The daughter ion mass spectra of the molecular ions of geoporphyrins from the New Albany bitumen and the 300 °C kerogen pyrolysate are summarized in Tables 3-1 and 3-2, respectively. The daughter ion mass spectra of the Ni(II) geoporphyrins and O=V(IV) geoporphyrins from both the bitumen and pyrolysate are compared in Tables 3-3 and 3-4, respectively. Many of these EI/MS/MS daughter ion mass spectra are collected in the Appendix. In both Tables 3-3 and 3-4, the relative abundances of the daughter ions are normalized relative to $[M-15]^+ = 100\%$ to clarify the correlation.

Table 3-1. Data from EI/MS/MS daughter ion mass spectra of the parent molecular ions of Ni(II) and O=V(IV) porphyrins from bitumen.

Compound	Molecular Ion m/z (% abundance)	Daughter Ions m/z(% abundance)[a]
Ni C_{27} Etio	464(100)	463(44) 462(9) 449(35) 448(8)
Ni C_{28} Etio	478(72)	477(27) 463(100) 462(8)
O=V C_{28} Etio	487(100)	486(10) 472(100) 471(9) 458(7) 457(6)
Ni C_{29} CAP	490(100)	489(10) 475(71) 474(9) 460(42) 459(7)
Ni C_{29} Etio	492(43)	477(100) 462(6)
O=V C_{29} Etio	501(93)	500(6) 486(100) 485(11) 472(5) 471(13)
Ni C_{30} CAP	504(71)	503(5) 489(100) 488(11) 475(12) 474(35) 473(9) 460(50) 459(17) 458(8)
O=V C_{30} CAP	513(100)	512(9) 498(84) 497 (10) 484(10) 483(16) 469(17)
Ni C_{30} Etio	506(56)	491(100) 477(10) 476(8) 475(8) 462(5)
O=V C_{30} Etio	515(100)	514(10) 500(92) 499(11) 486(7) 485(10)
Ni C_{31} CAP	518(100)	503(80) 502(16) 489(15) 488(17) 474(24) 473(8)
O=V C_{31} CAP	527(100)	526(10) 512(50) 497(10) 483(30)
Ni C_{31} Etio	520(100)[b]	519(7) 505(81) 504(12) 494(5)
O=V C_{31} Etio	529(89)	528(11) 514(100) 513(8) 500(14) 499(9)
Ni C_{32} CAP	532(100)	517(58) 503(14) 502(9) 488(23) 473(7)
O=V C_{32} CAP	541(100)	540(5) 526(36) 512(5) 511(7) 497(14)
Ni C_{32} Etio	534(100)	519(78) 505(14) 491(13) 490(11)
O=V C_{33} CAP	555(100)	554(5) 540(54) 539(12) 526(23) 511(32) 497(7) 496(5)

---

[a] Ions less than 5% omitted.

[b] Also contained about 8% of $[M+1]^+$ peak, m/z 521.

Table 3-2. Data from EI/MS/MS daughter ion mass spectra of the parent molecular ions of Ni(II) and O=V(IV) porphyrins from the 300 °C pyrolysate of kerogen.

Compound	Molecular Ion m/z (% abundance)	Daughter Ions m/z(% abundance)[a]
Ni C_{26} Etio	450(100)	449(67) 448(7) 435(51) 434(18)
Ni C_{27} Etio	464(100)	463(48) 462(5) 449(40) 448(12)
Ni C_{28} CAP	476(83)	475(10) 461(100) 460(15) 446(40) 445(7)
Ni C_{28} Etio	478(54)	477(12) 463(100) 448(8)
O=V C_{28} Etio	487(100)	486(15) 472(86) 471(9) 458(6) 457(10) 458(7)
Ni C_{29} CAP	490(100)	489(8) 475(97) 473(8) 461(8) 460(40) 446(6)
Ni C_{29} Etio	492(50)	477(100) 476(5) 462(10)
O=V C_{29} Etio	501(96)	500(5) 486(100) 485(5) 472(3) 471(14)
Ni C_{30} CAP	504(82)	489(100) 475(6) 474(35) 460(38) 459(15)
O=V C_{30} CAP	513(100)	512(13) 498(36) 483(12) 469(9) 468(7)
Ni C_{30} Etio	506(64)	505(7) 491(100) 490(10) 477(13) 476(16) 475(8) 462(13)
O=V C_{30} Etio	515(95)	514(7) 500(100) 499(12) 471(6)
Ni C_{31} CAP	518(88)	517(11) 503(100) 489(7) 488(22) 474(34) 473(11)
O=V C_{31} CAP	527(100)	526(12) 512(79) 511(10) 498(12) 497(10) 483(24)
Ni C_{32} CAP	532(100)	531(6) 517(85) 516(7) 503(18) 502(15) 489(8) 488(33) 487(8) 473(6)
O=V C_{32} CAP	541(100)	526(26) 512(11) 511(7) 497(39) 482(18)
Ni C_{33} CAP	546(100)	545(7) 531(77) 530(10) 517(30) 516(8) 503(18) 502(28) 501(6) 489(10) 488(12) 487(8) 474(12)

[a] Ions less then 5% omitted.

Table 3-3. Data from daughter ion mass spectra of Ni(II) porphyrins[a]

Sample[b]	Source[b]	M.W.	% Abundance (relative to M-15 = 100%)				
			M-1	M-29	M-30	M-44	Others
C_{26} E	PY	450	131	-	-	-	M-2 (14) M-16 (35)
C_{27} E	PY	464	120	-	6	-	M-2 (12) M-16 (30)
C_{27} E	BIT	464	125	-	-	-	M-2 (25) M-16 (22)
C_{28} C	PY	476	10	-	40	-	M-16 (15)
C_{28} E	PY	478	12	-	8	-	
C_{28} E	BIT	478	27	-	-	-	
C_{29} C	PY	490	8	8	41	6	
C_{29} C	BIT	490	14	6	59	-	M-16 (12)
C_{29} E	PY	492	-	-	10	-	
C_{29} E	BIT	492	-	-	6	-	
C_{30} C	PY	504	3	6	35	38	M-45 (15)
C_{30} C	BIT	504	5	12	35	50	M-16 (11) M-45 (17)
C_{30} E	PY	506	7	13	16	13	M-16 (10)
C_{30} E	BIT	506	3	10	18	3	
C_{31} C	PY	518	11	7	22	34	M-45 (11)
C_{31} C	BIT	518	5	19	21	30	M-16 (20) M-45 (10)
C_{31} E	BIT	520	10	-	-	-	M-16 (18)
C_{32} C	PY	532	6	21	18	38	
C_{32} C	BIT	532	12	24	16	40	M-59 (12)
C_{32} E	BIT	534	-	18	-	14	M-43 (17)
C_{33} C	PY	546	9	36	10	35	M-16 (13) M-43 (23) M-57 (13) M-58 (16) M-72 (16)

---

[a] The daughter ion mass spectra are normalized so that the intensity of the $[M\text{-}15]^+$ fragment ion is 100%.

[b] E= Etio porphyrin; C= CAP; BIT= bitumen; PY= pyrolysate.

Table 3-4. Data from daughter ion mass spectra of O=V(IV) porphyrins[a]

Sample[b]	Source[b]	M.W.	% Abundance (relative to M-15 = 100%)				
			M-1	M-29	M-30	M-44	Others
C_{28} E	BIT	487	10	7	6	-	M-16 (9)
C_{28} E	PY	487	17	11	-	-	M-16 (10)
C_{29} E	BIT	501	6	5	13	-	M-16 (11)
C_{29} E	PY	501	5	3	14	-	
C_{30} C	BIT	513	11	12	19	20	M-16 (12)
C_{30} C	PY	513	36	13	33	25	M-45 (19)
C_{30} E	BIT	515	11	8	11	5	M-16 (12)
C_{30} E	PY	515	7	-	3	6	M-16 (12)
C_{31} C	BIT	527	20	8	20	60	
C_{31} C	PY	527	16	15	12	30	M-16 (12)
C_{31} E	BIT	529	11	14	9	-	
C_{32} C	BIT	541	13	13	20	39	
C_{32} C	PY	541	7	42	26	150	M-59 (60)
C_{33} C	BIT	555	9	42	6	59	M-16 (22) M-58 (13)

[a] The daughter ion mass spectra are normalized so that the intensity of the $[M\text{-}15]^+$ fragment ion is 100%.

[b] E= Etio porphyrin; C= CAP; BIT= bitumen; PY= pyrolysate.

EI/MS/MS Analyses of the Ni(II) Geoporphyrins from the Bitumen and the Kerogen Pyrolysate

For both the bitumen and pyrolysate, the daughter ion mass spectra of the Ni(II) porphyrin molecular ions are fairly simple. The most commonly occurring daughter ions are:

(a) $[M\text{-}15]^+$ daughter ion. This ion corresponds to ß-cleavage of an ethyl group. It is either the most abundant or the second-most abundant daughter ion in all of the daughter ion mass spectra, including that of the C_{26} etio porphyrins. Clearly, porphyrins bearing ethyl groups are major contributors to the molecular ions of even the very low carbon number geoporphyrins (such as C_{26} and C_{27}). The data do not eliminate the possibility that there are porphyrin isomers present which are devoid of ethyl groups.

(b) $[M\text{-}1]^+$ daughter ion. This ion is abundant in the very low carbon number etio porphyrins. Because it is not usually observed in the daughter ion mass spectra of molecular ions of porphyrin standards, it may possibly arise from fragment ions produced from higher carbon number porphyrins, which have coincident mass with the molecular ions of these low carbon number porphyrins. Loss of 1 u has been noted after cleavage of several substituent groups from the porphyrin macrocycle (Van Berkel, unpublished data). A recent study by Van Berkel et al. (1989) revealed that the mass spectra of alkyl porphyrins which bear methyl groups and no other alkyl substituents show an intense $[M\text{-}1]^+$ daughter ion in addition to a $[M\text{-}15]^+$ ion, which must be formed by α-cleavage of the methyl group. This fragmentation pathway is not significant for the molecular ion of porphyrins with at least one ethyl (or higher alkyl) group present.

(c) $[M\text{-}29]^+$ daughter ion. This is a minor daughter ion which corresponds to a ß-cleavage of a propyl group. The low abundance of this daughter ion indicates that there are few etio or CAP porphyrins present which bear a propyl substituent.

(d) [M-30]$^+$ daughter ion. This ion may be attributed to the loss of two methyl groups corresponding to the ß-cleavage of two ethyl moieties. It was abundant for moderately high carbon number geoporphyrins (greater than C_{29}). The only exception to this trend was the C_{29} CAP which did show an abundant [M-30]$^+$ daughter ion.

(e) [M-44]$^+$ daughter ion. All of the Ni(II) CAP geoporphyrins except for the Ni(II) C_{28} and C_{29} compounds gave a significant [M-44]$^+$ daughter ion (Table 3-3). In contrast, for the etio porphyrins, the daughter ion mass spectra of the parent molecular ions contained little if any of this daughter ion. In fact, the trace amounts of the [M-44]$^+$ ion in the etio porphyrin daughter spectra could be attributed to the daughter ions of the molecular ion of the corresponding ^{60}Ni CAP porphyrins. The [M-44]$^+$ ion could be produced by a combination of losses of 15 and 29 u from ß-cleavage of ethyl and propyl groups, respectively. This is unlikely because only a few of the porphyrins contained propyl groups (see (c) above). It will be necessary to carry out extensive studies on a range of pure CAP porphyrins to elucidate the origin of this daughter ion.

The most abundant daughter ion which is not discussed above was the [M-16]$^+$ ion. This is probably formed by loss of a methyl group from the [M-1]$^+$ daughter ion because there is very good correlation between the abundances of these two ions. With the exception of the $[M-44]^+$ ion discussed above, daughter ions resulting from neutral losses of more than 30 u were not common. Such ions only occurred in the higher carbon number geoporphyrins in both the bitumen and pyrolysate samples. Since porphyrins fragment via β-cleavage of peripheral substituents upon CAD (Britton, 1985), this suggests that porphyrins bearing extended alkyl side chains (greater than C_2) were either absent or were minor contributors to the nickel geoporphyrin mixtures from both the bitumen and the kerogen pyrolysate.

Overall, the daughter ion mass spectra of the corresponding molecular ions of the Ni(II) porphyrins from New Albany bitumen and the 300 °C pyrolysate are very similar (Table 3-3). This similarity is a good indication that the Ni(II) geoporphyrins of New Albany bitumen and the kerogen pyrolysate have been formed via a similar pathway.

EI/MS/MS Analyses of the O=V(IV) Geoporphyrins from the Bitumen and the Kerogen Pyrolysate

The daughter ion mass spectra of the molecular ions of O=V(IV) geoporphyrins from the bitumen and the 300 °C pyrolysate are summarized in Tables 3-1 and 3-2, respectively, and the significant daughter ions are compared in Table 3-4. The daughter ion mass spectra of the O=V(IV) geoporphyrins closely resemble those of the Ni(II) geoporphyrins. Once again, the $[M-15]^+$ fragment was usually the major daughter ion (Tables 3-1 and 3-2), and the $[M-29]^+$, $[M-30]^+$, and

$[M\text{-}44]^+$ (for CAP) daughter ions were also significant. The $[M\text{-}1]^+$, and $[M\text{-}16]^+$ ions were usually minor contributors to the spectrum (Tables 3-1 and 3-2). The $[M\text{-}1]^+$ ion was intense in the daughter ion mass spectra of the molecular ions of the C_{31} CAP from the bitumen (20%), and the C_{30} CAP of the pyrolysate (36%); however, even in these cases, the relative intensities of the $[M\text{-}1]^+$ daughter ion were much lower than those observed in the daughter ion mass spectra of low carbon number Ni(II) geoporphyrins. Aside from the aforementioned $[M\text{-}44]^+$ ion, there were very few daughter ions resulting from losses of fragments of masses greater than 30 u. This indicates that porphyrins bearing extended alkyl side chains were either absent or were minor components of the O=V(IV) geoporphyrin mixtures from both the New Albany bitumen and the pyrolysate. The daughter ion mass spectra of the molecular ions of the O=V(IV) geoporphyrins from the New Albany bitumen and the 300 °C pyrolysate are very similar. Thus, it is also likely that the O=V(IV) geoporphyrins of New Albany bitumen and the kerogen pyrolysate have been formed via a similar pathway.

Comparison of the Ni(II) and O=V(IV) Geoporphyrins from the Bitumen and the Kerogen Pyrolysate

The daughter ion mass spectra of the molecular ions of the Ni(II) and O=V(IV) geoporphyrins of the same carbon number of New Albany bitumen and the 300 °C pyrolysate are very similar. Not only do they display similar fragment ions, but the relative abundances of the fragment ions are also generally in good agreement (Tables 3-3 and 3-4). The daughter ion mass spectra of the molecular ions of Ni(II) and O=V(IV) C_{30} etio porphyrins (Figures 3-2 and 3-3), and the Ni(II) and O=V(IV) C_{30} CAP porphyrins (Figures 3-4 and 3-5) from both the bitumen and kerogen pyrolysate can be used to illustrate this point. In view of the similarity of the carbon number ranges (Figure 3-1), and the daughter ion mass spectra, it seems most probable that the Ni(II) porphyrins and O=V(IV) porphyrins of both New Albany kerogen pyrolysate and bitumen have a common geological history, as was proposed previously (Van Berkel and Filby, 1987; Van Berkel et al., in press c). There is no evidence from these data that the geoporphyrins released from the kerogen are significantly different from the geoporphyrins isolated from the bitumen.

Significance of the $[M-15]^+$ Daughter Ion

The daughter ion mass spectra of the molecular ions of all of the porphyrins studied have the $[M-15]^+$ daughter ion as either the most abundant or the second-most abundant daughter ion resulting from collisionally activated dissociation (CAD) of the molecular ion. This indicates that geoporphyrins bearing at least one ethyl group make up a major contribution to the composition of each molecular ion. These data provide tentative evidence that the low carbon number geoporphyrins were formed via a Treibs'-type degradation of chlorophyll a, or other abundant biologically-occurring chlorophylls. In this type of pathway, only the functional

Figure 3-2.

EI/MS/MS daughter ion mass spectra of m/z 506 [Ni(II) C_{30} etioporphyrin]:
A. from New Albany bitumen
B. from 300 °C pyrolysate of New Albany kerogen

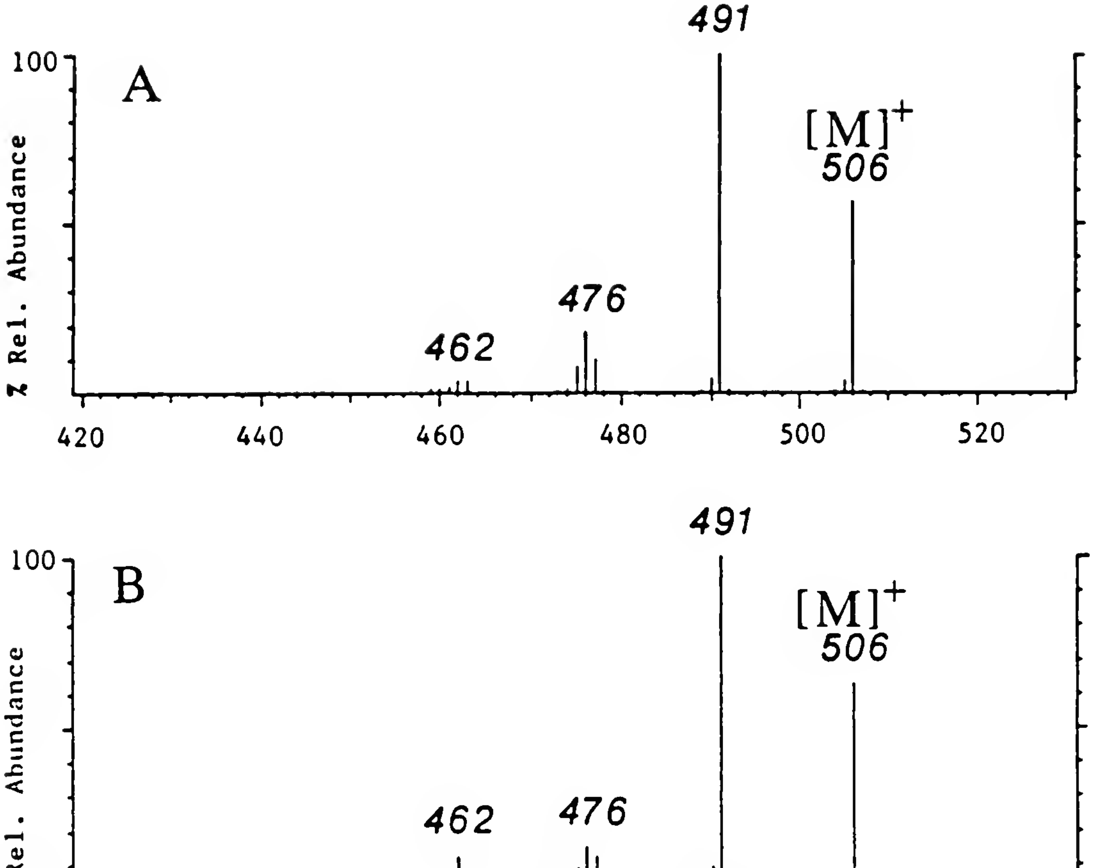
A
491
[M]+
506
476
462
100
% Rel. Abundance
420
440
460
480
500
520
B
491
[M]+
506
476
462
100
% Rel. Abundance
420
440
460
480
500
520

Figure 3-3.

Daughter ion mass spectra of m/z 515 [O=V(IV) C_{30} etioporphyrin]:
A. from New Albany bitumen
B. from 300 °C pyrolysate of New Albany kerogen

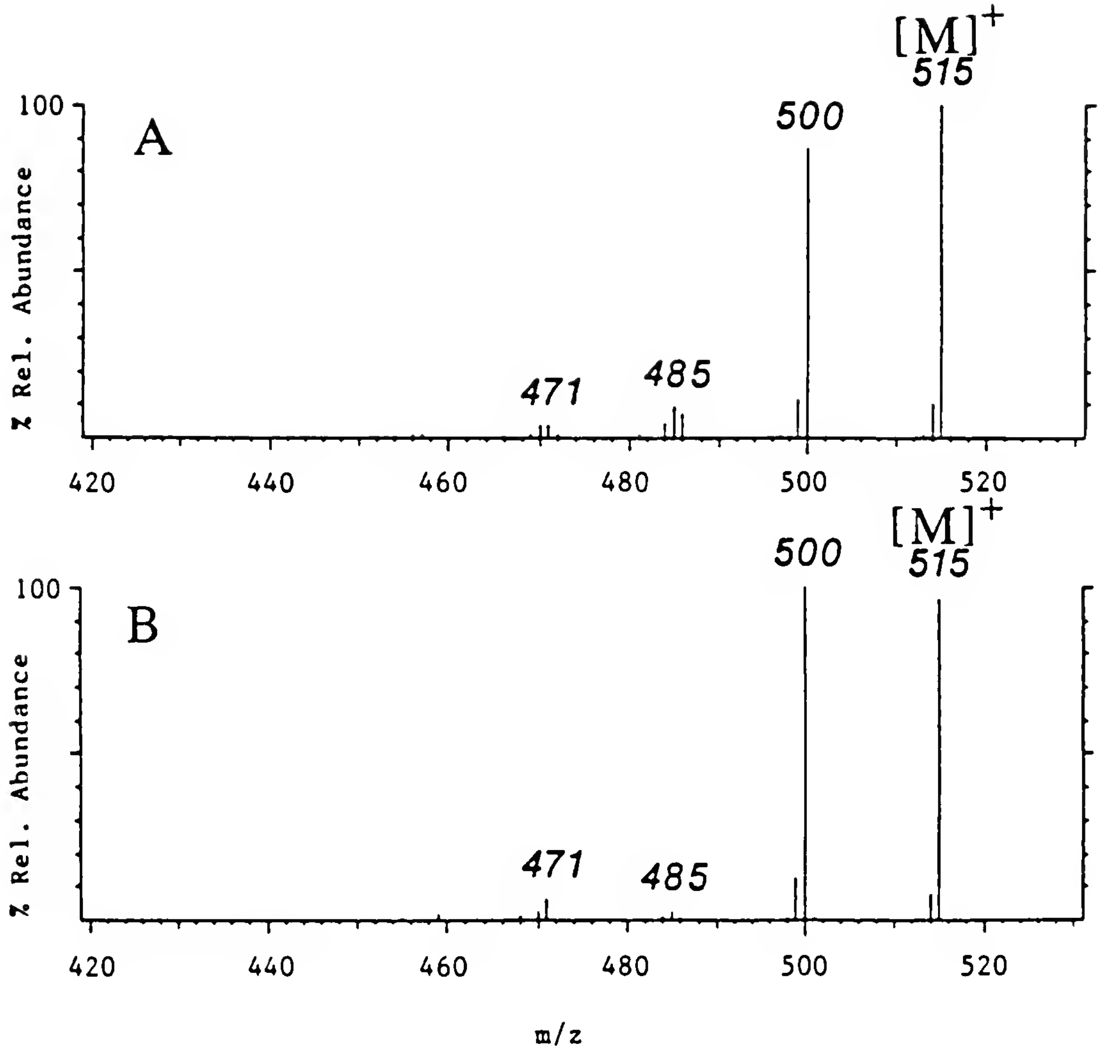
[M]+
515
500
100
A
% Rel. Abundance
471
485
420
440
460
480
500
520
[M]+
500
515
100
B
% Rel. Abundance
471
485
420
440
460
480
500
520
m/z

Figure 3-4.

Daughter ion mass spectra of m/z 504 [Ni(II) C_{30} CAP porphyrin]:
A. from New Albany bitumen
B. from 300 °C pyrolysate of New Albany kerogen

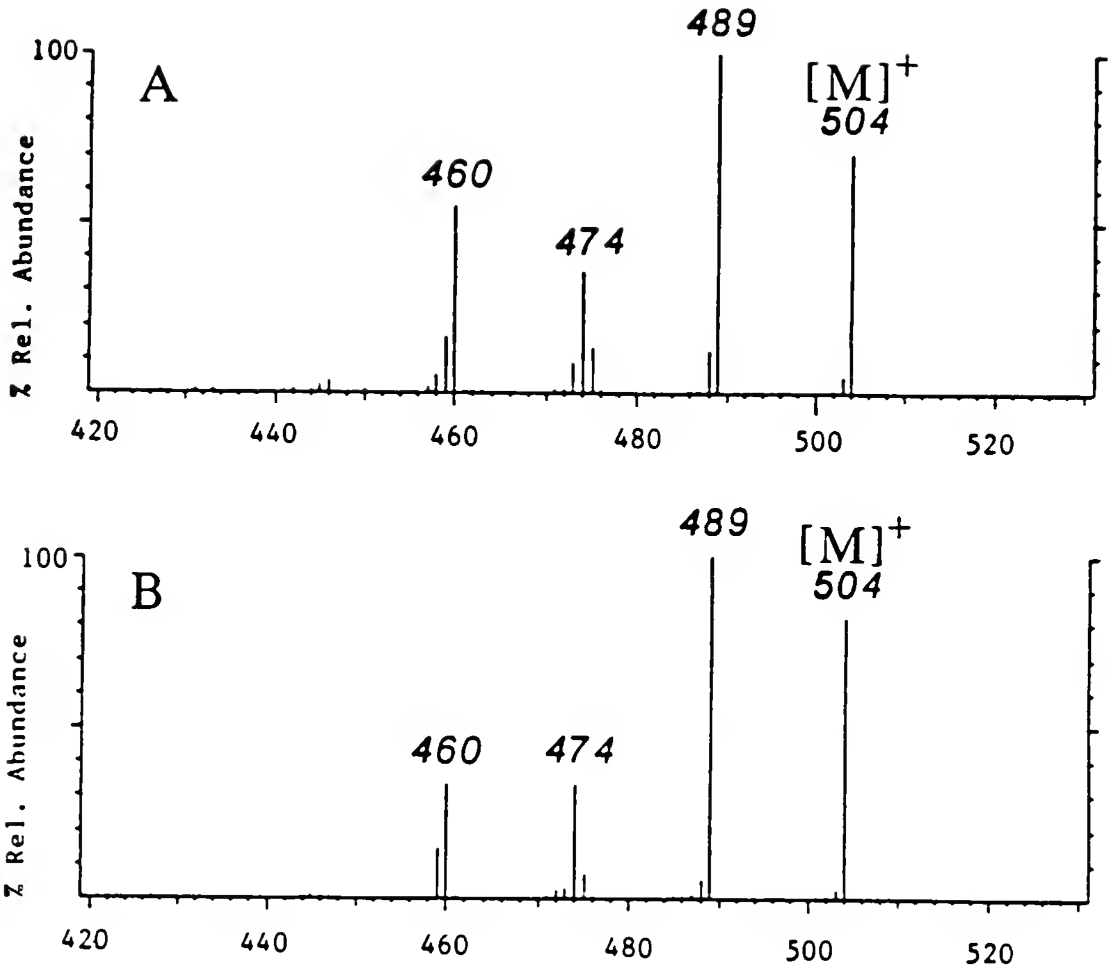
A
100
% Rel. Abundance
460
474
489
[M]$^+$
504
420
440
460
480
500
520
B
100
% Rel. Abundance
460
474
489
[M]$^+$
504
420
440
460
480
500
520

Figure 3-5.

Daughter ion mass spectra of m/z 513 [O=V(IV) C_{30} CAP porphyrin]:
A. from New Albany bitumen
B. from 300 °C pyrolysate of New Albany kerogen

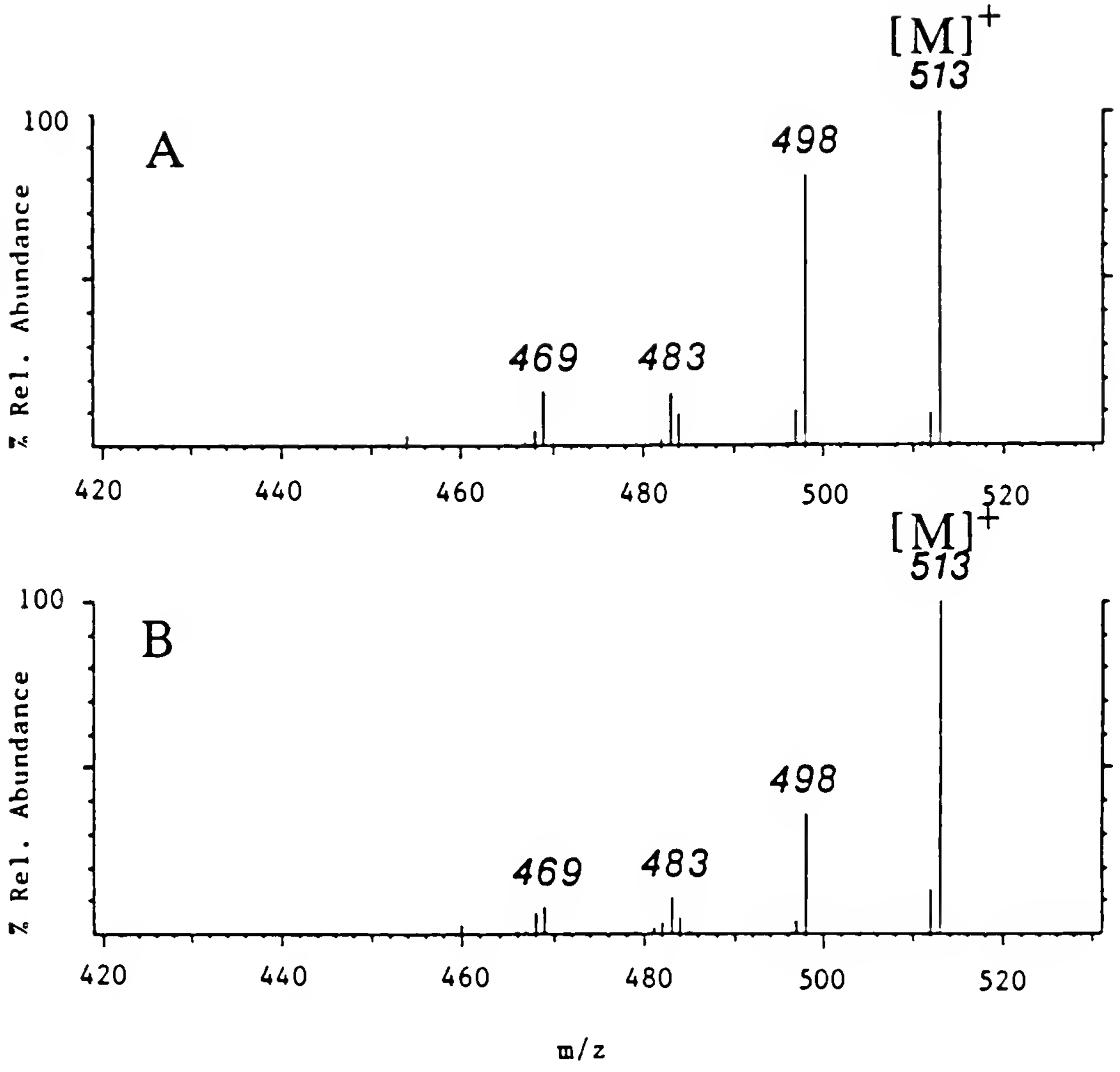
[M]+
513
100
A
498
469
483
% Rel. Abundance
420
440
460
480
500
520
[M]+
513
100
B
498
469
483
% Rel. Abundance
420
440
460
480
500
520
m/z

groups of the biological precursor would be modified, and the original alkyl substituents, including the ethyl group, would remain intact throughout the degradation pathway (Treibs, 1936). Thus, all of the geoporphyrins which were formed by such a pathway would be expected to bear at least one ethyl moiety because all of the abundant naturally-occurring chlorophylls contain an ethyl group. It is interesting to note that the low carbon number geoporphyrins from the New Albany shale, a sample of intermediate maturity (Van Berkel et al., in press b), resemble those of the immature Messel shale (Ocampo et al., 1987) in that they all bear at least one ethyl group. This also provides circumstantial evidence in favor of a Treibs' type decomposition pathway, because the porphyrins from the Messel shale were not generated by thermal cracking processes.

The studies on the Ni(II) and O=V(IV) geoporphyrins generated from the New Albany kerogen present no evidence that the compounds were produced from a thermal cracking process. If the low carbon number geoporphyrins were generated via the thermal cracking of alkyl substituents from higher carbon number alkyl geoporphyrins, it might be expected that there would be successive ß-like cleavage of the substituents until only methyl residues remained. Subsequently, the methyl groups might be cleaved off. Thus, a C_{28} etio porphyrin formed in this way would be expected to be 2,3,7,8,12,13,17,18-octamethyl-21H,23H-porphine (OMP) [R^1, R^2, R^3, R^4, R^5, R^6, R^7, R^8 = CH_3] shown as skeletal type (1) in Figure 2-1. Similarly, the C_{26} and C_{27} etio porphyrins would be expected to be devoid of ethyl substituents. There was no evidence for the generation of substantial amounts of very high carbon number (greater than C_{33}) porphyrins bearing extended (greater than C_2) alkyl substituents from the pyrolysis of the kerogen. Indeed the relative abundances of these compounds were slightly lower in the pyrolysate than in the bitumen (Figure 3-1). This implies that the very high carbon number geoporphyrins are not produced by thermal cracking of porphyrins linked to the kerogen via long alkyl chains (Mackenzie et al., 1980).

Complete structure elucidation of the porphyrins from New Albany bitumen and pyrolysates will be necessary in order to unambiguously determine the mechanism of the liberation of porphyrins from the kerogen of the New Albany shale.

Conclusions

Analyses of the daughter ion mass spectra of the molecular ions of Ni(II) and O=V(IV) porphyrins from the New Albany shale bitumen and the 300 °C kerogen pyrolysate yielded structural information on the individual carbon number geoporphyrins of the intact mixtures. The following conclusions were drawn from a combination of the EI/MS/MS data, and previous EI/MS studies (Van Berkel et al., in press b and c):

(a) The corresponding Ni(II) and O=V(IV) geoporphyrins from the New Albany shale bitumen are similar, and therefore probably have a common origin and geological history.

(b) All the Ni(II) and O=V(IV) porphyrins, including the low carbon number components (less than C_{30}), contain at least one ethyl group. This indicates that these compounds were probably derived from the modification of the functional groups of their chlorophyll precursors as opposed to being generated by thermal cracking of higher carbon number porphyrins.

(c) The daughter ion mass spectra of the molecular ions of the Ni(II) and O=V(IV) porphyrins from the 300 °C kerogen pyrolysate resemble those of the corresponding porphyrins from the New Albany shale bitumen. Each porphyrin contains at least one ethyl group. Thus, the porphyrins from the bitumen and the porphyrins from the kerogen pyrolysate appear to have a similar origin and history.

(d) There is no evidence that the porphyrins were released from the kerogen by carbon-carbon bond scission at 300 °C. Thus, the generation of the porphyrins from the kerogen appears to occur by an enhanced solubilization and/or desorption mechanism.

Clearly, pyrolysis studies on kerogens from other geological samples are needed to determine whether porphyrins are liberated from other kerogens by a similar mechanism.

CHAPTER 4

TANDEM MASS SPECTROMETRIC ANALYSES OF GEOPORPHYRINS FROM THE BITUMEN OF DEMINERALIZED SHALE

Introduction

The determination of the nature of the geoporphyrins in organic matter which is associated with the inorganic mineral matrix of the shale is another geochemical problem which has been studied by EI/MS/MS. This organic matter is isolated by solvent extraction from shale which has already been solvent extracted and demineralized using HCl and HF. In this chapter, bitumen-II describes the organic extract from the demineralized shale, and the organic extract from the intact shale is called bitumen-I.

The bitumen-II of the Henryville bed of the New Albany shale is of particular interest because the Ni(II) and O=V(IV) geoporphyrins from both the bitumen-I and a pyrolysate of the kerogen (obtained at 300 °C) of this shale have been studied in detail (Chapter 3; Van Berkel et al., in press b and c). By examining the geoporphyrins of the bitumen-II of the New Albany shale, it will be possible to compare the porphyrins from three different environments within the same shale. In this chapter, the daughter ion mass spectra of the molecular ions of both the Ni(II) and O=V(IV) porphyrins from the bitumen-II are reported. The data are compared with the daughter ion mass spectra of the molecular ions of the bitumen-I and the 300 °C kerogen pyrolysate, described in Chapter 3.

Experimental

Sample

A sample from the Henryville bed of the New Albany shale (Mississippian-Devonian, Clark County, Indiana) was used in this study. A detailed description of the sample type and location is presented elsewhere (Van Berkel et al., in press b). The vitrinite reflectance value for the Henryville bed (R_o = 0.5-0.6%) is just above the oil generation window for the source rocks in the region (Barrows and Cluff, 1984).

Sample Preparation and Porphyrin Isolation

The bitumen-I and bitumen-II extraction, kerogen isolation, and kerogen pyrolysis procedures have all been described previously and are summarized in Chapter 2 (Van Berkel and Filby, 1987; Van Berkel et al., in press c). The methods for the isolation and purification of the Ni(II) and O=V(IV) porphyrins from the New Albany bitumen-II are identical to those employed to isolate the geoporphyrins in the bitumen-I and from the kerogen pyrolysates (Van Berkel et al., in press b and c). The procedures are outlined in Chapter 2.

Tandem Mass Spectrometry

For the bitumen-II, all MS/MS spectra were obtained in the positive ion mode on a Finnigan MAT TSQ45 triple quadrupole mass spectrometer equipped with an INCOS data system. About 1 μg of porphyrin, dissolved in CH_2Cl_2, was deposited directly on the sample loop of a direct exposure probe. After the solvent evaporated, the probe was inserted into the mass spectrometer where it was rapidly heated to 600 °C at 10 °C sec^{-1}. The samples were ionized with an electron energy of 70 eV and an emission current of 0.3 mA. Daughter ion mass spectra were obtained using argon (1.3 mtorr) for collisionally activated dissociation in the second quadrupole with a collision energy of 20 eV. The experimental conditions for the analyses of the geoporphyrins from the bitumen-I and the 300 °C kerogen pyrolysate were described in Chapter 3.

The Ni(II) and O=V(IV) Geoporphyrins from New Albany Bitumen-II

The carbon number distributions of the total Ni(II) and O=V(IV) etio and CAP porphyrins from bitumen-II are compared with the corresponding distributions of the bitumen-I and the 300 °C pyrolysate in Figure 4-1. Both the Ni(II) porphyrin distributions of the bitumen-II, bitumen-I, and the pyrolysate are essentially the same. The O=V(IV) geoporphyrin distribution for the bitumen-II is different from those for the bitumen-I and the pyrolysate, which are similar. There are virtually no O=V(IV) etio porphyrins in the bitumen-II. The implication of these data is that the incorporation of O=V(IV) into the mineral associated

Figure 4-1.

Distributions of the CAP porphyrins (shaded blocks) and the etioporphyrins (open blocks) from the New Albany shale:

A. Ni(II) porphyrins from bitumen-II
B. O=V(IV) porphyrins from bitumen-II
C. Ni(II) porphyrins from bitumen-I
D. O=V(IV) porphyrins from bitumen-I
E. Ni(II) porphyrins from the 300 °C pyrolysate
F. O=V(IV) porphyrins from the 300 °C pyrolysate

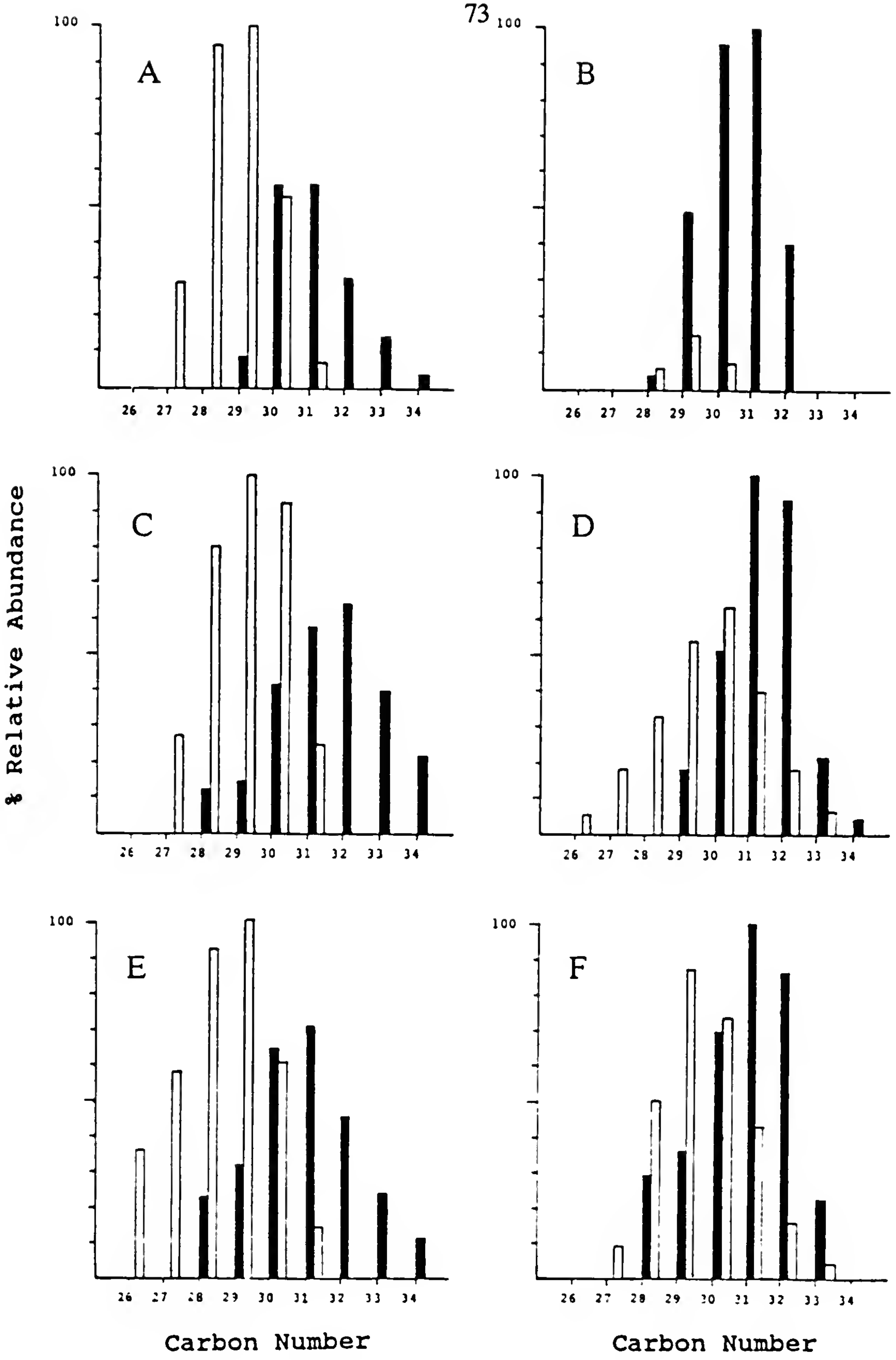
A
B
C
D
E
F
100
% Relative Abundance
26
27
28
29
30
31
32
33
34
Carbon Number
Carbon Number

bitumen is a more selective process than is the incorporation of the O=V(IV) porphyrins into either the bitumen-I or the kerogen. It is unclear why this is the case. It may be worthwhile to carry out studies on the partitioning of O=V(IV) porphyrins between the surfaces of minerals and hydrocarbons to determine whether some of the porphyrin skeletal types are preferentially bound on the mineral surface. If this is so, the molecules may have become associated with the bitumen during the demineralization procedure.

The O=V(IV) porphyrin mixtures from the pyrolysate and the bitumen were sufficiently clean to be used without further purification. It was necessary to separate the total Ni(II) porphyrin mixtures into fractions by thin layer chromatography (TLC) for two reasons:

(a) The total Ni(II) geoporphyrin mixtures from both the pyrolysate and the bitumen contained nonporphyrinic impurities which interfered with the EI/MS/MS analyses. The carbon number (C#) distributions for the etio and CAP porphyrins for each of the four TLC fractions: A (most polar), B, C, and D (least polar) are shown in Table 4-1.

(b) The TLC allows the separation of many of the Ni(II) CAP and etio porphyrins of the same carbon number. This is necessary for the study of the EI/MS/MS daughter ion mass spectra of ^{58}Ni(II) etio porphyrin molecular ions. Otherwise, the coincident ^{60}Ni(II) CAP makes interpretation of the daughter ion mass spectral data very difficult. Even after careful TLC separation, the higher

Table 4-1: Carbon number ranges for Ni(II) geoporphyrin skeletal types in TLC fractions A,B,C, and D.

Fraction	CAP C# Range	CAP Max	Etio C# Range	Etio Max
A	29-32	30	27-30*	28
B	29-32	31	27-30*	29
C	30-33	32	28-31*	30
D	30-38	33	30-35*	31

* Most abundant skeletal type.

carbon number (greater than C_{31}) etio and CAP porphyrins are present in the same fraction, D.

The daughter ion mass spectra of the Ni(II) and O=V(IV) geoporphyrin molecular ions from the New Albany bitumen-II are summarized in Table 4-2. In both Tables 4-3 and 4-4, the abundances of the daughter ions of the molecular ions of the Ni(II) and O=V(IV) porphyrins respectively are normalized relative to $[M-15]^+ = 100\%$ to clarify the correlation between the geoporphyrins of the bitumen-II, bitumen-I, and the 300 °C kerogen pyrolysate.

Table 4-2: EI/MS/MS Daughter spectra of the molecular ions of Ni(II) and O=V(IV) porphyrins from New Albany bitumen-II.[a]

Compound	Molecular Ion m/z (% abund.)	Daughter Ions m/z(% abundance)[b]
Ni C_{27} Etio	464 (100)	463(60) 449(59) 448(18) 447(11)
Ni C_{28} Etio	478 (43)	477(12) 463(100) 462(12) 448(13)
Ni C_{29} CAP	490 (58)	475(96) 460(100) 446(10)
O=V C_{29} CAP	499 (51)	498(10) 484(75) 483(13) 469(100) 454(37)
Ni C_{29} Etio	492 (30)	477(100)
Ni C_{30} CAP	504 (64)	489(73) 474(100) 473(10) 460(20)
O=V C_{30} CAP	513 (53)	498(100) 483(60) 469(27) 468(16)
Ni C_{30} Etio	506 (48)	491(100) 476(24)
Ni C_{31} CAP	518 (68)	503(100) 488(37) 474(51) 473(18)
O=V C_{31} CAP	527 (56)	526(12) 512(100) 498(14) 497(53) 483(63) 482(27)
Ni C_{31} Etio	520 (83)	505(100) 491(38) 490(31) 477(28) 462(23)
Ni C_{32} CAP M	532 (80)	517(100) 503(22) 502(21) 518(40) 474(11)
Ni C_{32} CAP L	532 (85)	517(100) 503(94) 502 (14) 489(30) 488(65) 475(52) 474(32) 473(30) 456(18) 459(25)
O=V C_{32} CAP	541 (73)	526(100) 511(28) 497(43) 496(15)

[a] See experimental for details of EI/MS/MS conditions.

[b] Ions less than 5% omitted.

L= less polar; M= more polar

Table 4-3: Data from EI/MS/MS daughter ion mass spectra of the molecular ions of Ni(II) porphyrins from New Albany bitumen-II, bitumen-I, and 300 °C kerogen pyrolysate normalized to $[M\text{-}15]^+$ = 100%.[a]

Sample[b]	Source[b]	M.W.	% Abundance (relative to M-15 = 100%)				
			M-1	M-29	M-30	M-44	Others
C_{27} E	BIT-II	464	102	-	-	-	M-16 (18)
C_{27} E	BIT-I	464	125	-	-	-	M-2 (25) M-16 (22)
C_{27} E	PY	464	120	-	6	-	M-2 (12) M-16 (30)
C_{28} E	BIT-II	478	12	-	13	-	M-16 (12)
C_{28} E	BIT-I	478	27	-	-	-	
C_{28} E	PY	478	12	-	8	-	
C_{29} C	BIT-II	490	-	-	104	10	
C_{29} C	BIT-I	490	14	6	59	-	M-16 (12)
C_{29} C	PY	490	8	8	41	6	
C_{29} E	BIT-II	492	-	-	6	-	
C_{29} E	BIT-I	492	-	-	6	-	
C_{29} E	PY	492	-	-	10	-	
C_{30} C	BIT-II	504	5	5	136	27	
C_{30} C	BIT-I	504	5	12	35	50	M-16 (11) M-45 (17)
C_{30} C	PY L	504	3	6	35	38	M-45 (15)
C_{30} C	PY M	504	8	-	80	16	
C_{30} E	BIT-II	506	-	4	24	3	
C_{30} E	BIT-I	506	3	10	18	3	
C_{30} E	PY	506	7	13	16	13	M-16 (10)
C_{31} C	BIT-II	518	-	6	37	51	M-45 (18)
C_{31} C	BIT-I	518	5	19	21	30	M-16 (20) M-45 (10)
C_{31} C	PY	518	11	7	22	34	M-45 (11)
C_{31} E	BIT-II	520	-	38	31	-	M-43 (28)
C_{31} E	BIT-I	520	10	-	-	-	M-16 (18)
C_{32} C	BIT-II M	532	2	22	21	40	M-58 (11)
C_{32} C	BIT-I	532	12	24	16	40	M-59 (12)
C_{32} C	PY	532	6	21	18	38	
C_{32} C	BIT-II L	532	-	94	12	65	M-43 (30) M-57 (52) M-58 (32) M-59 (30) M-73 (25)

---

[a] The daughter spectra are normalized so that the intensity of the $[M\text{-}15]^+$ fragment ion is 100%.

[b] L= less polar; M= more polar; E= Etioporphyrin; C= CAP; BIT= Bitumen; PY= pyrolysate.

Table 4-4: Data from EI/MS/MS Daughter ion mass spectra of the molecular ions of O=V(IV) porphyrins from New Albany bitumen-II, bitumen-I, and 300 °C kerogen pyrolysate normalized to $[M\text{-}15]^+$ = 100%.[a]

Sample[b]	Source[b]	M.W.	% Abundance (relative to M-15 = 100%)				
			M-1	M-29	M-30	M-44	Others
C_{29} C	BIT-II	499	13	-	133	49	M-1 (13)
C_{30} C	BIT-II	513	-	5	60	27	M-16 (16) M-45 (16)
C_{30} C	BIT-I	513	11	12	19	20	M-16 (12)
C_{30} C	PY	513	36	13	33	25	M-45 (19)
C_{31} C	BIT-II	527	12	14	53	63	M-45 (27)
C_{31} C	BIT-I	527	20	8	20	60	
C_{31} C	PY	527	16	15	12	30	M-16 (12)
C_{32} C	BIT-II	541	-	-	28	43	M-45 (15)
C_{32} C	BIT-I	541	13	13	20	39	
C_{32} C	PY	541	7	42	26	150	M-59 (60)

[a] The daughter spectra are normalized so that the intensity of the $[M\text{-}15]^+$ fragment ion is 100%.

[b] C= CAP; BIT= Bitumen; PY= pyrolysate.

EI/MS/MS Analyses of the Ni(II) Geoporphyrins from the Bitumen-II

The daughter ion mass spectra of the Ni(II) geoporphyrin molecular ions from the bitumen-II are fairly simple (Tables 4-2 and 4-3). The most commonly occurring daughter ions are:

(a) $[M\text{-}15]^+$ daughter ion. This ion usually corresponds to ß-cleavage of an ethyl group, unless it is accompanied by a large $[M\text{-}1]^+$ daughter ion. In that case it is probably the product of α-cleavage of a methyl group on a porphyrin which is devoid of higher alkyl substituents (Van Berkel et al., 1989). The $[M\text{-}15]^+$ ion is the most abundant daughter ion in most of the daughter ion mass spectra (Table 4-3).

(b) $[M\text{-}1]^+$ daughter ion. This ion is abundant in the daughter ion mass spectrum of the molecular ion of the C_{27} etio porphyrins only. Based on the work of Van Berkel et al. (1989), it seems likely that the major contributor of this molecular ion is a porphyrin with no ethyl side chains. If this is the case, the major component to this molecular ion must be 2,3,7,8,12,13,17-heptamethylporphine. Work is in progress to determine whether this deduction is valid. The data do not eliminate the possibility that there are other isomers present which make a minor contribution to the intensity of the molecular ion.

(c) $[M\text{-}29]^+$ daughter ion. This daughter ion is usually of low abundance. It corresponds to ß-cleavage of a propyl group. The low abundance of this daughter ion indicates that there are very few etio or CAP porphyrins present which bear a propyl substituent. Previous EI/MS/MS studies on etioporphyrin-I and octaethylporphyrin revealed that the ethyl groups do not undergo α-cleavage to a significant extent (Johnson et al., 1986).

(d) [M-30]$^+$ daughter ion. This ion may be attributed to the loss of two methyl groups, corresponding to the ß-cleavage of two ethyl moieties. It was usually a minor daughter ion, but it was the most abundant daughter ion of the molecular ions of both C_{29} and C_{30} CAP geoporphyrins. The C_{30} CAP geoporphyrin of the bitumen-II yields a very different daughter ion mass spectrum from those of the bitumen-I or the pyrolysate.

(e) [M-44]$^+$ daughter ion. Although the origin of the [M-44]$^+$ daughter ion is not known, the ion is a characteristic daughter ion of CAP porphyrins. It is no more than a very minor daughter ion for etio porphyrins. At present it is uncertain whether this ion is a diagnostic daughter ion of all the CAP porphyrins or is indicative of specific skeletal types. Certainly, it occurs in the daughter ion mass spectra of the molecular ions of DPEP porphyrin. EI/MS/MS studies on the molecular ion of the $C_3$1 pentamethyl-diethyl DPEP porphyrin isolated from Gilsonite (Eocene, Uinta Basin, Utah, USA) revealed that the [M-44]$^+$ ion was the only abundant ion generated by loss of fragments greater than 30 u (Britton, unpublished). Van Berkel et al. (1989) have made similar observations on studying the porphyrinic mineral Abelsonite which is the Ni(II) complex of 2(a).

With the exception of the [M-44]$^+$ ion discussed above, there are very few daughter ions resulting from neutral losses of more than 30 u. In fact, these ions are only significant for the less polar C_{32} CAP (Table 4-3). This indicates that porphyrins bearing extended alkyl side chains (greater than C_2) were either absent or were minor contributors to the Ni(II) geoporphyrin mixtures from bitumen-II.

Isomeric Ni(II) CAP Porphyrins

Some of the same carbon number etio and CAP porphyrins occur in more than one of the TLC fractions. This can be accounted for in two ways:

(a) The same compound is distributed between two fractions because of incomplete resolution of the bands. In this case the daughter ion mass spectra of the molecular ions should be identical.

(b) There are isomeric porphyrins present which are separated on the TLC. These may have different daughter ion mass spectra from each other.

In the case of the C_{30} and C_{32} CAP porphyrins, there is clear evidence for the presence of isomers as the daughter ion mass spectra of the molecular ions are sharply different (Tables 4-2 and 4-3; Figure 4-2). In the daughter ion mass spectrum of the more polar C_{32} CAP, the $[M-44]^+$ ion is the only daughter ion produced by losses of fragments greater than 30 u. The less polar isomer shows a much more abundant $[M-29]^+$ and $[M-57]^+$ daughter ions than the more polar isomer. It is possible that the more polar isomer is a true DPEP, and the other isomer is a different skeletal type of CAP, but this is speculation at present. The C_{30} CAP porphyrin in the bitumen-II is more polar than the porphyrin studied in bitumen-I; however, a similar isomer was detected in the kerogen pyrolysate (Table 4-3).

Figure 4-2.

EI/MS/MS daughter ion mass spectra of m/z 532 [Ni(II) C_{32} CAP porphyrin]:
A. from TLC fraction C (more polar)
B. from TLC fraction D (less polar)

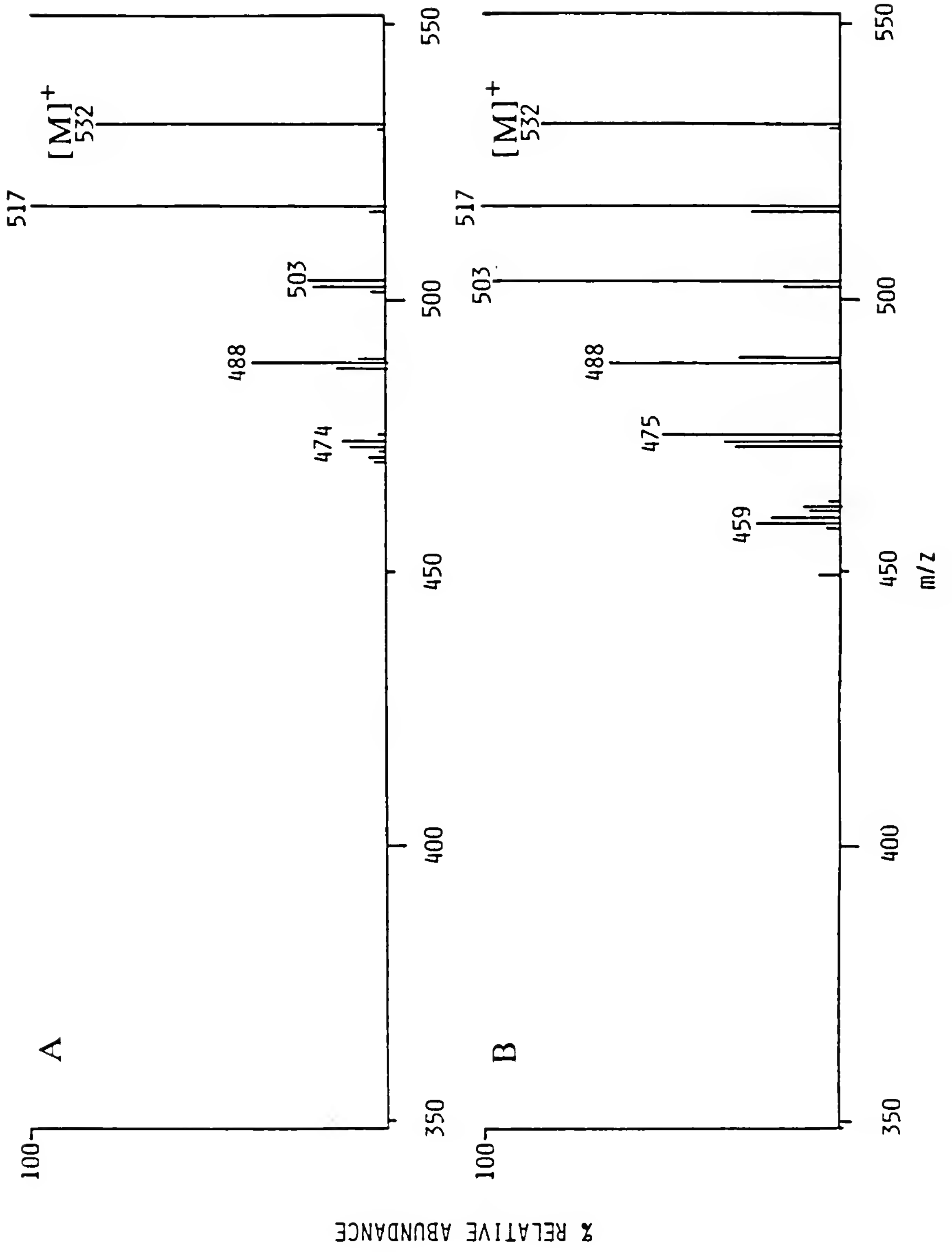
A
100
517
[M]+
532
503
488
474
350
400
450
500
550
B
100
517
[M]+
532
503
488
475
459
350
400
450
500
550
m/z
% RELATIVE ABUNDANCE

Comparison of the EI/MS/MS Daughter Ion Mass Spectra of Ni(II) Geporphyrins from Bitumen-II, Bitumen-I, and the 300 °C Kerogen Pyrolysate

The daughter ion mass spectra of the molecular ions of the corresponding porphyrins of the bitumen-I, bitumen-II, and the 300 °C kerogen pyrolysate are nearly all very similar (Table 4-3; Figures 4-3 and 4-4). This similarity is a good indication that the Ni(II) porphyrins from the New Albany bitumen-II, bitumen-I, and the 300 °C kerogen pyrolysate are largely generated via a similar pathway.

EI/MS/MS Analyses of the O=V(IV) Geoporphyrins from the Bitumen-II

The daughter ion mass spectra of the molecular ions of O=V(IV) geoporphyrins from the bitumen-II are summarized in Tables 4-2 and 4-4. The $[M-15]^+$ ions are dominant along with the $[M-44]^+$ ions (Tables 4-2 and 4-4). The $[M-29]^+$ daughter ions were not abundant and there were no significant $[M-1]^+$ ions (Table 4-4). The $[M-30]^+$ ion was abundant in all the daughter ion mass spectra, particularly in the daughter ion mass spectra of C_{29} and C_{30} CAP porphyrins. Aside from the $[M-44]^+$ ion, there were very few daughter ions resulting from losses of fragments of masses greater than 30 u. This indicates that porphyrins bearing extended alkyl side chains were either absent or were minor components of the O=V(IV) geoporphyrin mixture from the New Albany bitumen-II. With the exception of the C_{30} CAP, the daughter ion mass spectra of the molecular ions of the O=V(IV) geoporphyrins from the New Albany bitumen-II, bitumen-I, and the 300 °C kerogen pyrolysate are similar (Table 4-4; Figure 4-5). It is also likely that

Figure 4-3.

EI/MS/MS daughter ion mass spectra of m/z 464 [Ni(II) C_{27} etioporphyrin]:
A. from bitumen-II
B. from bitumen-I
C. from the 300 °C kerogen pyrolysate

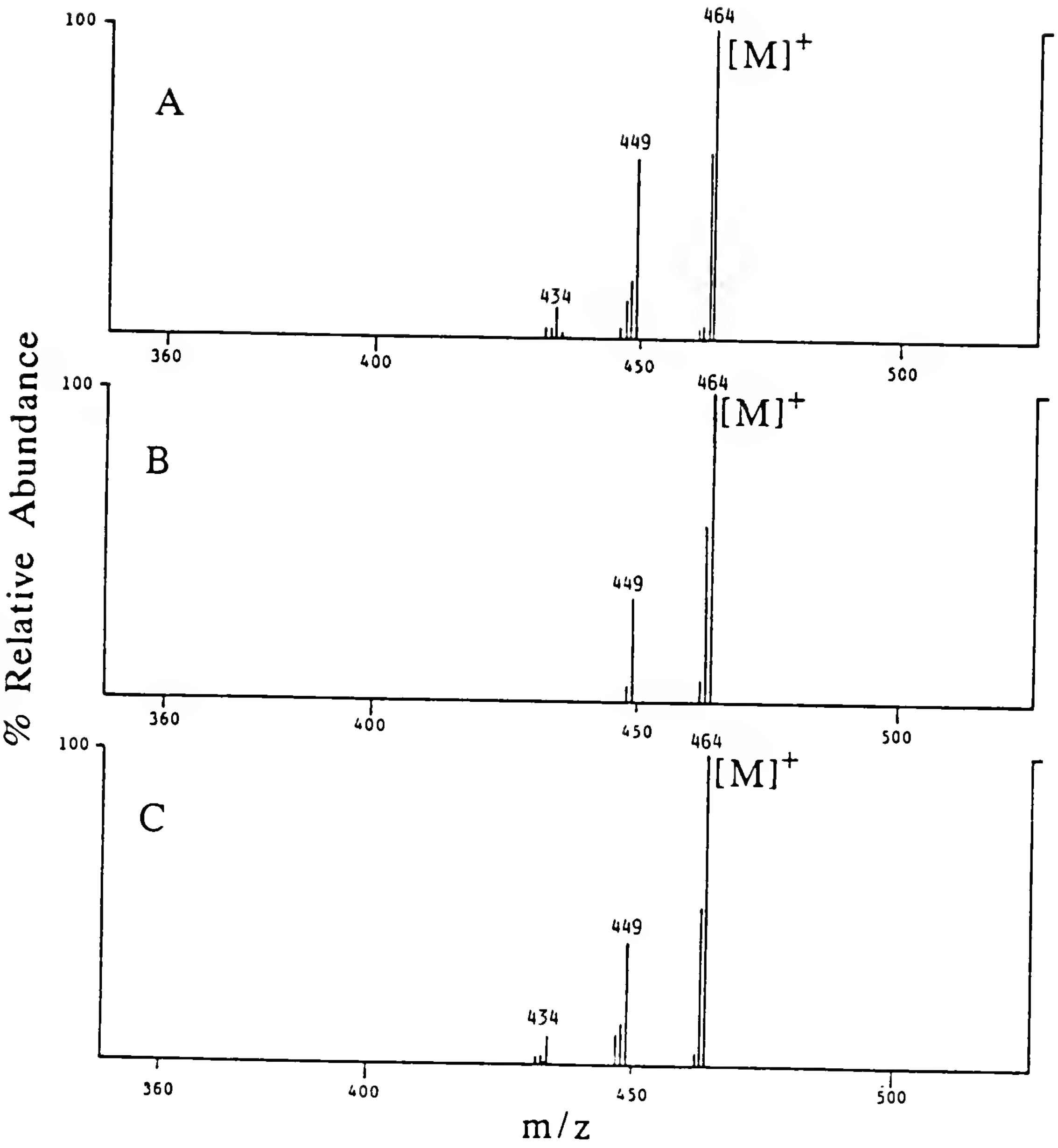
100
464
[M]$^+$
A
449
434
360
400
450
500
100
464
[M]$^+$
B
449
360
400
450
500
100
464
[M]$^+$
C
449
434
360
400
450
500
% Relative Abundance
m/z

Figure 4-4.

EI/MS/MS daughter ion mass spectra of m/z 518 [Ni(II) C_{31} CAP porphyrin]
A. from bitumen-II
B. from bitumen-I
C. from the 300 °C kerogen pyrolysate

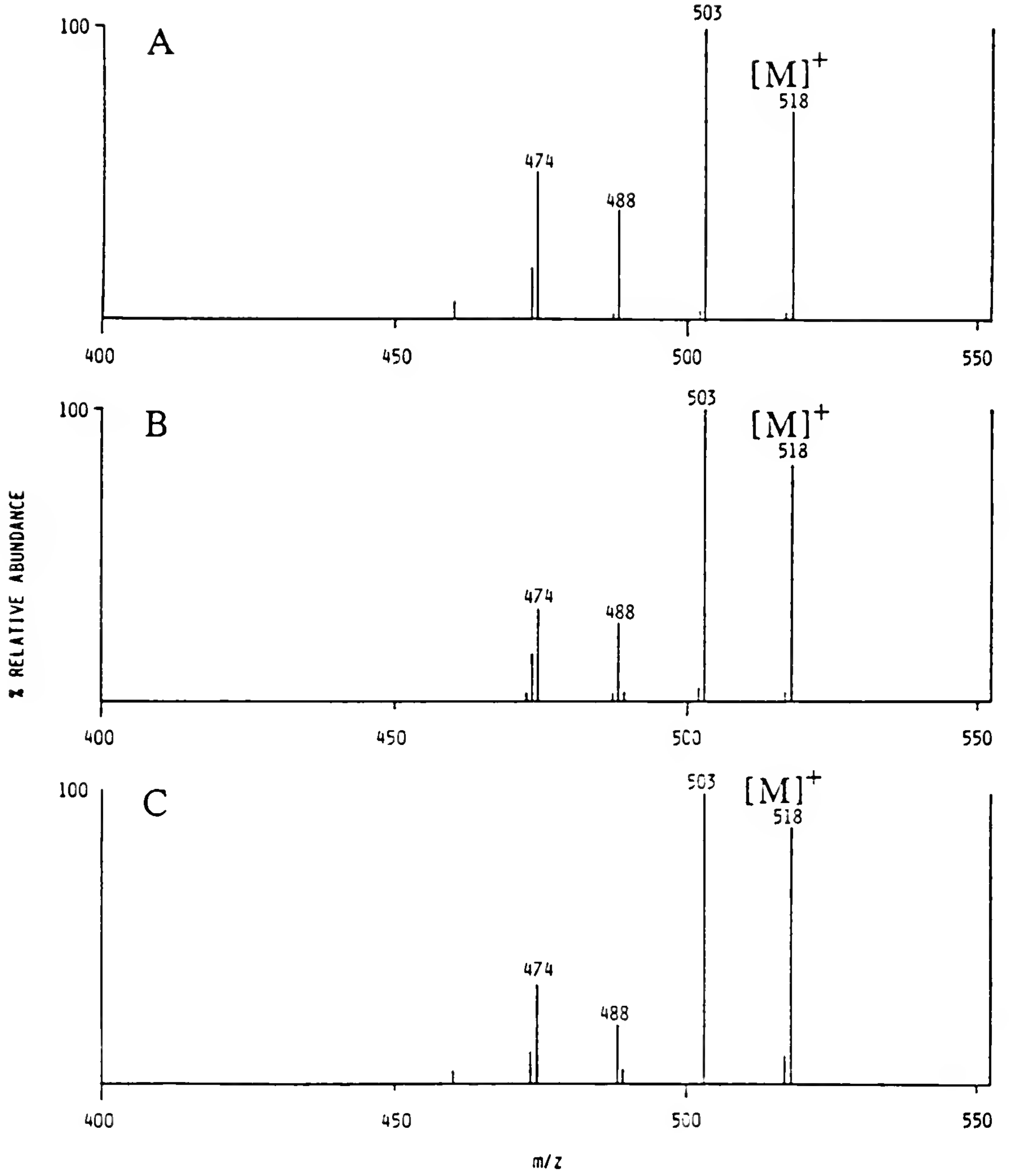
A
B
C
100
503
[M]$^+$
518
474
488
400
450
500
550
% RELATIVE ABUNDANCE
m/z

Figure 4-5.

EI/MS/MS daughter ion mass spectra of m/z 527 [O=V(IV) C_{31} CAP porphyri
A. from bitumen-II
B. from bitumen-I
C. from the 300 °C kerogen pyrolysate

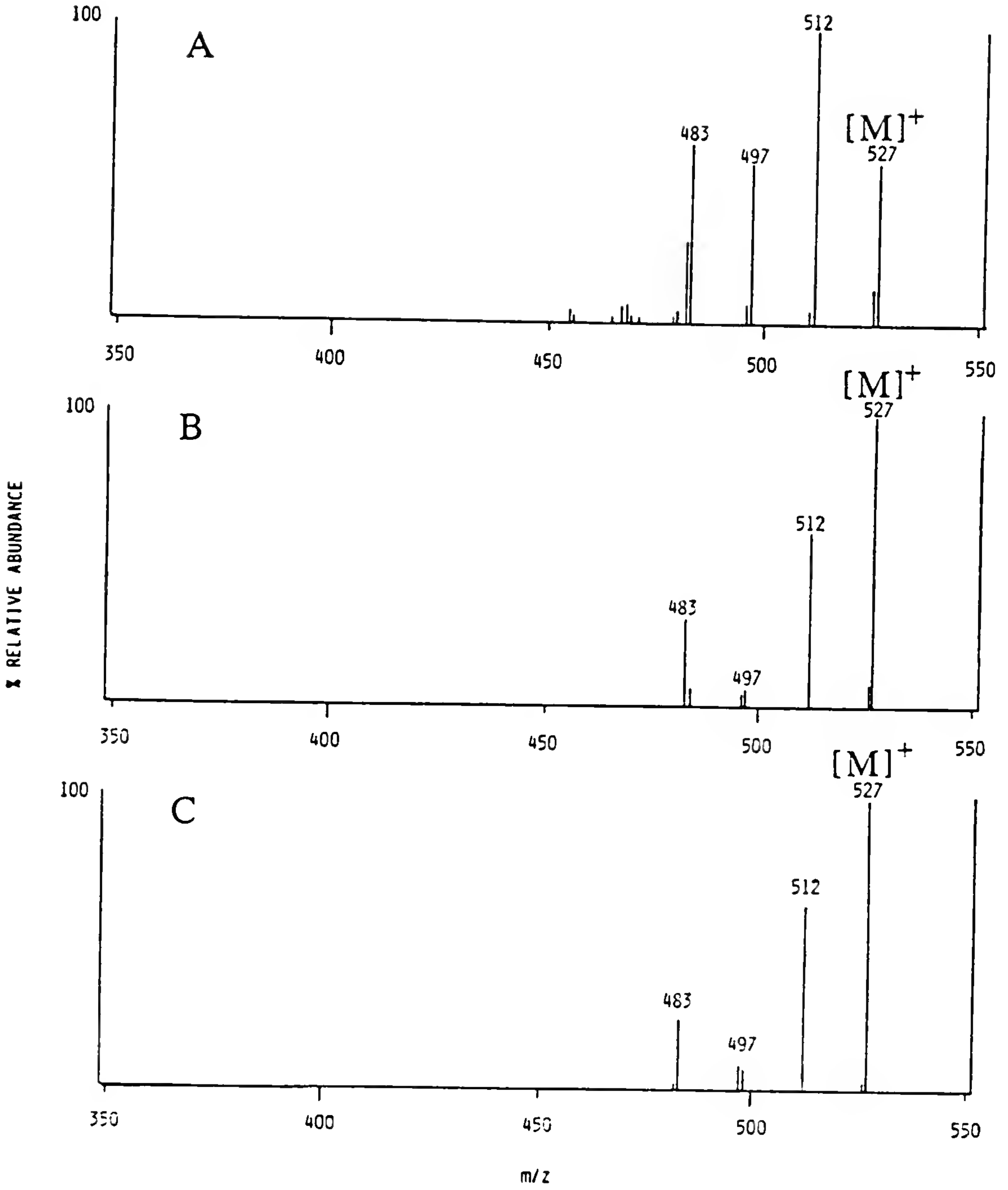
100
A
512
483
497
[M]+
527
350
400
450
500
550
100
B
[M]+
527
512
483
497
350
400
450
500
550
100
C
[M]+
527
512
483
497
350
400
450
500
550
% RELATIVE ABUNDANCE
m/z

the O=V(IV) porphyrins of New Albany bitumen-II, bitumen-I, and the kerogen pyrolysate have been formed via similar pathways.

Comparison of the Ni(II) and O=V(IV) Geoporphyrins from the Bitumen-II

The daughter ion mass spectra of the molecular ions of the Ni(II) and O=V(IV) geoporphyrins of the same carbon number of New Albany bitumen-II closely resemble each other (Tables 4-3 and 4-4). The daughter ion mass spectra of the molecular ions of Ni(II) and O=V(IV) C_{30} CAP porphyrins can be used to illustrate this point (Figure 4-6). These data indicate that the Ni(II) and O=V(IV) geoporphyrins of the New Albany bitumen-II probably have a common origin and geological history.

Conclusions

Analyses of the daughter ion mass spectra of the molecular ions of Ni(II) and O=V(IV) porphyrins from the New Albany shale bitumen-II yielded structural information on the individual carbon number geoporphyrins of the intact mixtures. The following conclusions were drawn from the EI/MS/MS data, and by comparison with previous EI/MS and EI/MS/MS studies on the bitumen-I and kerogen pyrolysates (Chapter 3; Van Berkel et al., in press b and c):

(a) The carbon number distribution of the O=V(IV) porphyrins of the bitumen-II is comprised almost exclusively of CAP porphyrins. This distribution is markedly different from those of the bitumen-I and the kerogen pyrolysates, both of which contain substantial quantities of the etio porphyrins. Thus, it appears

Figure 4-6.

EI/MS/MS daughter ion mass spectra of parent ions from bitumen-II:
A. parent ion is m/z 504 [Ni(II) C_{30} CAP porphyrin]
B. parent ion is m/z 513 [O=V(IV) C_{30} CAP porphyrin

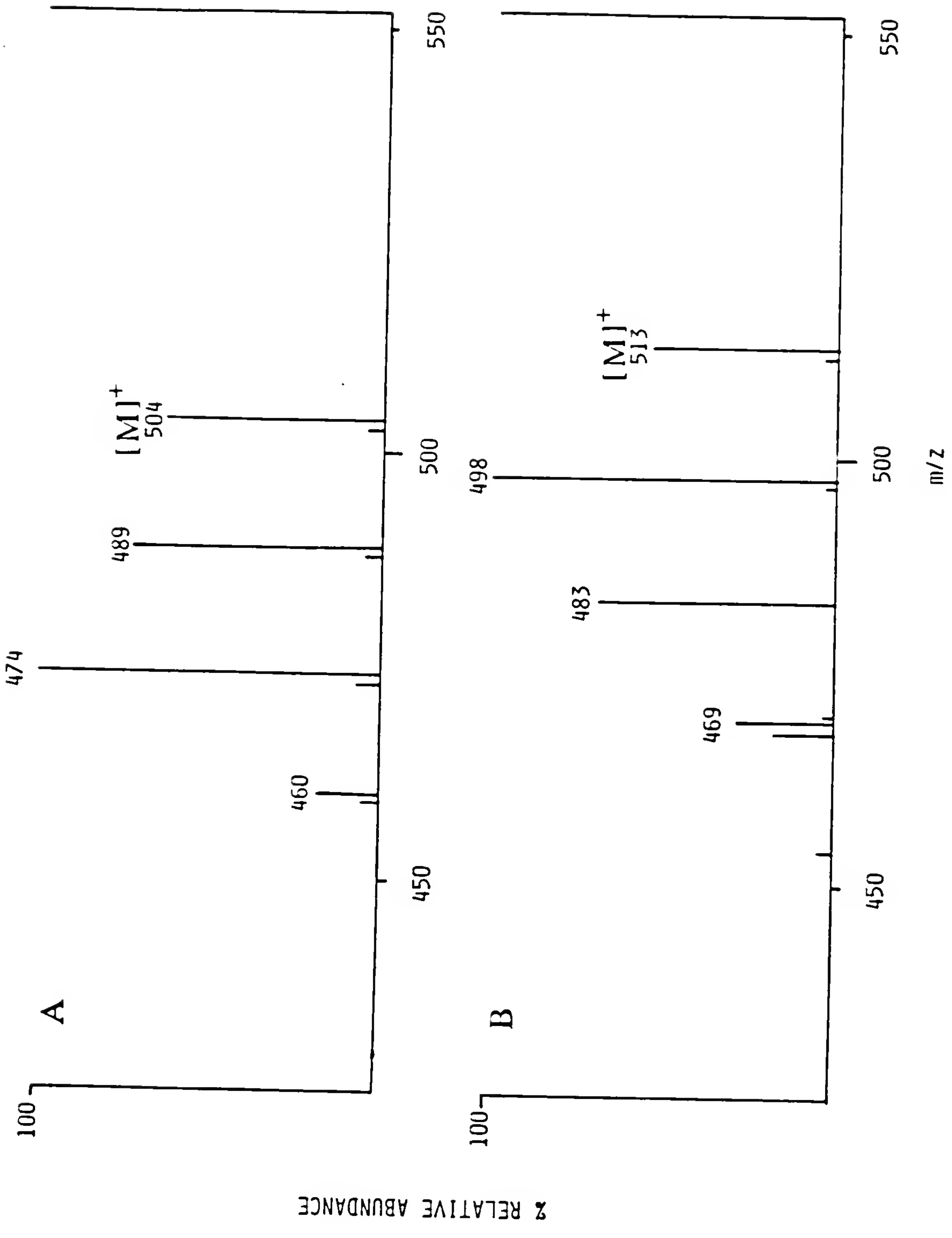
A
100
460
474
489
[M]+
504
450
500
550
B
100
469
483
498
[M]+
513
450
500
550
m/z
% RELATIVE ABUNDANCE

that the mineral associated bitumen preferentially incorporates O=V(IV) CAP porphyrins rather than O=V(IV) etio porphyrins.

(b) The corresponding Ni(II) and O=V(IV) geoporphyrins from the New Albany shale bitumen-II are similar, and therefore probably have a common origin and geological history.

(c) The daughter ion mass spectra of the parent molecular ions of the Ni(II) and O=V(IV) porphyrins from the bitumen-II resemble those of the corresponding porphyrins from the New Albany shale bitumen-I and the 300 °C kerogen pyrolysate. Thus, the Ni(II) and O=V(IV) porphyrins from the bitumen-I, bitumen-II, and the kerogen pyrolysate appear to have a similar origin and geological history.

(d) There is no evidence that the minor porphyrin skeletal types (Figure 2-1, numbers 7-10) are preferentially associated with the bitumen-II.

Clearly, studies on the carbon number distributions of the bitumen-II from other geological samples are needed to determine whether there is a similar selectivity of incorporation of O=V(IV) CAP porphyrins in the bitumen-II of other shales.

PART 2: NEW STRATEGIES FOR AND FUNDAMENTAL STUDIES OF PORPHYRIN STRUCTURE ELUCIDATION BY MS AND MS/MS

CHAPTER 5

DOUBLY CHARGED PORPHYRIN ION TANDEM MASS SPECTROMETRY: IMPLICATIONS FOR STRUCTURE ELUCIDATION

Introduction

Electron ionization (EI) strips neutral molecules of one or more electrons, leaving them singly or multiply charged. Excited molecular ions may then fragment into singly or multiply charged fragment ions. When doubly charged ions do form under EI conditions, they are rarely found in abundances exceeding 1% relative to that of the base peak (McLafferty and Bursey, 1967). There are several characteristics of molecules which enhance their ability to form doubly charged ions (Vouros and Biemann, 1969). One is the ability to separate charge, as this increases the stability of doubly charged ions. The presence of double bonds also favors the formation of doubly charged ions, as π-electrons are in higher energy orbitals than σ-electrons, and are easier to remove, and also because conjugated systems favor charge separation. Similarly, molecules containing heteroatoms are also more likely to yield doubly charged ions because nonbonding electrons are easier to remove than bonding electrons. Porphyrins, which are large aromatic molecules, and contain nitrogens, yield relatively high intensities of doubly charged molecular and fragment ions (Jackson et al., 1965).

The primary purpose of this study is to investigate some of the fundamental aspects of doubly charged porphyrin ion formation and fragmentation. Doubly charged porphyrin ions may yield structural information that is unobtainable or less conveniently obtainable from singly charged porphyrin ions. Doubly charged ions in mass spectra are usually ignored, although in a few cases they have been found to offer unique structural information not obtainable from the singly charged ions, such as differentiation of isomers (Vouros and Biemann, 1969). Doubly charged ions often behave quite differently than corresponding singly charged ions for several reasons (Ast et al., 1988). First, corresponding doubly and singly charged ions usually differ in that one is an even and the other an odd-electron species. Second, fragmentations occurring in doubly charged ions are often driven by coulombic repulsions between the two like charges. Finally, removal of a second electron under EI conditions may lead to significant structural changes in the ion. Doubly charged ions can yield structural information from the fact that they carry two charges, and that the positions of these charges can often be determined (Ast et al., 1972a). In this chapter, doubly charged porphyrin ion MS and MS/MS are shown to be useful in terms of porphyrin structure elucidation: not in terms of determining the positions of the charges, but because doubly charged porphyrin ions fragment more efficiently than corresponding singly charged porphyrin ions.

Most early studies of doubly charged ion mass spectra were performed with double-focusing sector mass spectrometers in which doubly charged ions from the source were converted to singly charged ions by charge exchange in the field-free region preceding the first sector (Beynon et al., 1970; Ast et al., 1972b). Only ions having the unique energy-to-charge ratio of singly charged ions arising from charge exchange reactions were transmitted. Similar charge exchange techniques have also been developed for triple quadrupole mass spectrometers (Kenttämaa et al., 1983). One method involves setting the potential on Q3 and associated lenses more positive than the ion source. Only singly charged positive daughter ions formed via charge exchange reactions are transmitted. The other technique involves scanning Q3 at twice the rate that Q1 is scanned to detect singly charged (but not fragmented) daughter ions arising from charge exchange reactions. These types of experiments do avoid interferences from $[M/2]^{+\cdot}$ ions which coincide with the m/z of $[M]^{2+}$ (Jones et al., 1982). There are, however, some disadvantages to these techniques in terms of structure elucidation (Kenttämaa et al., 1983). First, the resultant spectra do not necessarily yield the distribution of doubly charged ions formed in the source because the extent of charge exchange as well as the extent of fragmentation of the resultant singly charged ions depends on the specific doubly charged ion involved. Second, kinetic energy is distributed among the daughter ions proportionally by mass, so the lower mass fragment ions may have the necessary energy-to-charge ratio to be detected when potential barriers are used.

Collisionally activated dissociation (CAD) of doubly charged ions which do not participate in charge exchange reactions could avoid the drawbacks of the MS techniques described above. Without charge exchange reactions, there is no need for an energy barrier, so all daughter ions can be detected. The distribution of doubly charged ions formed in the source should also be more accurately reflected by the resultant spectra without the discrimination which can arise from charge exchange. Most reports of doubly charged ion MS/MS indicate that when doubly charged ions dissociate upon collision with a neutral gas, most of the daughter ions are singly charged (Kenttämaa et al., 1983). One major driving force in CAD reactions of doubly charged parent ions is separation of charge, which is why the two charges from the parent ion usually end up on separate ions. Although most studies have involved positively charged ions, CAD of the $[M]^{2-}$ ion from the disodium salt of adenosine triphosphate $[MNa_2]$ resulted in two singly charged negative ions (Thomson et al., 1982). Collision of doubly charged parent ions with a metal surface also yielded daughter ions that were all singly charged, except for $[C_7H_6]^{2+}$, a particularly stable doubly charged daughter ion arising from dissociation of $[C_7H_8]^{2+}$ (Mabud et al., 1986). These studies have usually dealt with relatively small organic molecules which have limited ability to maintain two charges upon CAD. Probably the earliest studies in which doubly charged daughter ions were reported to arise from doubly charged parent ions involved the metastable decomposition of 2-hydroxyanthraquinone resulting in expulsion of neutral CO

(Beynon et al., 1959). Doubly charged daughter ions have been reported recently to arise from CAD of larger doubly charged parent ions such as small peptides (m.w. less than 1400 u) (Barber et al., 1988), and polycyclic aromatic hydrocarbons (PAHs) (Boyd et al., 1988; Sim et al., 1989). Certainly another driving force involved in CAD of doubly charged parent ions is the stability of even-electron ions, as opposed to odd-electron ions. In all of these cases, doubly charged parent ions can yield doubly charged daughter ions because these daughter ions are stabilized by charge separation within the same large ion, or by resonance maintained by an even number of electrons.

This chapter presents the first detailed study of doubly charged porphyrin ions by MS/MS. It is also the first report of CAD of doubly charged ions resulting almost exclusively in doubly charged daughter ions. The present study complements the existing literature by demonstrating the enhancement in structure elucidation which can be provided by MS/MS of doubly charged ions that do not undergo charge exchange.

Experimental

Mass spectral data were obtained with a Finnigan MAT TSQ45 triple quadrupole mass spectrometer with an INCOS data system. The solid porphyrin samples were dissolved in methylene chloride. Five μL of solution (containing 2 μg of porphyrin) were placed in glass vials. After the solvent was evaporated at 50 °C, the glass vials were placed into a solids probe. The solids probe was programmed to heat the sample vial from 90 °C to 500 °C at 120 °C/min. The Ni(II) deuteroporphyrin IX dimethyl ester (Ni(II) D-IX DME) was analyzed by both solids probe and by direct exposure probe (DEP). The DEP consists of a rhenium filament which is resistively heated. Two μL of the porphyrin solution were placed onto the filament, and the methylene chloride was allowed to evaporate. The DEP was then heated from ambient to 700 °C at 600 °C/min. Both types of sample introduction gave very similar results for this compound. The analyzer pressure was 2.5 X 10^{-7} torr. For EI, the filament current was 0.3 mA with an electron energy of 70 eV. For normal mass spectra, quadrupole 1 was scanned from m/z 150 to m/z 800 in 1.6 s, while quadrupoles 2 and 3 were operated in the RF-only mode, transmitting all masses. For daughter spectra, quadrupole 1 was programmed to pass only the parent ion selected. Quadrupole 2 (Q2), the collision cell, was operated in the RF-only mode, and contained 1.9 mtorr of N_2. The third quadrupole was scanned from m/z 30 to just above the m/z of the singly charged parent ion at 100 u per 0.1 s. The collision energy (Q2 offset) was set between 10 and 25 eV according to the specific experiment. The instrument was tuned by placing solid Cr(III) OEP Cl into an aluminum solids probe vial that had a cap with a small hole in it. By heating the solids probe to about 250 °C, the metalloporphyrin vaporized at a steady rate so that both singly and doubly charged ions could be monitored. Every effort was made to simultaneously enhance both the singly and doubly charged regions by adjusting the lens voltages.

The Ni(II) D-IX DME was synthesized according to standard methods (Buchler, 1975). All of the other metalloporphyrins are derivatives of 2,3,7,8,12,13,17,18-octaethyl-21H,23H-porphine (OEP). The free-base OEP, and Co(II), Cr(III), Cu(II), Fe(III), Mg(II), Mn(III), Ni(II), and Zn(II) OEP derivatives were obtained from the Aldrich Chemical Company. The Al(III), Ga(III), Hg(II), In(III), Sc(III), Sn(IV), Ti(IV), Tl(IV), and V(IV) OEP derivatives were all prepared according to standard methods (Buchler, 1975). The metal(III) porphyrins all contained one axial chloride ligand, while the Sn(IV) porphyrin contained two axial chloride ligands. The Ti(IV) and V(IV) porphyrins contained an oxygen atom as a ligand.

The Effect of the Metal Ion on Electron Ionization of Metalloporphyrins

Under EI conditions, porphyrins undergo peripheral substituent fragmentations that are usually "benzylic" in character, by cleavage of the bond β to the porphyrin nucleus as described in Chapter 1 (Jackson et al., 1965). OEP and metalated OEP derivatives contain eight peripheral ethyl substituents, and lose up to eight methyl groups as a result of ß-cleavages. The EI mass spectrum of Zn(II) OEP (Figure 5-1) shows the singly charged ß-cleavage fragments at low relative abundances, while the doubly charged fragment ions are at much greater relative abundances. The radical electron symbol normally associated with singly charged ions in EI mass

Figure 5-1.

Electron ionization mass spectrum of Zn(II) OEP

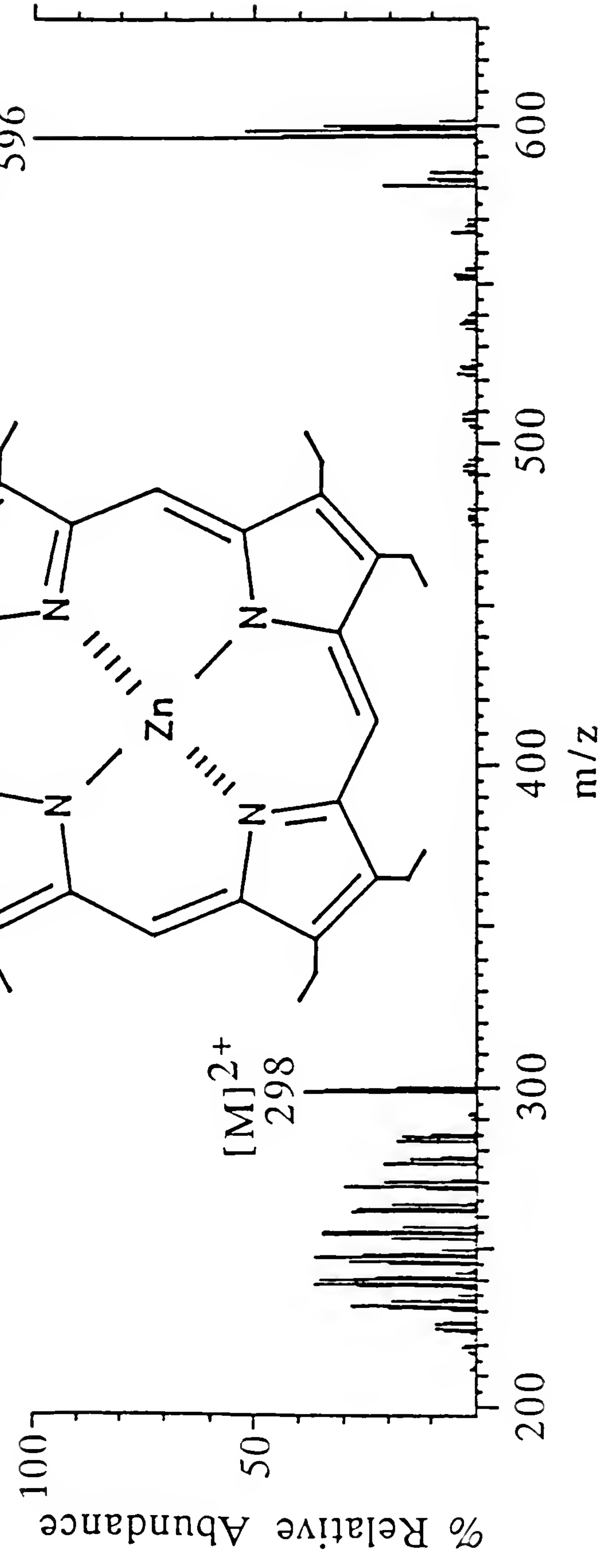
[M]$^+$
596
[M]$^{2+}$
298
Zn
N
N
N
N
m/z
200
300
400
500
600
% Relative Abundance
100
50

spectra is not used in labeling such ions in this chapter in order to avoid ambiguity arising from odd numbers of electrons in some of the metals. Close inspection of Figure 5-1 reveals that there are doubly charged fragment ions corresponding to loss of more than the eight methyl groups which can be attributed solely to ß-cleavage. Therefore, α-cleavage from the doubly charged molecular ion must also be occurring. The loss of a methyl group from a doubly charged ion appears as an m/z loss of 7.5 u, rather than the loss of 15 u for the loss of a methyl group from a singly charged ion. The quadrupole mass spectrometer used for this study was tuned for only unit resolution, so loss of 7.5 mass units may appear in the centroided mass spectrum as loss of 7 and/or loss of 8 mass units, resulting in a doublet. Also, instead of occurring at m/2, where m is the mass of the singly charged ion, doubly charged ions often arise at (m-1)/2, corresponding to a loss of a hydrogen atom (Beynon, 1960).

Mass spectra from 17 metalated OEP derivatives plus free-base OEP (Table 5-1) have been obtained; spectra for three of the compounds are shown in Figure 5-2. Based on these data, several important observations can be made. First, for all 17 metalloporphyrins, the relative abundances of the doubly charged fragment ions were much greater than those of their singly charged counterparts. Also, the abundances of the doubly charged ß-cleavage fragment ions relative to the base peak (either $[M]^+$ or $[M - Cl]^+$) were dependent on the specific metal, while the abundances of the singly charged fragment ions relative to the base peak were practically independent of the metal.

Table 5-1. A list of the 18 porphyrins studied, the ground state valence electron configurations, electronegativities, and ionic radii of the metals, the calculated Buchler Stability Indexes, the revised stability indexes, and the ratio of the sum of the relative abundances of the doubly charged fragment ions to the sum of the relative abundances of the singly charged fragment ions.

Porphyrin	Valence Electron Configuration of Metal	Pauling Electro-negativity of metal[a]	Ionic Radius of metal (pm)[a]	Buchler Stability Index	$\Sigma F^{2+}/\Sigma F^{+}$	Revised Stability Index
free-base OEP	--	--	--	--	1.70	--
Hg(II) OEP	$6s^2$	1.9	103.4	3.68	5.16	3.68
Mg(II) OEP	$3s^2$	1.2	61.10	3.93	3.56	3.93
Zn(II) OEP	$4s^2$	1.6	69.56	4.60	4.83	4.60
Sc(III) OEP Cl	$3d^1 4s^2$	1.3	78.57	4.96	2.26	4.96
Co(II) OEP	$3d^7 4s^2$	1.8	69.56	5.18	3.46	5.18
Ni(II) OEP	$3d^8 4s^2$	1.8	67.68	5.32	3.13	5.32
Tl(III) OEP Cl	$6s^2 6p^1$	1.8	92.15	5.86	2.55	5.86
Cu(II) OEP	$3d^{10} 4s^1$	2.0	67.68	5.91	5.99	5.91
In(III) OEP Cl	$5s^2 5p^1$	1.7	78.57	6.49	7.78	6.49
Mn(III) OEP Cl	$3d^5 4s^2$	1.5	60.14	7.48	6.25	5.67
Mn(II)			77.60	3.87		
Cr(III) OEP Cl	$3d^5 4s^1$	1.6	62.08	7.73	5.45	5.83
Cr(II)			81.48	3.93		
Ga(III) OEP Cl	$4s^2 4p^1$	1.6	60.14	7.98	10.28	7.98
O=Ti(IV) OEP	$3d^2 4s^2$	1.5	65.96	9.10	2.83	3.44
Ti(II)			87.30	3.44		
Fe(III) OEP Cl	$3d^6 4s^2$	1.9	62.08	9.18	6.75	7.17
Fe(II)			73.72	5.16		
Al(III) OEP Cl	$3s^2 3p^1$	1.5	48.50	9.28	13.53	9.28
Sn(IV) OEP Cl_2		1.9	71.00	10.70	9.22	7.33
Sn(II)			95.88	3.96		
O=V(IV) OEP	$3d^3 4s^1$	1.6	58.20	11.00	2.44	3.75
V(II)			85.36	3.75		

[a] from Lange's Handbook of Chemistry, McGraw-Hill, New York, 1973

Figure 5-2.

Electron ionization mass spectra of:
A. Ga(III) OEP Cl
B. Mg(II) OEP
C. OEP

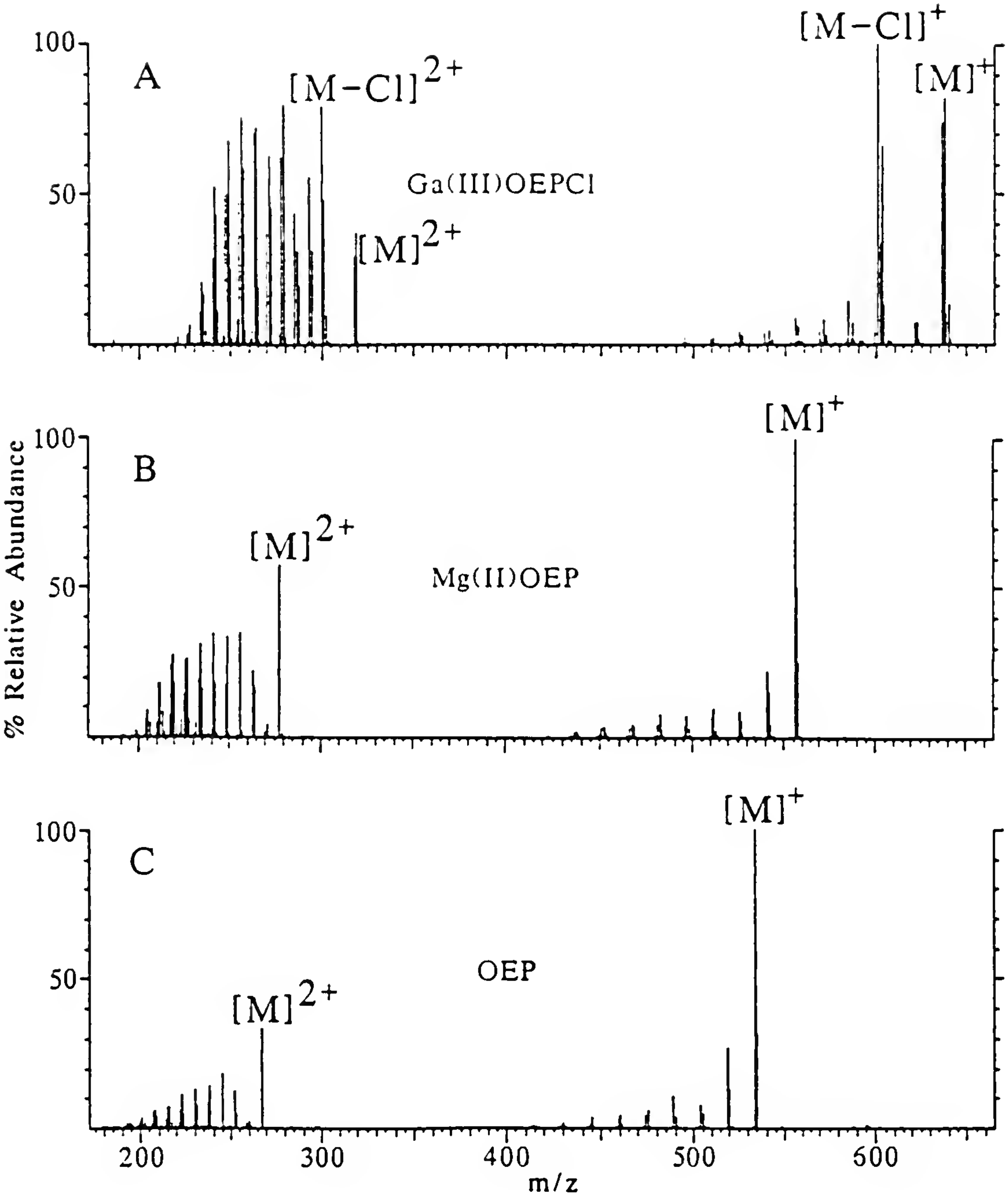
100
50
A
[M-Cl]$^{2+}$
[M]$^{2+}$
Ga(III)OEPCl
[M-Cl]$^{+}$
[M]$^{+}$
B
[M]$^{2+}$
Mg(II)OEP
[M]$^{+}$
C
[M]$^{2+}$
OEP
[M]$^{+}$
% Relative Abundance
200
300
400
500
600
m/z

The data from the doubly charged ions in the mass spectra were correlated to a stability index originally defined by Buchler to describe the stability of metalloporphyrins toward demetalation in solutions (Buchler, 1975). Buchler defined the stability index, S_i, as

$$S_i = \frac{100(\text{Pauling electronegativity of metal})(\text{charge on metal})}{(\text{ionic radius of metal in pm})}$$

The lower the stability index of a metalloporphyrin, the more reactive it is toward demetalation reactions in solution. Although this is an index for metalloporphyrins under very different conditions than used to obtain mass spectral data, it depends only on parameters of the metal itself. Thus, it would not be surprising if a correlation existed between the stability index and the doubly charged ion mass spectra of metalloporphyrins.

The ratio of the sum of the relative abundances of all doubly charged β-cleavage fragment ions to the sum of the relative abundances of all singly charged β-cleavage fragment ions, $\Sigma F^{2+}/\Sigma F^{+}$, is plotted against the Buchler Stability Index for the 17 metalated OEP derivatives in Figure 5-3. The $\Sigma F^{2+}/\Sigma F^{+}$ value is a measure of the extent to which doubly charged β-cleavage fragment ions form in the source. The greater the $\Sigma F^{2+}/\Sigma F^{+}$ value, the greater the relative abundance of doubly charged fragment ions compared to singly charged fragment ions. Only fragment ions resulting from β-cleavage of peripheral substituents were summed.

Figure 5-3.

The ratio of the sum of relative intensities of all doubly charged fragment ions to the sum of relative intensities of all singly charged fragment ions, $\Sigma F^{2+}/\Sigma F^{+}$, plotted against the Buchler Stability Index. The $\Sigma F^{2+}/\Sigma F^{+}$ ratio for free-base OEP is shown at an arbitrary stability index value for comparison.

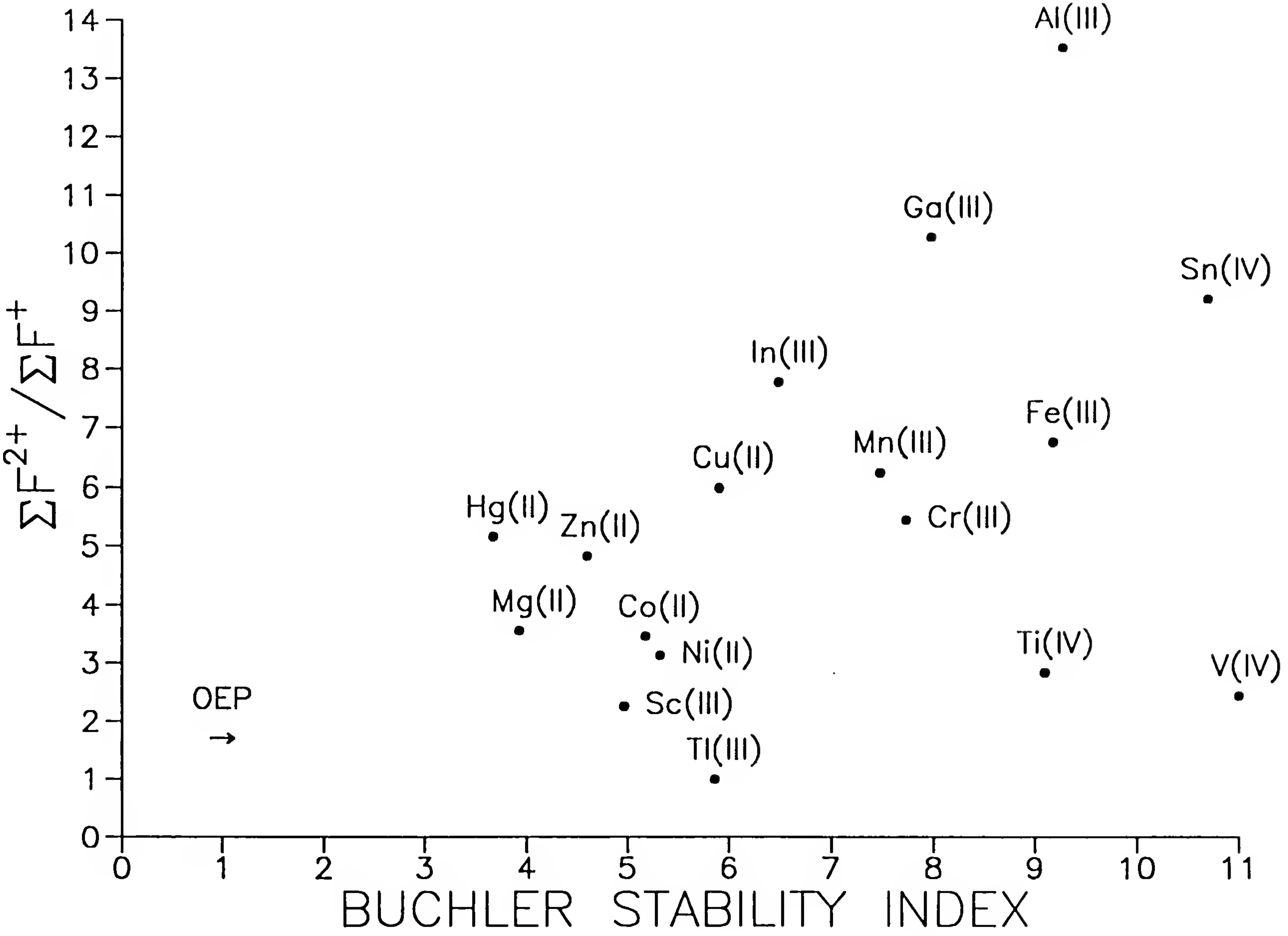
$\sum F^{2+}/\sum F^{+}$
14
13
12
11
10
9
8
7
6
5
4
3
2
1
0
0
1
2
3
4
5
6
7
8
9
10
11
BUCHLER STABILITY INDEX
Al(III)
Ga(III)
Sn(IV)
In(III)
Fe(III)
Mn(III)
Cu(II)
Cr(III)
Hg(II)
Zn(II)
Mg(II)
Co(II)
Ni(II)
Ti(IV)
V(IV)
OEP
→
Sc(III)
Tl(III)

Singly and doubly charged fragment ions arising only from the loss of chloride ligands were not included for this calculation. For Hg(II) OEP and Tl(III) OEP Cl, which demetalated significantly in solution and/or upon ionization, the relative abundances of both the metalated and nonmetalated β-cleavage fragment ions were summed to calculate $\Sigma F^{2+}/\Sigma F^{+}$. The rather large ionic radii of Tl(III) and Hg(II) compared to the other metals (Table 5-1) facilitates demetalation. Tl(III) OEP Cl is actually quite stable toward demetalation in solution, but has been shown to demetalate readily upon electron ionization (Smith, 1972). Hg(II) OEP is less stable in solution than Tl(III) OEP Cl, but it is unclear how much of the demetalation observed in the Hg(II) OEP mass spectrum occurred in the methylene chloride solution, and how much of it occurred in the EI source. The $\Sigma F^{2+}/\Sigma F^{+}$ value for metal-free OEP is also plotted in Figure 5-3 for comparison.

Although the plot in Figure 5-3 indicates only a limited correlation between $\Sigma F^{2+}/\Sigma F^{+}$ and the Buchler Stability Index, it does lead to some interesting observations. First, the metal-free OEP has a lower $\Sigma F^{2+}/\Sigma F^{+}$ value than most of the metalated OEP derivatives. The $\Sigma F^{2+}/\Sigma F^{+}$ value of Tl(III) OEP Cl is lower than that of OEP, but this is probably due to the fact that the relative abundances of both singly and doubly charged metalated β-cleavage fragment ions in the Tl(III) OEP Cl mass spectrum are very small compared to those of their nonmetalated counterparts. Second, there does seem to be a linear relationship between the Al(III), Ga(III), and In(III) OEP derivatives. These metals are all in the same group, and have filled valence shells. Two other metals with filled valence shells, Zn(II) and Mg(II), also lie along this line. Third, most of the metals which lie to the right of this line have additional ligands (Cl or O), and can exist in lower oxidation states which are also stable. Recent work with doubly charged aluminum and iron acetylacetonates indicates that doubly charged Fe(III) compounds probably do reduce to Fe(II) compounds upon loss of a ligand via CAD (Ast, 1988). That is, iron compounds, and presumably other transition metal compounds, can change their valency depending on whether they are losing a neutral radical or a neutral molecule, in order to maintain an even number of electrons. In the present study, Sn(IV), Fe(III), Mn(III), Cr(III), Ti(IV), and V(IV) are also stable in the (II) oxidation state. With this in mind, a revised stability index, which was determined in the same manner as the Buchler Stability Index, was calculated for these metalloporphyrins using different values for charge and ionic radius.

This revised stability index was only calculated for metals which had oxidation states greater than (II), and was not calculated for metals which have filled valence shells in the (III) oxidation state. Thus, the revised stability index is the same as the Buchler Stability Index for all (II) metal OEP derivatives, and for Sc(III), Al(III), Ga(III), In(III), and Tl(III) OEP derivatives. Among the metalloporphyrins for which a revised stability index was determined, there is a fundamental difference between the two types of ligands. The oxygen ligands in O=Ti(IV) OEP and O=V(IV) OEP are not removed upon ionization, whereas the chloride ligands in the other compounds can be removed upon ionization. Thus, it seems reasonable to calculate the revised stability indexes for O=Ti(IV) OEP and O=V(IV) OEP with the metals having charges and radii corresponding to the (II) oxidation state. The chlorinated Sn(IV), Fe(III), Mn(III), and Cr(III) OEP derivatives all yield both chlorinated and nonchlorinated ions in the mass spectra. This suggests that these metals are present in both the original and the (II) oxidation states. The revised stability indexes for these metalloporphyrins was obtained by averaging the Buchler Stability Indexes for both oxidation states, and are listed in Table 5-1. The correlation between $\Sigma F^{2+}/\Sigma F^{+}$ and this revised stability index is significantly improved, as shown in Figure 5-4.

In general, the higher the revised stability index of a metalloporphyrin, the greater the relative abundance of doubly charged fragment ions. This is due to the fact that metalloporphyrins having a higher stability index have a greater charge localization on the metal, and increased withdrawal of electron density from the periphery. This results in the weakening of peripheral bonds and increased β-cleavage fragmentation of peripheral substituents. Indeed, it appears to enhance α-cleavage of such substituents as well. Metal-free OEP has a rather low $\Sigma F^{2+}/\Sigma F^{+}$ value because it does not contain a metal to withdraw electron density from the periphery. It is unclear how valid the $\Sigma F^{2+}/\Sigma F^{+}$ values for Hg(II) OEP and Tl(III) OEP Cl are, as these metalloporphyrins demetalate to a significant extent. The other metalloporphyrins studied do exhibit an increase in $\Sigma F^{2+}/\Sigma F^{+}$

Figure 5-4.

The $\Sigma F^{2+}/\Sigma F^{+}$ values plotted against a revised stability index which takes into account changes in valence which can occur among Sn and transition metals having ligands

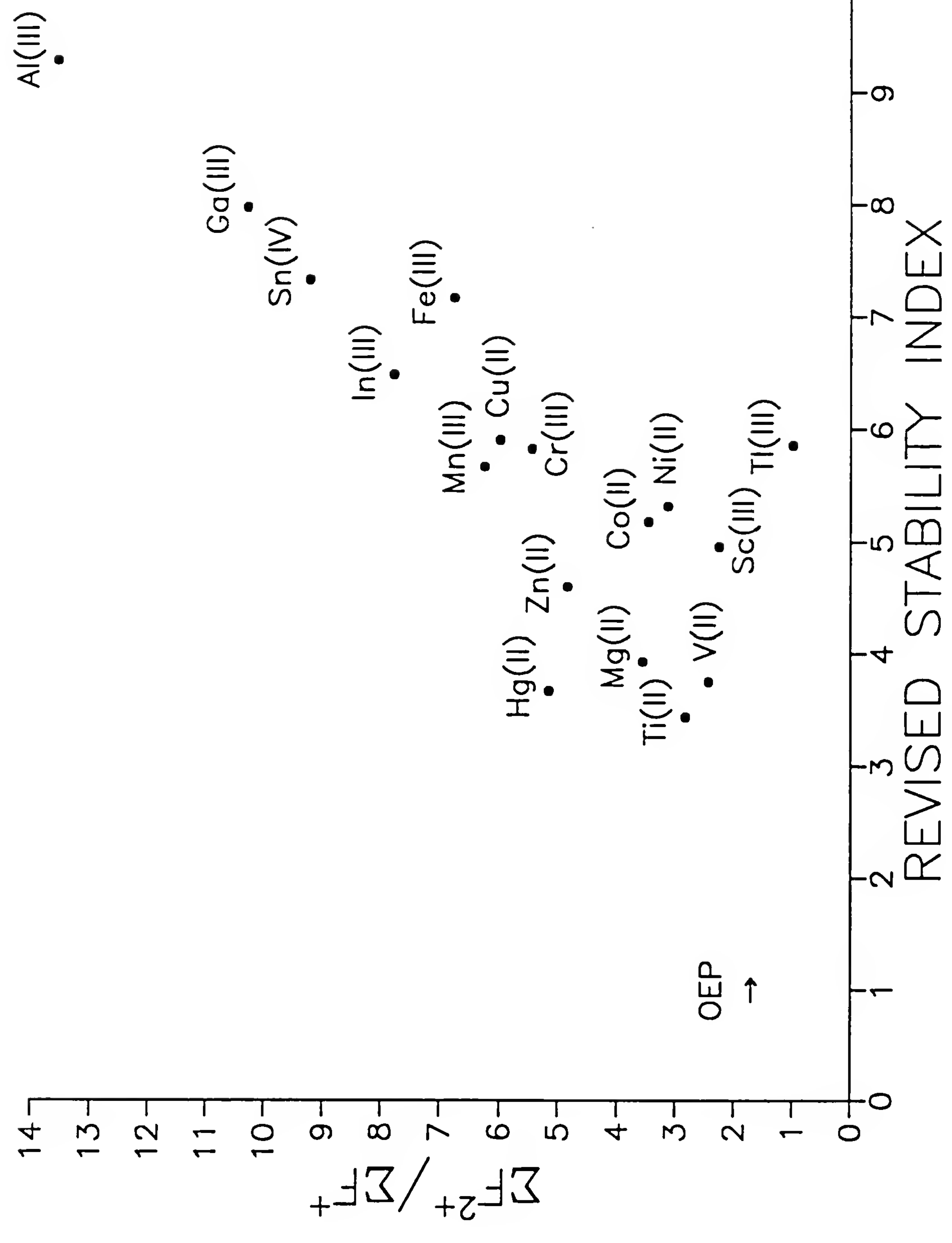
ΣF2+/ΣF+
0
1
2
3
4
5
6
7
8
9
10
11
12
13
14
REVISED STABILITY INDEX
0
1
2
3
4
5
6
7
8
9
10
OEP →
Al(III)
Ga(III)
Sn(IV)
Fe(III)
In(III)
Cu(II)
Mn(III)
Cr(III)
Ni(II)
Tl(III)
Co(II)
Sc(III)
Zn(II)
Hg(II)
Mg(II)
V(II)
Ti(II)

with an increase in the revised stability index. That is, the extent of doubly charged β-cleavage fragment ion formation by metalloporphyrins depends upon the specific metal.

This phenomenon is of use in the structure elucidation of porphyrins, since it can provide a way in which to control fragmentation in the source under EI conditions, via replacement of the metal in solution (Buchler, 1975) prior to mass spectrometric analysis. It should be pointed out that some metal complexes are extremely difficult to demetalate under mild conditions, so this method may not be feasible in such cases. Replacement of a metal of low stability index with one of high stability index, for instance, increases the extent of fragmentation of the metalloporphyrin. This is especially useful in MS/MS studies of ß-cleavage fragment ions, since increasing their relative abundance can compensate for the inefficiencies of CAD and transmission through a second mass analyzer. Metalation of free-base porphyrins also increases the extent of EI fragmentation. Similarly, the extent of fragmentation may instead be diminished, in order to enhance the sensitivity of MS/MS measurements on molecular ions. Hg(II) and Tl(III) porphyrins should probably be converted to metalloporphyrins which do not readily demetalate, as demetalation reduces the absolute intensities of all metalated ions. The singly charged fragment ions are at much lower intensities and exhibit far less dependence on the metal, compared to the doubly charged fragment ions.

The EI mass spectrum of nickel (II) deuteroporphyrin-IX dimethyl ester (Ni(II)D-IX DME) (Figure 5-5) indicates that fragmentation pathways for singly charged porphyrin ions can differ from those for doubly charged ions. The most obvious difference in this case is the near total lack of doubly charged di-ester molecular ions, $[M]^{2+}$, or doubly charged mono-ester ions, $[M - CH_2CO_2CH_3]^{2+}$, in the spectrum. Note that the two ester groups (73 u each) are the only substituents which may be lost by β-cleavage. This type of ester fragmentation occurs in doubly charged ions but not in singly charged ions (Jackson et al., 1965). Another difference is the existence of a doubly charged ion at m/z 244 with no singly charged counterpart appearing at m/z 488. This doubly charged ion has been shown to arise from other doubly charged ions, and can also be assigned a resonance stabilized structure when formed from the doubly charged molecular ion (Clezy et al., 1974). Once again, there is enhancement of α-cleavages occurring in the doubly charged region over those appearing in the singly charged region. The fact that separate fragmentation pathways can exist for corresponding doubly and singly charged ions suggests that doubly charged porphyrin ions may offer unique structural information.

Enhanced CAD Fragmentation of Doubly Charged Porphyrin Ions

The development of methods to analyze doubly charged ions by MS/MS may prove quite useful in the structure elucidation of many compounds. This is because doubly charged ions are expected to fragment more extensively than singly charged

Figure 5-5.

Electron ionization mass spectrum of Ni(II) deutero IX dimethyl ester obtained with a direct exposure probe

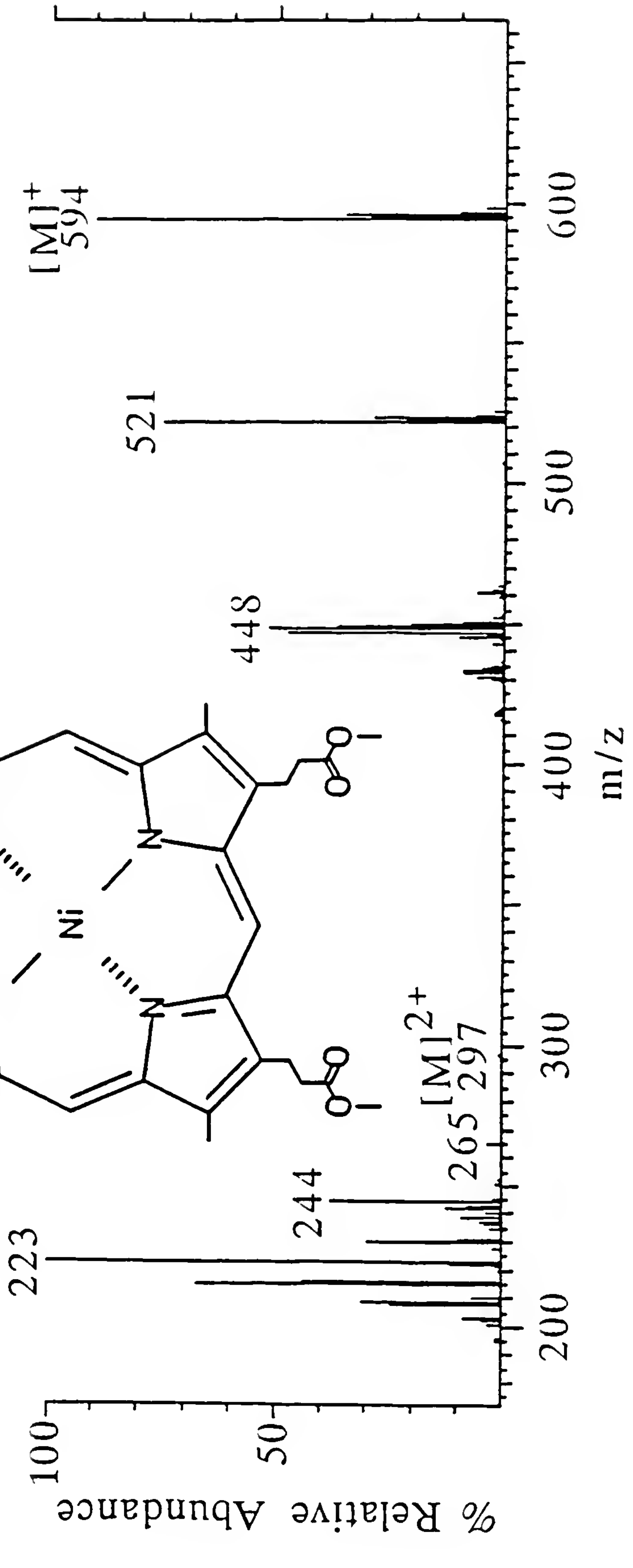
% Relative Abundance
100
50
m/z
200
300
400
500
600
223
244
265
[M]$^{2+}$ 297
448
521
[M]$^{+}$ 594
Ni
N
N
N
N
O
O
O
O

ions for two major reasons. First, in a mass spectrometer operated at fixed accelerating voltage, doubly charged ions experience twice the kinetic energy of singly charged ions of the same mass. Increased kinetic energy leads to increased fragmentation upon collision with neutral gas species in the quadrupole collision cell. Second, doubly charged ions may have lower critical energies of dissociation because they have fewer bonding electrons than corresponding singly charged ions.

The major difference between this MS/MS study of doubly charged ions and previous reports dealing with other molecular systems is that under the normal MS/MS conditions described, doubly charged porphyrin ions do not undergo charge exchange reactions to any significant extent in the collision cell. Most previous MS/MS studies of doubly charged ions resulted in singly charged daughter ions due to charge exchange reactions. These studies involved the $[M]^{2+}$ ions of compounds such as acetylenes (Appling et al., 1983), halogenated alkanes (Hanner et al., 1982), n-alkanes (Jones et al., 1982), toluene (Ast et al., 1972a), and simple aromatics (Beynon et al., 1971). Doubly charged porphyrin ions are very different from the $[M]^{2+}$ ions of these other compounds because they are large, resonance-stabilized ions very capable of maintaining two charges upon CAD. The structure of a doubly charged metal-free porphyrin ion in solution has been suggested as having the positive charges localized on diagonally opposed nitrogens, based upon ^1H NMR studies (Chakraborty et al., 1982). The structure of the same ion in the gas phase, however, may be very different than in solution in terms of localization of positive charges. This doubly charged macrocyclic ion is resonance stabilized, and is not likely to undergo charge exchange. This results in the doubly charged porphyrin ions yielding daughter ions which are almost exclusively doubly charged. Metalloporphyrins have been reported to delocalize π-electrons in the same way metal-free porphyrins do, and are also resonance stabilized (Chakraborty et al., 1982).

One does not typically scan the third quadrupole, Q3, much above the m/z of the parent ion selected in Q1 when obtaining daughter ion mass spectra with a triple quadrupole mass spectrometer. However, when the parent ion is doubly charged, it is important to scan Q3 to at least twice the m/z of the parent ion to detect any singly charged daughter ions that are formed. In the present study, even when the mass spectrometer was tuned to favor the singly charged region, the daughter ions of positive doubly charged porphyrin molecular and fragment ions are almost exclusively doubly charged (Figure 5-6). Although the instrument used cannot directly differentiate lower mass singly charged ions from doubly charged ions, the most abundant daughter ions are most certainly doubly charged. This conclusion is based on the fact that the major daughter ions are separated by 7.5 u, corresponding to successive losses of 15 u, a $\cdot CH_3$ group, from a doubly charged ion. Recall that singly charged OEP ions fragment via β-cleavage of the peripheral ethyl substituents upon CAD, so a similar fragmentation pattern with doubly charged OEP ions is not unexpected. The 7.5 u separation between peaks was

Figure 5-6.

The daughter ion mass spectrum of the $[M]^{2+}$ ion of OEP (m/z 267) obtained with the mass spectrometer tuned to favor the singly charged region

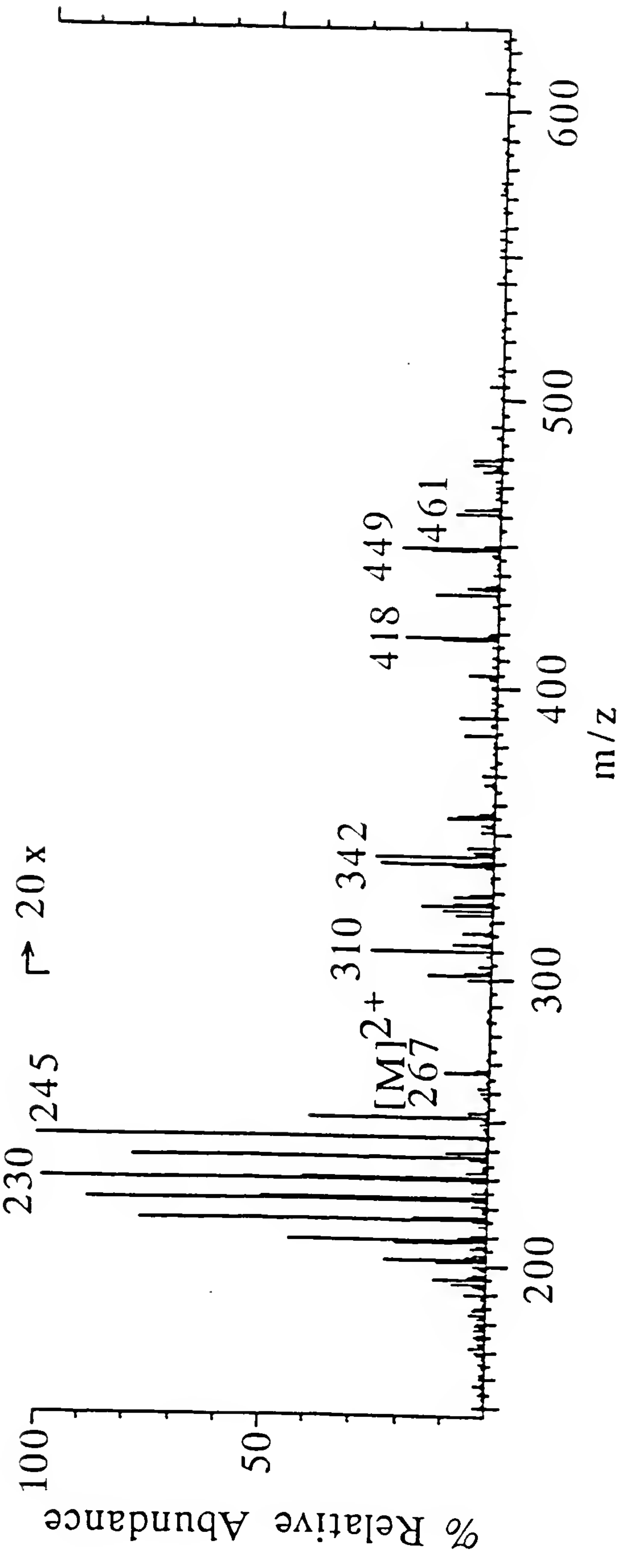
% Relative Abundance
100
50
m/z
200
300
400
500
600
230
245
[M]$^{2+}$
267
310
342
418
449
461
20 x

also seen in the doubly charged fragment ion region of EI/MS data, and these are known to be doubly charged from high resolution experiments on a magnetic sector instrument. The singly charged daughter ions which do appear in the daughter ion mass spectra of doubly charged parent ions are at low abundances, are difficult to reproduce, and are not diagnostically useful. In fact, metalloporphyrins yield far lower abundances of singly charged daughter ions from doubly charged parent ions than does the free-base porphyrin depicted in Figure 5-6. Thus, in the following MS/MS daughter ion mass spectra of doubly charged parent ions, the singly charged region is not shown.

One of the benefits the charge exchange methods offer that this technique does not is avoiding interferences from $[M/2]^{+\cdot}$ ions which coincide with the m/z of $[M]^{2+}$ (Jones et al., 1982). This is typically not a problem with porphyrins of less than 40 carbons, because the doubly and singly charged regions are usually well separated in m/z. For such interferences to occur under EI conditions, a porphyrin would have to lose peripheral substituents of mass totaling more than 1/2 of the molecular weight of the intact porphyrin. Another disadvantage of this technique is that, with Q3 tuned to provide unit mass resolution, adjacent doubly charged ions (separated by 1/2 u) are not resolved. Even if the mass filter is set to resolve half-masses, the data system software is designed to provide unit resolution spectra with integer m/z values. This can sometimes complicate structure elucidation.

The daughter ion mass spectra of singly and doubly charged ions of the same mass were obtained for numerous metalated OEP derivatives. An example of such an experiment is the comparison of the daughter ion mass spectra of m/z 584 and m/z 292 (Figure 5-7) which are the $[M - Cl]^+$ and $[M - Cl]^{2+}$ ions, respectively, of Cr(III) OEP Cl. The singly charged parent ion yields far fewer ß-cleavage daughter ions under CAD than does the doubly charged parent ion. In fact, the doubly charged parent yields more than eight different daughter ions, indicating that even α-cleavage is occurring during CAD of the doubly charged ions. Such increased fragmentation can be valuable in terms of structure elucidation.

When daughter ion mass spectra of singly and doubly charged molecular ions (i.e., $[M]^+$ and $[M]^{2+}$) of this same compound are compared, another interesting difference arises (Figure 5-8). The ß-cleavage daughter ions of the singly charged parent ion are predominantly chlorinated, although some nonchlorinated daughter ions of low abundance do appear. In contrast, the doubly charged parent ion yields predominantly nonchlorinated daughter ions. This is another example of different fragmentation pathways existing for singly and doubly charged ions; such pathways must be recognized for doubly charged ion MS/MS to be of use in structure elucidation.

Daughter ion mass spectra of both the singly and doubly charged molecular ions of O=V(IV) OEP were obtained at various Q2 offset voltages to determine the extent of CAD of doubly charged ions compared to that of singly charged ions

Figure 5-7.

Daughter ion mass spectra from Cr(III) OEP Cl:
A. parent ion is $[M\text{-}Cl]^{+}$
B. parent ion is $[M\text{-}Cl]^{2+}$

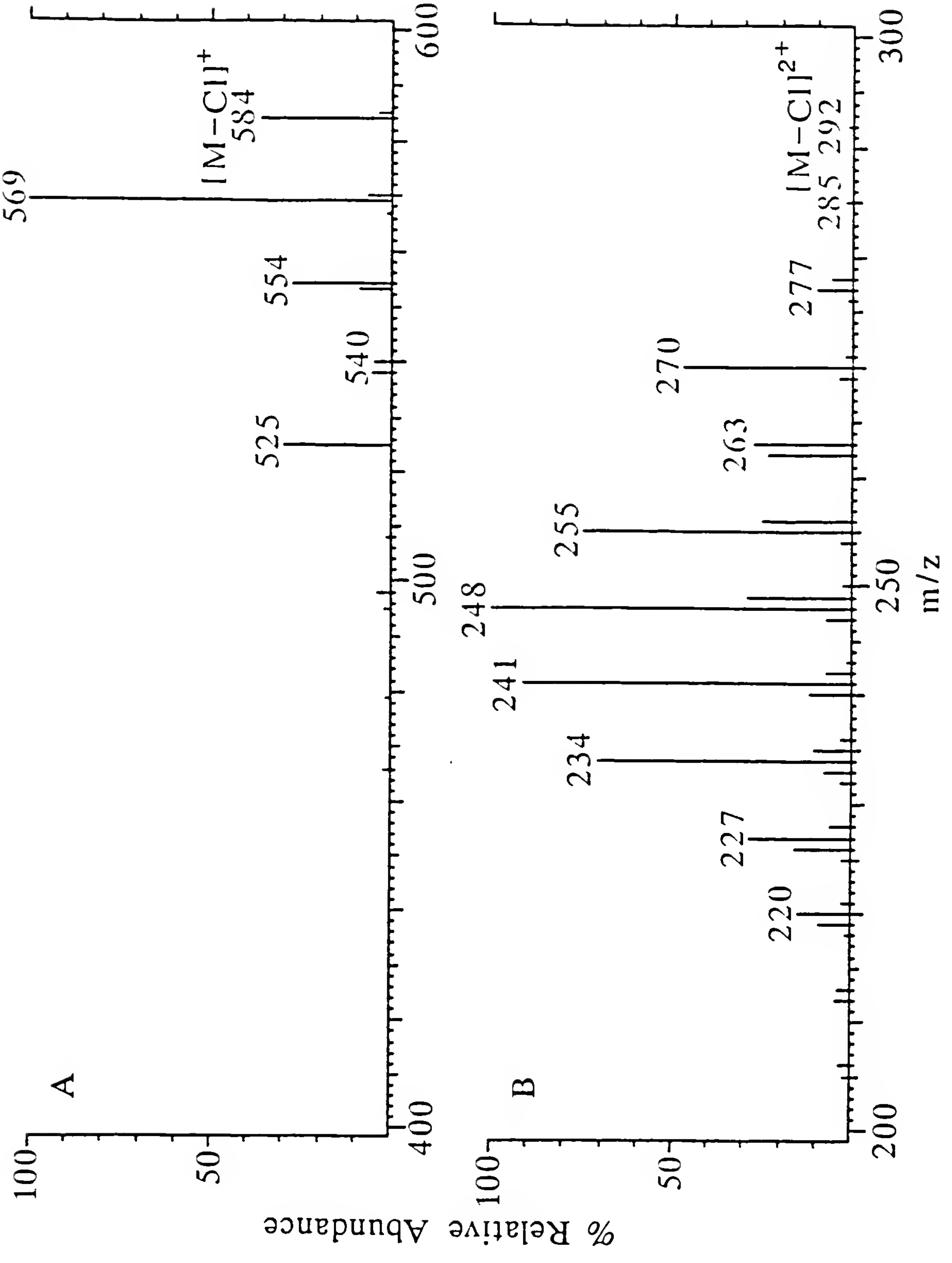
A
569
[M−Cl]+
584
554
540
525
400
500
600
B
[M−Cl]2+
285
292
277
270
263
255
248
241
234
227
220
200
250
300
m/z
100
50
% Relative Abundance

Figure 5-8.

Daughter ion mass spectra from Cr(III) OEP Cl:
A. parent ion is $[M]^+$
B. parent ion is $[M]^{2+}$

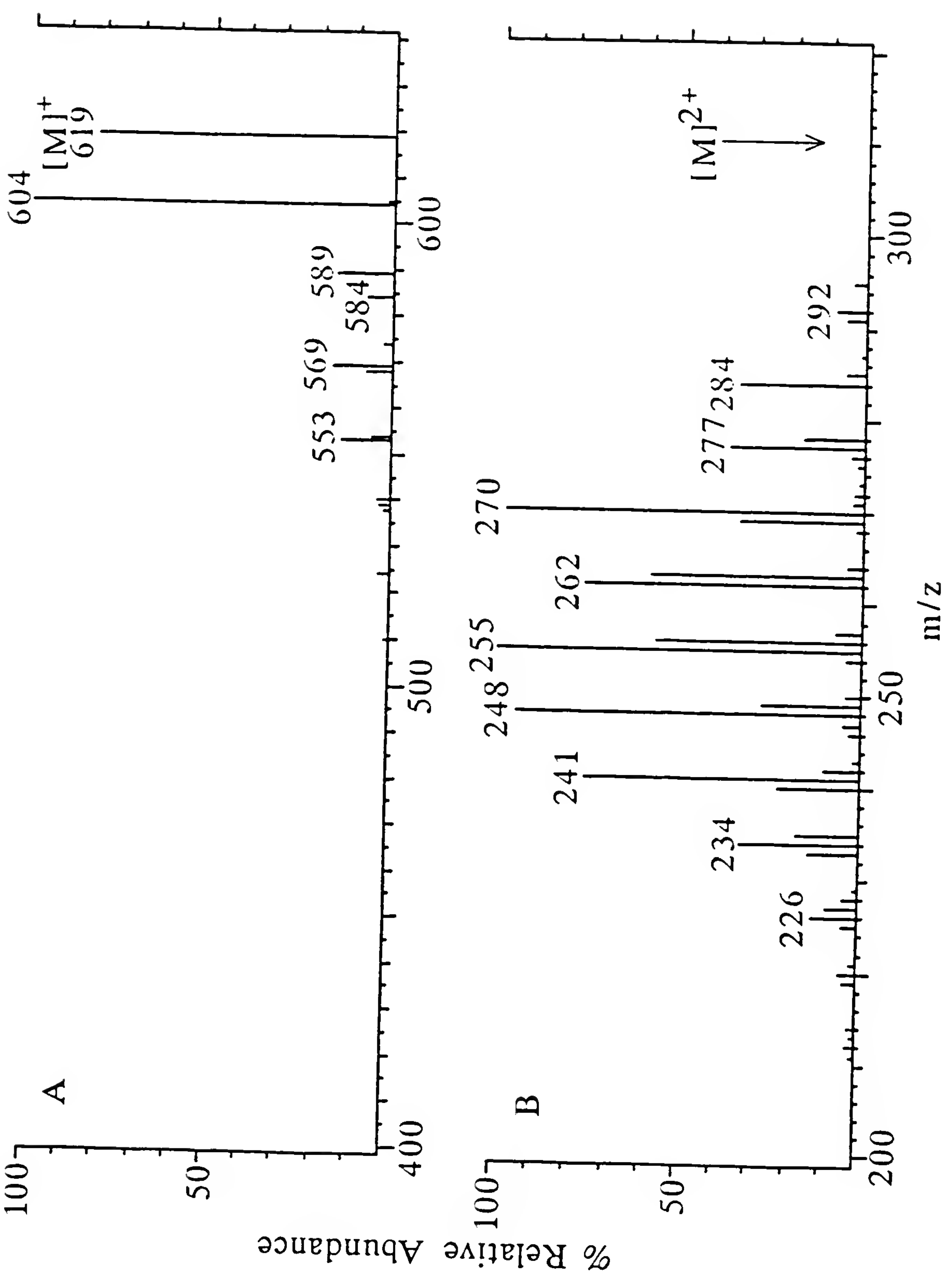
A
[M]$^+$
619
604
589
584
569
553
400
500
600
B
[M]$^{2+}$
292
284
277
270
262
255
248
241
234
226
200
250
300
100
50
% Relative Abundance
m/z

at various collision energies. At all Q2 offset voltages from 10 V to 25 V, the doubly charged ions fragmented more extensively than did the singly charged parent ions. In fact, the doubly charged parent ions yielded α-cleavage daughter ions, losing 11 carbons, at collision energies as low as 15 eV. The singly charged parent ions did not lose more than 5 carbons even at 25 eV (Figure 5-9).

Daughter ion mass spectra were also obtained for singly and doubly charged ions of the same mass at the same effective collision energies (Figure 5-10). The singly charged molecular ion of Co(II) OEP, m/z 591, was accelerated into Q2 by a Q2 offset voltage of 20 volts, while the doubly charged ion, m/z 296, was accelerated by 10 volts. The two spectra indicate different fragmentation patterns for the two ions,even though the collision energy was 20 eV for each. The average number of carbons lost by the parent ion in each case was calculated from the following equation:

$$\text{Ave. C\# lost} = \frac{\Sigma\, nA_n}{\Sigma\, A_n}$$

where A_n = percent relative abundance of an ion corresponding to loss of n carbons. The doubly charged parent ion fragments more extensively, with an average of four carbons lost, compared to an average of only two carbons lost from the singly charged parent ion. This evidence suggests that the doubly charged porphyrin ions have lower critical energies of dissociation than do corresponding singly charged porphyrin ions.

Figure 5-9.

The maximum number of carbons lost by both singly and doubly charged molecular ions of O=V(IV) OEP at various Q2 offset voltages

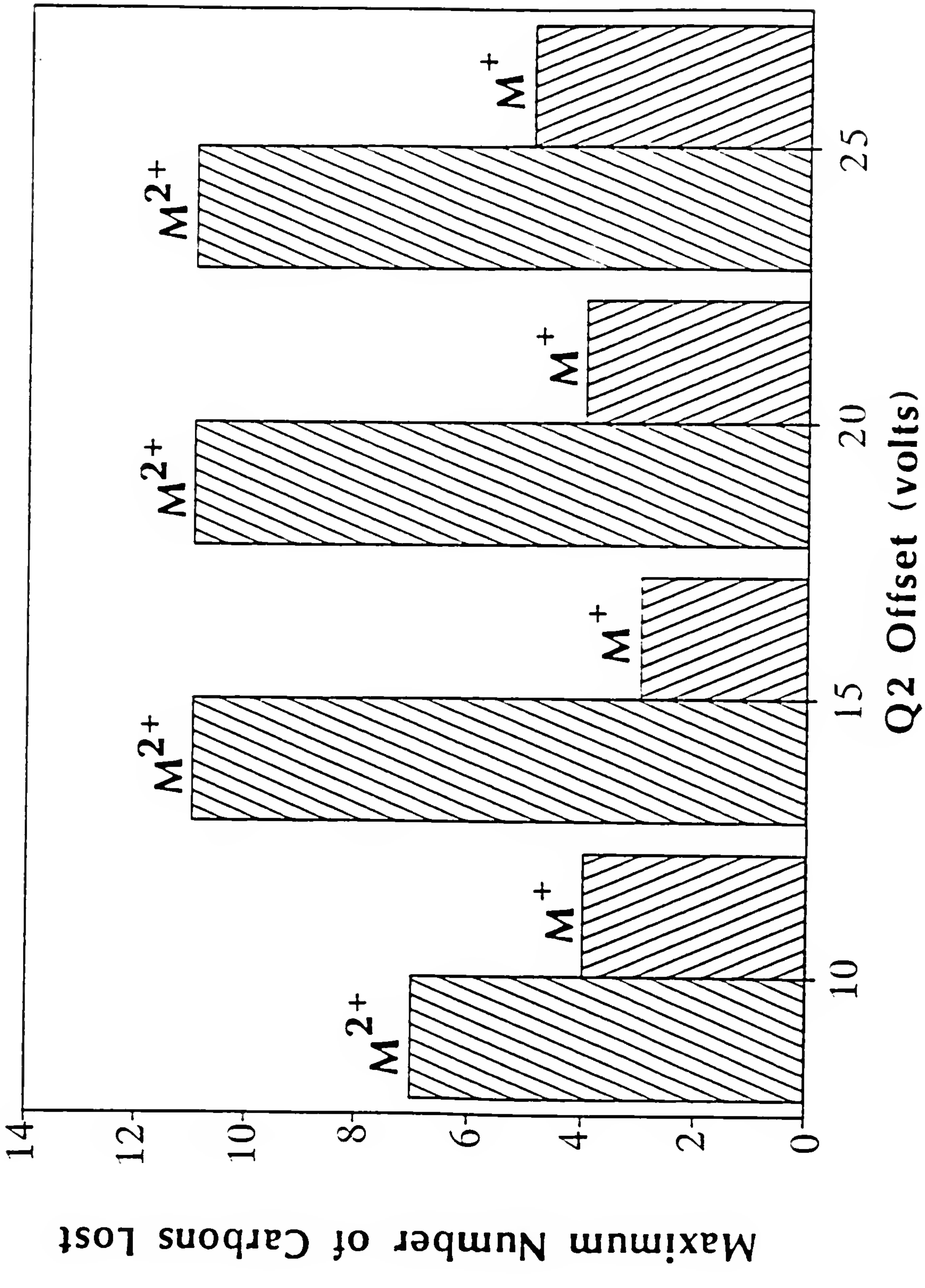
Maximum Number of Carbons Lost
0
2
4
6
8
10
12
14
Q2 Offset (volts)
10
15
20
25
M2+
M+
M2+
M+
M2+
M+
M2+
M+

Figure 5-10.

Daughter ion mass spectra of singly and doubly charged molecular ions of Co(II) OEP ate the same effective collision energies (20 eV):

A. parent ion is $[M]^{+}$, Q2 offset is 20 V, average number of carbons lost is 2

B. parent ion is $[M]^{2+}$, Q2 offset is 10 V, average number of carbons lost is 4

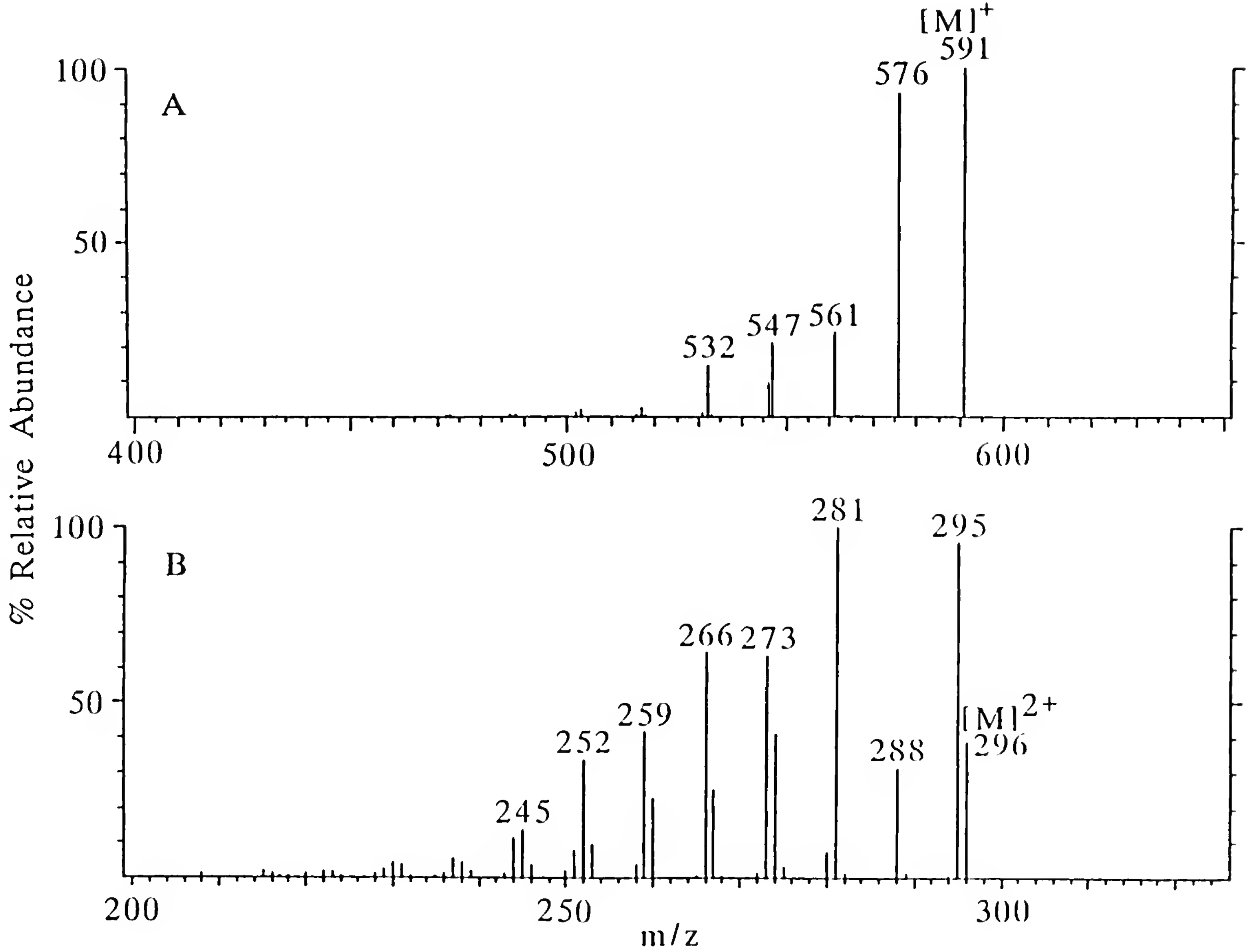
A
B
% Relative Abundance
100
50
100
50
400
500
600
200
250
300
m/z
[M]+
591
576
561
547
532
281
295
266
273
259
252
245
288
[M]2+
296

Conclusions

Doubly charged porphyrin ions have several features which singly charged porphyrin ions do not share, and these can be exploited for structure elucidation by EI/MS and EI/MS/MS. The intensities of doubly charged metalloporphyrin ß-cleavage fragment ions formed in the source under EI conditions are dependent on a revised stability index of the metal, so the extent of such fragmentation may be controlled by selection of the metal. This is particularly useful for MS/MS, because either molecular or fragment ions can be made more abundant for subsequent mass selection and fragmentation. Different fragmentation pathways can also exist for corresponding doubly and singly charged ions, and this fact could be of use in elucidating structures of other complex ions. Another characteristic of doubly charged ions is that they have greater kinetic energies at the same collision cell offset voltage than do singly charged ions of the same mass, which leads to increased fragmentation in MS/MS experiments. Doubly charged porphyrin ions even yield α-cleavage fragment and daughter ions, which singly charged ions rarely do. Doubly charged porphyrin molecular and fragment ions form rather abundantly under EI conditions, and offer unique opportunities in terms of structure elucidation by MS/MS.

CHAPTER 6

POSITIVE CHEMICAL IONIZATION OF PORPHYRINS: THE CASE FOR SURFACE-INDUCED DECOMPOSITION

Introduction

Porphyrins and metalloporphyrins fragment in a unique manner under positive hydrogen and positive ammonia chemical ionization conditions, although the mechanisms involved are not clearly understood. The meso-bridge bonds of porphyrins are known to be reduced under both H_2CI and NH_3CI conditions (Shaw et al., 1981; Jiang et al., 1984). An example of a porphyrin (OEP) and its corresponding reduced form, called a porphyrinogen (OEP + 6H), are depicted in Figure 6-1. Porphyrinogens are not aromatic, and are therefore much more susceptible to cleavage of the meso-bridge bonds than are porphyrins. Thus, porphyrin reduction to porphyrinogens under H_2CI or NH_3CI conditions yields pyrrole fragment ions, which are very useful for sequencing the pyrroles around the porphyrin macrocycle (Tolf et al., 1986; Kurlansik et al., 1984). The mono-, di-, and tri-pyrroles which form may each contain 0, 1, or 2 meso-carbons, as shown in Figure 6-2 for monopyrroles.

There has been some debate as to how the reduction and fragmentation come about, dating back to initial CIMS studies on porphyrins by Eglinton et al. (1979).

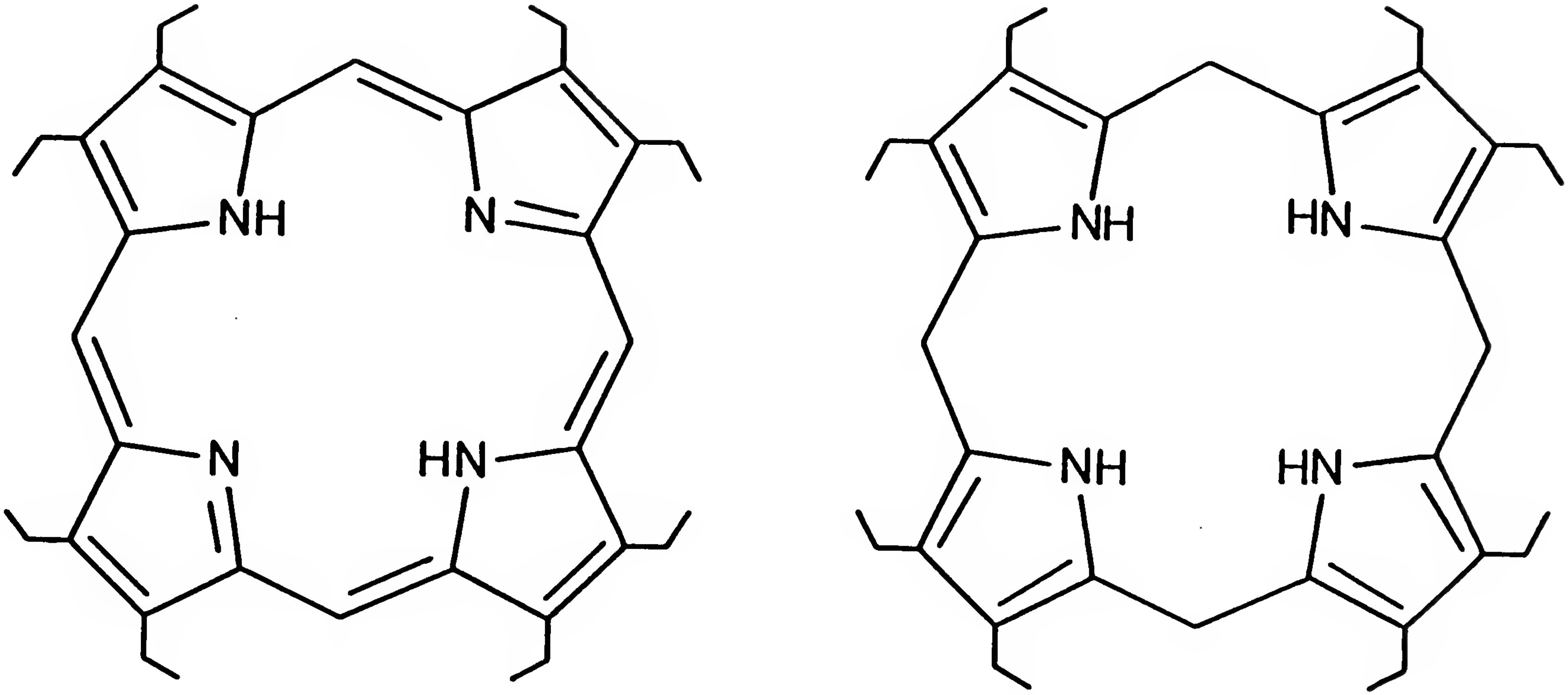

Porphyrin

Porphyrinogen

Figure 6-1.

Structures of a porphyrin (OEP) and a porphyrinogen (OEP + 6H)

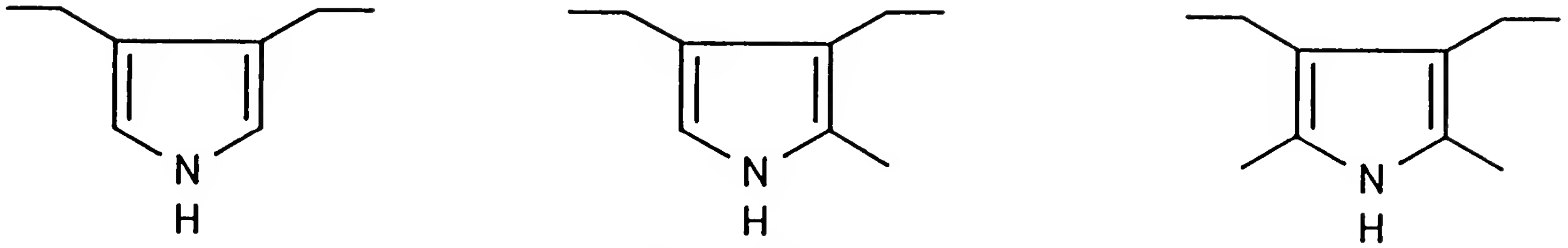

0 meso-carbons 1 meso-carbon 2 meso-carbons

Figure 6-2.

Monopyrrole structures resulting from meso-bridge cleavages of OEP

Djerassi and co-workers believe it occurs in the gas phase, but they present two conflicting theories, neither of which is plausible (Tolf et al., 1986, p. 1365). They hypothesize that the porphyrin molecule is protonated, and thus ionized, upon "attack by the reagent gas", under ammonia desorption chemical ionization conditions. Djerassi and co-workers go on to state that "further attack by the reagent gas then occurs with the formation of the protonated *porphyrinogen*". This is not a plausible theory because the porphyrin, once ionized, would be accelerated out of the ion source almost immediately. Analyte ions, upon formation, do not remain in the ion source nearly long enough to repeatedly react with reagent gas species. Djerassi and co-workers then suggest that "the porphyrinogen ions are unstable and are subject to continued nonspecific attack by the reagent gas at the meso carbon positions" which "can result in formation of mono-, di-, and tri-pyrrolic fragments" (Tolf et al., 1986, p. 1366). Again, just as the protonated porphyrin spends very little time in the ion source, the protonated porphyrinogen ions will not spend enough time in the ion source to be repeatedly attacked by the reagent gas. The figure illustrating this process which accompanies the text (Tolf et al., 1986, p. 1366) is even more implausible. It depicts positively charged reagent ions reacting with the positively charged protonated porphyrinogen ion. Ions of like charge, of course, repel each other, and would not react with one another in the gas phase as indicated.

A more feasible explanation of the mechanism of porphyrin reduction and fragmentation under CI conditions is that of surface-induced decomposition. In other words, porphyrin molecules condense on the walls of the ion source and are reduced. The resulting porphyrinogens then decompose, yielding the various pyrroles which vaporize and are ionized. Such interactions between neutral porphyrin molecules and the CI ion volume surface would not be surprising. The alkyl porphyrins discussed throughout this dissertation all have boiling points above 250 °C at ion source pressures, with many vaporizing above 300 °C. The stainless steel ion volume, or ion source, can only be heated to 190 °C. Thus, any porphyrin analyte which is not initially ionized in the CI plasma may condense on the walls of the ion volume. The condensed porphyrins can then be reduced on the metal surfaces by the CI plasma, a reaction which has been demonstrated for other compounds (Budzikiewicz, 1988). The porphyrinogens which result from reduction of the porphyrins can decompose via cleavages of their meso-bridge bonds, resulting in mono-, di-, and tri-pyrroles, each containing 0, 1, or 2 meso-carbons. As the filament of the DEP heats up to a maximum temperature of 1350 °C, radiative heat from the probe vaporizes the pyrrolic decomposition products, which are more volatile than the porphyrin (Figure 6-3). The pyrroles which vaporize are then ionized by the CI plasma. Similar results occur with the solids probe. Although the solids probe can only be heated to 500 °C, the entire probe tip is heated and butts up against the back of the ion volume. Thus, heating of the ion volume by

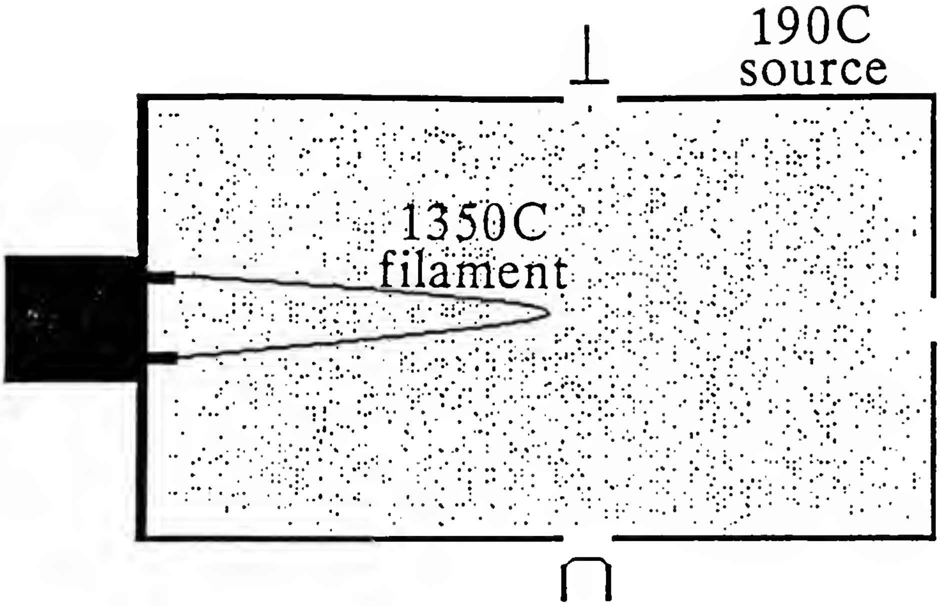
190C
source
1350C
filament

Figure 6-3.

Diagram of a CI ion volume indicating maximum temperatures of the DEP filament and the ion volume walls the solids probe probably occurs predominantly by direct, rather than by radiative, heating.

The important role that surfaces within the source perform can be used to explain the effect of source temperature on the CI mass spectra of porphyrins. The CH_4 CI mass spectrum of a standard free-base porphyrin was found to depend on the temperature of the ion source (Eglinton et al., 1979). When the ion source was heated to 300 °C, the mass spectrum consisted of the protonated molecular ion as the base peak, with monopyrrolic ions of intensities of less than 10 % of the base peak. When the source was cooled to 250 °C, the relative abundances of the monopyrrolic ions were 50 to 90 % that of the protonated molecular ion. Upon cooling the source to 200 °C, the intensities of the monopyrrolic ions were 4 to 5 times greater than the intensity of the protonated molecular ion. This is certainly what would be expected to occur if surfaces within the ion source were involved in decomposition of the porphyrin. The higher the source temperature, the shorter the residence time on surfaces within the source for the porphyrins which collide with these surfaces, and the less likely they are to undergo surface-assisted decomposition reactions. At lower source temperatures, the nonvolatile porphyrins are more likely to condense on the surfaces, better enabling them to undergo surface-assisted decomposition.

There has been some recent work by other groups supporting this theory. Pyrrolic ions are not formed when porphyrins are analyzed by low pressure ammonia or hydrogen CI, as in a quadrupole ion trap (Van Berkel et al., in press a). Even with the ion trap pressurized with 1 mtorr of hydrogen and reaction times of up to 2 seconds, no ions from reduction products were observed. There are several major differences between the ionization regions of an ion trap mass spectrometer (ITMS) and of a triple quadrupole mass spectrometer which may account for these results. First, the ITMS is operated at pressures three orders of magnitude lower than the CI ion source of a triple quadrupole mass spectrometer. This means that the partial pressures of reagent gas species required for reduction reactions are much lower in an ITMS, resulting in decreased rates of reduction. Second, the solids probe of an ITMS is placed outside of the trap. This results in most of the porphyrins condensing on the Rulon probe insert instead of on stainless steel surfaces inside of the trap. Third, and most importantly, the trap is normally kept at 100 °C, which may be too cool to facilitate the reduction, decomposition, and vaporization necessary for pyrrolic ions to be observed. The solids probe does not significantly heat the large thermal mass of the ring electrode in an ITMS because of the lack of direct thermal contact.

Although it is widely accepted that the pyrroles arise out of porphyrins reducing to porphyrinogens, another set of recent experiments has supported this assertion (Van Berkel et al., in press a). This work was performed on a double-focusing dual sector instrument in which the collision cell was not pressurized with a target gas. The resulting EI/MS/MS metastable daughter ion mass spectrum of a porphyrinogen $[M]^+$ ion prepared by Raney nickel reduction before introduction into the ion source was compared to the H_2CI/MS/MS metastable daughter ion mass spectrum of a porphyrinogen $[M]^+$ ion that formed in a high pressure ion source. Both of these metastable daughter ion mass spectra were very similar, suggesting that the porphyrinogen parent ion $[M]^+$ was the same whether prepared outside the mass spectrometer or within the ion source.

Data presented here also support the theory that the pyrrolic ions arise from surface-induced decomposition. These experiments also indicate that the surface of the ion volume may have a significant impact upon positive chemical ionization mass spectra of nonvolatile compounds. Ions which appear to be fragment ions in the CI mass spectra of such compounds may actually be produced by CI of surface-induced decomposition products. One rapidly growing area of mass spectrometry is analysis of higher molecular weight compounds of low volatility. This chapter describes the important role that surfaces within the ion source can play in terms of positive chemical ionization of nonvolatile compounds. It leads to interesting implications concerning mass spectra of other types of nonvolatile compounds besides porphyrins which may undergo surface-induced decomposition reactions within the ion source. The nature of the ion volume surface may be another variable, such as choice of the CI reagent gas, pressure, and source temperature, which can be utilized to optimize certain mass spectra.

Experimental

A porphyrin standard (2,3,7,8,12,13,17,18,-octaethyl-21H,23H-porphine) known as OEP, and 8 metalated OEP derivatives were studied under positive H_2CI and positive NH_3CI conditions. The free-base OEP, and Co(II), Cr(III), Cu(II), Fe(III), Mg(II), Mn(III), Ni(II), and Zn(II) OEP derivatives were obtained from the Aldrich Chemical Company. The metal(III) porphyrins all contained one axial chloride ligand. All of the experiments were performed on a Finnigan MAT TSQ45 triple quadrupole mass spectrometer, with removable CI ion volumes. The source was pressurized with 0.9 torr H_2 for the H_2CI experiments, and 0.4 torr NH_3 for the NH_3CI experiments. For the direct exposure probe (DEP) experiments, the porphyrin samples were dissolved in methylene chloride and deposited on the rhenium filament of the DEP such that less than 1 μg of sample was analyzed. The DEP was then inserted into the ion source and heated from ambient to 1350 °C at 600 °C/min. For the solids probe experiments, about 2 μg of porphyrin was dissolved in 5 μL of methylene chloride. This solution was placed in a 5 μL glass vial. The solvent was allowed to evaporate at 50 °C. The vial was inserted into the solids probe and heated from 90 to 400 °C at 100 °C/min. Collision energies and argon pressures were 25 eV and 1.0 mtorr.

Surface-induced Decomposition

When porphyrins or metalloporphyrins are introduced via a DEP into a high pressure NH_3 or H_2 chemical ionization source, two positive ion peaks typically arise (Figure 6-4). The negative ion peak(s) which arise are discussed in Chapter 7. The first peak occurs as the compound vaporizes off the probe filament (about 250 to 350 °C). As the DEP is further heated to a maximum temperature of 1350 °C, the second peak appears, beginning around 900 °C. This second peak results from the condensed porphyrins on the ion volume surfaces reducing and decomposing to form pyrroles. These pyrroles vaporize as the ion volume temperature increases, and are ionized by reagent gas ions.

The positive NH_3CI and H_2CI mass spectra of both free-base porphyrins and of metalloporphyrins are characterized by these two peaks. When a solids probe is employed for sample introduction, the positive NH_3CI mass chromatograms of the protonated Mg(II) OEP ion and a representative monopyrrolic ion (m/z 138) do not track each other (Figure 6-5). If the pyrrolic ions were formed by fragmentation of the protonated porphyrin ion in the gas phase, the intensity of the pyrrolic ions should increase and decrease with that of the molecular ion (Kurlansik et al., 1984). If the pyrrolic ions arise out of fragmentation of the protonated porphyrinogen ion in the gas phase, the mass chromatograms of the pyrrolic ions should track that from the protonated porphyrinogen ion. In fact, protonated porphyrinogen ions were not even detected whenever samples were introduced via a solids probe. This evidence supports the idea that pyrroles arise out of surface-induced reduction and decomposition of porphyrins.

Positive NH_3CI mass chromatograms from Co(II) OEP introduced by the DEP indicate two separate peaks as the DEP is heated from ambient to 1350 °C (Figure

Figure 6-4.

Mass chromatograms of the reconstructed ion current (RIC) from OEP under both positive and negative H_2CI conditions with DEP introduction

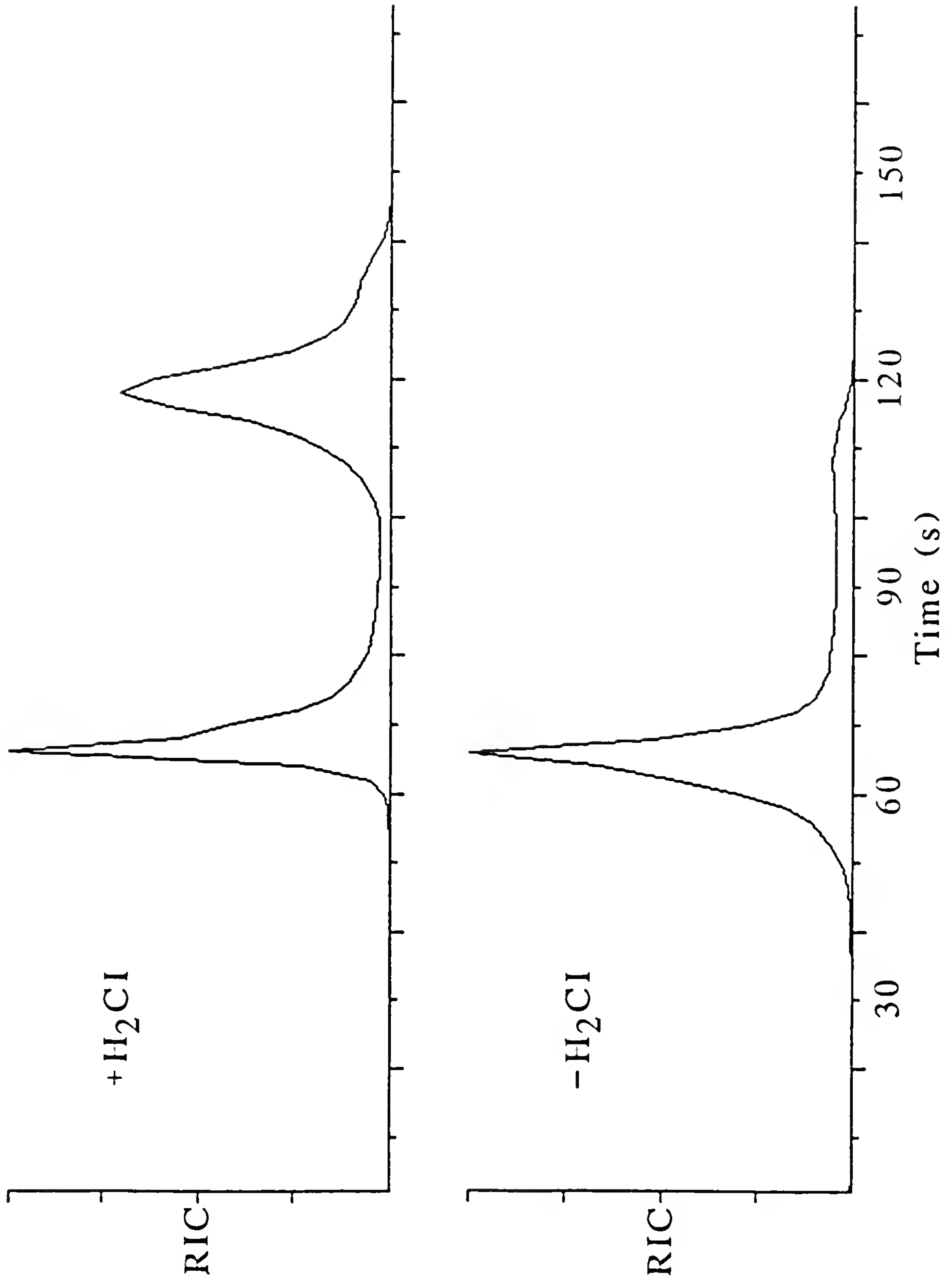
+H2CI
RIC
-H2CI
RIC
30
60
90
120
150
Time (s)

Figure 6-5.

Mass chromatograms of the protonated molecular ion (m/z 557) and a monopyrrolic ion (m/z 138) from Mg(II) OEP upon NH_3CI with solids probe introduction

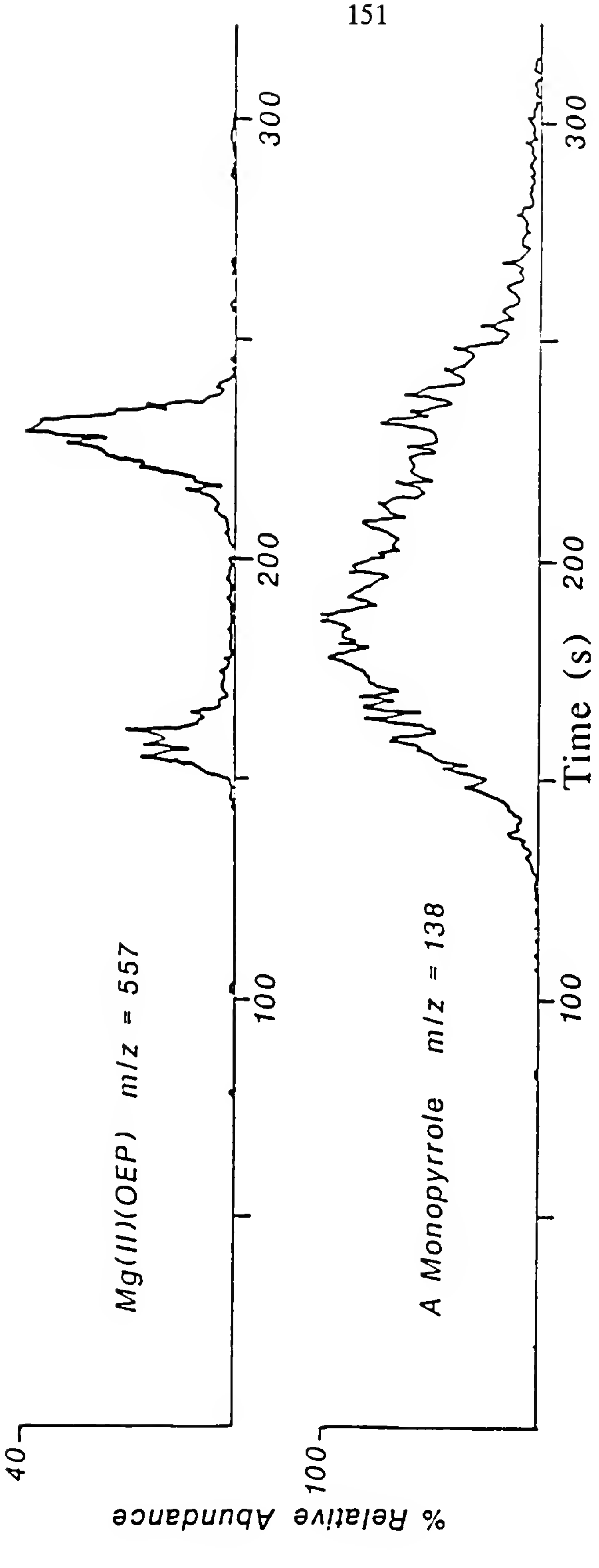
% Relative Abundance
40
100
Mg(III)(OEP) m/z = 557
A Monopyrrole m/z = 138
100
200
300
100
200
300
Time (s)

6-6). The first peak, appearing as the DEP reaches about 300 °C, corresponds to the Co(II) OEP vaporizing from the probe filament. It consists of the protonated molecular ion, m/z 592, as well as small relative abundances of monopyrrolic ions such as m/z 136 and m/z 138 which result from the reduction and cleavage of the meso-bridge bonds. These monopyrrolic ions in the first peak probably do not result from gas phase reactions involving protonated molecular ions because their mass chromatograms do not track that from the protonated molecular ion. They could conceivably result from gas phase reactions involving protonated porphyrinogen ions. Collisionally activated dissociation of porphyrinogen ions has been shown to result in pyrrolic ions (Chapter 8), but this has not been shown for metalloporphyrins. In fact, in this present study, parent ion mass spectra of m/z 136, 138, and 140 from OEP and Co(II) OEP did not yield significant abundances of parent ions. This suggests that these pyrroles may arise out of some other mechanism such as CI of products of surface-induced decomposition of porphyrins on the rhenium filament itself, or on the stainless steel posts of the filament. The two posts are connected to the filament, and probably reach the necessary temperatures for reduction, decomposition, and vaporization of pyrroles before other surfaces within the ion volume.

The second peak appears when the DEP reaches about 900 °C, and results from monopyrroles vaporizing off the ion volume. The mass spectra from each of these mass chromatographic peaks indicate that surface-induced decomposition can be quite useful for structure elucidation, because it greatly enhances pyrrolic ion

Figure 6-6.

Mass chromatograms of monopyrrolic ions (m/z 136, m/z 138, and m/z 140), the protonated molecular ion (m/z 592), and the reconstructed ion current (RIC) from Co(II) OEP upon positive NH_3CI with DEP introduction. Spectra from the intervals marked A and B are shown in Figure 6-7.

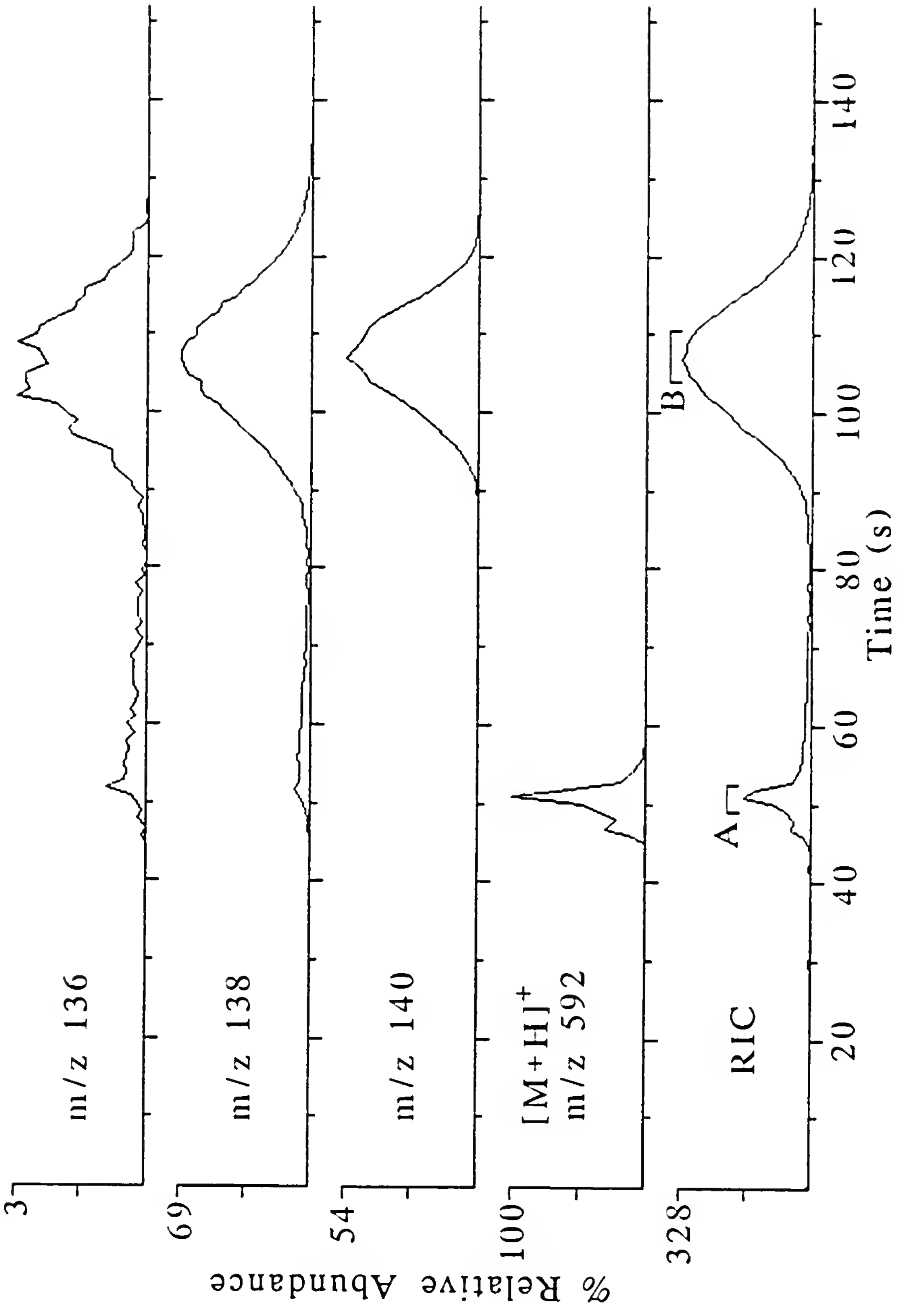
m/z 136
m/z 138
m/z 140
[M+H]$^+$
m/z 592
RIC
3
69
54
100
328
% Relative Abundance
A
B
20
40
60
80
100
120
140
Time (s)

formation (Figure 6-7). The mass spectrum from the first peak alone does not yield much pyrrolic structure information, and there may not be enough pyrrolic ion intensity in this peak on which to perform subsequent MS/MS studies. The mass spectrum from the second peak yields much higher relative abundances of pyrrolic ions, complementing the limited structural information obtainable from the first peak.

This second peak contains no protonated molecular ions, but does include m/z 140, a reduced monopyrrole. This particular monopyrrolic ion was not detected in the first peak. It arises only after the porphyrin molecule interacts with the surface of the ion volume. Daughter ion mass spectra indicate that this monopyrrolic ion is a reduced form of the m/z 136 and m/z 138 monopyrroles resulting from surface-induced reduction (Figure 6-8). These results do not rule out the possibility of some reduction and fragmentation occurring in the gas phase. For instance, if m/z 136 and m/z 138 ions, which are seen in the first mass chromatographic peak, result from decomposition on the filament posts, reduction to m/z 140 may be expected to occur on these posts as well. This work does indicate, however, that the primary mechanism by which the monopyrroles arise is the surface-induced decomposition of porphyrins.

Further evidence of this surface-induced decomposition mechanism is obtained when the porphyrin or metalloporphyrin solution is deposited directly on the inner surface of the CI ion volume pressurized with 0.9 torr H_2. In each case, the same

Figure 6-7.

Positive NH_3CI mass spectra from intervals marked A and B in Figure 6-6.

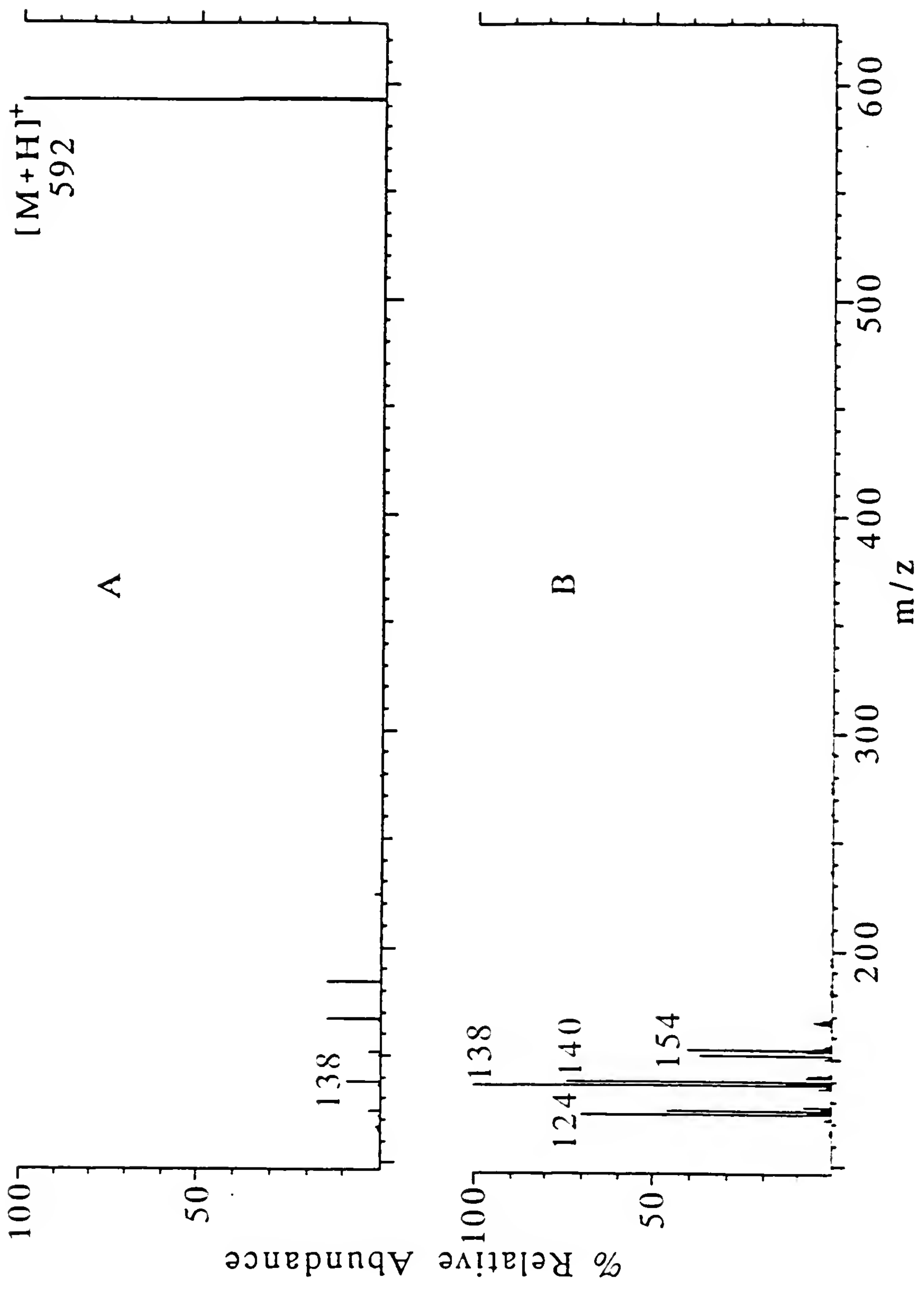
A
[M+H]$^+$
592
138
B
138
124
140
154
100
50
100
50
% Relative Abundance
200
300
400
500
600
m/z

Figure 6-8.

Positive H_2CI/MS/MS daughter ion mass spectra of monopyrroles from OEP:
A. parent ion is m/z 136
B. parent ion is m/z 138
C. parent ion is m/z 140

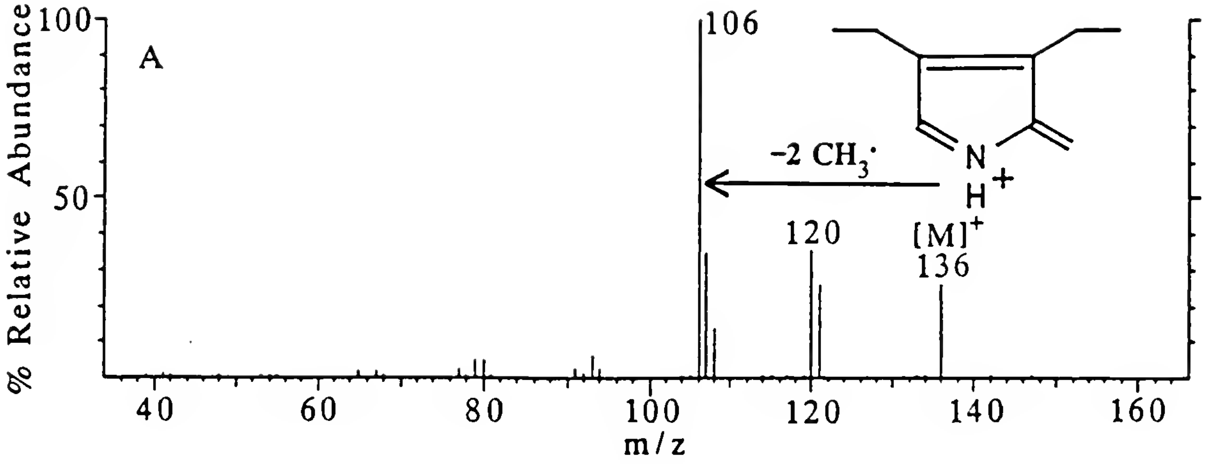
% Relative Abundance
100
50
A
106
-2 $CH_3^\cdot$
N
H+
120
[M]+
136
40
60
80
100
120
140
160
m/z

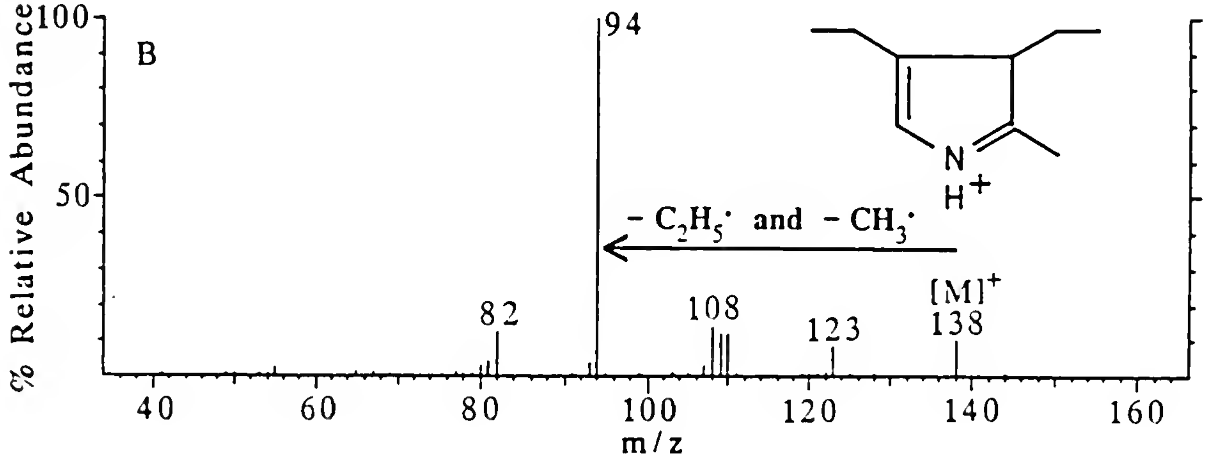
% Relative Abundance
100
50
B
94
N
H+
- $C_2H_5^\cdot$ and - $CH_3^\cdot$
82
108
123
[M]+
138
40
60
80
100
120
140
160
m/z

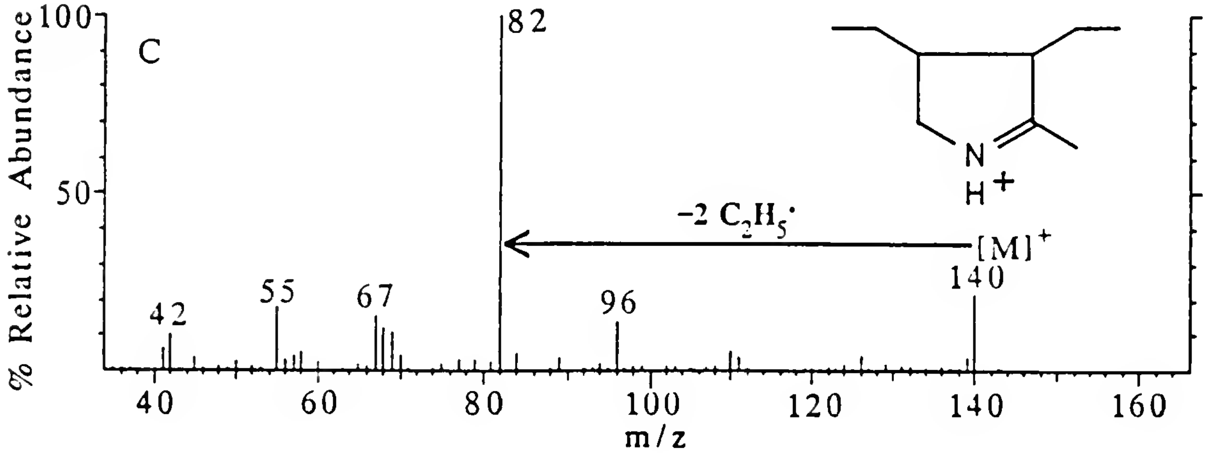
% Relative Abundance
100
50
C
82
N
H+
-2 $C_2H_5^\cdot$
[M]+
140
42
55
67
96
40
60
80
100
120
140
160
m/z

amount of porphyrin solution is deposited on the ion volume wall which is placed on the DEP filament for conventional DEP experiments. Upon evaporation of the methylene chloride solvent, 0.5 to 1 μg of solid porphyrin remains condensed on the stainless steel surface. When a clean DEP filament is inserted into the H_2 plasma and heated, only one mass chromatographic peak is observed. This peak appears when the DEP filament reaches temperatures exceeding 900 °C. The mass spectra from these high temperature peaks are very similar to those mass spectra from the second (high temperature) peaks in conventional DEP experiments for both OEP (Figure 6-9) and Co(II) OEP (Figure 6-10). This is certainly strong evidence in favor of the surface-induced decomposition mechanism for porphyrins under high pressure CI conditions. For both free-base OEP and Co(II) OEP, monopyrrolic and dipyrrolic ions are observed when porphyrins are analyzed by direct deposition on the ion volume surface. No significant abundances of ions of m/z greater than the dipyrrolic ions are observed in either the conventional or direct deposition experiments under the conditions specified, although the mass range scanned extended past the m/z of the molecular porphyrinogen ions. This may be because the maximum attainable temperature of the ion volume walls when the DEP filament is heated to 1350 °C is too low for the less volatile higher molecular weight species to vaporize. Pyrrolic ions have also been observed in a sector mass spectrometer when a free-base porphyrin sample was deposited directly on the ion source repeller plate which was gradually heated by the ionization filament (Van Berkel et al., in press a).

Figure 6-9.

Positive H_2CI mass spectra of OEP:
A. OEP deposited on DEP filament
B. OEP deposited directly on ion volume wall

The inset RIC traces show the interval over which the mass spectra were obtained.

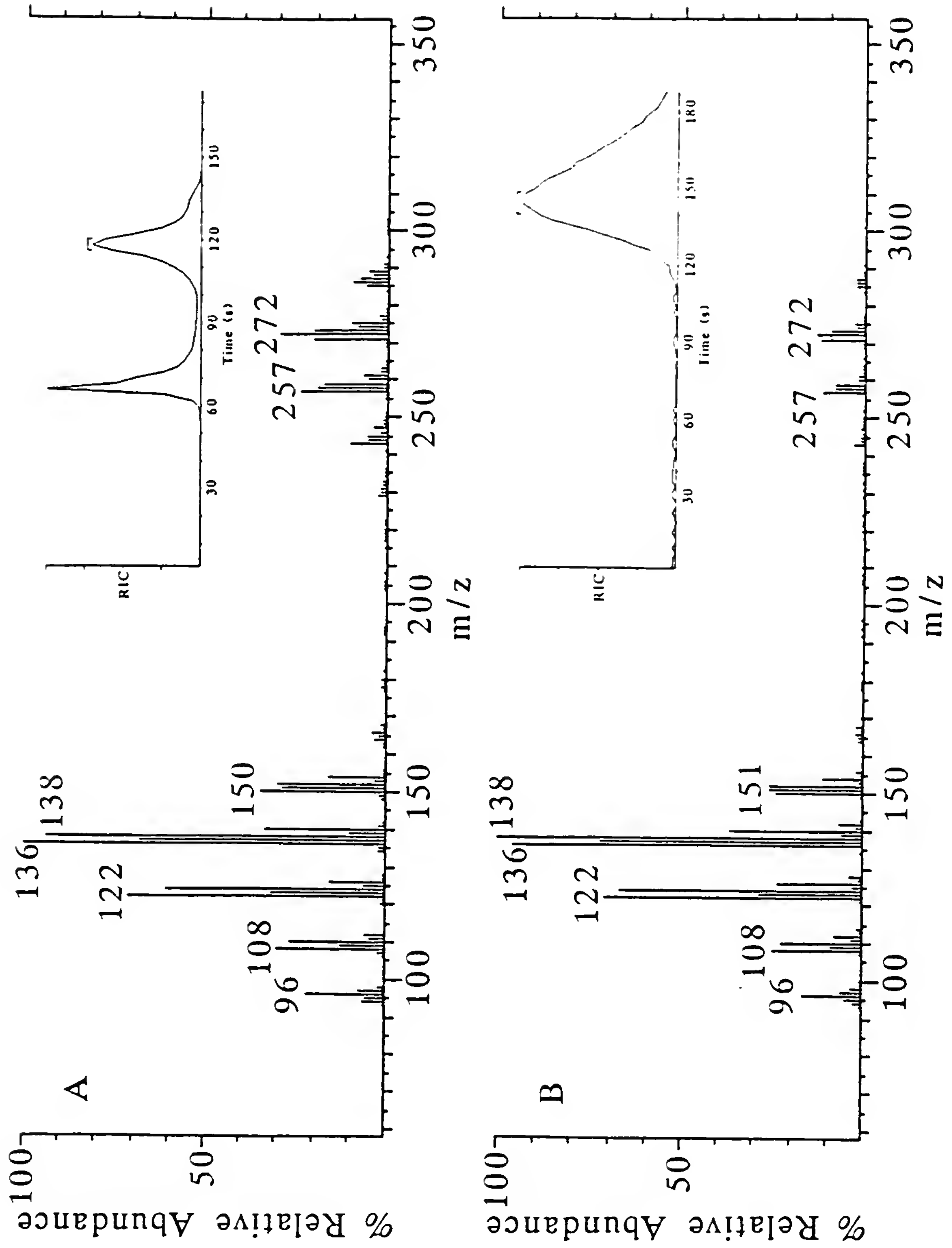
A
% Relative Abundance
100
50
96
108
122
136
138
150
257
272
m/z
100
150
200
250
300
350
RIC
Time (s)
30
60
90
120
150
B
% Relative Abundance
100
50
96
108
122
136
138
151
257
272
m/z
100
150
200
250
300
350
RIC
Time (s)
30
60
90
120
150
180

Figure 6-10.

Positive H_2CI mass spectra of Co(II) OEP:
A. Co(II) OEP deposited on DEP filament
B. Co(II) OEP deposited directly on ion volume wall

The inset RIC traces show the interval over
which the mass spectra were obtained.

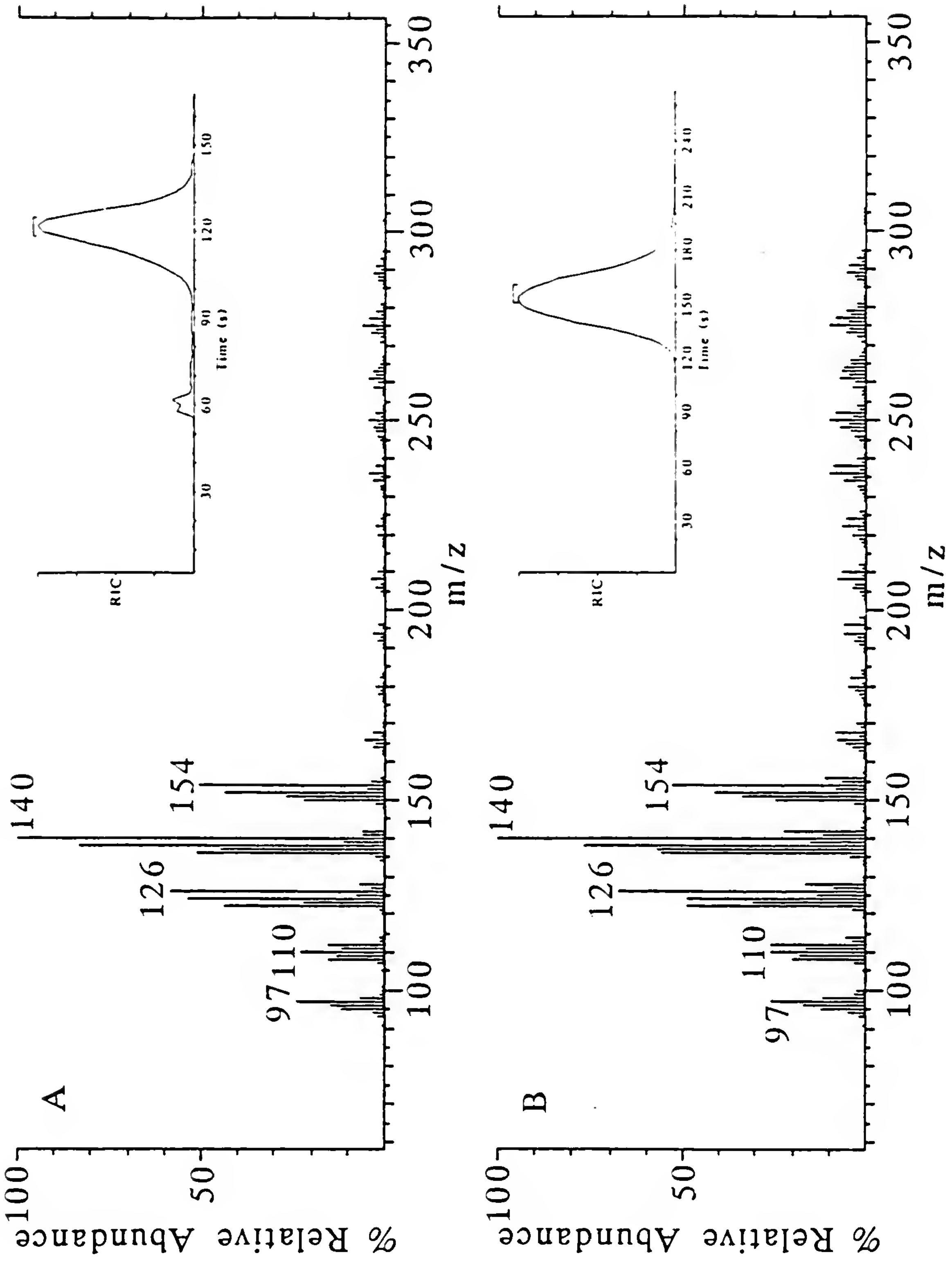
A
B
% Relative Abundance
100
50
m/z
100
150
200
250
300
350
97
110
126
140
154
RIC
Time (s)
30
60
90
120
150
180
210
240

The reagent gas does play a major role in the surface-induced decomposition of porphyrins under CI conditions. The more reducing the reagent gas, the greater the extent to which pyrrolic ions form. Strongly reducing reagent gases such as hydrogen and ammonia are much more efficient than methane or isobutane in yielding pyrrolic ions upon chemical ionization of porphyrins in a high pressure CI source, yet pyrrolic ions are observed in each instance (Eglinton et al., 1979; Van Berkel et al., in press a). Electron ionization does not result in significant abundances of pyrroles vaporizing off of the ion source walls, even though porphyrin/surface interactions are expected to occur under EI conditions. High DEP temperature peaks of low intensity are seen in EI experiments, but they consist of hydrocarbon homologs of less than m/z 100. Any porphyrin molecules which do condense on the EI ion volume surface presumably are not reduced to porphyrinogens due to the lack of a high pressure of a reducing gas (NH_3 or H_2). Otherwise, both porphyrinogens and pyrrole fragments would vaporize, ionize, and be detected, as these species are much more volatile than are porphyrins.

The Effect of the Metal on Positive CI of Metalloporphyrins

An intriguing question which remains is whether or not metalloporphyrins are first reduced to metalated porphyrinogens, or if they demetalate to free-base porphyrins before reduction to porphyrinogens. This is significant in terms of describing the process of surface-induced decomposition of porphyrins. If a metalloporphyrin must demetalate prior to reduction and decomposition, then metalloporphyrins which demetalate most easily may be predicted to be more efficient at yielding pyrroles than metalloporphyrins which are more stable toward demetalation. On the other hand, if metalloporphyrins are reduced to metalated porphyrinogens and then decompose, the stability of the meso-bridge bonds of the metalated porphyrinogen becomes an important consideration.

Evidence indicating that metalloporphyrins demetalate prior to reduction and decomposition may come from MS/MS studies of reduced metalloporphyrin ions in which they fragment very differently than free-base porphyrinogen ions. Upon CAD, free-base porphyrinogen ions yield mono-, di- and tri-pyrrolic ions due to cleavage of the reduced meso-bridge bonds (Van Berkel et al., in press a; Chapter 8). In a study involving CAD of reduced metalloporphyrins, however, Sundararaman et al. did not report pyrrolic daughter ions (1984). Instead, the dihydro, tetrahydro, and hexahydro metalated species studied fragmented upon CAD via α- and β-cleavages of peripheral substituents, indicating that one or more of the pyrrole rings were reduced instead of the meso-bridge bonds. This could support the idea that metalloporphyrins first demetalate and then decompose on the surfaces as free-base porphyrins, because when metalloporphyrins decompose on the ion volume surfaces, meso-bridge bonds are cleaved rather than peripheral substituents. On the other hand it is possible that reduced metalated porphyrins isomerize differently in the gas phase than those condensed on the ion volume surfaces.

It is difficult to compare data from reduced free-base and reduced metalated porphyrins because reduced metalated porphyrinogen ions do not form as readily in the source as free-base porphyrinogen ions. Sundararaman et al. reported daughter ion mass spectra of relatively small $[M + 6H]^+$ peaks observed in the H_2CI mass spectra of Ni(II), Cu(II), and O=V(IV) porphyrins (1984). However, in the Ni(II) and Cu(II) cases, it is unclear if these ions are actually $[M + 6H]^+$ ions and not $[M+4H]^+$ containing a higher isotope of the metal. With copper and nickel metalloporphyrins, the natural abundance of the metal isotopes must be considered. They may have actually been fragmenting $[M+4H]^+$ ions from ^{65}Cu and ^{60}Ni complexes, instead of the $[M+6H]^+$ ions from ^{63}Cu and ^{58}Ni complexes which they reported. The relative abundances of the naturally occurring ^{65}Cu and ^{60}Ni isotopes are 30.9% and 26.2%, respectively. The relative abundances of the naturally occurring ^{63}Cu and ^{58}Ni isotopes are 69.1% and 67.8%, respectively. Studies in this laboratory focussing on NH_3CI and H_2CI of cobalt(II) porphyrins (selected because cobalt is monoisotopic) failed to yield positively charged cobalt porphyrinogen ions with either DEP or solids probe introduction. In the case of the vanadyl complexes, losses of H_2O were reported in the daughter ion mass spectrum of $[M + 6H]^+$, suggesting that two of the six additional hydrogens in the reduced vanadyl complex are bound to the oxygen atom. In any event, the structures of reduced metalloporphyrins remain unclear. More work is needed to determine the role of the metal ion in surface-induced decomposition of metalloporphyrins under positive CI conditions.

Just as the nature of the metal ion in metalloporphyrins was shown to have an effect on the extent to which they formed doubly charged fragment ions under EI conditions, chelated metals may also affect the extent to which metalloporphyrins fragment or decompose under CI conditions. If metalloporphyrins demetalate prior to reduction and decomposition to pyrroles, then the degree of pyrrole formation should be proportional to the ease of demetalation. In order to determine whether the chelated metal has an effect on positive chemical ionization mass spectra of metalloporphyrins, NH_3CI/MS experiments were performed with a solids probe for a suite of 8 metalated OEP derivatives, and free-base OEP as well. The mass spectra for three of the porphyrins are shown in Figure 6-11. Each of the samples yielded the expected protonated molecular ions under NH_3CI conditions, although no ions with the chloride ligand intact appeared for the trivalent metal complexes. The samples also formed both monopyrrolic and dipyrrolic fragment ions together with a variety of NH_3 pyrrole adducts. Three of the metalloporphyrins, Fe(III) OEP Cl, Mn(III) OEP Cl, and Cu(II) OEP, are likely to undergo reduction in the ammonia plasma. In reducing solutions, Cu(II) porphyrins have been observed to be reduced to Cu(I) (Buchler, 1975). Under NH_3 desorption CI conditions, Cu(II) porphyrins have been observed to completely demetalate and fragment as metal-free porphyrins (Tolf et al., 1986), presumably due to reduction of Cu(II) to Cu(I),

Figure 6-11.

Positive NH_3CI mass spectra (with solids probe introduction) of:
A. Co(II) OEP
B. Zn(II) OEP
C. Mg(II) OEP

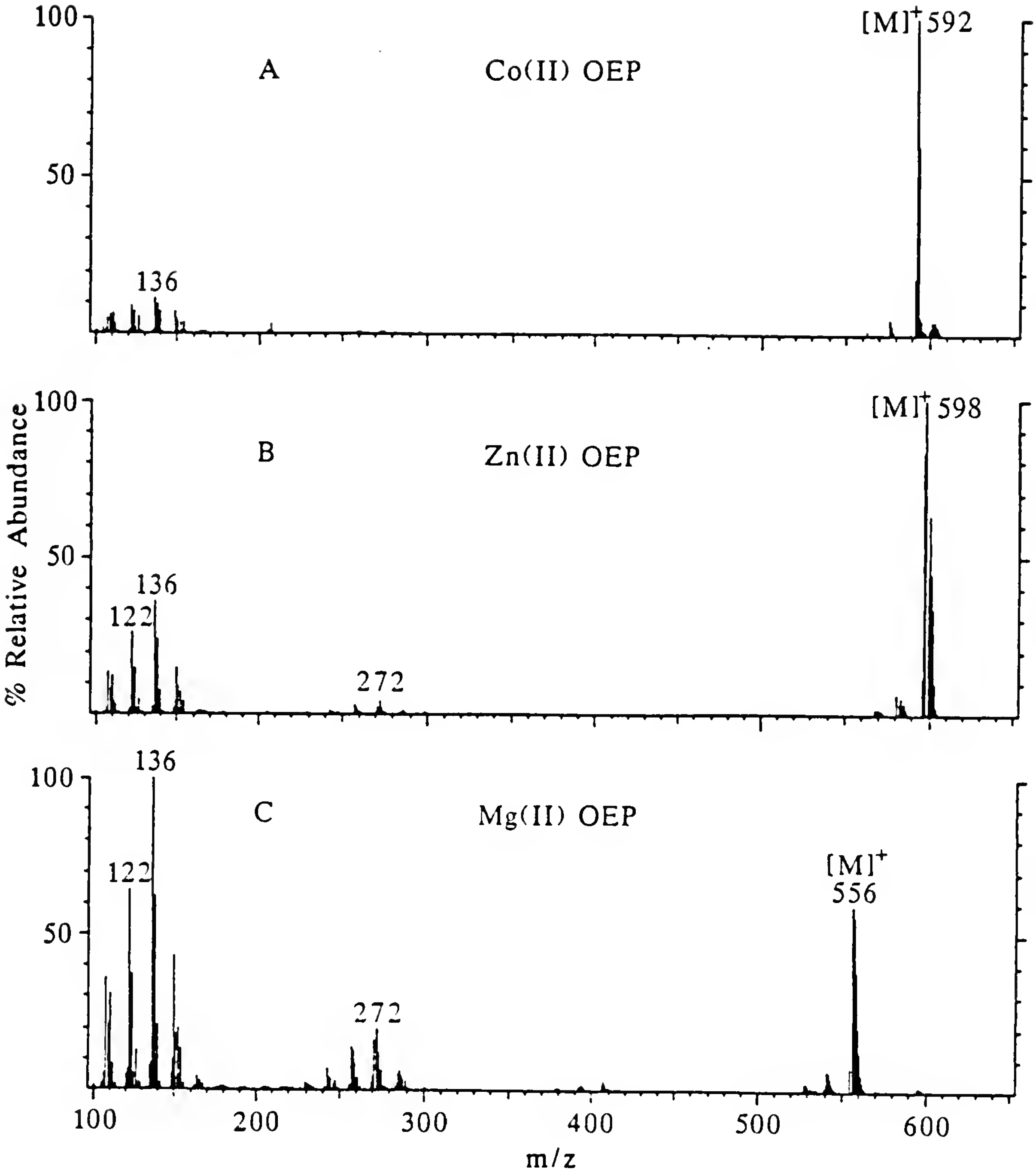
A
Co(II) OEP
[M]$^+$ 592
136
B
Zn(II) OEP
[M]$^+$ 598
122
136
272
C
Mg(II) OEP
[M]$^+$
556
122
136
272
% Relative Abundance
100
50
100
50
100
50
100
200
300
400
500
600
m/z

which is readily extruded from the macrocycle. If Cu(II) porphyrins are reduced under NH_3CI conditions, it is likely that Fe(III) and Mn(III) porphyrins are also reduced in the NH_3 plasma, as these metal ions have higher standard reduction potentials than Cu(II) in solution (CRC Handbook of Chemistry and Physics, 1979):

$$\mathrm{Cu(II)} + e^- \leftrightarrow \mathrm{Cu(I)} \qquad E^\circ = +0.158\ \mathrm{V}$$

$$\mathrm{Fe(III)} + e^- \leftrightarrow \mathrm{Fe(II)} \qquad E^\circ = +0.770\ \mathrm{V}$$

$$\mathrm{Mn(III)} + e^- \leftrightarrow \mathrm{Mn(II)} \qquad E^\circ = +1.51\ \mathrm{V}$$

The extent of pyrrole formation is dependent on the specific metal in the metalloporphyrin, as shown by the nomograms in Figure 6-12. The first nomogram displays the Buchler Stability Indices for metal ions from the metalloporphyrins studied, including the values for Mn(II) and Fe(II) metalloporphyrins which likely form upon reduction of the Mn(III) and Fe(III) metalloporphyrins in the source. No Buchler Stability Index was calculated for Cu(I) metalloporphyrins because Cu(II) metalloporphyrins demetalate upon reduction of Cu(II) to Cu(I). The other three nomograms demonstrate correlations between the intensities, I, of the protonated molecular ion, and of monopyrroles of m/z 124, of m/z 138, and of the sum of the intensities of monopyrroles. While the order of the metalloporphyrins in each nomogram is not exactly the same, the trend is that metalloporphyrins of greater stability index yield lower relative abundances of pyrrolic ions, compared to the protonated molecular ion. These nomograms also offer evidence that Cu(II) OEP is reduced and demetalated in the NH_3 plasma. While both Cu(II) OEP and

Figure 6-12.

Nomograms comparing the effect of metals in metalloporphyrins under positive NH_3CI conditions on the extent of monopyrrole formation with the Buchler Stability Index. The relative intensity of a particular ion is denoted by I, while M denotes the molecular ion.

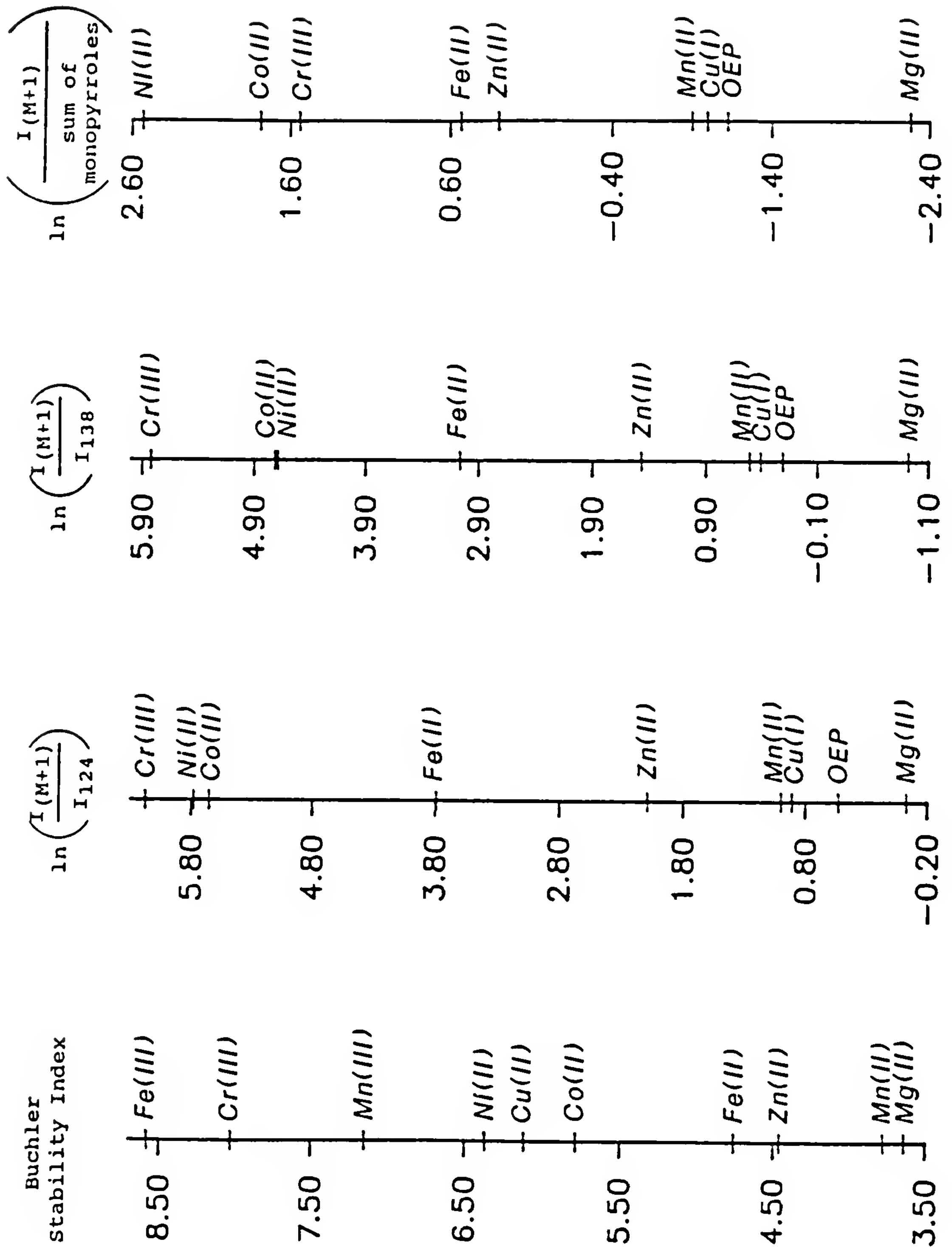
Buchler Stability Index
8.50
7.50
6.50
5.50
4.50
3.50
Fe(III)
Cr(III)
Mn(III)
Ni(II)
Cu(II)
Co(II)
Fe(II)
Zn(II)
Mn(II)
Mg(II)
$\ln\left(\frac{I_{(M+1)}}{I_{124}}\right)$
5.80
4.80
3.80
2.80
1.80
0.80
−0.20
Cr(III)
Ni(II)
Co(II)
Fe(II)
Zn(II)
Mn(II)
Cu(I)
OEP
Mg(II)
$\ln\left(\frac{I_{(M+1)}}{I_{138}}\right)$
5.90
4.90
3.90
2.90
1.90
0.90
−0.10
−1.10
Cr(III)
Co(II)
Ni(II)
Fe(II)
Zn(II)
Mn(II)
Cu(I)
OEP
Mg(II)
$\ln\left(\frac{I_{(M+1)}}{\text{sum of monopyrroles}}\right)$
2.60
1.60
0.60
−0.40
−1.40
−2.40
Ni(II)
Co(II)
Cr(III)
Fe(II)
Zn(II)
Mn(II)
Cu(I)
OEP
Mg(II)

Ni(II) OEP have very similar stability indices, Cu(II) OEP yields significantly higher intensities of pyrroles than does Ni(II) OEP. In fact, Cu(II) OEP behaves very much like metal-free OEP, as is expected if Cu(II) is reduced to Cu(I) and extruded from the macrocycle. The correlation of pyrrole formation for Fe(III) OEP Cl and Mn(III) OEP Cl is much better with Fe(II) OEP and Mn(II) OEP than with Fe(III) OEP Cl and Mn(III) OEP Cl, indicating that these two trivalent metal ions are also reduced under NH_3CI conditions, as expected.

This study is meant only to convey general trends in behavior of various metalloporphyrins under NH_3CI conditions. It cannot be expected to yield the strong correlation that the effect of the metals have upon EI fragmentation because formation of pyrroles does not occur via gas-phase fragmentations. Surface-induced decomposition reactions cause several problems for quantitation with the instrument used in these studies. First of all, the nature of the surface of the ion volume may not be exactly the same for all of the metalloporphyrins analyzed. Between analyses of metalloporphyrins, clean glass vial blanks were analyzed, and no pyrrole or porphyrin ions were detected in the background. However, this is no indication that metalloporphyrin or porphyrinogen molecules were not still condensed on the surface of the ion volume. It is likely that various sample molecules were indeed condensed on the ion volume, but the ion volume could not be heated enough to entirely vaporize them or their decomposition products. If the ion volume was removed after each experiment and cleaned, there is no guarantee that the ion volume would be placed in exactly the same position in the ion source. Any slight deviation in its position with respect to the extraction lenses and ionizer filament could result in different ionization conditions for each analysis. It is not known how much of each sample remained undetected on the ion volume surface, but the data were obtained consistently for each porphyrin, and should provide information on the relative effects of various metals under NH_3CI conditions. It is clear that the chelated metals do have an effect on the positive NH_3CI mass spectra of metalloporphyrins, but complications due to reduction of the oxidation state of the metal, and to surface-induced decomposition make this effect difficult to quantitate. The effect of the metal ions on the extent to which metalloporphyrins decompose on the ion volume surface under positive CI conditions appears to depend on the stability of the metalloporphyrin toward demetalation. This is added evidence suggesting that metalloporphyrins demetalate prior to reduction and decomposition on the metal ion volume surface in the positive CI source.

Another difference between the positive CI mass spectra of metalloporphyrin ions and of free-base porphyrin ions also appears to involve the metal. In the present study, the monopyrrolic ion regions in the mass spectra of free-base and metalated porphyrins are slightly different. The mass spectra from surface-induced decomposition of Co(II) OEP in Figure 6-10 display relatively abundant reduced monopyrrolic ions such as m/z 126, 140, and 154. Conversely, the mass spectra from surface-induced decomposition of free-base OEP in Figure 6-9 display greater relative abundances of monopyrrolic ions such as m/z 122, 136, and 150. Although it is quite apparent that the metal ions have significant effects on the positive CI mass spectra of metalloporphyrins, much about their specific role in the surface-induced decomposition process remains to be determined.

Conclusions

Positive chemical ionization provides structural information about porphyrins which is complementary to that obtainable from EI experiments. Under both $+H_2CI$ and $+NH_3CI$ conditions, porphyrins and metalloporphyrins decompose to a significant extent on the ion volume surface, yielding pyrrolic ions. These pyrrolic ions are useful for sequencing the pyrrole rings around the porphyrin macrocycle. While this work does not rule out the possibility of limited reduction and decomposition of porphyrins and metalloporphyrins in the gas phase, it does demonstrate that surface-induced decomposition mechanisms are the dominant processes involved in pyrrole formation. A better understanding of these processes allows the CI techniques to be more useful for structure elucidation.

This work leads to interesting implications concerning mass spectra of other types of nonvolatile compounds which may undergo surface-induced decomposition reactions within the ion source. Mass spectrometric analyses of compounds of higher molecular weight and lower volatility are becoming increasingly important lately, especially those of polymers and biomolecules. The surfaces in the ion source may play a major role in the manner in which these molecules fragment or decompose. Perhaps the nature of the ion volume surface is a variable such as choice of the CI reagent gas, pressure, and source temperature, which can be utilized to optimize certain mass spectra.

The chelated metal is observed to have an effect on the extent to which various metalloporphyrins demetalate and decompose on the ion volume; however, this effect is difficult to quantitate. First of all, the oxidation states of the metals are difficult to discern in the CI reagent gas plasma, so some physical constants are difficult to assign to them. Secondly, the ion volume cannot be heated enough to vaporize all the porphyrins and products which are condensed on it. Thus, it is difficult to judge the extent to which decomposition reactions actually took place. However, it is possible to observe trends in the positive CI mass spectra of metalloporphyrins. The lower the Buchler stability index of a metalloporphyrin, the greater its tendency to form pyrrolic ions. The oxidation states of metals may not be known for some metalloporphyrins in the CI reagent gas plasma, making determination of the Buchler stability index difficult. In many cases, such as for Cu(II), Fe(III), and Mn(III) OEP derivatives under NH_3CI conditions, the metals are probably reduced. This is an important consideration in calculating the appropriate stability index values.

CHAPTER 7

ELECTRON CAPTURE NEGATIVE CHEMICAL IONIZATION OF PORPHYRINS

Introduction

Electron capture negative chemical ionization (ECNCI) occurs in a CI plasma when a neutral analyte molecule picks up a thermal electron. This ionization technique is generally two to three orders of magnitude more sensitive than positive CI techniques for compounds with high electronegativity and large cross sections for electron capture (Hunt et al., 1976). Compounds which do not contain electronegative species are ionized inefficiently in this manner. Halogenated compounds are typically the best candidates for ECNCI, although molecules containing other heteroatoms are often ionizable by this method as well. Alkyl porphyrins contain four nitrogen atoms, and are good candidates for ECNCI. Few reports concerning ECNCI of porphyrins appear in the literature, most of which deal with metalloporphyrins (Henis et al., 1981; Dillow et al., 1986; Dillow and Gregor 1988). This chapter deals with some fundamental aspects of ECNCI mass spectrometric analyses of both free-base and metalated porphyrins.

One of the motivations for this work is to determine the value of ECNCI for structure elucidation of porphyrins. An ionization technique is desired which would yield exclusively molecular ions in the ion source. Such an ionization technique would generate carbon-number range information about complex mixtures of porphyrins, such as geoporphyrins. It would also allow subsequent analyses by MS/MS daughter ion scans of strictly the molecular ions in question. Positive chemical ionization mass spectra of porphyrins yields molecular and/or protonated molecular ions, but can also yield abundant pyrrolic ions resulting from CI of surface-induced decomposition products (Chapter 6). This results in reduced sensitivity, as ion current is spread out over a variety of decomposition product ions. The pyrrolic ions do not offer structural information about individual porphyrins in complex mixtures because it is impossible to assign them to specific precursor porphyrin structures. Daughter ion mass spectra of positively charged porphyrin molecular ions produced in a CI plasma yield structural information about peripheral substituents, but not their sequence around the macrocycle (Chapter 8). This information is obtainable from daughter ion mass spectra of hexahydro porphyrin (porphyrinogen) ions, but such ions do not form abundantly from metalated porphyrin derivatives (Chapter 6). Electron ionization (EI) of porphyrins yields abundant singly and doubly charged molecular and fragment ions (Chapter 5). Again, sensitivity is reduced because ion current is spread out over a variety of fragment ions. The mass spectrometric analysis of a complex mixture of geoporphyrins is hampered when true molecular ions are indistinguishable from fragment ions of higher molecular weight geoporphyrins. For example, in the reports of EI/MS/MS daughter ion mass spectrometric analyses of complex mixtures of geoporphyrins (Johnson et al., 1986; Quirke et al., 1989), the mass-to-charge ratio (m/z) of the selected parent ion may actually correspond to both a molecular ion and a fragment ion from a higher molecular weight geoporphyrin. This is a potential interference in such analyses, where the goal is to obtain structural information strictly from the molecular geoporphyrin ions, and may limit such techniques to obtaining structural information from the higher carbon-number species in a mixture. The limitations inherent in EI and positive CI mass spectrometric analyses of porphyrins suggest the characterization of other ionization methods. The work in this chapter addresses the question of the utility of ECNCI of porphyrins for structure elucidation.

Negative ions arise out of very different processes than do positive ions in the CI source, but both form at the same time. Ions of both polarities can be monitored during the same experiment through the use of two conversion dynodes in front of the electron-multiplier (EM). The positively biased (+3 kV) dynode converts negative ions impinging upon it to positive ions which can be detected by the EM; positive ions striking the -3 kV dynode will produce negative ions or electrons which can be detected by the more positively biased EM. These conversion dynodes allow acquisition of pulsed positive ion/negative ion chemical ionization (PPINICI) data (Hunt et al., 1976). This means that the data system can rapidly switch back and forth between acquisition of positive and negative ion mass spectra. The ECNCI mass spectra presented in this chapter were all obtained by PPINICI, allowing them to be compared to the corresponding positive ion mass spectra, which are better characterized for porphyrins.

Experimental

Free-base OEP (2,3,7,8,12,13,17,18,-octaethyl-21H,23H-porphine) and several metalated OEP derivatives were analyzed by electron capture negative hydrogen chemical ionization MS and MS/MS. The sources of the OEP, Mn(III) OEP Cl, O=V(IV) OEP, and Co(II) OEP were described in Chapter 6. The sources of the O=V(IV) porphyrins from demineralized shale was discussed in Chapter 4. The O=V(IV) porphyrins from the demineralized shale were stored dry overnight, as were all porphyrin samples discussed in this dissertation. All of the experiments were performed on a Finnigan MAT TSQ45 triple quadrupole mass spectrometer, with removable CI ion volumes. The source was pressurized with 0.9 torr H_2. The porphyrin samples were dissolved in methylene chloride and deposited on the rhenium filament of the DEP such that less than 1 μg of sample was analyzed. The DEP was then inserted into the ion source and heated from ambient to 1350 °C at 600 °C/min. Collision energies and argon pressures were 25 eV and 1.0 mtorr.

Structural Information from ECNCI

The electron capture negative hydrogen chemical ionization mass spectra of porphyrins from the first mass chromatographic peak differ drastically from the corresponding positive hydrogen chemical ionization mass spectra from the first mass chromatographic peak. A comparison of the $+H_2CI$ and $-H_2CI$ mass spectra averaged over the initial mass chromatographic peak in each case for Mn(III) OEP Cl is shown in Figure 7-1. The ECNCI mass spectrum is much simpler than the $+H_2CI$ mass spectrum. No fragment ions aside from the $[M-Cl]^-$ ion appear in the ECNCI mass spectrum. The $+H_2CI$ mass spectrum, however, also yields mono-, di-, and tri-pyrrolic ions, as well as a porphyrinogen ion at m/z 540 corresponding to loss of the metal and reduction of the porphyrin. Apparently, the pyrrole neutrals resulting from the surface-induced decomposition process described in Chapter 6 are not efficiently ionized by ECNCI.

In both mass spectra, the base peak arises from loss of the chloride ligand from the molecular ion, but only the ECNCI mass spectrum includes a relatively abundant molecular ion. In fact, in subsequent ECNCI analyses of Mn(III) OEP Cl, the molecular ion was often the base peak. In a study of the vapor absorption spectrum of Mn(III) OEP Cl, it was determined that the major gas phase species is actually Mn(II) OEP (Edwards et al., 1970). In that study, EI mass spectral data from Mn(III) OEP Cl indicated that Mn(II) OEP is about 200 times more abundant than Mn(III) OEP Cl in the gas phase. It appears that ECNCI provides a unique

Figure 7-1.

Hydrogen chemical ionization mass spectra of Mn(III) OEP Cl, m.w 622:
A. positive H_2CI
B. ECNCI

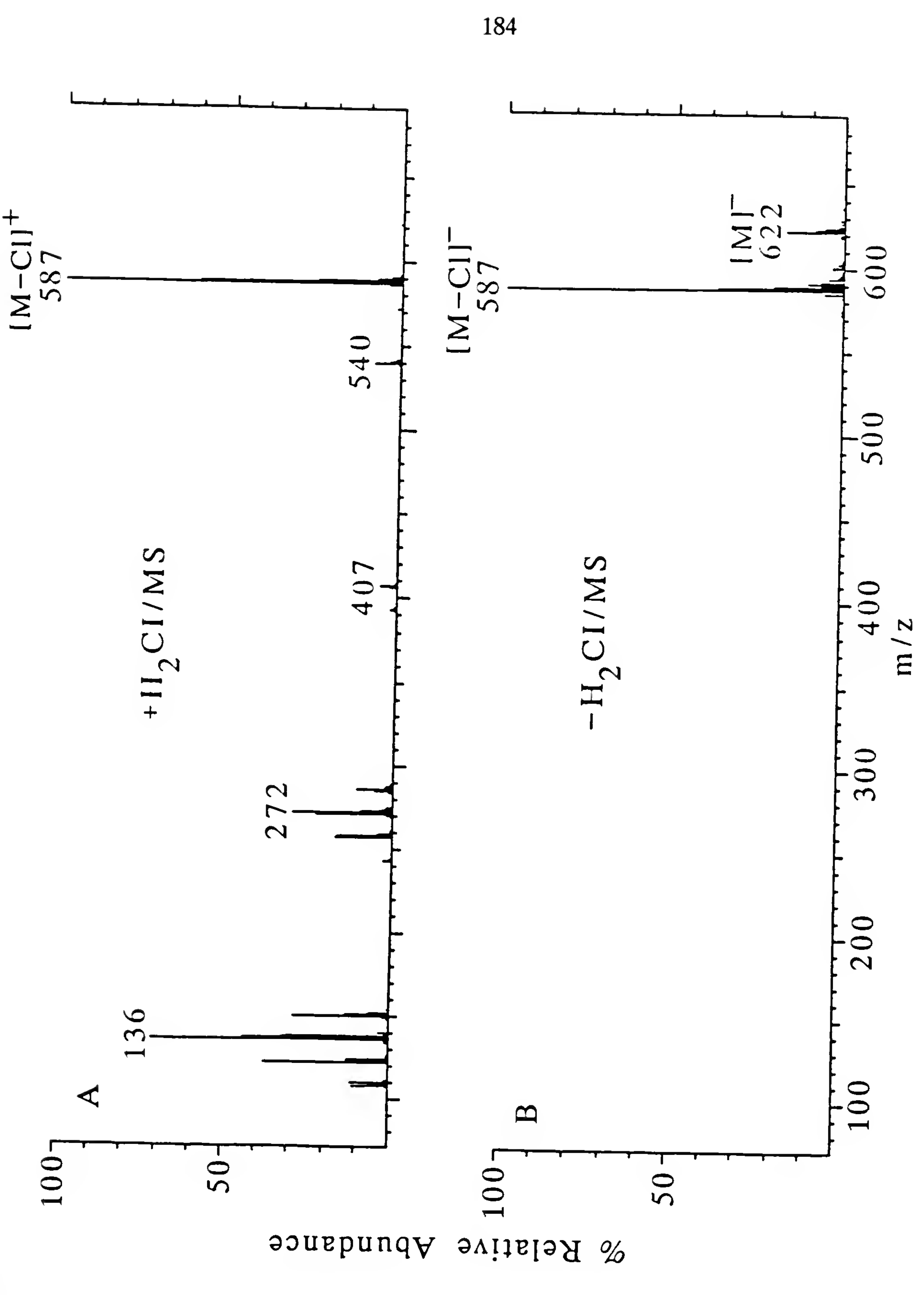
A
+H2CI/MS
136
272
407
540
[M−Cl]+
587
B
−H2CI/MS
[M−Cl]−
587
[M]−
622
100
200
300
400
500
600
m/z
100
50
100
50
% Relative Abundance

means of observing the relatively low abundances of Mn(III) OEP Cl, compared to Mn(II) OEP, in the gas phase. Electron capture negative chemical ionization is apparently quite efficient at ionizing the chlorinated species containing trivalent metal ions. Electron capture negative chemical ionization does not, however, provide information about the true relative abundances of ions in the ion source.

Just as negatively charged porphyrin ions are more stable than positively charged porphyrin ions toward fragmentation in the ion source, they are also more stable toward fragmentation by CAD. In fact, the $[M]^-$ and $[M - Cl]^-$ negative ions are quite difficult to fragment via CAD. As previously mentioned, ECNCI tends to be a more sensitive technique than positive CI for compounds with electronegative species. The ECNCI technique should be even more sensitive for porphyrin analysis compared to positive CI, because negative ion intensity is distributed over a narrower range of fragment ions. Data from PPINICI experiments with porphyrins analyzed under the conditions described in this chapter typically indicate that ECNCI is 10 to 50 times more sensitive than positive CI for porphyrins.

The simplicity of the ECNCI mass spectrum suggests that this technique would be ideal for obtaining carbon-number distribution data for complex mixtures of porphyrins, such as those in petroleum samples (Chapter 2). Most geoporphyrins are chelates of either Ni(II) or O=V(IV), and do not contain axial chloride ligands which are easily cleaved. They would be expected to produce only $[M]^-$ ions, with no significantly abundant fragment ions. Thus, geoporphyrin carbon-number distribution data from ECNCI should be unambiguous. Since these geoporphyrins are typically available for analysis in only trace amounts (ppm or less), the increased sensitivity of ECNCI would also be advantageous.

Hydrogenated Negative Ions

Unfortunately, ECNCI of O=V(IV) porphyrins suffers from a major drawback. The $-H_2CI$ mass spectra of O=V(IV) porphyrins can yield abundant hydrogenated ions. A comparison of the molecular ion region of the PPINICI mass spectra of O=V(IV) OEP with H_2 as the reagent gas is made in Figure 7-2. The $+H_2CI$ mass spectrum yields predominantly molecular ions ($[M]^+$, m/z 599) and protonated molecular ions (m/z 600), although impurities possibly due to Co(II) OEP appear at m/z 591 and m/z 592. The $[M]^-$ molecular ion in the ECNCI mass spectrum is overshadowed by hydrogenated product ions formed by addition of 2, 4, 6, and 8 hydrogens. The hydrogenated product ions appear at m/z 601, 603, 605, and 607. Formation of such hydrogenated product ions could make ECNCI analyses of complex mixtures of vanadyl geoporphyrins rather difficult, if not useless. Hydrogenation product ion envelopes from different vanadyl porphyrin structures could overlap, causing severe interferences.

This is shown in Figures 7-3 and 7-4 for O=V(IV) geoporphyrins extracted from a demineralized shale. Mass spectra from identical samples of O=V(IV) geoporphyrin mixtures that had been isolated by thin layer chromatography (Chapter 4) were obtained on successive days under the same PPINICI conditions.

Figure 7-2.

Hydrogen chemical ionization mass spectra of O=V(IV) OEP, m.w. 599:
A. positive H_2CI
B. ECNCI

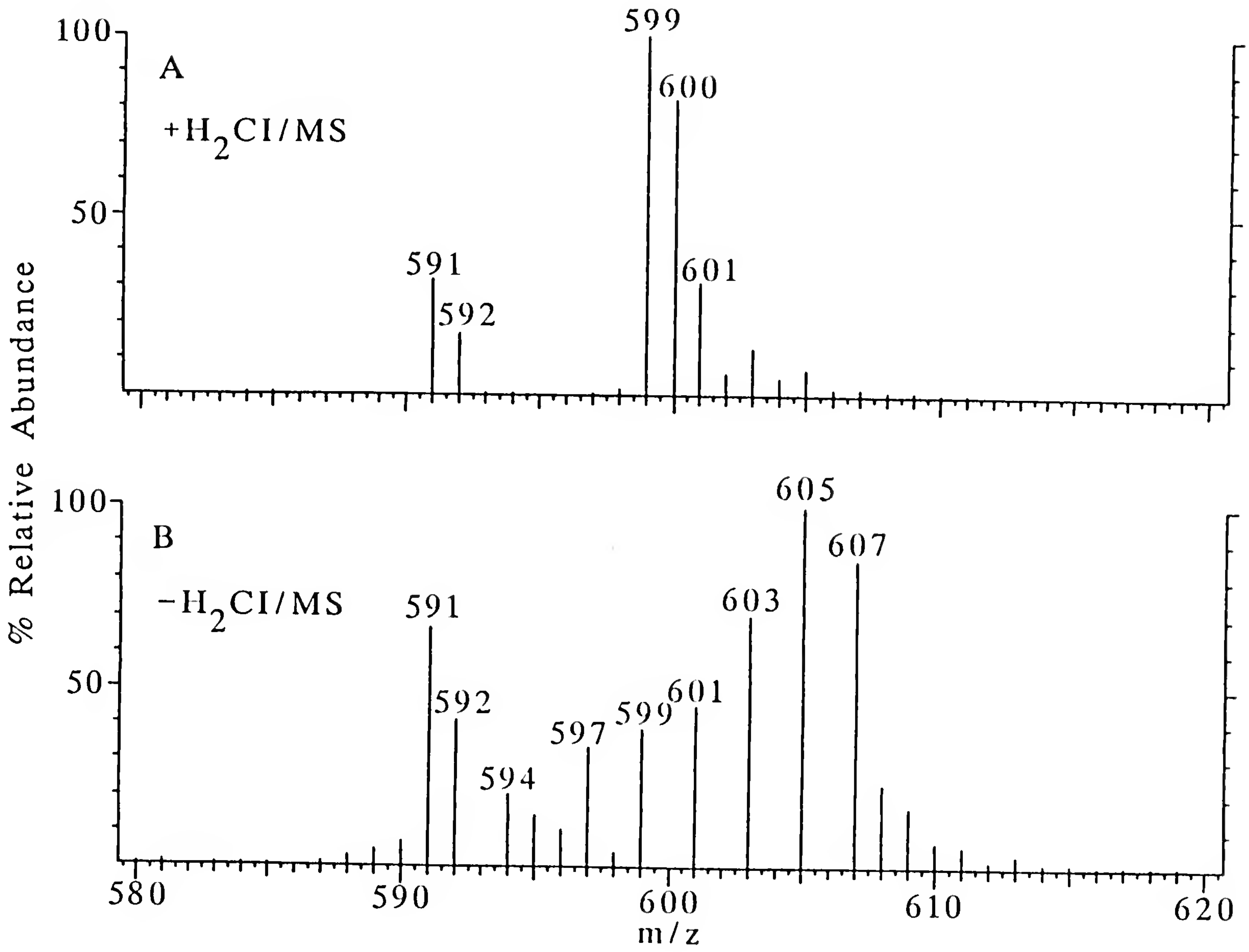
A
+H_2CI/MS
B
−H_2CI/MS
% Relative Abundance
100
50
100
50
591
592
599
600
601
591
592
594
597
599
601
603
605
607
580
590
600
610
620
m/z

Figure 7-3.

Positive H_2CI mass spectra of O=V(IV) porphyrins from demineralized shale analyzed on successive days

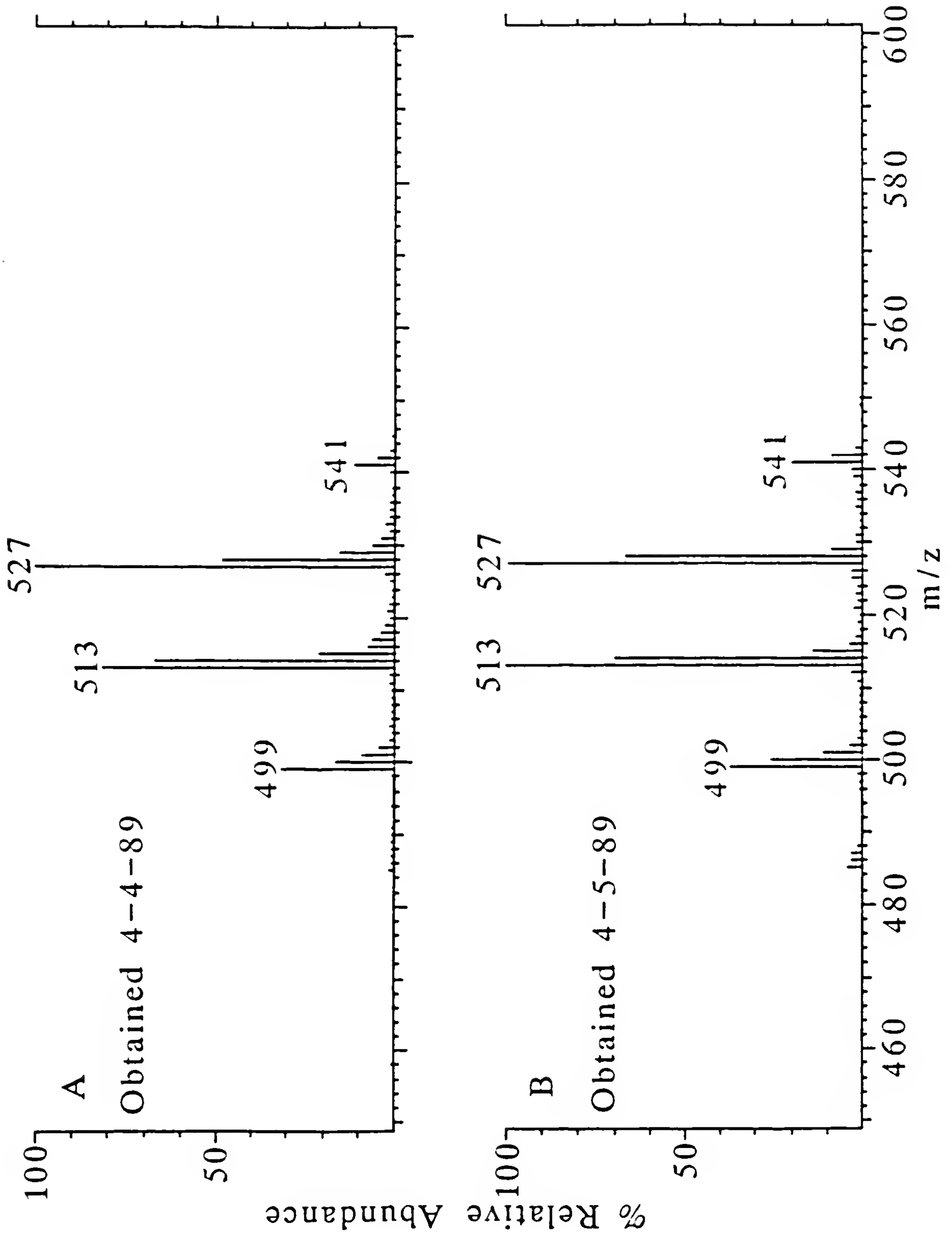
A
Obtained 4-4-89
499
513
527
541
B
Obtained 4-5-89
499
513
527
541
100
50
100
50
% Relative Abundance
460
480
500
520
540
560
580
600
m/z

Figure 7-4.

Electron capture negative H_2CI mass spectra of O=V(IV) porphyrins from demineralized shale analyzed on successive days

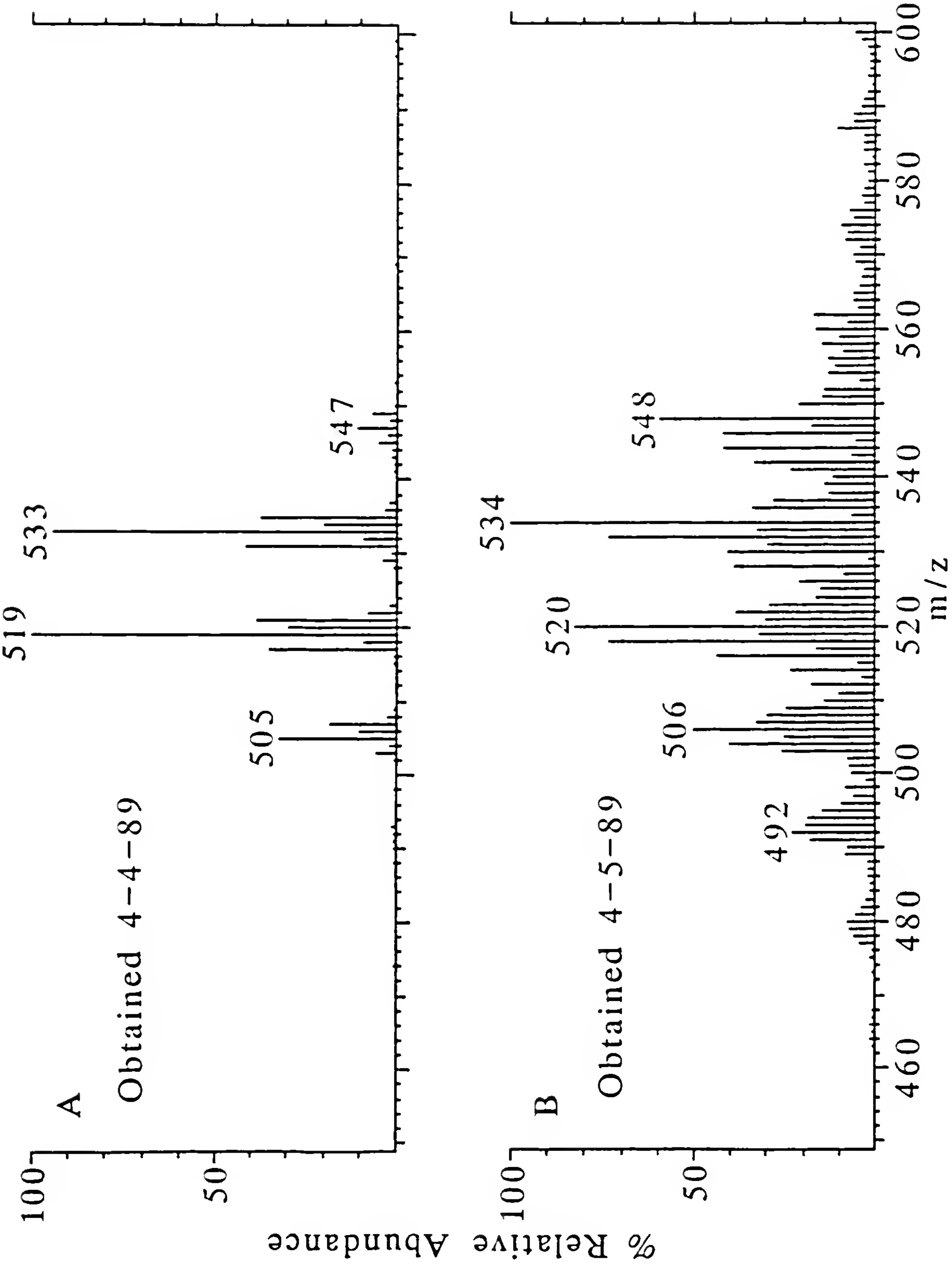
A
Obtained 4-4-89
505
519
533
547
B
Obtained 4-5-89
492
506
520
534
548
100
50
100
50
% Relative Abundance
460
480
500
520
540
560
580
600
m/z

The mass spectra from the two $+H_2CI$ experiments are very similar (Figure 7-3). These spectra contain predominantly molecular and protonated molecular ions, as verified by EI experiments. The two corresponding ECNCI mass spectra are very different from the $+H_2CI$ mass spectra. The major ions appearing in the ECNCI mass spectrum in Figure 7-4A are 6 u higher than those in the $+H_2CI$ mass spectrum (Figure 7-3A), even though the two spectra were recorded at the same time by PPINICI. The major ions appearing in the ECNCI mass spectrum correspond to hexahydro vanadyl porphyrin species, $[M + 6H]^+$. Apparently, electron capture negative chemical ionization is much more efficient at ionizing these reduced species than it is for ionizing the porphyrins. Another problem with the ECNCI mass spectra of these geoporphyrins is that they are not as reproducible as the corresponding positive H_2CI mass spectra. The two $+H_2CI$ mass spectra in Figure 7-3 were obtained on successive days, and are very similar. The two ECNCI mass spectra in Figure 7-4 were also obtained on successive days, yet appear very different. The ECNCI mass spectrum obtained on the second day consists of more extensively hydrogenated ions (Figure 7-4B). It is possible, though unlikely, that the sample degraded upon being stored dry overnight; however, neither the EI nor positive H_2CI mass spectra obtained of the sample yielded any such degradation products. Recalling that the corresponding positive and ECNCI mass spectra in Figures 7-3 and 7-4 were obtained simultaneously by PPINICI, it is more likely that the hydrogenation observed in the ECNCI mass spectra arose out of a surface-assisted process. The nature of the surfaces within the ion source could have been different on successive days, accounting for the lack of reproducibility of the ECNCI mass spectra. Surface-assisted hydrogenation under ECNCI conditions has been reported previously (Sears et al., 1987), as have other wall-catalyzed reactions including chlorination (Kassel et al., 1986) and oxidation (Stemmler and Buchanan 1989).

The ECNCI mass spectra of O=V(IV) porphyrins are of questionable value for two main reasons. First, it is not always possible to correlate the relatively abundant m/z values appearing in the ECNCI mass spectra with molecular ions. Second, the ECNCI mass spectra are not as reproducible from one day to the next, as the EI and $+H_2CI$ mass spectra are. Both of these problems severely limit the utility of ECNCI for analyzing O=V(IV) geoporphyrins, especially in complex mixtures. In petroleum samples, for instance, etioporphyrins and cycloalkanoporphyrins of the same carbon-number differ by only 2 u, and usually occur as pseudohomologous series. Hydrogenation product ion envelopes from different O=V(IV) porphyrin structures would therefore overlap. This could make it extremely difficult to determine the carbon-number of hydrogenated products ions, or whether they resulted from etioporphyrins or cycloalkanoporphyrins.

Upon ECNCI, Co(II) OEP yields two distinct peaks as the DEP is heated, shown by the mass chromatograms in Figure 7-5. The first one appears at about 300 °C, and consists entirely of the negative molecular ion, m/z 591 (Figure 7-6A).

Figure 7-5.

Electron capture negative H_2CI mass chromatograms of the molecular ion (m/z 591) and a hydrogenated product ion (m/z 597) from Co(II) OEP. The mass spectra for the intervals marked A and B are shown in Figure 7-6.

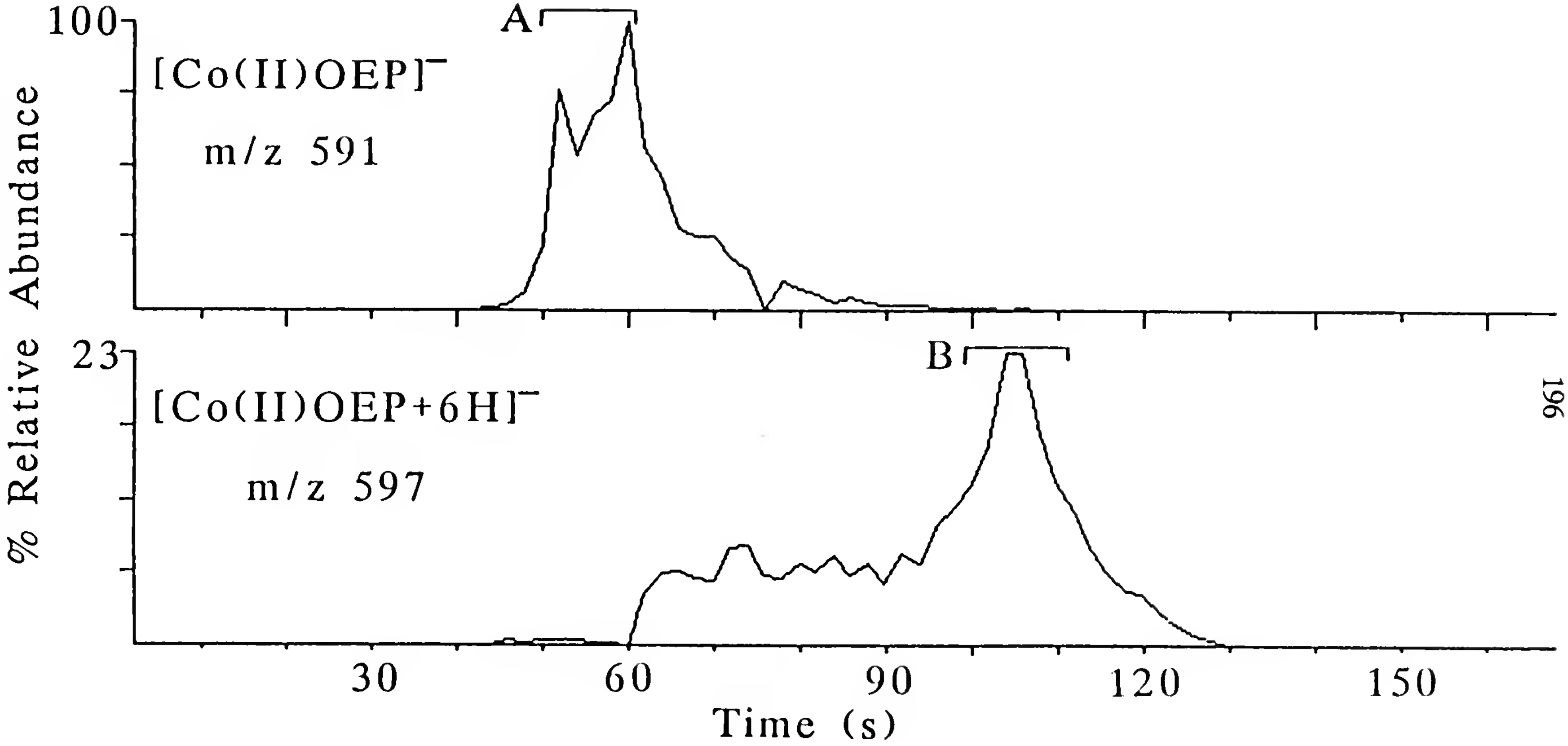
100
23
% Relative Abundance
[Co(II)OEP]⁻
m/z 591
A
[Co(II)OEP+6H]⁻
m/z 597
B
30
60
90
120
150
Time (s)

Figure 7-6.

Mass spectra from ECNCI analysis of Co(II) OEP:
A. from first peak in Figure 7-5
B. from second peak in Figure 7-5

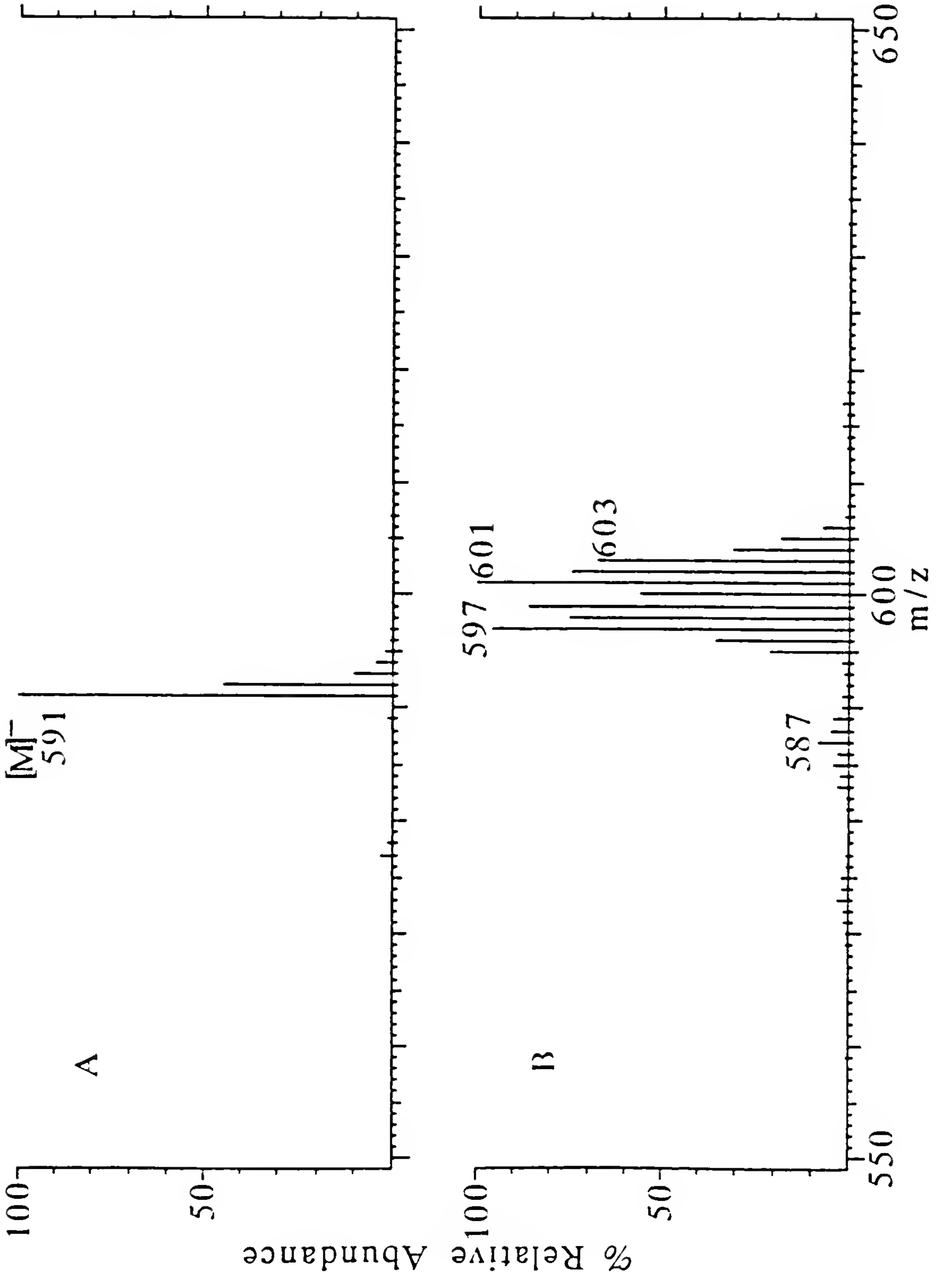
A
[M]⁻
591
B
597
601
603
587
100
50
550
600
650
m/z
% Relative Abundance

Cobalt(II) OEP was selected because cobalt is monoisotopic, making the extent of hydrogenation clear. This negative ion is very stable and is difficult to fragment via CAD. The second peak arising in the negative ion H_2CI mass spectrum of Co(II) OEP is smaller than the first, and appears when the DEP reaches 900 °C. It consists of hydrogenated cobalt OEP adducts resulting from surface-induced reduction (Figure 7-6B). The $[Co(II)\ OEP + 6H]^-$ ion (m/z 597) was selected for a daughter ion MS/MS experiment. It fragmented much more efficiently upon CAD than did the m/z 591 ion, yielding m/z 568 and m/z 449 daughter ions (Figure 7-7). The m/z 568 corresponds to α-cleavage of a peripheral ethyl substituent. The origin of the m/z 449 ion is unclear; further experiments are needed to better identify this daughter ion. Such novel fragmentations of reduced negative ions suggest this to be potentially useful in terms of structure elucidation of individual porphyrins, but not in complex mixtures. Further studies of ECNCI of porphyrins are needed in order to make use of the hydrogenated product ions for structure elucidation.

Relative Sensitivities of ECNCI Toward Free-base and Metalated Porphyrins

Both H_2CI/MS and NH_3CI/MS analyses of free-base (metal-free) porphyrins often yield corresponding iron metalloporphyrin ions, even when care is taken to avoid contact of the porphyrin sample with metal during sample preparation. Free-base porphyrins can abstract traces of transition metal ions from solvents, resulting

Figure 7-7.

Daughter ion mass spectrum from the ECNCI-produced hydrogenated product ion (m/z 597) from Co(II) OEP

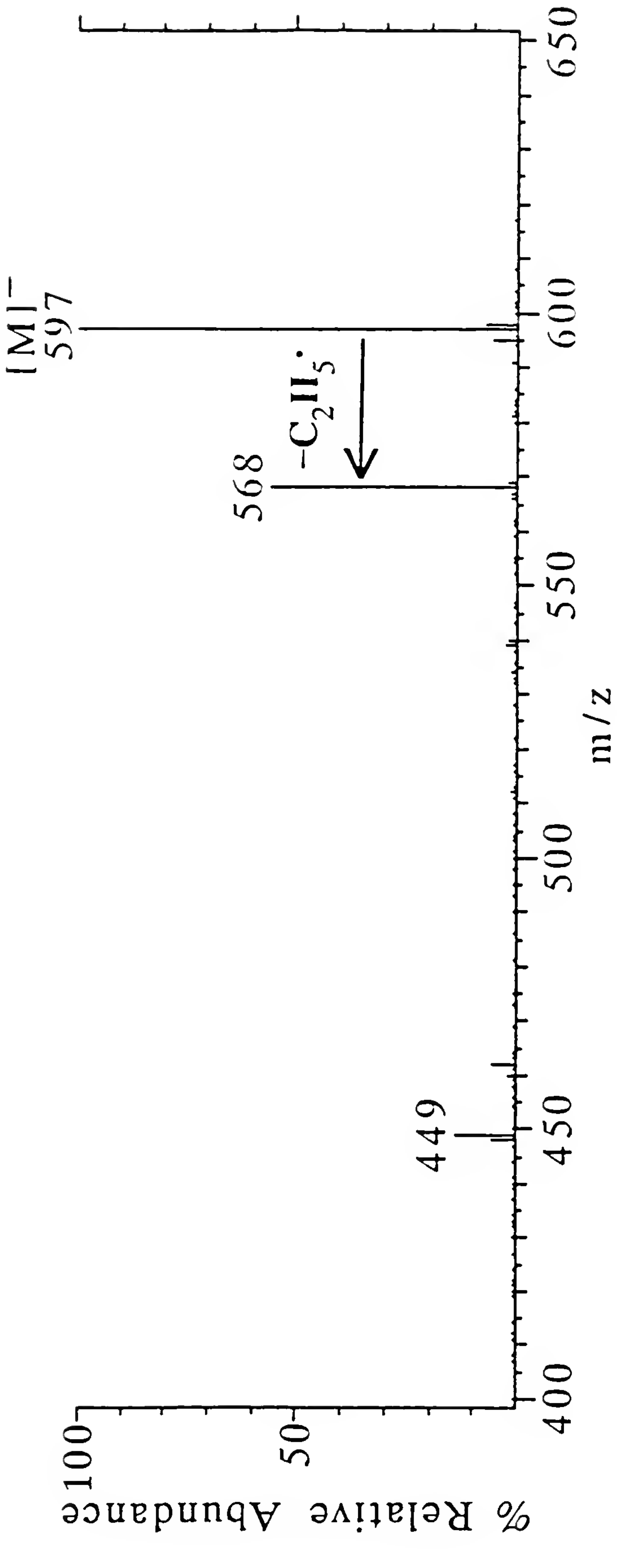
% Relative Abundance
100
50
m/z
400
450
500
550
600
650
449
568
[M]⁻
597
−C₂H₅·

in trace levels of metalloporphyrin impurities (Jackson et al., 1965). Metalloporphyrins might also form when free-base porphyrins interact with metal surfaces within the ion volume. Certain metalloporphyrins have been reported to undergo extensive metal exchange on metal surfaces within the ion source, including replacement of Cd and Pb by Ni (Henis et al., 1981), and replacement of Mg by Fe (Dillow and Gregor, 1988). In order to determine if the iron porphyrin ions arise from impurities in the solution or form on the stainless steel ion volume, EI and positive and negative H_2CI/MS data were obtained from the same sample of OEP. Both the EI and positive hydrogen chemical ionization mass spectra yield iron porphyrin ions that are significantly less abundant than the molecular ion, m/z 534, but these metalloporphyrin ions in the negative ion mass spectrum are far more abundant than are any of the ions in the molecular ion region (Figure 7-8). Note that the EI/MS spectrum in Figure 7-8C is expanded by a factor of 100 at m/z values greater than m/z 560, indicating that m/z 588 appears at merely 0.25 % of the abundance of the base peak molecular ion. This EI experiment was inconclusive in terms of determining the origin of the iron porphyrin impurity. Some metalloporphyrins were clearly observed in the EI mass spectrum, albeit at very low relative abundances. The presence of other ions in this region could be impurities as well, or may correspond to Ni(II), Cu(II), and/or Zn(II) derivatives of OEP which formed on the stainless steel surface of the ion volume.

Figure 7-8.

Three types of mass spectra from OEP:
A. positive H_2CI
B. electron-capture negative H_2CI
C. electron ionization

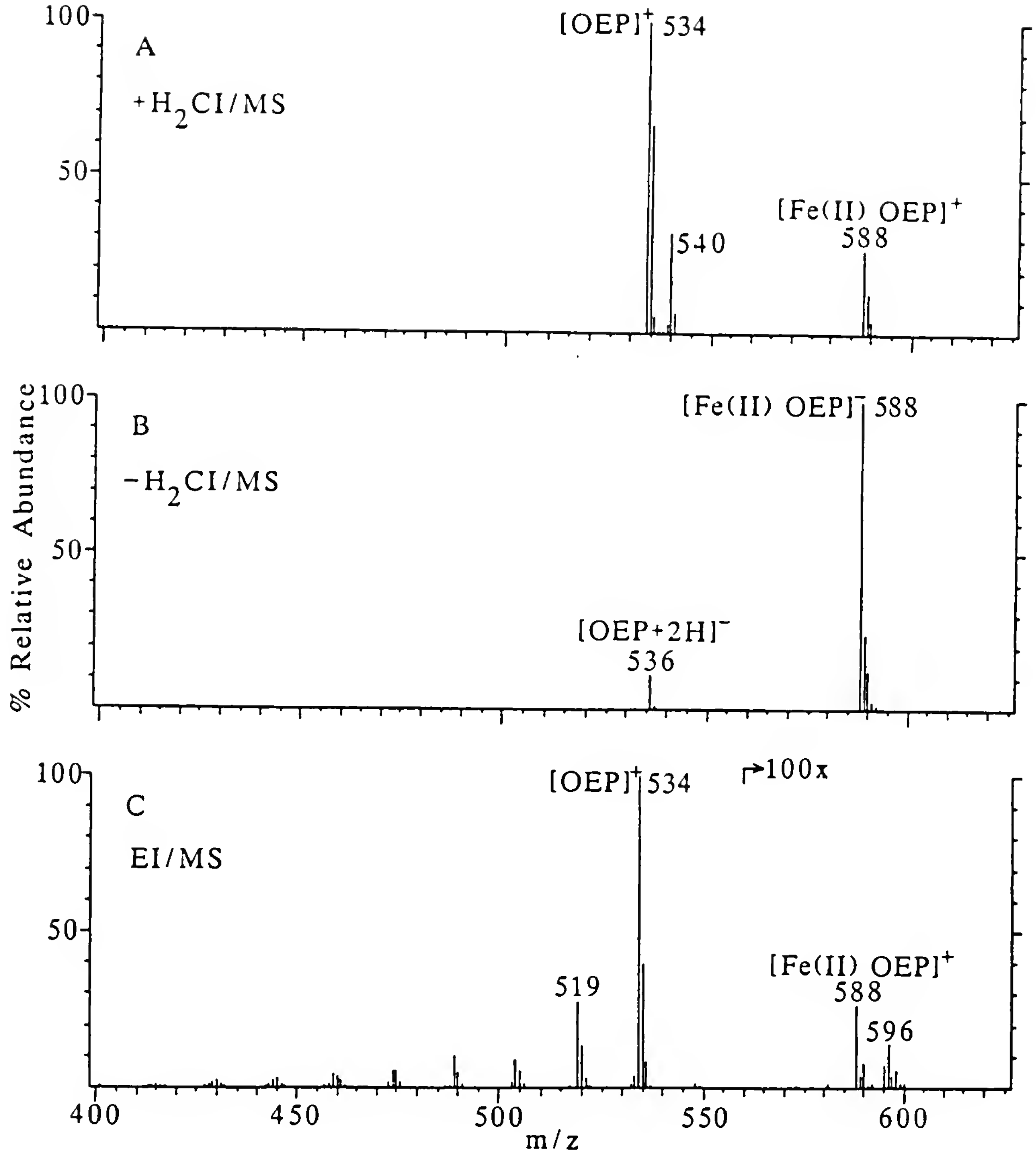
A
+H2CI/MS
[OEP]+ 534
540
[Fe(II) OEP]+
588
B
−H2CI/MS
[Fe(II) OEP]− 588
[OEP+2H]−
536
C
EI/MS
[OEP]+ 534
100x
519
[Fe(II) OEP]+
588
596
% Relative Abundance
100
50
400
450
500
550
600
m/z

When the stainless steel ion volume was electroplated with copper, and the negative H_2CI/MS experiment repeated, a remarkable decrease in the abundance of the iron metalloporphyrin was observed, as shown in Figure 7-9. This indicates that pick up of iron most probably occurs on the surface of the ion volume. Differences between the mass spectra in Figures 7-8 (A and B) and 7-9 (A and B) are likely due to the fact that each group of spectra were obtained on different days. The nature of the surfaces involved in metalation reactions is difficult to reproduce, so differences in the relative abundances of iron metalloporphyrins are not unexpected. It is noteworthy that m/z 588, the iron metalloporphyrin ion, is only detected at lower DEP temperatures (around 300 °C) in all three spectra in Figure 7-9, indicating that products of porphyrin/surface interactions are observed at low DEP temperatures as well as at the high DEP temperatures discussed in Chapter 6. It is also interesting that copper plating does not seem to result in metalation of OEP by copper to the extent that stainless steel results in pick-up of iron by OEP. When OEP is introduced via a glass vial in a heated solids probe, the iron chelate is also observed. When the glass vial is replaced by a copper probe extension, and OEP is deposited directly on the copper piece, both OEP and its iron derivative are detected, however, no copper chelate is observed. There may be a correlation between metal atoms and the extent to which they can be extracted from the metal lattice by free-base porphyrins.

Figure 7-9.

Mass spectra from OEP:
A. positive H_2CI in stainless steel ion volume
B. ECNCI in stainless steel ion volume
C. ECNCI in copper-plated ion volume

The inset RIC traces show the time interval over which the mass spectra were obtained.

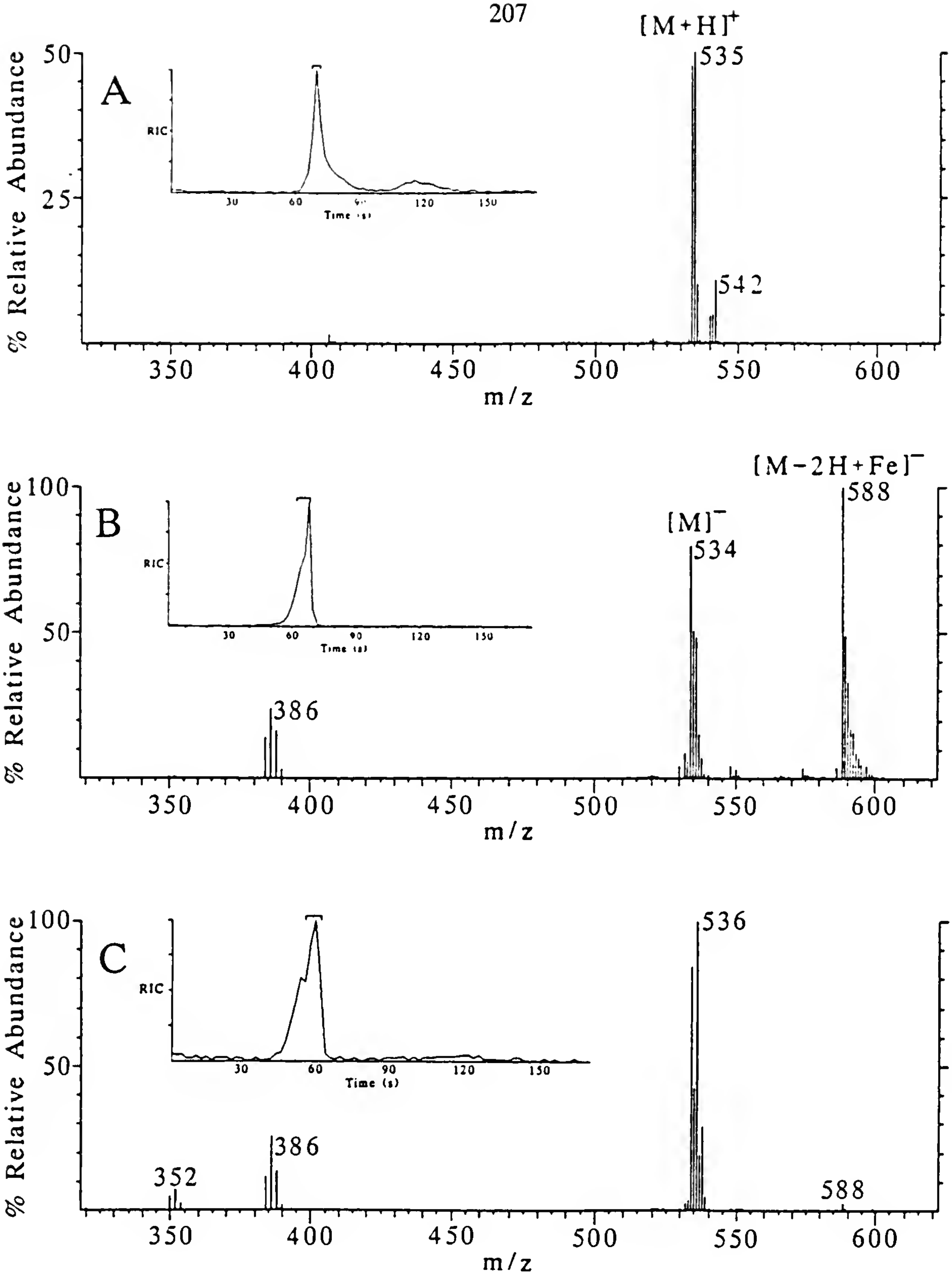
[M+H]$^+$
535
542
A
RIC
30
60
90
120
150
Time (s)
% Relative Abundance
50
25
350
400
450
500
550
600
m/z
[M-2H+Fe]$^-$
588
[M]$^-$
534
386
B
RIC
30
60
90
120
150
Time (s)
% Relative Abundance
100
50
350
400
450
500
550
600
m/z
536
352
386
588
C
RIC
30
60
90
120
150
Time (s)
% Relative Abundance
100
50
350
400
450
500
550
600
m/z

The drastic differences between the relative intensities of the free-base and iron porphyrin ions under positive and negative H_2CI conditions suggest two possible explanations. The first one is that the free-base porphyrin metalates on the stainless steel surface by a mechanism resulting in the iron chelate having a negative charge which does not result from ECNCI. The other possibility is that ECNCI selectively favors ionization of metalloporphyrins over free-base porphyrins. This second scenario would result in unusually high intensities of the iron porphyrin regardless of whether it is an impurity in the OEP sample, or if it forms in the source. This latter explanation is supported by a previous investigation in which free-base porphyrins were not found to ionize significantly by ECNCI, but metalloporphyrins were ionized very efficiently by ECNCI (Sundararaman et al., 1982). Metalloporphyrins may ionize more efficiently by ECNCI than free-base porphyrins because they contain metal ions which can capture low energy electrons into empty metal orbitals. Formation of negative molecular ions by capture of thermal electrons into empty metal orbitals has been reported for various metal coordination compounds, including Co(II), Ni(II), and Cu(II) polydentate Schiff base complexes (Gilbert et al., 1973; Taylor and Dillard, 1974).

To determine the relative sensitivities of positive and negative H_2CI toward free-base and metalated porphyrins, a 1:1 molar mixture of OEP and Co(II) OEP was analyzed by EI and PPINICI methods. In every case, both the free-base OEP and Co(II) OEP vaporized off of the DEP filament within the same mass chromatographic peak. Averaged mass spectra were obtained over the entire peak, to safeguard against bias toward a particular ion. It is difficult to tell from the EI/MS data that the sample was a equimolar mixture of OEP (m.w. 534) and Co(II) OEP (m.w. 591) (Figure 7-10). The EI mass spectrum indicates that OEP is more prevalent in the ion source than is Co(II) OEP. Not only are the singly and doubly charged molecular ions more abundant for OEP, but the corresponding fragment ions seem more predominant for OEP as well. One possible explanation is that the Co(II) OEP may have somehow demetalated. This is doubtful because subsequent EI/MS analysis of pure Co(II) OEP resulted in no free-base porphyrin ions being observed. Another possibility is that the Co(II) OEP did not all dissolve, while all of the OEP did. Although the OEP dissolves much more easily than the Co(II) OEP, this explanation is also doubtful because the solution was sonicated for over two hours, and no undissolved solids were seen when light was passed through the solution. Perhaps EI of the free-base porphyrin is favored over EI of the metalloporphyrin. This unexpected behavior could have serious ramifications for mixture analyses, and warrants further investigation.

The $+H_2$CI/MS and $-H_2$CI/MS data from the PPINICI experiment are also rather surprising (Figure 7-11). For this experiment, the pyrrolic ion mass regions were not scanned; rather, only the mass ranges of the molecular ions, protonated molecular ions, and hydrogenated product ions were scanned. This was done to maximize the number of data points collected for each compound, as the OEP and

Figure 7-10.

Electron ionization mass spectrum of a 1:1 molar mixture of OEP and Co(II) OEP

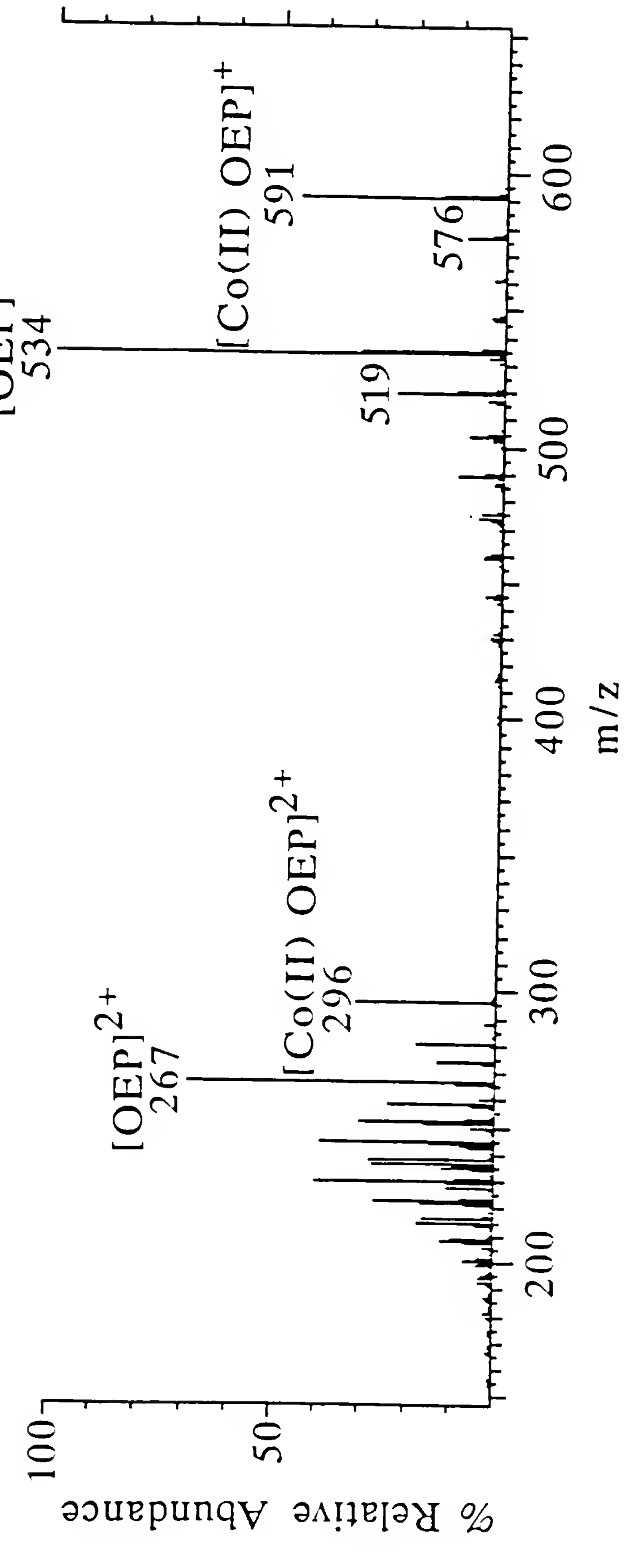
[OEP]$^{2+}$
267
[Co(II) OEP]$^{2+}$
296
[OEP]$^{+}$
534
519
[Co(II) OEP]$^{+}$
591
576
200
300
400
500
600
m/z
100
50
% Relative Abundance

Figure 7-11.

PPINICI mass spectra from a 1:1 molar mixture of OEP and Co(II) OEP:
A. positive H_2CI
B. Electron capture negative H_2CI

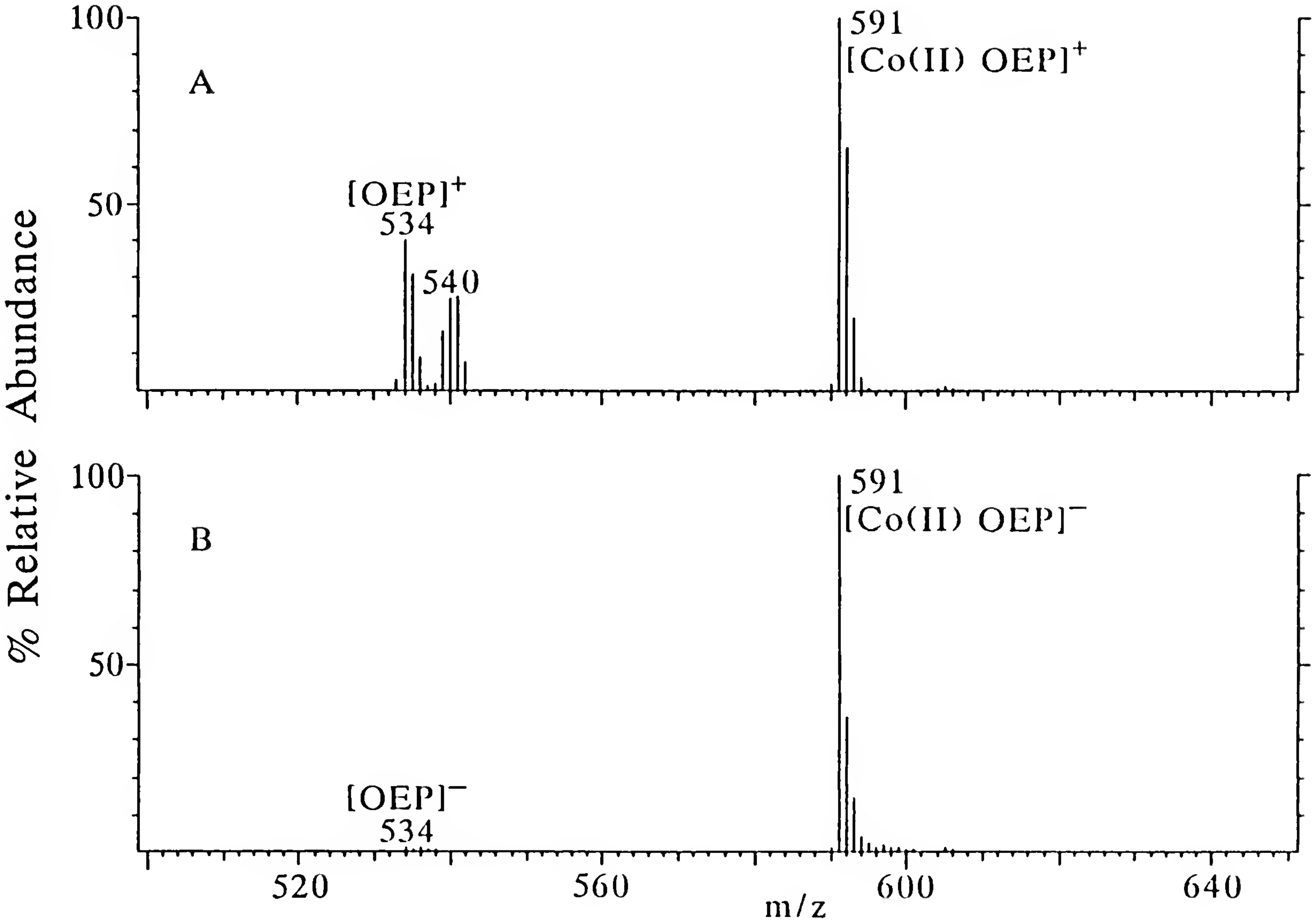
% Relative Abundance
100
50
A
[OEP]$^+$
534
540
591
[Co(II) OEP]$^+$
100
50
B
[OEP]$^-$
534
591
[Co(II) OEP]$^-$
520
560
600
640
m/z

Co(II) OEP vaporize over a very short period of time. The $+H_2CI$ mass spectrum reveals a base peak corresponding to the Co(II) OEP, with the peak corresponding to OEP at less than half the relative abundance of the base peak. These are very different results than those obtained by EI, in which OEP produced the base peak. However, the $+H_2CI$/MS data are not unexpected if one takes into account the relatively abundant hydrogenated OEP ions (porphyrinogen ions). The sum of the relative abundances of OEP and porphyrinogen ions is close to the sum of relative abundances of the Co(II) OEP and associated hydrogenated ions. A small difference in the relative abundances of the OEP and Co(II) OEP ions would not be unanticipated, since the ionization cross sections may not be the same for the free-base and metalated porphyrins.

The $-H_2CI$ mass spectrum in Figure 7-11 indicates that ECNCI definitely favors ionization of Co(II) OEP over OEP. The base peak corresponds to the molecular Co(II) OEP ion, and the ^{13}C isotope peaks at m/z 592 and m/z 593 are of the relative abundances expected. The peaks corresponding to OEP, however, are only about 2% relative to the base peak, even though equimolar quantities of OEP and Co(II) OEP were analyzed. This means that mixtures of metal-free and metalated porphyrins cannot be accurately analyzed by $-H_2CI$ techniques. Apparently, metalloporphyrins are so much more adept at capturing thermal electrons than free-base porphyrins, that when the two types of porphyrins are mixed, the sensitivity of ECNCI for free-base porphyrins will be 10 to 100 times lower. This has serious ramifications for ECNCI analyses of free-base porphyrins which may contain impurities of metalloporphyrins, or which may metalate within the ion source.

Conclusions

Electron capture negative chemical ionization is very attractive in terms of structure elucidation of geoporphyrins, but suffers from several drawbacks which severely limit its practical utility. This ionization technique is appealing because it is extremely sensitive and yields predominantly molecular porphyrin ions, with little or no fragmentation. This is particularly useful for geoporphyrin mixtures because unambiguous carbon-number information strictly from molecular ions is potentially available. Thus, ECNCI would seem to be a potential complement to other ionization techniques for structure elucidation of geoporphyrins.

Unfortunately, applications of ECNCI techniques to porphyrins result in a myriad of problems which are not easily understood nor controlled. One result of ECNCI of porphyrins is that the negatively charged molecular ions are extremely difficult to fragment via CAD. Thus, information about the peripheral substituents or sequence of pyrrolic rings is not available from ECNCI/MS/MS experiments with the molecular ions .

Another, more serious problem with ECNCI of porphyrins is hydrogenation. Metalloporphyrins are especially prone to form hydrogenated products under ECNCI conditions. Often, the molecular ions appear at much lower relative abundances than the clusters of hydrogenated product ions. This can make ECNCI/MS analysis of complex mixtures of metalloporphyrins, such as geoporphyrins, futile. Hydrogenation is not very reproducible. However, if more were known about the process and if it could be controlled, this might not be a limiting factor for porphyrin analysis by ECNCI/MS. In fact, it was shown that negatively charged hydrogenated product ions fragment much more efficiently than do the corresponding negatively charged porphyrin ions upon CAD. If these hydrogenated product ions could somehow be correlated to porphyrin structures, then CAD of these ions may eventually be useful in terms of structure elucidation.

One problem with ECNCI of porphyrins which does not seem resolvable, is that ECNCI is much more sensitive toward metalloporphyrins than toward free-base porphyrins. This makes such analyses of mixtures of free-base and metalated porphyrins of limited utility. In fact, free-base porphyrins are so proficient at metalation, that even ECNCI/MS analyses of free-base porphyrins can be difficult. Trace metal impurities in the sample solution may result in trace levels of metalloporphyrins which appear as the dominant peaks in the mass spectrum. The free-base porphyrins may also pick up iron from the stainless steel ion volume, resulting in predominantly iron porphyrins being detected. The relative abundance of iron porphyrins has been shown to decrease when a copper-plated ion volume is utilized for ECNCI/MS analysis of a free-base porphyrin. Further work is required to address this and other problems before ECNCI/MS analyses of porphyrins are routinely useful for structure elucidation.

CHAPTER 8

STRUCTURE ELUCIDATION OF GEOPORPHYRINS BY DESORPTION TANDEM MASS SPECTROMETRY: CARBON-NUMBER, PYRROLIC STRUCTURE, AND SEQUENCING INFORMATION FROM THE SAME EXPERIMENT

Introduction

Three types of structural information are usually required for structure elucidation of porphyrins. These are the porphyrin's molecular weight, or carbon-number, the identities of peripheral substituents, and the sequence of the pyrrolic rings around the porphyrin macrocycle. Separate mass spectrometric experiments with a variety of ionization techniques are normally required to obtain all of this information. Electron ionization (EI) of porphyrins typically yields both molecular ions, $[M]^+$, and fragment ions primarily from β-cleavage of peripheral substituents (Jackson et al., 1965). Thus, EI techniques can provide information about a porphyrin's carbon number and its peripheral substituents, but offer little information about the sequence of the pyrrolic rings around the macrocycle. In contrast, hydrogen chemical ionization (H_2CI) of porphyrins can result in reduction of the porphyrins to porphyrinogens, yielding both $[M]^+$ and $[M + 6H]^+$ ions (Shaw et al., 1981). In addition, cleavage of the meso-bridges of the porphyrinogen yields mono-, di-, and tri-pyrroles which are then ionized. These are clearly useful in sequencing the pyrroles; however, obtaining information about the nature of the peripheral substituents is less straightforward by H_2CI than with EI techniques. Tandem mass spectrometry (MS/MS) in conjunction with H_2CI may be used to obtain all of the required information in the same experiment, and has definite advantages over performing separate EI and CI experiments.

Two mass spectrometric methods are described which facilitate obtaining all three types of structural information in the same H_2CI experiment. The first method involves obtaining H_2CI/MS/MS daughter ion mass spectra from the porphyrins upon vaporization off of the direct exposure probe (DEP) filament. Once this occurs, the collision gas is removed from the collision cell, and the DEP continues to heat. Pyrrolic ions, resulting from the surface-induced decomposition and ionization processes described in Chapter 6, are subsequently analyzed by MS. The second method involves MS/MS of both the porphyrin molecular ion and the corresponding porphyrinogen ion.

Experimental

Mass spectrometric data were obtained with a Finnigan MAT TSQ45 triple quadrupole mass spectrometer, with an INCOS data system, operated in the positive ion mode. The origins of OEP and Zn(II) OEP which are analyzed in this chapter are discussed in Chapter 5. The solid porphyrin samples were dissolved in methylene chloride. One μL of solution (containing about 2 μg of porphyrin) were placed onto a direct exposure probe, consisting of a resistively heated rhenium filament. The methylene chloride was allowed to evaporate prior to insertion of the probe into the ion source. For the electron ionization experiment, the metalloporphyrin studied was 2,3,7,8,12,13,17,18-octaethyl-21H,23H-porphine zinc(II), denoted as Zn(II) OEP, which was purchased from Aldrich, Milwaukee, WI. The EI mass spectrum was obtained with an electron energy of 70 eV, an emission current of 0.3 mA, a source temperature of 190 °C, and an analyzer pressure of 2.5 X 10^{-7} torr. Quadrupole 1 (Q1) was scanned from a mass-to-charge ratio (m/z) of 200 to m/z 650 in 0.75 s, while quadrupoles 2 and 3 (Q2 and Q3) were operated in the RF-only mode, transmitting all masses. The DEP was then heated from ambient to 700 °C at 600 °C/min.

For the chemical ionization experiments, metal-free 2,3,7,8,12,13,17,18-octaethyl-21H,23H-porphine, also purchased from Aldrich and denoted as OEP, was studied. The H_2CI data were obtained with an electron energy of 100eV, an emission current of 0.3 mA, a source temperature of 190 °C, an analyzer pressure of 8.0 X 10^{-5} torr, and a source pressure of 0.9 torr H_2. For the first method involving MS/MS of the porphyrins and MS of the decomposition products, Q1 was programmed to pass only m/z 534 until the DEP reached 600 °C. The collision cell, Q2, was operated in the RF-only mode, and contained 2 mtorr argon. The third quadrupole, Q3, was scanned from m/z 350 to m/z 550 in 0.33 s. The collision energy was set at 30 eV. When the DEP reached 600 °C, the argon was pumped out of Q2 in less than 2 s. Both Q2 and Q3 were then switched to the

RF-only mode, passing all m/z ratios, and Q1 was scanned from m/z 80 to m/z 280 in 0.33 s. The collision energy (Q2 offset) was also reduced to 8.2 eV at this point. Conventional MS data were obtained until 1 minute after the DEP reached its maximum temperature of 1350 °C. For the second method, involving daughter ion mass spectra from both the porphyrin and its corresponding porphyrinogen, Q1 was programmed to sequentially pass only m/z 534 and then only m/z 540 every 0.91 s. The collision cell was operated in the RF-only mode, and contained 2 mtorr argon. The third quadrupole was scanned from m/z 45 to m/z 600 in 0.91 s. The collision energy (Q2 offset) was set at 30 eV when m/z 534 was selected as the parent ion, and at 25 eV when m/z 540 was chosen as the parent ion. By sequentially selecting m/z 534 and m/z 540 as parent ions, and then deconvoluting the data, two separate daughter ion mass spectra were obtained from the same sample simultaneously.

Traditional Mass Spectrometric Methods of Porphyrin Structure Elucidation

Electron Ionization MS

Electron ionization occurs when a gaseous neutral molecule, M, interacts with a (typically) 70eV electron. This usually results in the ejection of an electron from the neutral molecule, leaving a positively charged molecular ion, $M^{+\cdot}$. As mentioned previously, the radical symbol is not used in this dissertation for porphyrins to avoid ambiguity due to metals containing odd numbers of electrons. The EI process also deposits internal energy into the molecular ion, which may then fragment. In the case of electron ionization of porphyrin ions, these fragment ions often result from β-cleavage of the peripheral substituents. Thus, both the molecular and the β-cleavage fragment ions form in the source, and can then be mass analyzed. An example of an EI mass spectrum was displayed for Zn(II) OEP in Chapter 5 (Figure 5-1). The ions having m/z values between 200 and 300 are doubly charged (i.e. $[M]^{2+}$ and doubly charged fragment ions) (Chapter 5).

The EI mass spectrum of Zn(II) OEP is an example of how the EI/MS technique can be employed in determining the molecular weight of porphyrins, as well as the nature of the peripheral substituents. The singly charged molecular ion, $[M]^+$ is typically the base peak, with the singly charged β-cleavage fragment ions having much lower relative abundances. Clearly, this technique offers no information about the sequence of the pyrrolic rings around the macrocycle, and even the identities of the peripheral substituents can be difficult to discern owing to the isotopic pattern. Electron ionization is often used to determine the carbon number ranges of porphyrins, such as those of bitumen and kerogen (Chapter 3); however, β-cleavage fragment ions from higher carbon number species may coincide in m/z with lower carbon number molecular ions. Interferences of this type may be diminished by ionizing at lower ionization energies, but this results in decreased sensitivity. Thus, EIMS has limited utility as a structure elucidation tool for geoporphyrin mixtures.

Chemical Ionization MS

Chemical ionization of porphyrins can provide complementary structural information to that obtainable by EIMS. Chemical ionization occurs when the ion source is pressurized with 0.4 to 1.0 torr of a reagent gas, commonly methane, ammonia, or hydrogen. The reagent gas is ionized by high energy electrons; the resultant reagent ions can then ionize sample molecules, either by protonation or charge exchange, for subsequent mass analysis. This technique is often called "soft ionization" because not as much energy is deposited into the sample ions, which therefore do not typically fragment as much as with EI.

Porphyrins, however, undergo unique fragmentation pathways under CI conditions, especially with reducing reagent gases such as H_2 and NH_3. Free-base porphyrins can be reduced to porphyrinogens under H_2CI or NH_3CI conditions, as discussed in Chapter 6. An example of this was shown in Chapter 6 (Figure 6-1), where metal-free OEP, m.w. 534, is reduced to its corresponding porphyrinogen (OEP + 6H), m.w 540, under positive H_2CI conditions. The resultant porphyrinogens are not fully conjugated, and tend to fragment within the source by cleavage of the meso-bridges. Scission of these meso-bridge bonds and reactions with reagent ions yields mono-, di-, and tri-pyrrolic ions. These ions are very useful in sequencing the pyrrolic rings around the porphyrin. The dipyrrolic ions are especially useful in sequencing pyrroles in asymmetrical porphyrins, as these ions correspond to adjacent pyrrolic rings. These dipyrrolic ions do not result from recombination reactions, but arise directly from the porphyrinogen (Shaw et al., 1981). Pyrrolic rings which are diagonally across from each other do not therefore form dipyrrolic ions.

A typical H_2CI mass spectrum of free-base OEP, m.w. 534, was shown in Chapter 1 (Figure 1-9). Neutral OEP is ionized via both charge exchange (resulting in m/z 534) and protonation (resulting in m/z 535). The porphyrinogen ion appears at m/z 540, corresponding to the addition of six hydrogens to the porphyrin: reduction of the four meso-bridges, and addition of hydrogens to two nitrogens. Mono-, di-, and tri-pyrrolic ions can be seen in three distinct regions: m/z 100-155, m/z 240-290, and m/z 390-425, respectively. Even though all eight peripheral substituents are identical for OEP, several different peaks can arise in each pyrrolic region, depending on the number of meso-carbons retained by each ion, and on the extent to which cleavage of peripheral substituents occurs. This ionization technique, as with EI, can provide carbon-number information, but unlike with EI, H_2CI may also offer information about the sequence of the pyrroles around the porphyrin macrocycle. However, the extent to which pyrrolic ions appear in the source is very dependent on source temperature and can even be compound dependent, as discussed in Chapter 6. Even when the conditions are optimized, and the relative abundances of pyrrolic ions are greater than in Figure 1-9, information about the peripheral substituents is limited. Determining the number of peripheral carbons is difficult because each pyrrolic ion may contain 0, 1, or 2 meso-carbons.

The capabilities and limitations of H_2CI/MS for porphyrin structure elucidation can be illustrated by the following example. A demetalated C_{31} DPEP porphyrin which had already been well-characterized by ^{1}H NMR was analyzed by H_2CI/MS. The structure of the porphyrin is given in Figure 8-1 along with structures of the various dipyrroles which can result from cleavage of the meso-bridge bonds. The dipyrrolic region from the H_2CI mass spectrum of this demetalated C_{31} DPEP reveals some of the difficulties associated with this technique for structure elucidation of porphyrins (Figure 8-2). For example, as discussed in Chapter 1, little information about the nature of the peripheral substituents is available solely from this method due to the fact that the dipyrrolic ions may contain 0, 1, or 2 meso-carbons. This is depicted in Figure 8-2, as each dipyrrole corresponds to more than one peak in the mass spectrum, and vice-versa. Certainly, in a single-component sample, one could predict the theoretical relative abundances arising from a dipyrrolic ion containing various numbers of meso-carbons, but complications arise. One must know the relative tendencies of dipyrrolic ions to form with 0, 1, and 2 meso-carbons, as these may not be identical for all of the dipyrroles. It is then necessary to add the theoretical relative abundances for different dipyrrolic ions of coincident mass, which further complicates matters. Fragmentation of the ions in the source may also contribute to confusion, as it would be unclear whether or not m/z 201 or m/z 202 in Figure 8-2 result from dipyrrolic ions fragmenting or from surface-induced decomposition of the porphyrin. Finally, as mentioned in Chapter 1, H_2CI/MS techniques are of limited value for complex mixtures, as there

Figure 8-1.

Structures of a demetalated C_{31} DPEP (characterized by ^1H NMR) and the associated dipyrroles which can result from scission of the meso-bridge bonds

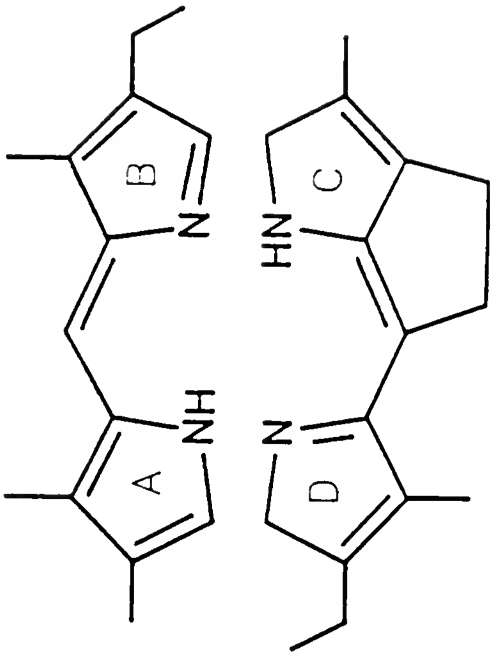
B
N
NH
A
C
HN
N
D

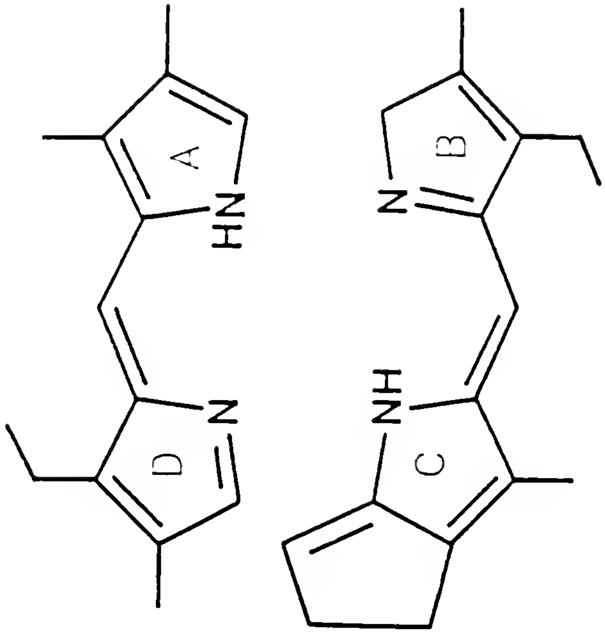
A
HN
N
D
B
N
NH
C

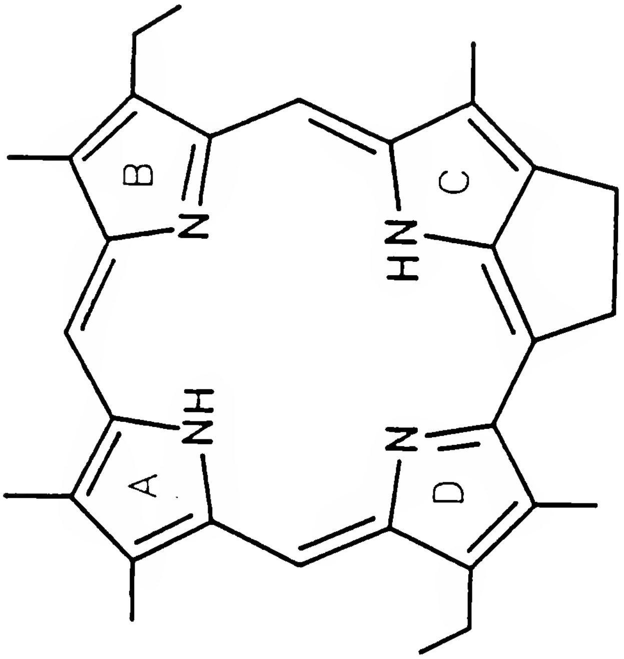
B
N
C
HN
NH
A
N
D

Figure 8-2.

Positive H_2CI mass spectrum of dipyrrolic ions from the demetalated C_{31} DPEP in Figure 8-1. The labels above the groups of peaks correspond to the dipyrroles shown in Figure 8-1.

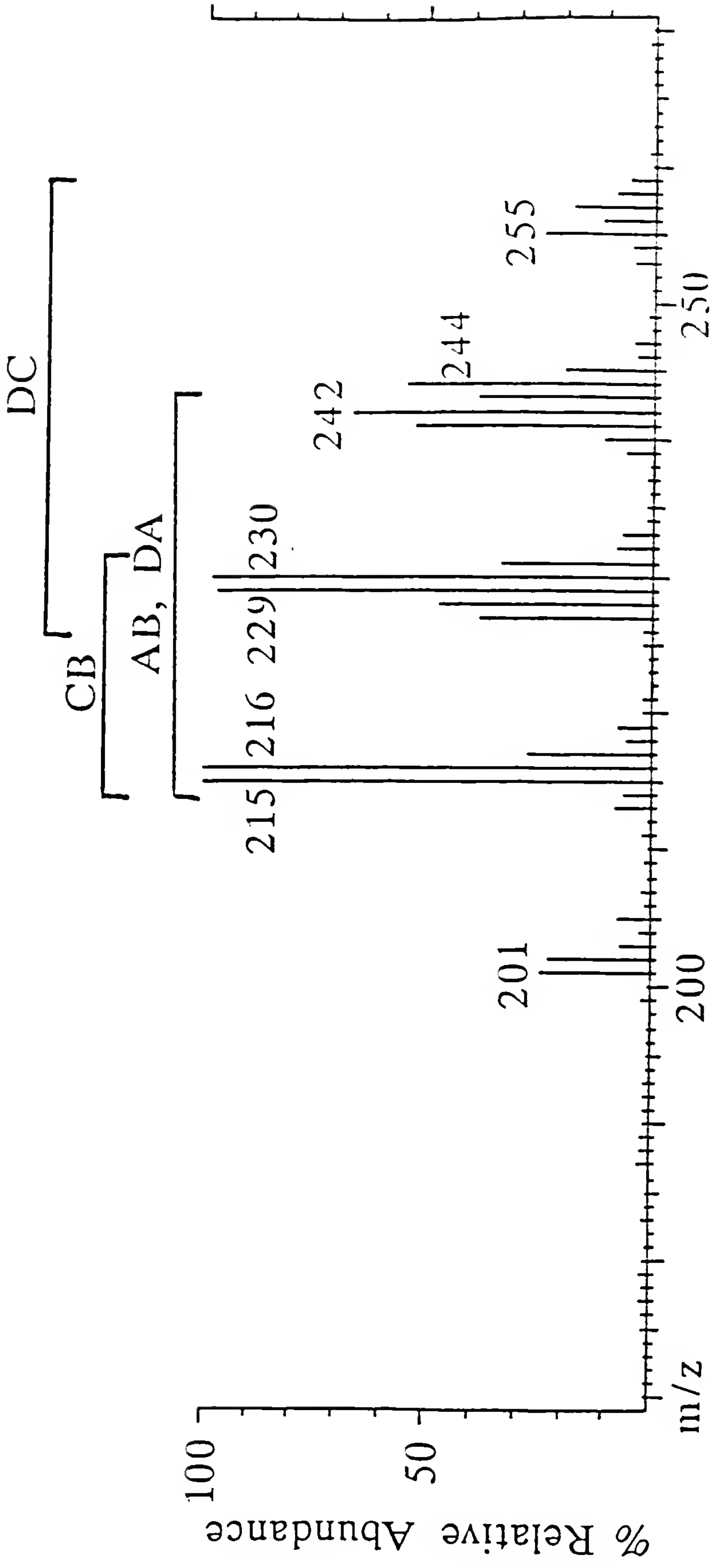
% Relative Abundance
100
50
m/z
200
250
201
215
216
229
230
242
244
255
CB
AB, DA
DC

is no way to determine which molecular porphyrins in the mixture give rise to specific pyrrolic ions.

MS/MS of Porphyrins and MS of Decomposition Products

Normal mass spectrometry (MS) certainly can be useful in structure elucidation of porphyrins, but in order to obtain both peripheral substituent and pyrrolic sequencing information, separate EI/MS and CI/MS experiments must be performed. The first method is a combination of separate MS/MS and MS scan functions within the same experiment. For the first part of this experiment, the porphyrin molecular ion is chosen as the parent ion in an MS/MS daughter ion experiment. Upon collisionally activated dissociation (CAD) with argon, the porphyrin fragments via β-cleavage of peripheral substituents. This scan mode provides information about the structures of peripheral substituents and the molecular weight of the porphyrin. After the porphyrin has vaporized off of the DEP filament and has been fragmented by CAD, argon is rapidly pumped out of the collision cell in less than 2 s.

The mass chromatograms from such an experiment involving OEP are shown in Figure 8-3 for a monopyrrolic ion (m/z 138), a dipyrrolic ion (m/z 275), the molecular ion (m/z 534), and reconstructed ion current. Note that the first peak results from MS/MS of the parent molecular porphyrin ion. The mass spectrum from this peak (Figure 8-4) is useful for determining the nature of the peripheral substituents. The second peak results from MS analysis of ionized pyrroles which

Figure 8-3.

Mass chromatograms of a monopyrrole (m/z 138), a dipyrrole (m/z 275), molecular ion (m/z 534), and reconstructed ion current from combined positive $H_2CI/MS/MS$ and positive H_2CI/MS experiments involving OEP introduced via a solids probe

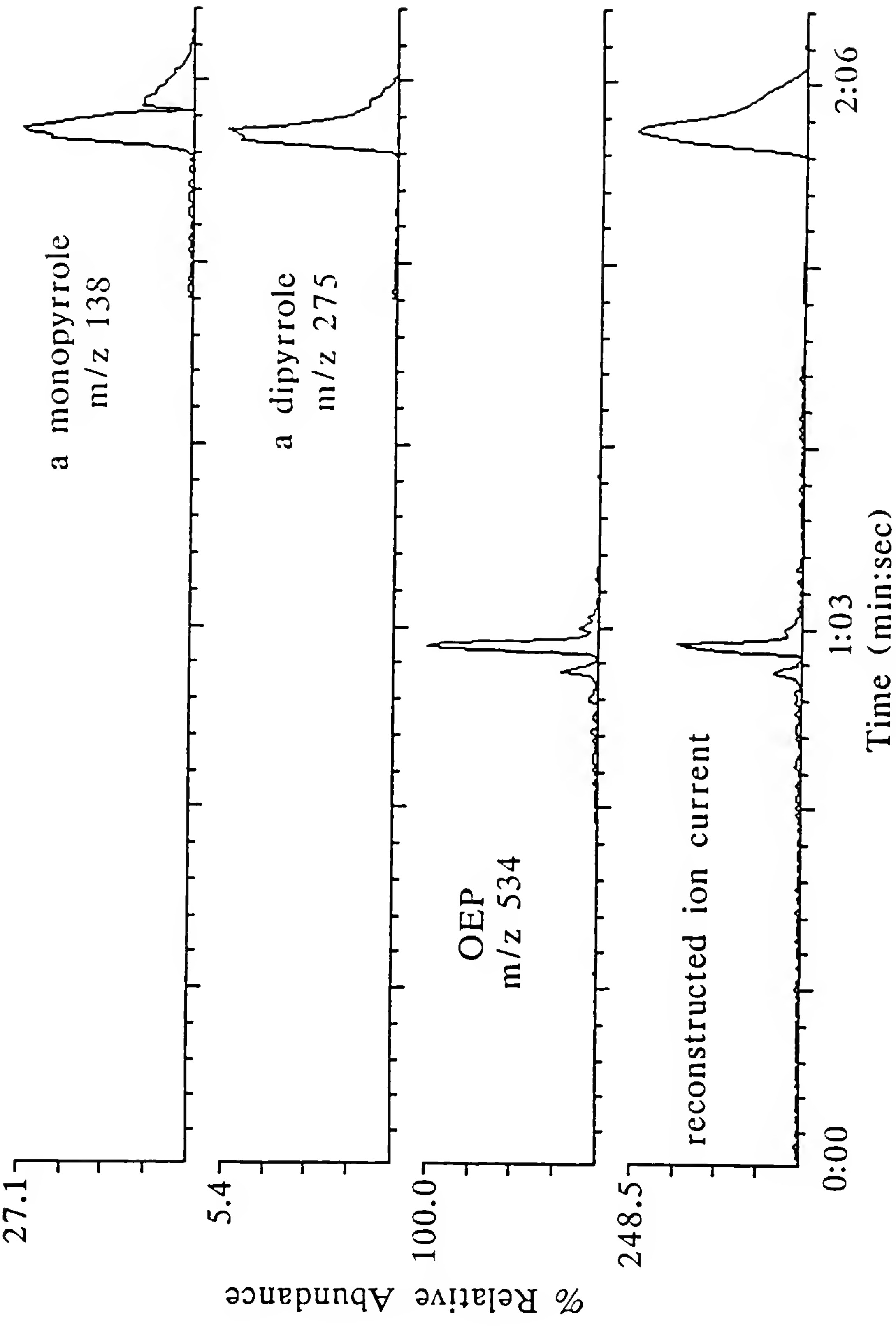
a monopyrrole
m/z 138
a dipyrrole
m/z 275
OEP
m/z 534
reconstructed ion current
27.1
5.4
100.0
248.5
% Relative Abundance
0:00
1:03
2:06
Time (min:sec)

Figure 8-4.

Mass spectrum from the first mass chromatographic peak in the combined positive H_2CI/MS/MS and positive H_2CI/MS experiments involving OEP introduced via a solids probe

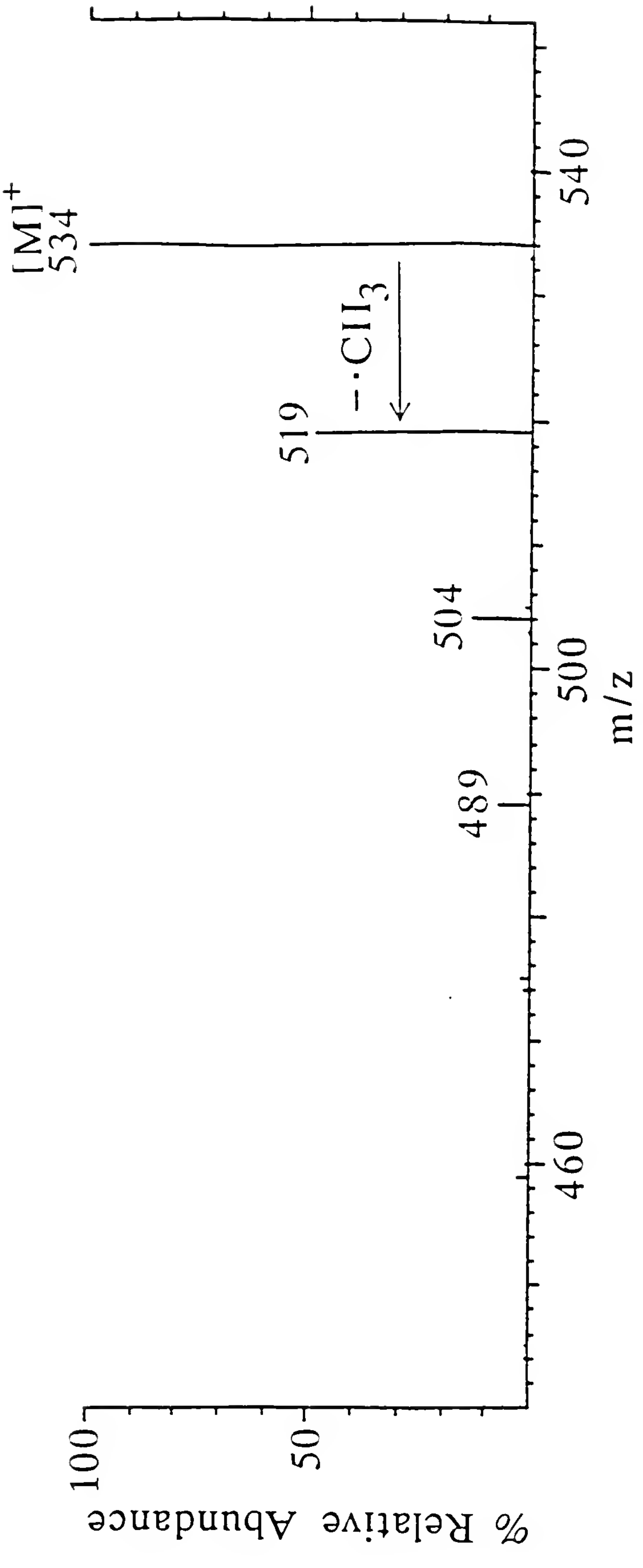
% Relative Abundance
100
50
m/z
460
500
540
489
504
519
534
[M]+
−·CH3

arise out of surface-induced decomposition. The mass spectrum from this peak (Figure 8-5) is useful for determining the sequence of the pyrroles around the porphyrin macrocycle.

Daughter ion experiments do require that conventional MS data are available for the sample in question, because the m/z of the desired parent ion must be known. For this reason, the method of porphyrin analysis outlined above actually requires that separate H_2CI/MS and $H_2CI/MS/MS$ experiments be performed. This is still more convenient than performing separate EI and CI experiments. On the other hand, the initial H_2CI/MS experiment can obviate the need for the H_2CI/MS in the combined scan experiment if, during this initial experiment, the DEP is heated enough to liberate pyrroles from the source walls. In other words, this technique does not actually provide three types of structural information in the same experiment, but rather in the same type (H_2CI) of experiment. This method does suffer from the same limitations for structure elucidation of porphyrins described previously for H_2CI/MS techniques, except that it can provide information about the structures of the peripheral substituents.

MS/MS of Porphyrins and Porphyrinogens

One of the more serious limitations in the techniques discussed above is that they are not very useful for structure elucidation of porphyrins in complex mixtures. In each case, at least part of the method consists of a conventional MS scan. Such scans detect ions that cannot be assigned to the specific porphyrins from which they

Figure 8-5.

Mass spectrum from the second mass chromatographic peak in the combined positive $H_2CI/MS/MS$ and positive H_2CI/MS experiments involving OEP introduced via a solids probe

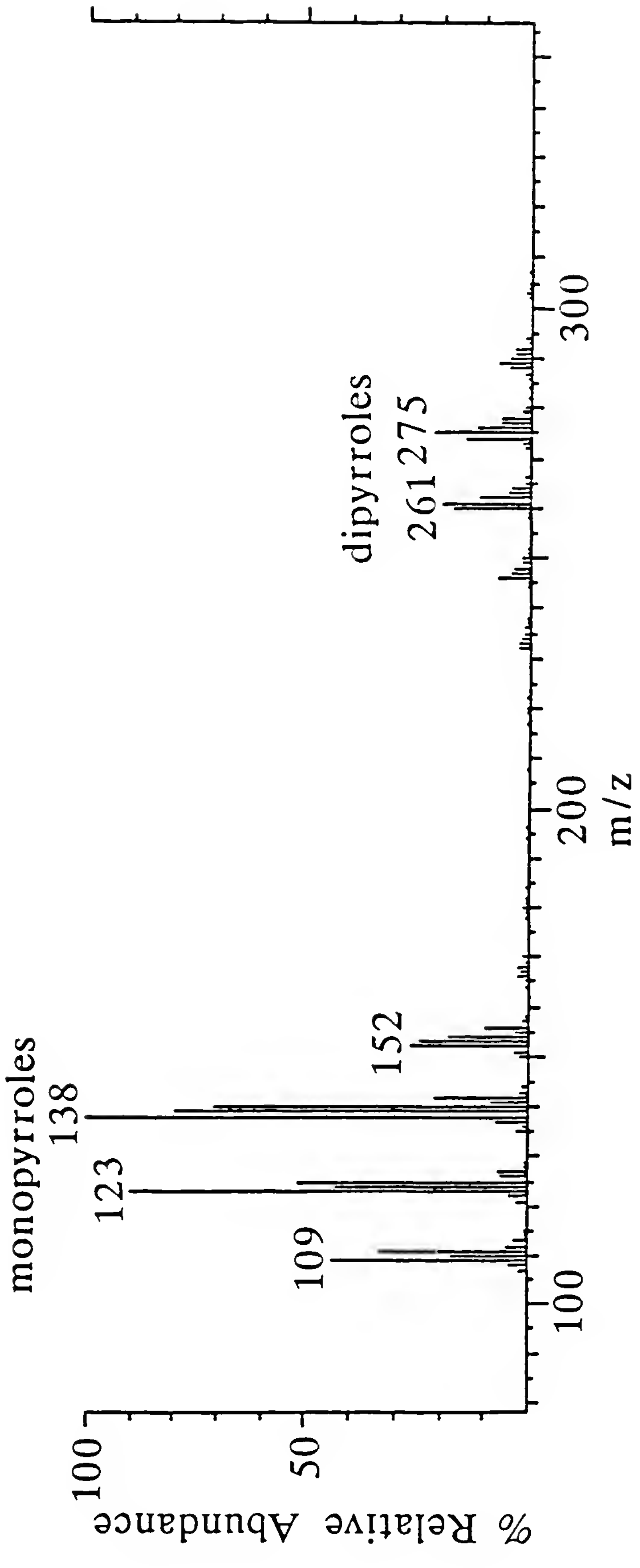
% Relative Abundance
100
50
m/z
100
200
300
monopyrroles
109
123
138
152
dipyrroles
261
275

arise in a complex mixture. One method for obtaining all three types of structural information from the same experiment does not include conventional MS scans, and is therefore quite useful for porphyrin mixture analysis.

When a porphyrin molecular ion, $[M]^+$, is selected as the parent ion and undergoes CAD, β-cleavage of peripheral substituents is the main fragmentation pathway (Johnson et al., 1986). Thus, MS/MS can be useful in determining the identities of peripheral substituents as was shown previously. Selecting a porphyrinogen ion, $[M + 6H]^+$, to fragment via CAD results in scission of the meso-bridge bonds, and yields mono-, di-, and tri-pyrrolic daughter ions. Van Berkel et al. (1988) have shown similar results with protonated porphyrinogen ions, $[M + 7H]^+$ which arise upon NH_3CI. Thus, MS/MS can also be very useful in sequencing the pyrroles around the macrocycle. All of the daughter ions arising from CAD originate from the specific parent m/z chosen. This makes mixture analysis possible because the daughter ions can be assigned to a specific porphyrinogen or porphyrin ion.

The data system associated with the triple quadrupole mass spectrometer is able to repeatedly cycle between passing selected parent ions into Q2 for CAD. That is, it can select a porphyrin $[M]^+$ ion as the parent ion by having Q1 pass only a particular m/z (e.g. m/z 534 for OEP) for a certain length of time, and then pass only the corresponding porphyrinogen ion, m/z 540, for another period of time. The data system can sequentially pass these two m/z's in the same experiment, and then deconvolute the data into two separate daughter ion mass spectra. The two daughter ion mass spectra shown in Figure 8-6 were obtained in this manner. Structural information about the peripheral substituents is obtainable from CAD of the molecular ion, $[OEP]^+$, while pyrrolic sequencing information can be obtained from CAD of the porphyrinogen ion, $[OEP + 6H]^+$.

This technique appears, however, to be limited to free-base porphyrins. Reduced metalloporphyrins do not form as abundantly as free-base porphyrinogens with the instrumentation and conditions employed in this dissertation (Chapter 6). The structures of reduced metalloporphyrins remain unclear. This technique could only be extended to include metalloporphyrins if the meso-bridge bonds of metalloporphyrins could be efficiently and reproducibly reduced. If one or more of the pyrrole rings are reduced instead of the meso-bridge bonds, as has been reported to occur, (Sundararaman et al., 1984), peripheral substituents would be cleaved upon CAD instead of meso-bridge bonds. In this case, this technique would not be useful for structure elucidation of metalloporphyrins.

As mentioned earlier, MS/MS techniques do require a separate MS experiment to determine the m/z of the desired parent ion. Therefore, this method does not technically yield three types of structural information from only one experiment. Performing two H_2CI experiments is certainly much more convenient than tuning for and performing separate EI and CI experiments. More importantly, this technique is quite useful for mixture analysis of free-base porphyrins. After the MS

Figure 8-6.

Positive H_2CI/MS/MS daughter ion mass spectra from OEP:
A. parent ion is $[OEP]^+$
B. parent ion is $[OEP + 6H]^+$

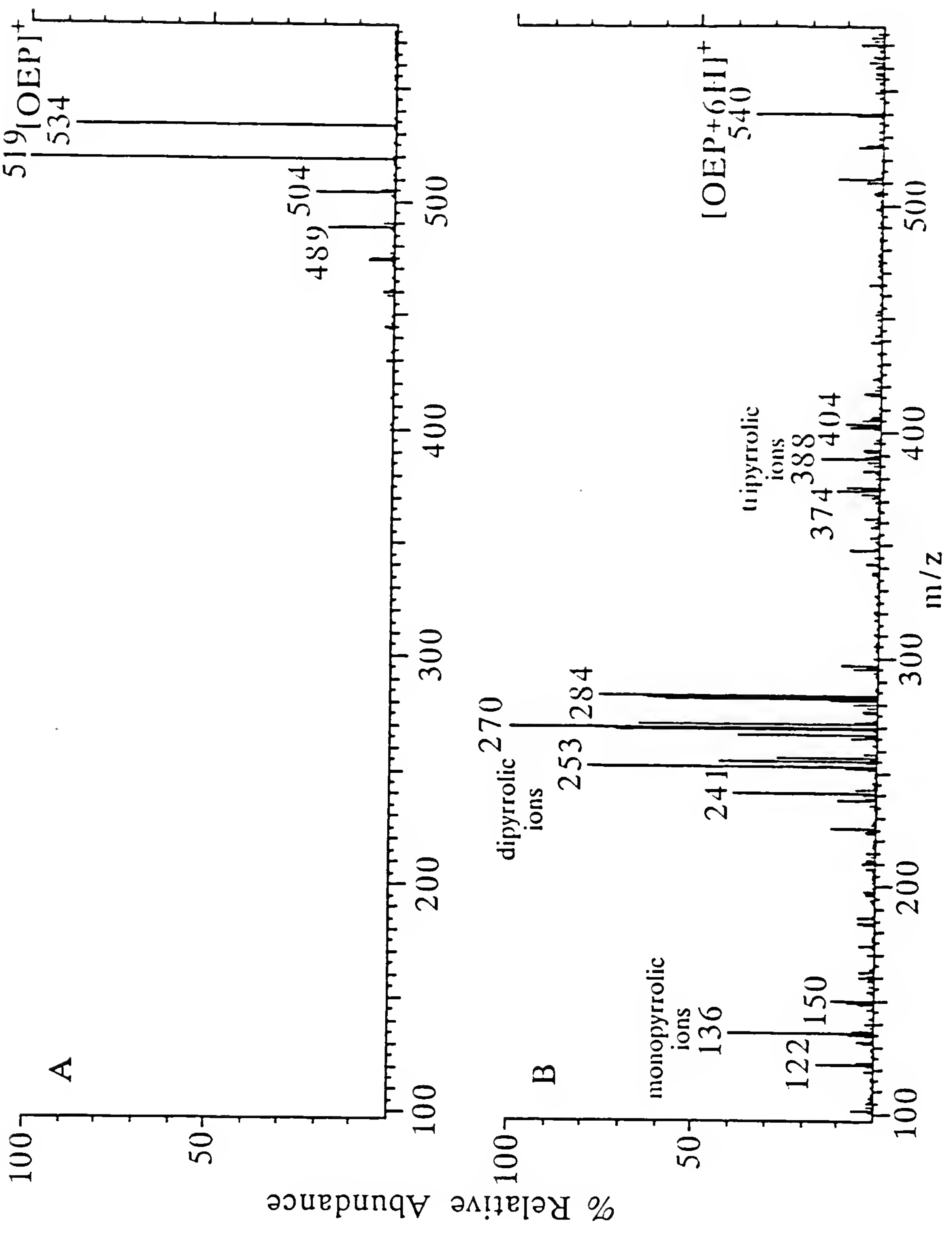
A
[OEP]$^+$
534
519
504
489
B
[OEP+6H]$^+$
540
monopyrrolic ions
122
136
150
dipyrrolic ions
241
253
270
284
tripyrrolic ions
374
388
404
100
50
% Relative Abundance
100
200
300
400
500
m/z

data is obtained from a mixture of such porphyrins, this method could be employed to obtain all three types of structural information for several different porphyrins, all during the same experiment. Not only is this method useful for mixture analysis, but it also saves time and requires less sample than methods requiring separate experiments for each porphyrin in a mixture. On the other hand, this method, as is the case with all H_2CI porphyrin structure elucidation techniques does not simplify complications arising from pyrrolic ions of coincident mass and pyrrolic ion containing variable numbers of meso-carbons.

Conclusions

Two mass spectrometric methods have been presented which yield carbon-number, pyrrolic structure, and sequencing information. Both are superior to conventional MS techniques because separate EI and CI experiments are not required. The first method, involving MS/MS of porphyrins and subsequent MS of decomposition products is not useful for mixtures of porphyrins, but is useful for analyzing metalloporphyrins. There is no reason to combine the MS/MS and MS scan modes into the same experiment, unless the m/z of the pure porphyrin standard is known prior to analysis. If the m/z of the porphyrin is not known, the MS experiment must be performed initially anyway. After that, only the MS/MS daughter ion mass spectrum is required.

The second technique, involving sequential CAD of free-base porphyrin and porphyrinogen ions, is very useful for mixture analysis of porphyrins, but is not useful for analyzing metalloporphyrins. It can provide both pyrrolic structure and sequencing information for several different porphyrin structures in a mixture in the same MS/MS experiment. This structure elucidation technique has several advantages over the other ones described. As mentioned earlier, this method saves time and is much more useful for analyzing complex mixtures. It also provides control over the extent to which fragmentation occurs. By adjusting the collision gas pressure and the collision energy, the analyst can optimize the daughter ion mass spectra to enhance the type of structural information desired. Such control is not as easily available with normal MS experiments. This method does appear limited to free-base porphyrins, so metalloporphyrin samples should be demetalated prior to analysis by the H_2CI/MS/MS method described here. Demetalation can be achieved without affecting the structure of the porphyrin skeleton (Buchler, 1975). This CI/MS/MS method may also require somewhat higher collision energies compared to EI/MS/MS experiments because CI is a softer ionization technique, and does not deposit as much internal energy into the ions in the source as does EI. Overall however, these disadvantages are minor, and can be easily dealt with. This technique is very useful for structure elucidation of porphyrins, and should enjoy wide use.

It is important to make note of two limitations common to structure elucidation of porphyrins by tandem mass spectrometry. The first is common to all chemical ionization techniques in which pyrrolic ions form and are used to determine the sequence of pyrroles around the porphyrin macrocycle, and has been discussed throughout this chapter. This concerns complications due to meso-carbons and coincident masses. This is not a serious liability to porphyrin structure elucidation, as the mono-, di- and tri-pyrrolic ion structures observed in such mass spectra are usually understandable. Such CI techniques have been employed for years, and have been quite useful. The contention in this chapter, however, is that such techniques do involve potential confusion not conducive to structure elucidation of unknown porphyrin structures. Perhaps MS/MS experiments involving the pyrrolic ions can lessen any potential structural confusion. The other limitation in terms of porphyrin structure elucidation is one which has not been addressed earlier, and is common to all mass spectrometric techniques discussed. It involves the fact that tandem mass spectrometry can only provide information about which pyrrole ring contains a specific peripheral substituent, not the position of that substituent on the pyrrole. For instance, if one of the pyrrole rings contains an ethyl and a methyl substituent, such as rings B and D in the C_{31} DPEP pictured in Figure 8-1, there is no way to distinguish the position of the ethyl group from the position of the methyl group on those pyrrole rings. In cases where this is of vital importance, mass spectrometry is not useful, and some other means such as ^1H NMR must be employed.

CHAPTER 9

SUMMARY AND FUTURE WORK

Summary

The work presented in this dissertation covers a variety of mass spectrometric techniques which can be utilized to enhance structure elucidation of porphyrins. Fundamental concepts of mass spectrometric structure elucidation by both new strategies and traditional methods have been explored. These have led to a better understanding of the complicated mechanisms involved in mass spectrometric analyses of porphyrins. Included in this dissertation are examples of geochemical questions about geoporphyrin biomarkers which are addressed by analytical tandem mass spectrometry. Although this dissertation focusses on porphyrin analysis with a triple quadrupole mass spectrometer, much of it is applicable to mass spectrometric analyses of other types of metalated and nonvolatile compounds as well.

Part 1 of this dissertation centers on geochemical applications of tandem mass spectrometric analysis of porphyrins. Geochemistry and petroleum exploration are two of many areas with interests in structure elucidation of porphyrins. As discussed in Part 1, geoporphyrins originate from ancient chlorophylls. Their structures are indicative of the depositional environment and geological history of the petroleum samples in which they are found. Geoporphyrins are very useful biomarkers, providing information about sample maturity and migration. Tandem mass spectrometry has been found to be useful for determining the structures of these complex molecules which are found in trace quantities in complicated mixtures.

Several questions about the metalloporphyrins found in a sample of New Albany shale are addressed in Part 1. First, geoporphyrins presumably originate as magnesium compounds (chlorophylls), yet are present today almost exclusively as Ni(II) and O=V(IV) compounds. Daughter ion mass spectra of corresponding Ni(II) and O=V(IV) porphyrins from the shale are similar suggesting that these geoporphyrins have a common origin and geological history. Second, information about the nature of kerogen, about which very little is known, was obtained by comparing the daughter ion mass spectra of porphyrins both from bitumen and from 300 °C kerogen pyrolysates. These MS/MS spectra are very similar as well, suggesting that release of the porphyrins from the kerogen occurs via enhanced solubilization and/or desorption, rather than scission of carbon-carbon bonds. This supports the theory that porphyrins are not bound to the kerogen by carbon-carbon linkages. These results also imply that the geoporphyrins in the kerogen pyrolysates do not offer any additional information not available from the bitumen. Since the bitumen is organically extractable, it is a much simpler matrix from which to obtain porphyrins than is the kerogen. Thus, analyses of geoporphyrins from kerogen pyrolysates are probably unnecessary for fingerprinting geoporphyrin biomarkers, as long as the bitumen is available. Third, daughter ion mass spectra of corresponding Ni(II) and O=V(IV) porphyrins from demineralized bitumen result in only one difference from the corresponding porphyrins in kerogen and bitumen from intact shale. This difference is that the O=V(IV) porphyrins found in demineralized shale are almost exclusively cycloalkanoporphyrins (CAPs), instead of the expected mix of CAPs and etio porphyrins. For some reason, it seems that mineral associated bitumen preferentially incorporates O=V(IV) CAP porphyrins over O=V(IV) etio porphyrins. Otherwise, the geoporphyrins found in all bitumen and kerogen samples were determined to have had similar origins and geological histories.

Part 2 of this dissertation focusses on new strategies for and fundamental studies of structure elucidation of porphyrins by tandem mass spectrometry. Chapter 5 specifically addresses formation and utility of doubly charged porphyrin ions. Electron ionization of porphyrins results in unusually abundant doubly charged ions. These ions can be useful in terms of structure elucidation for several reasons. They fragment much more efficiently than do corresponding singly charged porphyrin ions both in the ion source, and upon collisionally activated dissociation (CAD). In the ion source, the extent of fragmentation of the doubly charged metalloporphyrin ions was found to depend on the size, charge, and electronegativity of the metal. Thus, transmetalation was found to offer a method by which the extent of fragmentation in an EI source could be controlled. Doubly charged porphyrin ions were also found to fragment much more extensively upon CAD than corresponding singly charged ions. This is useful for structure elucidation of porphyrins because it allows the available collision energy for a given mass spectrometer to be effectively doubled. Doubly charged porphyrin ions were also found to fragment via different pathways than singly charged porphyrin ions in both the ion source and upon CAD. Doubly charged porphyrin ion analysis can enhance structure elucidation by producing ions which do not arise as singly charged species.

Chapter 6 concentrates on positive chemical ionization of porphyrins, and on the mechanism by which pyrrolic ions form under such conditions. Evidence is presented which supportes the idea that pyrroles in the CI ion source arise from surface-induced decomposition of porphyrins on the walls of the ion volume. This evidence refutes published reports of the pyrrolic ions resulting from gas-phase reductions of porphyrins. This work leads to interesting implications concerning mass spectra of other nonvolatile compounds which may also decompose upon interactions with surfaces within the ion source. Perhaps the nature of the surfaces within the ion source is a variable which can be used to optimize certain mass spectra. The chelated metal was also observed to have an effect on the extent to which metalloporphyrins decompose to form pyrroles in a CI source. Unfortunately, such surface reactions do not lend themselves to quantitation as easily or reproducibly as one might hope.

Electron capture negative chemical ionization of porphyrins is addressed in Chapter 7. Although this technique seems theoretically useful, it suffers from several practical drawbacks. This ionization technique is extremely sensitive and typically results in a molecular ion with minimal fragmentation. This seems rather useful for geoporphyrin analysis, as it could yield unambiguous carbon-number information about molecular ions without interferences from fragment ions. Unfortunately, ECNCI of porphyrins can result in extensive hydrogenation, which can make structure elucidation of pure compounds, not to mention complex mixtures, difficult if not impossible. This hydrogenation is not very reproducible, nor does it appear to be controllable. The hydrogenated product ions fragment much more efficiently than do negatively charged porphyrin ions; however, the analytical utility of this seems limited due to the ambiguity of the structures of the hydrogenated product ions. Another problem with ECNCI is that it is much more sensitive toward metalloporphyrins than it is toward free-base porphyrins. This can be a major problem for ECNCI analysis of mixtures of free-base and metalated porphyrins. It appears to be a problem as well for ECNCI analyses of even pure free-base compounds because even trace impurities of metalloporphyrins arising from trace amounts of metals in the porphyrin solution or from abstraction of metals from the ion source yield much more intense ion signals than do the more abundant free-base porphyrins because metalloporphyrins are so efficiently ionized.

Finally, Chapter 8 introduces two MS/MS techniques which offer carbon-number, pyrrolic structure, and pyrrole sequencing information from the same experiment. Both are compared to conventional EI/MS and CI/MS techniques, and are shown to be superior for porphyrin structure elucidation. The traditional EI/MS method is limited by the fact that it offers no information about the sequence of pyrroles around the porphyrin macrocycle. The conventional CI/MS techniques are shown to offer structural information which is complementary to that from EI/MS, but the CI/MS methods are not useful for complex mixtures. One of the new techniques presented consists of a combined H_2CI experiment. The first part entails H_2CI/MS/MS daughter ion experiments with the porphyrin molecular ions. It offers information about the peripheral substituents and carbon-number. The second part involves H_2CI/MS analysis of the pyrrolic ions arising out of surface-induced decomposition of the porphyrins and subsequent ionization. This part yields information about the sequence of the pyrroles around the porphyrin macrocycle. Unfortunately, as this method includes H_2CI/MS analysis of decomposition products, it is not useful for complex mixtures. A second method was presented which can be utilized for complex mixtures of porphyrins. This one consisted of performing H_2CI/MS/MS daughter ion scans on both the molecular porphyrin ion and on its corresponding porphyrinogen ion on alternate scans. The daughter ions from the molecular ion gave information about the peripheral substituents and the carbon-number of the porphyrin. The porphyrinogen ions, which arise from reduced porphyrins, yielded pyrrolic ions upon CAD. These can be used to sequence pyrroles around the porphyrin. The main drawback with the second method is that it seems to be useful for free-base porphyrins, but not for metalloporphyrins.

This dissertation answers several questions about geoporphyrins, suggests various mechanisms for phenomena which are not well understood, and presents several new strategies which can enhance structure elucidation of porphyrins. As is typical of research, however, it brings up as many questions as it answers. The results detailed in this dissertation suggest many areas in which more research is needed.

Suggested Future Work with Geoporphyrin Biomarkers

There are several diverse topics addressed by this dissertation, resulting in the need for further research in a number of areas. One of these areas is the very broad field of geochemistry. One of the first topics that will be addressed upon completion of this dissertation is a comparison of the high carbon-number (greater than 40 carbons) geoporphyrins from New Albany shale with those from Boscan oil. None of the work described in Part 1 of this dissertation dealt with such porphyrins; from that standpoint, such future work would be a logical extension. It is an important task for another reason as well, however, because analysis of the high carbon-number geoporphyrins from Boscan oil has already been completed (Britton, 1985). This would mean that a direct comparison between the structures of these geoporphyrins from both Boscan oil and New Albany shale could be accomplished. Another geochemical topic which should continue to be of interest is that of the structure of the kerogen matrix. This is thought to be a highly polymerized matrix, but very little is known about it because it is not soluble in organic solvents nor in acids. Complete structure elucidation of the porphyrins from New Albany bitumen and pyrolysates will be necessary in order to unambiguously determine the mechanism of the liberation of porphyrins from the kerogen of the New Albany shale. This mechanism may provide added insight into the nature of kerogen. Pyrolysis studies on kerogens from other geological samples are needed as well, to determine whether porphyrins are liberated from other kerogens by similar mechanisms. It would also be interesting to determine if certain types of metalloporphyrins are preferentially incorporated into the mineral associated bitumen, as the preliminary studies in Chapter 4 indicate. This could have serious ramifications in terms of comparing geoporphyrins from different geological samples.

Suggested Future Work with Chemical Ionization of Porphyrins

Much future mass spectrometric research will undoubtedly focus on chemical ionization of porphyrins. The idea that pyrrolic ions observed upon positive chemical ionization of porphyrins result from surface-induced decomposition reactions rather than from gas-phase fragmentations is gaining wider acceptance. The plethora of data concerning chemical ionization of porphyrins must be more critically evaluated in order to determine whether or not gas-phase reduction and fragmentation also play a significant role in the production of pyrrolic ions in a CI source. Further work remains to be done to determine the actual mechanisms involved in surface-induced decomposition of porphyrins under positive CI conditions.

Another challenge which lies ahead is to quantitatively determine the effect of the chelated metal on surface-induced decomposition of metalloporphyrins under positive CI conditions. The preliminary results in Chapter 6 indicate that the metal does have an effect. This would not be surprising, as decomposition of metalloporphyrins on a metal surface is thought to occur after demetalation. Since the ease with which a metalloporphyrin demetalates is a function of parameters of the metal itself, physical properties of the chelated metals probably have a noticeable effect on the extent of decomposition. An extension of the study in Chapter 6 to include all eighteen OEP derivatives studied in Chapter 5 under H_2CI conditions by DEP is desireable, but not feasible with the Finnigan MAT TSQ45 because the ion source cannot be heated above 190 °C. Introduction via DEP results in two easily distinguishable mass chromatographic peaks: one consisting of predominantly molecular and protonated molecular ions, and the other consisting of surface-induced decomposition product ions. Although the DEP attains much higher temperatures than the solids probe, there is no way to easily determine to what temperatures it is able to heat the ion volume. Again, comparing the extent of decomposition of various metalloporphyrins on the surface is difficult, if not impossible, with the instrument employed. Even if the ion volume is cleaned before each analysis, and the DEP is able to heat the ion volume to a high enough temperature to liberate all of the pyrroles formed, there is no indication of the extent to which porphyrins are left on the surface at the end of the analysis. To determine this, the ion volume could be rinsed in a solvent, and then a UV-vis spectrophotometer used to quantitate the porphyrin residue. It would be much simpler to employ an ion source which can be somewhat rapidly heated to temperatures above 400 °C. With a source such as this, one could obtain a mass spectrum of all of the species remaining on the ion volume. This could yield invaluable information about the mechanisms involved in surface-induced decomposition of porphyrins under positive CI conditions.

Another interesting extension of the research presented in this dissertation would be a quantitative appraisal of the effect of metal ions on the ease with which they are ionized by electron capture negative chemical ionization. Just as there is a significant difference between the efficiencies of ECNCI for free-base and metalated porphyrins, there may be differences in the efficiencies of ECNCI among metalloporphyrins having identical skeletons. If metalloporphyrins capture thermal electrons into empty metal orbitals, those containing unoccupied orbitals at the lowest energy levels should ionize most efficiently. The experiments involved in determining the effects of the metal ions are not trivial, and may only be useful for certain metals. First of all, there is little or no fragmentation occurring among the negatively charged ions, so there are no built-in internal standards as with EI (Chapter 5). To obtain a measure of the abundance of negatively charged molecular ions, for instance, one would probably need to add an internal standard consisting of another similar metalloporphyrin to each of the metalloporphyrins in question. The ratios of the relative abundances of the analytes to the standard are probably more reliable than comparing absolute abundances of analyte ions from separate analyses. Ions from the internal standard must not overlap those from the analyte, so the metal and skeleton of the internal standard should be chosen carefully. The efficiency of the internal standard toward ECNCI must be similar to those of the analytes in order to obtain sufficient signal from the internal standard without saturation of the thermal electron population. It is also imperative that the total amount of analyte and internal standard analyzed does not saturate the thermal electron population. In a preliminary study of 17 metalated OEP derivatives by electron capture negative hydrogen chemical ionization mass spectrometry, several problems arose which make such analyses difficult. First of all, trace amounts of impurities in some of the samples dominated those ECNCI mass spectra. Secondly, some of the metalated OEP compounds hydrogenated much more extensively than the others, most notably the Zn(II) and Ni(II) compounds. As many of the metalloporphyrins studied did not hydrogenate to any significant extent, hydrogenated product ions were not useful as an internal standard. Obviously, much work remains if trends in the ECNCI mass spectra of metalloporphyrins are to be related to the metal ions.

One last set of questions still deserving attention concerns the problems associated with ECNCI of porphyrins. Hydrogenation of porphyrins remains an uncontrollable and irreproducible phenomenon. This is quite unfortunate, not only because this process may prevent use of ECNCI for porphyrin mixture analysis, but also because hydrogenated product ions fragment so much more efficiently than do negatively charged molecular porphyrin ions. The ECNCI methods would be much more useful in terms of structure elucidation of porphyrins if hydrogenation were controllable, reproducible, and/or better understood from a structural standpoint. Work also remains to be done in determining the origin of the iron porphyrin adducts in the ECNCI mass spectra of free-base porphyrins. If the free-base porphyrins are actually abstracting the iron from the source, the mechanism for this process must be understood so predictions can be made for ECNCI of other similar compounds. It is also important to determine why iron seems to be so readily abstracted from stainless steel, while copper does not seem prone to such abstraction from metallic copper surfaces.

This dissertation lays a foundation for further research in an important field of study. It supports and refutes some existing literature. This work offers new information about structure elucidation of porphyrins by tandem mass spectrometry, much of which should also extend to mass spectrometric analyses of other types of compounds. This dissertation is presented in the hope that it will serve not only as a useful reference, but also as a springboard for future research.

APPENDIX

EI/MS/MS DAUGHTER ION MASS SPECTRA OF Ni(II) AND O=V(IV) GEOPORPHYRINS FROM THE BITUMEN AND KEROGEN FROM NEW ALBANY SHALE

The mass spectra on the following pages are examples of comparisons made in Chapter 3 concerning the similarities between various geoporphyrins found in New Albany shale. All MS/MS daughter ion mass spectra were obtained, in the positive ion mode, on a Finnigan MAT TSQ45 triple quadrupole mass spectrometer equipped with an INCOS data system. The samples were placed in glass vials and introduced via a solids probe in which samples were heated from ambient to 400 °C at 99 °C/min. The samples were ionized with an electron energy of 70 eV and an emission current of 0.3 mA. Daughter ion mass spectra were obtained using nitrogen (1.9 mtorr) for collisionally activated dissociation in the second quadrupole with a collision energy of 20 eV. In each case, the parent ion m/z selected consists of predominantly molecular ions.

DAUGHTERS OF m/z 506 FROM NICKEL C_{30} ETIO

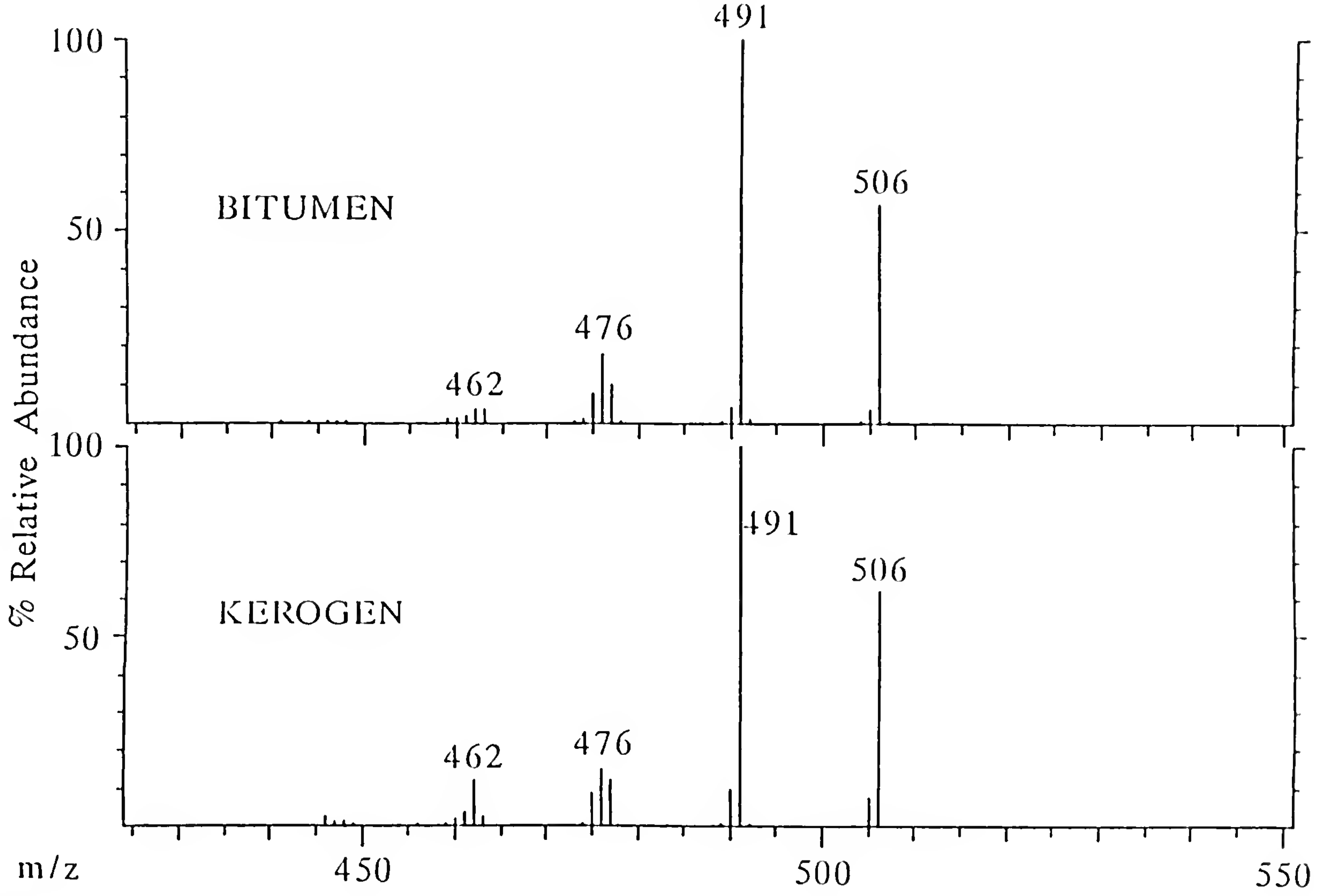

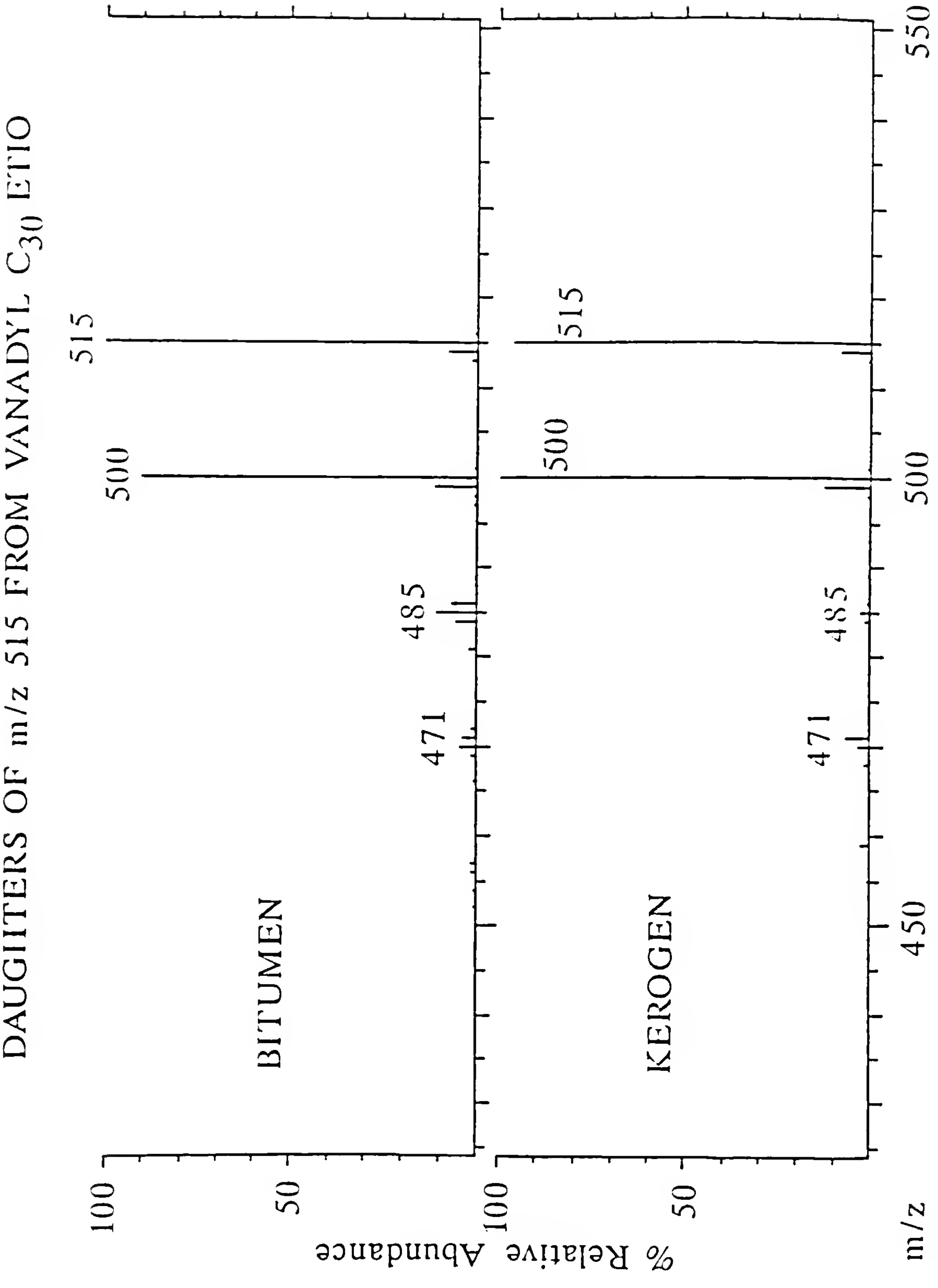

DAUGHTERS OF m/z 515 FROM VANADYL C_{30} ETIO

DAUGHTERS OF m/z 518 FROM NICKEL C_{31} CAP

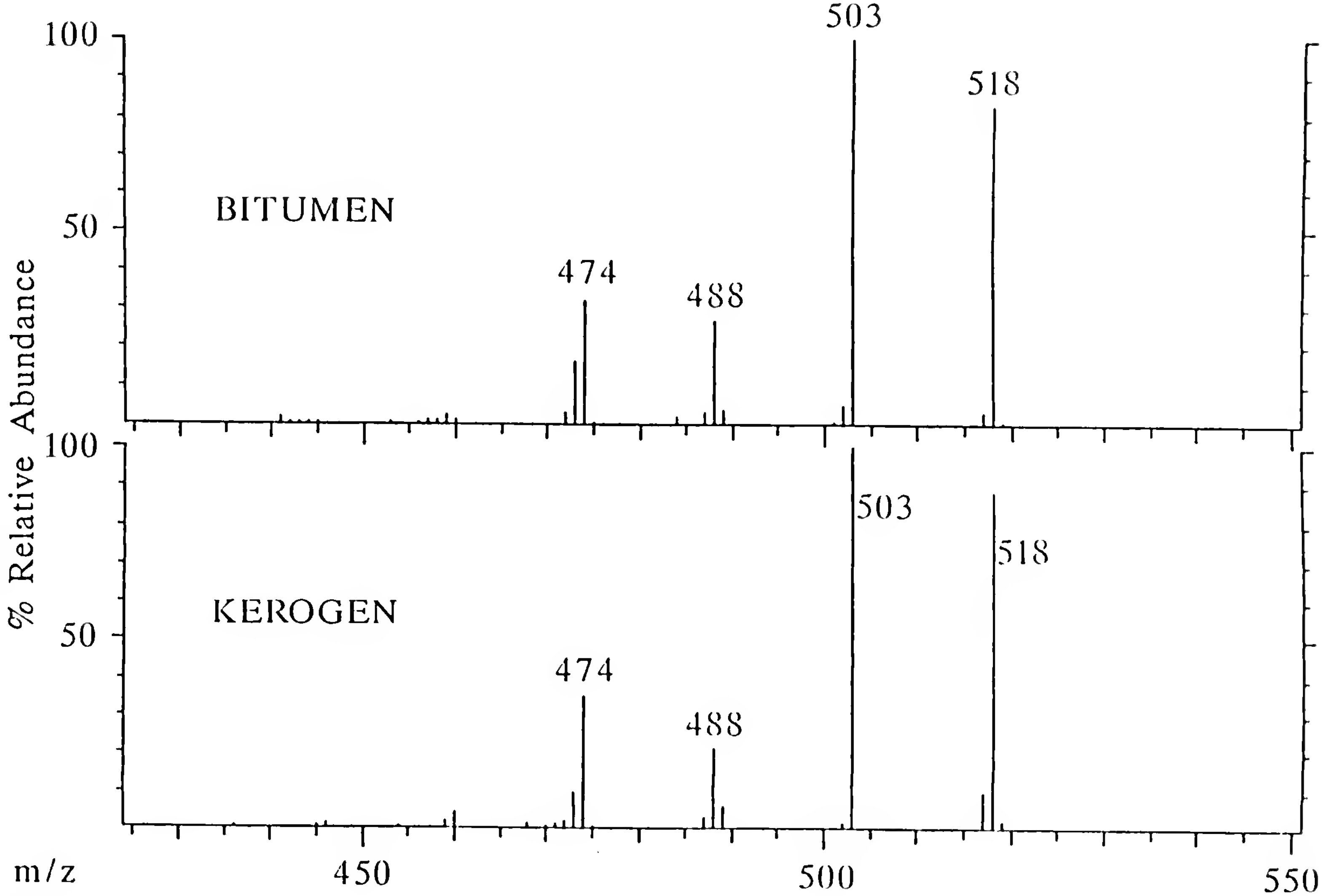

DAUGHTERS OF m/z 527 FROM VANADYL C_{31} CAP

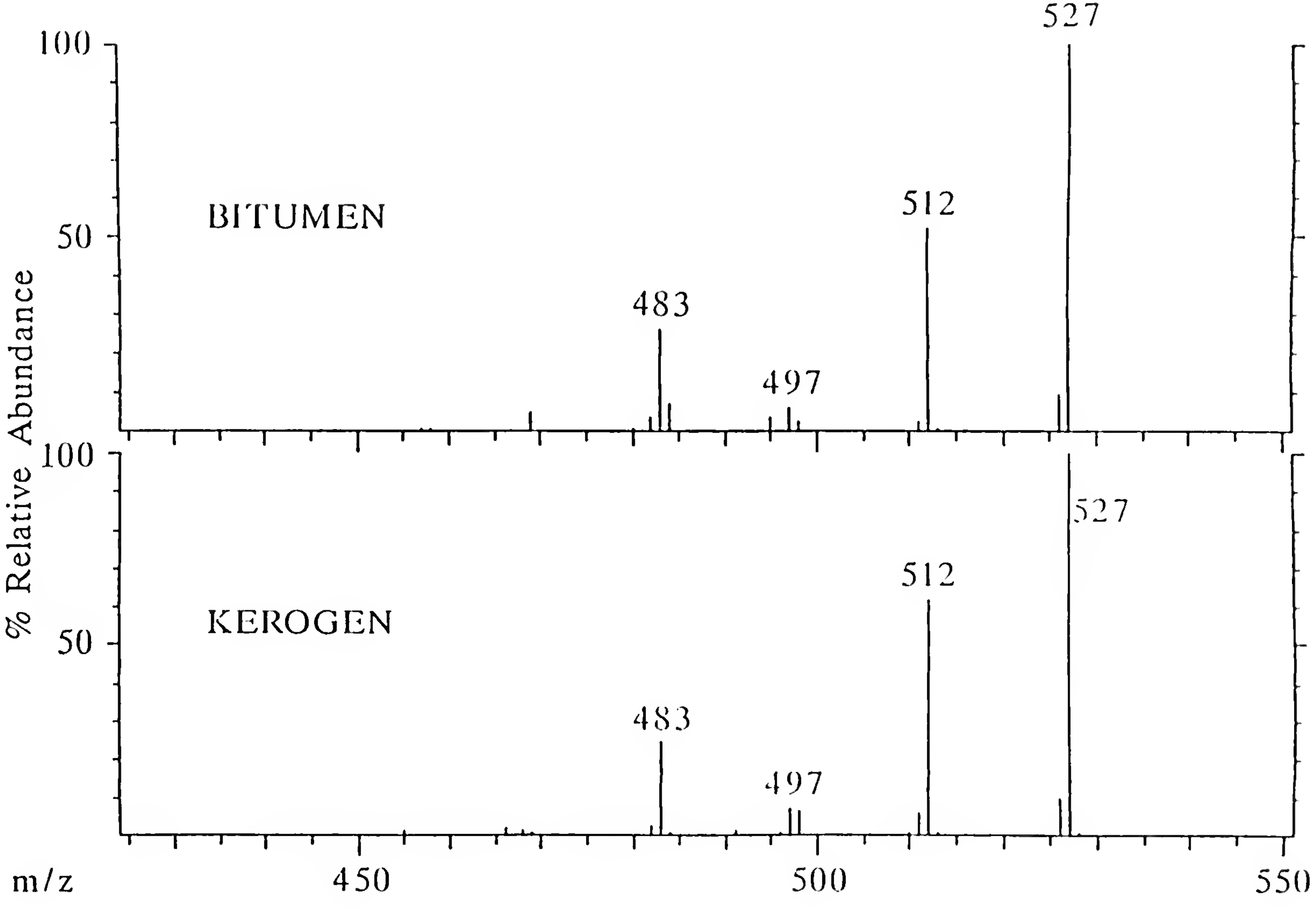

EI/MS/MS OF C_{28} ETIO M^+ FROM KEROGEN

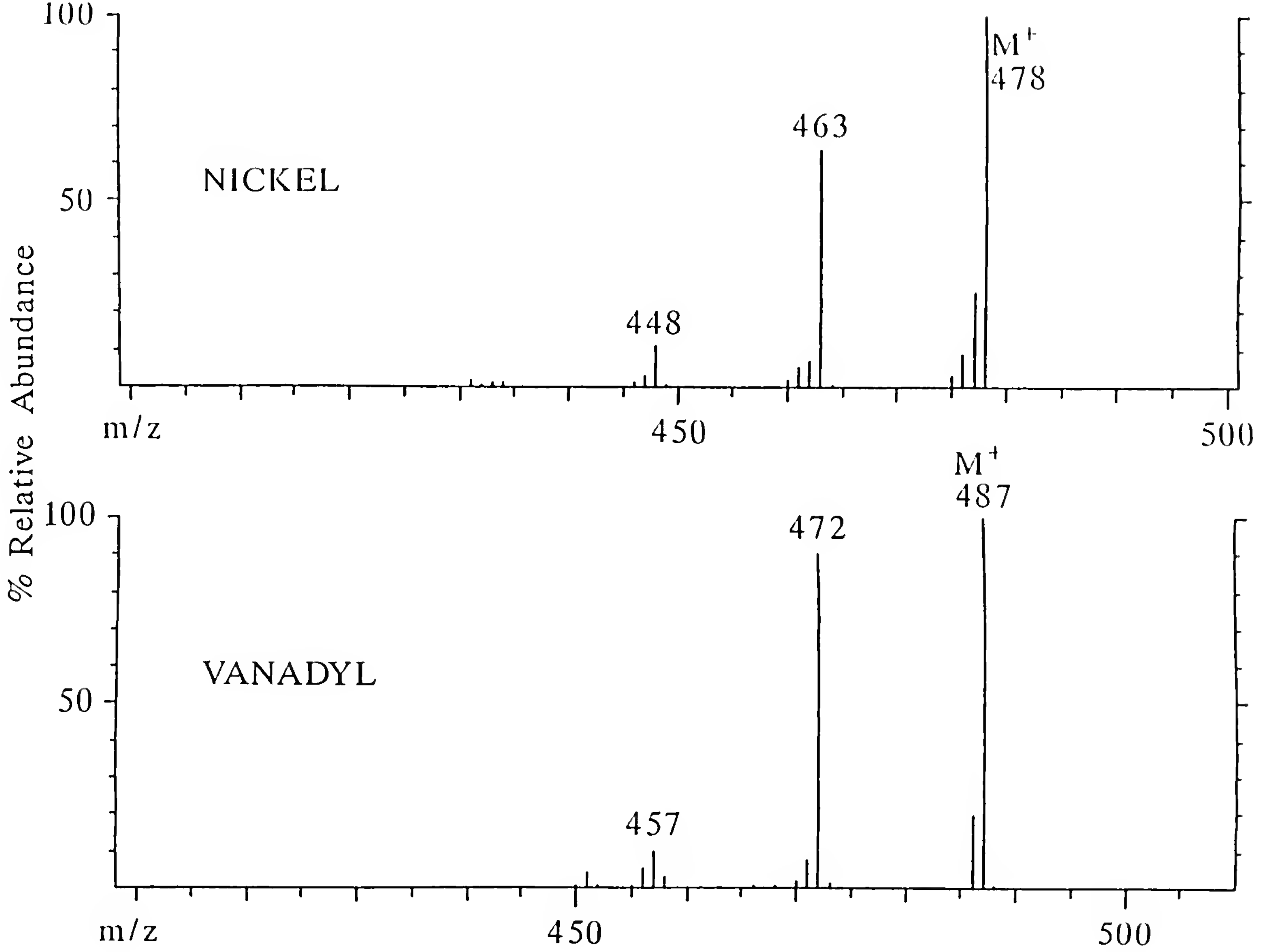

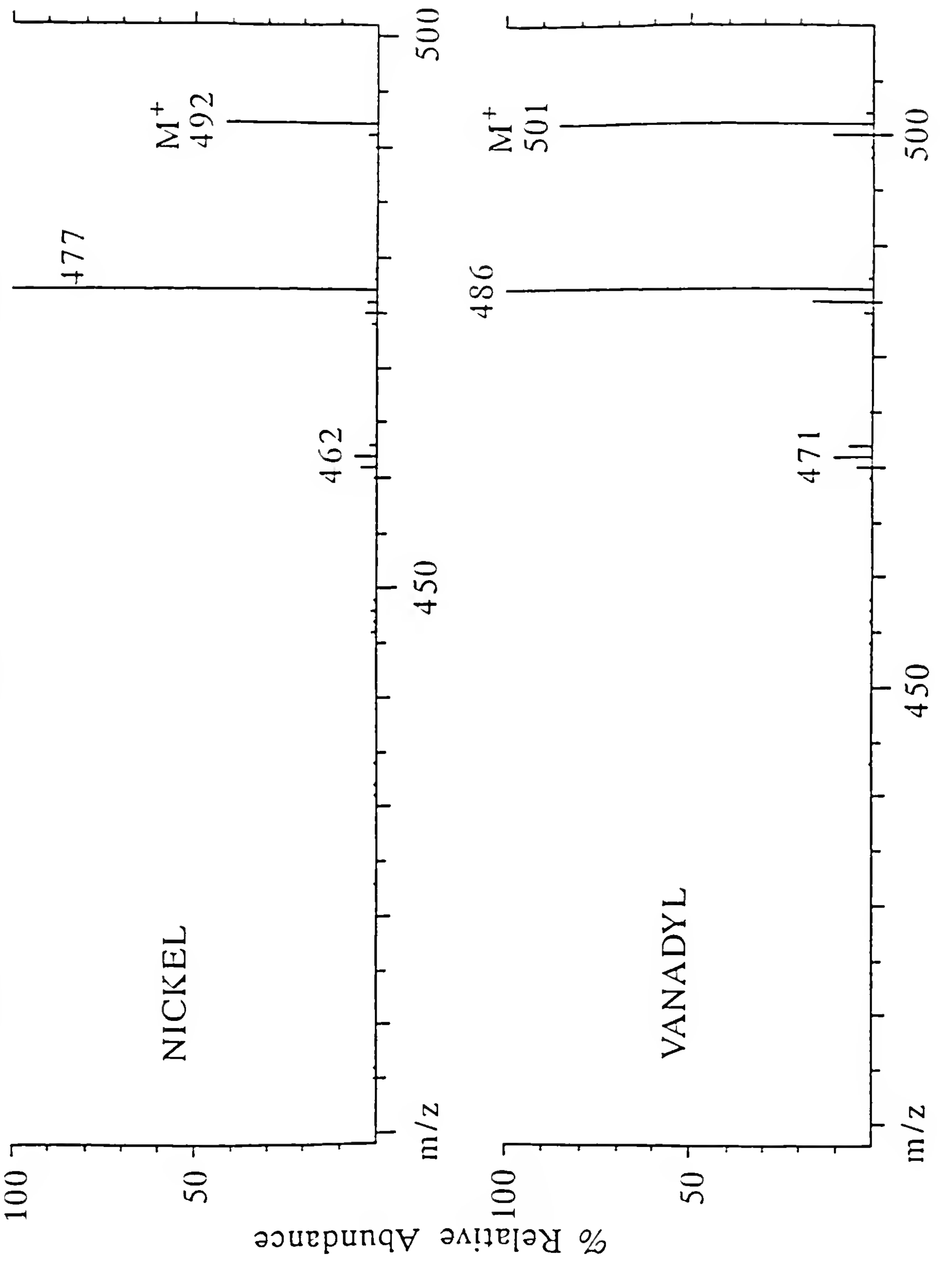

EI/MS/MS OF C_{29} ETIO M^+ FROM BITUMEN

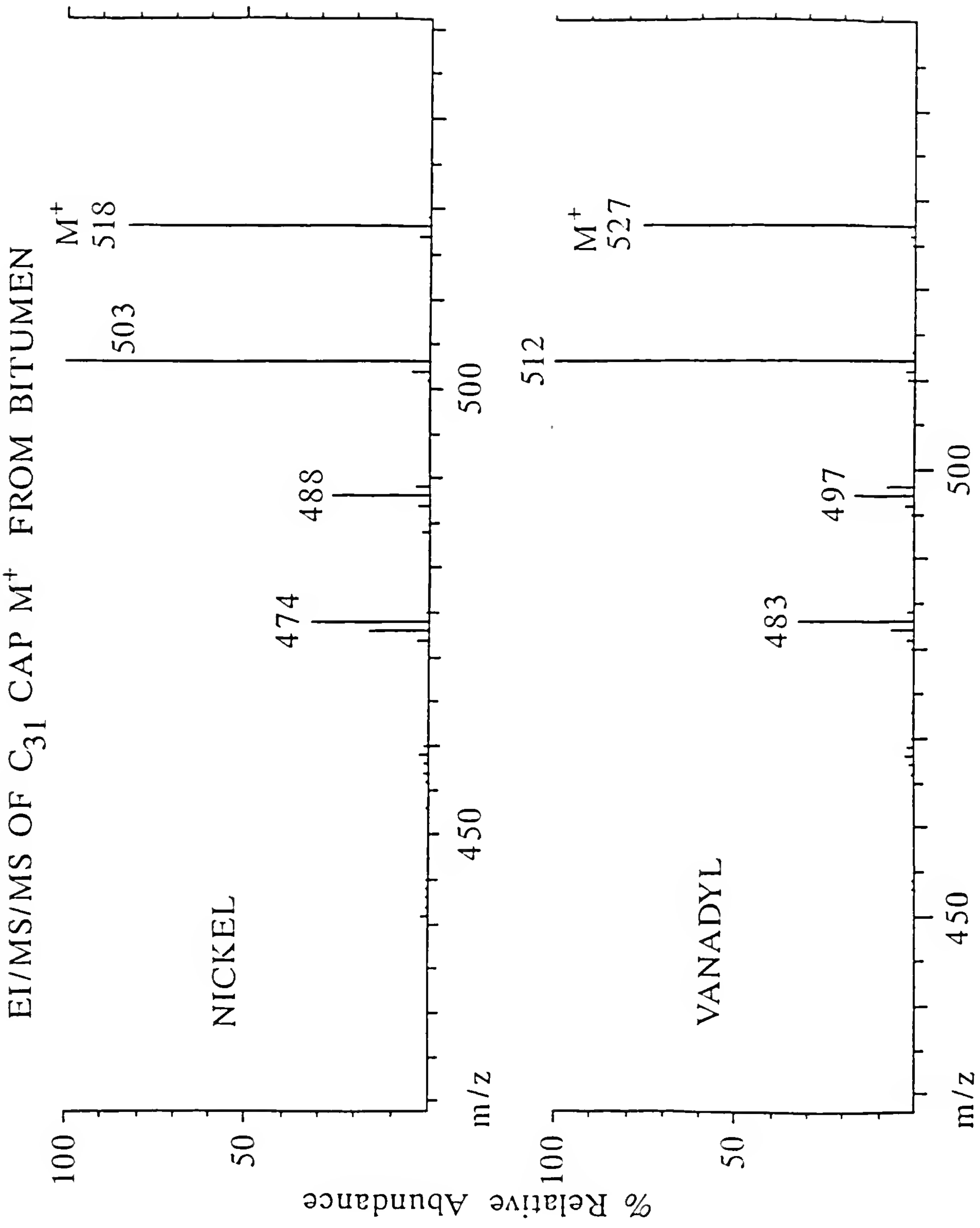
EI/MS/MS OF C_{31} CAP M^+ FROM BITUMEN
NICKEL
474
488
503
518
M^+
450
500
m/z
VANADYL
483
497
512
527
M^+
450
500
m/z
100
50
100
50
% Relative Abundance

EI/MS/MS OF C_{32} CAP M^+ FROM KEROGEN

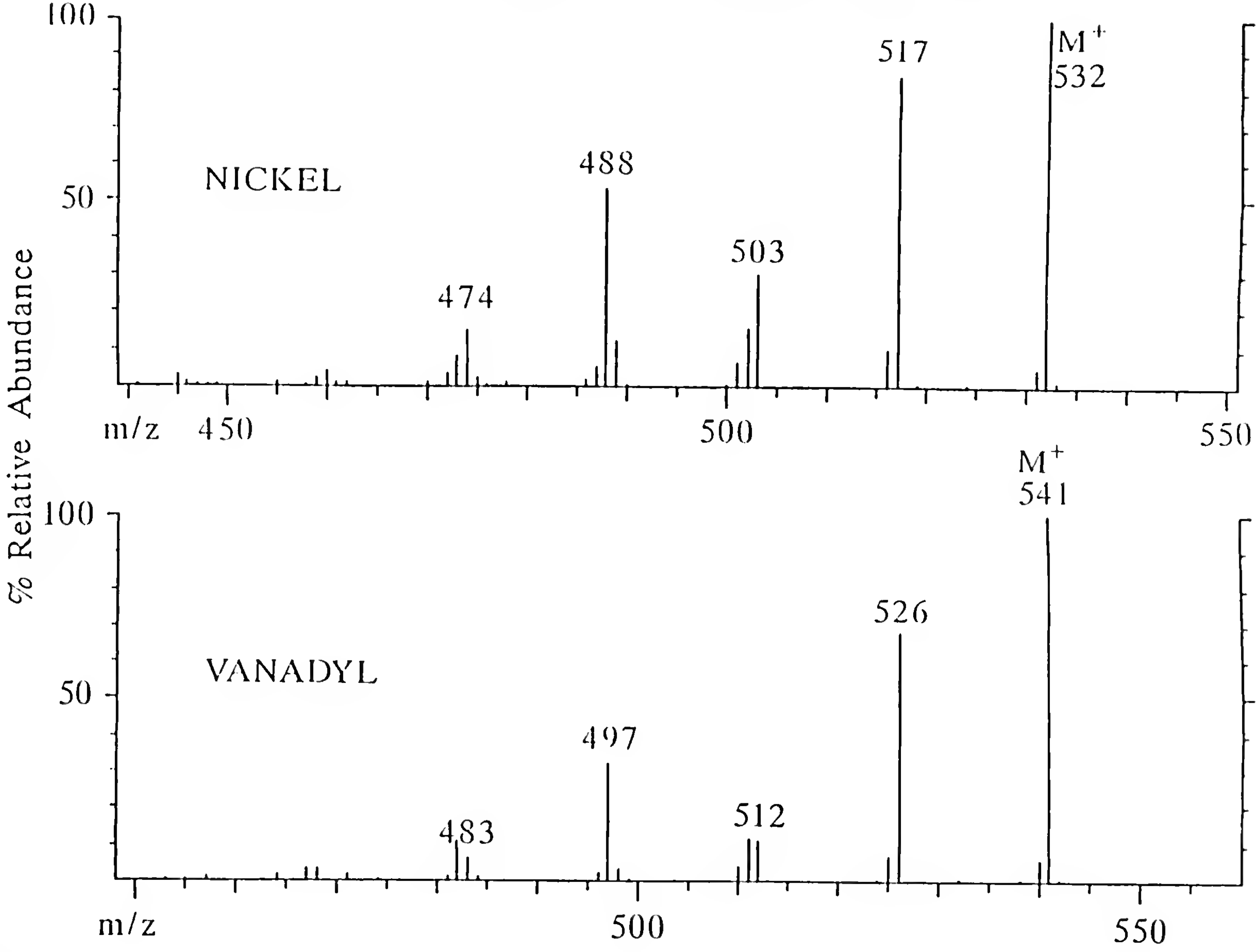

LITERATURE CITED

Appling, J.R., Jones, B.E., Abbey, L.E., Bostwick, D.E., and Moran, T.F. (1983) Doubly charged ion mass spectra 7 -- acetylenes. Org. Mass Spectrom., 18, 282-294.

Ast, T., Beynon, J.H., and Cooks, R.G. (1972a) Charge localization: doubly charged ion reactions in toluene. Org. Mass Spectrom., 6, 741-747.

Ast, T., Beynon, J.H., and Cooks, R.G. (1972b) The doubly charged ion mass spectra of hydrocarbons. Org. Mass Spectrom., 6, 749-763.

Ast, T., Kralj, B., Kramer, V., Zigon, D. (1988) A study of doubly charged ions in aluminum and iron acetylacetonates. Int. J. Mass Spectrom. Ion Proc., 86, 329-339.

Baker, E.W. and Louda, J.W. (1983) Thermal aspects of chlorophyll geochemistry. In M. Bjørøy et al. (Editors), Advances in Organic Geochemistry 1981, Wiley, Chichester, U.K., pp. 401-421.

Baker, E.W. and Louda, J.W. (1986) Porphyrins in the geologic record. In R.B. Johns (Editor), Biological Markers of the Sedimentary Record, Elsevier, Amsterdam pp. 125-225.

Baker, E.W. and Palmer, S.E. (1978) Geochemistry of porphyrins. In D. Dolphin (Editor), The Porphyrins, Vol. 1, Academic Press, New York, NY, pp. 486-552.

Barber, M., Bell, D.J., Morris, M.R., Tetler, L.W., and Woods, M.D. (1988) Mass spectra of doubly charged ions. Proceedings of the 36th ASMS Conference on Mass Spectrometry and Allied Topics, San Francisco, California, June 5-10, 1988, pp. 115-116.

Barrows, M.H. and Cluff, R.M. (1984) New Albany shale Group (Devonian-Mississippian) source rocks and hydrocarbon generation in the Illinois Basin. Am. Assoc. Petrol. Geol. Memoir, 35, 111-138.

Barwise, A.J.G. (1987) Mechanisms involved in altering deoxophylloerythroetioporphyrin-etioporphyrin ratios in sediments and oils. In R.H. Filby and J.F. Branthaver (Editors), Metal Complexes in Fossil Fuels. ACS Symposium Series, 344, American Chemical Society, Washington, D.C., pp. 100-109.

Barwise, A.J.G., Evershed, R.P., Wolff, G.A., Eglinton, G., and Maxwell, J.R. (1986) High-performance liquid chromatographic analysis of free-base porphyrins I. An improved method. J. Chromatogr., 368, 1-9.

Barwise, A.J.G. and Roberts, I. (1984) Diagenetic and catagenetic pathways for porphyrins in sediments. Org. Geochem., 6, 167-176.

Baum, R.M. (1988) Metalloporphyrin research makes strides in biomedical applications. Chem. Eng. News, 66, 18-22.

Beynon, J.H. (1960) Mass Spectrometry and its Applications to Organic Chemistry, Elsevier, Amsterdam, p. 311.

Beynon, J.H., Caprioli, R.M., Baitinger, W.E., and Amy, J.W. (1970) The ion kinetic energy spectra of some aromatic hydrocarbons. Org. Mass Spectrom., 3, 455-477.

Beynon, J.H., Lester, G.R., and Williams, A.E. (1959) Some specific molecular rearrangements in the mass spectra of organic compounds. J. Phys. Chem., 63, 1861-1868.

Beynon, J.H., Mathias, A., and Williams, A.E. (1971) 'Doubly charged ion' mass spectra of some simple aromatic compounds. Org. Mass Spectrom., 5, 303-310.

Bonnett, R. and Czechowski, F. (1981) Metals and metal complexes in coal. Trans. Roy. Soc. Lond., Ser. A, 300, 51-63.

Bonnett, R. and Hughes, P.S. (1989) Porphyrin analysis and coal rank: a porphyrin index of coalification. Presented at the American Chemical Society 197th National Meeting and Exposition in Dallas, Texas, April 9-14, 1989.

Boyd, R.K., Jamieson, W.D., and Sim, P.G. (1988) Collision-induced dissociation reactions of doubly charged ions of polycyclic aromatic hydrocarbons. Proceedings of the 36th ASMS Conference on Mass Spectrometry and Allied Topics, San Francisco, California, June 5-10, 1988, pp. 99-100.

Britton, E.D. (1985) Analysis of High Carbon-number Geoporphyrins in Boscan Oil by Tandem Mass Spectrometry, Master's Thesis, University of Florida.

Brodbelt, J.S., Cooks, R.G., Wood, K.V., and Jackson, T.J. (1986) The analysis of metalloporphyrins in petroleum using tandem mass spectrometry. Fuel Sci. Tech. Int., 4, 683-698.

Buchler, J.W. (1975) Static Coordination Chemistry of Metalloporphyrins. In K.M. Smith (Editor), Porphyrins and Metalloporphyrins, Elsevier, Amsterdam, pp. 157-231.

Budzikiewicz, H. (1978) Mass spectra of porphyrins and related compounds. In D. Dolphin (Editor), The Porphyrins, Vol. III, Academic Press, New York, NY, pp. 395-461.

Budzikiewicz, H. (1988) Reactions between substrate molecules and chemical ionization reagent gases prior to ionization. Org. Mass Spectrom., 23, 561-565.

Chakraborty, S., Clezy, P.S., Sternhell, S., and van Thuc, L. (1982) The chemistry of pyrrolic compounds. LII the preferred pathway of electron delocation in metalloporphyrins. Aust. J. Chem., 35, 2315-2323.

Chicarelli, M.I., Kaur, S., and Maxwell, J.R. (1987) Sedimentary porphyrins: unexpected structures, occurrence and possible origins. In R.H. Filby and J.F. Branthaver (Editors), Metal Complexes in Fossil Fuels ACS Symposium. Series, 344, American Chemical Society, Washington, D.C., pp. 40-67.

Clezy, P.S., Lim, C.L., and Shannon, J.S. (1974) Chemistry of pyrrolic compounds. XXVIII the synthesis of acrylic acid porphyrins: porphyrin mass spectra. Aust. J. Chem., 27, 2431-2437.

CRC Handbook of Chemistry and Physics, R.C. Weast (Editor), (1979) CRC Press, Inc., Boca Raton, pp. D155-D156.

Dillow, G.W. and Gregor, I.K. (1988) Gas-phase reactions of electrons, halide ions and radicals with (meso-tetraphenylporphinato)metal(II) complexes under negative ion chemical ionization conditions. Org. Mass Spectrom., 23, 777-782.

Dillow, G.W., Gregor, I.K., and Guilhaus, M. (1986) Adduct ion formation by metal complexes under methane negative chemical ionization conditions. Org. Mass Spectrom., 21, 151-156.

Eckardt, C.B. and Maxwell, J.R. (1989) Are iron porphyrins restricted to coals? Presented at the American Chemical Society 197th National Meeting and Exposition in Dallas, Texas, April 9-14, 1989.

Edwards, L., Dolphin, D.H., and Gouterman, M. (1970) Porphyrins XVI. vapor absorption spectra and redox reactions: octalkylporphins. J. Mol. Spectrosc., 35, 90-109.

Eglinton, T.I. and Douglas, A.G. (1988) Quantitative study of biomarker hydrocarbons released from kerogen during hydrous pyrolysis. Energy and Fuels, 2, 81-88.

Eglinton, G., HajIbrahim, S.K., Maxwell, J.R., Quirke, J.M.E., Shaw, G.J., and Wardroper, A.M.K. (1979) Lipids of aquatic sediments, recent and ancient. Phil. Trans. R. Soc. Lond. A, 293, 69-91.

Freeman, D.H., Angeles, R.M. and Keller, S. (1988) Determination of the geoporphyrins in Athabasca tar sands using semi-automatic chromatographic deasphaltation. Preprints Div. Pet. Chem. Amer. Chem. Soc., June 5-11, 231-238.

Gilbert, W.C., Taylor, L.T., Dillard, J.G. (1973) Mass spectrometric study of polydentate Schiff base coordination compounds. I. cobalt(II), nickel(II), and copper(II) complexes of salen and oaben. J. Amer. Chem. Soc., 95, 2477-2482.

Hanner, A.W., Abbey, L.E., Bostwick, D.E., Burgess, E.M. and Moran, T.F. (1982) Doubly charged ion mass spectra IV -- chlorinated and brominated alkanes. Org. Mass Spectrom., 17, 19-28.

Henis, N.B.H., Busch, K.L., Bursey, M.M. (1981) Methane enhanced negative ionization mass spectra of some biologically important chelate compounds: porphyrins, dithiophosphates and dithiolates. Inorg. Chim. Acta, 53, L31-L33.

Hunt, D.F., Stafford, G.C., Crow, F.W., Russel, J.W. (1976) Pulsed positive negative ion chemical ionization mass spectrometry. Anal. Chem., 48, 2098-2105.

Jackson, A.H., Kenner, G.W., Smith, K.M., Aplin, R.T. Budzikiewicz, H. and Djerassi, C. (1965) The mass spectra of porphyrins. Tetrahedron, 21, 2913-2924.

Jiang, X.-Y., Wegmann-Szente, A., Tolf, B.-R., Kehres, L.A., Bunnenberg, E. and Djerassi, C. (1984) Enhanced structure determination of beta-pyrrole and N-substituted porphyrins by desorption chemical ionization mass spectrometry. Tetrahedron Lett., 25, 4083-4086.

Johnson, J.V., Britton, E.D., Yost, R.A., Quirke, J.M.E. and Cuesta, L.L. (1986) Tandem mass spectrometric studies on high carbon number geoporphyrins. Anal. Chem., 58, 1325-1329.

Jones, B.E., Abbey, L.E., Chatham, H.L., Hanner, A.W., Teleshefsky, L.A., Burgess, E.M., and Moran, T.F. (1982) Doubly charged ion mass spectra III -- N-alkanes. Org. Mass Spectrom., 17, 10-18.

Kassel, D.B., Kayganich, K.A., and Watson, J.T. (1986) Detection of $(M+Cl)^-$ ions under conditions for electron capture negative chemical ionization (EC-NCI) mass spectrometry. Abstracts from the 34th Annual Conference on Mass Spectrometry and Allied Topics, Cincinnati, Ohio, June 8-13, 1986, pp. 523-524.

Kenttämaa, H.I., Wood, K.V., Busch, K.L., and Cooks, R.G. (1983) Scanning a triple quadrupole mass spectrometer for doubly charged ions. Org. Mass Spectrom., 18, 561-567.

Kurlansik, L., Williams, T.J., Strong, J.M., Anderson, L.W. and Campana, J.E. (1984) Desorption ionization mass spectrometry of synthetic porphyrins. Biomed. Mass Spectrom., 11, 475-481.

Mabud, MD.A., DeKrey, M.J., Cooks, R.G., and Ast, T. (1986) Charge exchange of doubly charged organic ions at metal surfaces. Int. J. Mass Spectrom. Ion Processes, 69, 277-284.

Mackenzie, A.S., Quirke, J.M.E. and Maxwell, J.R. (1980) Molecular parameters of maturation in the Toarcian shales, Paris Basin, France II. Evolution of metalloporphyrins. In J.R. Maxwell and A.G. Douglas (Editors), Advances in Organic Geochemistry 1979, Pergamon, Oxford, U.K., pp. 181-192.

McLafferty, F.W. (Editor) (1983) Tandem Mass Spectrometry, Wiley, New York, NY, 506pp.

McLafferty, F.W. and Bursey, M.M. (1967) A specific rearrangement of doubly-charged ions formed by electron impact. Chem. Comm., 533-535.

Musselman, B., Kessel, D., and Chang, C.K. (1988) Fast atom bombardment mass spectrometry of high-molecular-weight fraction of porphyrin-based photodynamic therapy drugs. Biomed. Environ. Mass Spectrom., 15, 257-263.

Ocampo, R., Callot, H.J. and Albrecht, P. (1987) Porphyrins of Bacterial and Algal Origin. In R.H. Filby and J.F. Branthaver (Editors), Metal Complexes in Fossil Fuels. ACS Symposium Series, 344, American Chemical Society, Washington, D.C., pp. 68-73.

Palmer, S.E. and Baker, E.W. (1978) Copper porphyrins in deep sea sediments: a possible indicator of terrestrial matter. Science, 201, 49-51.

Philp, R.P. (1986) Geochemistry in the search for oil. Chem. Eng. News, 64, 28-43.

Prowse, W.G., Chicarelli, M.I., Keely, B.J., Kaur, S., and Maxwell, J.R. (1987) Characterization of fossil porphyrins of the "di-DPEP" type. Geochem. Cosmochim. Acta, 51, 2875-2877.

Quirke, J.M.E. (1987) Techniques for isolation and characterisation of geoporphyrins and chlorins. In R.H. Filby and J.F. Branthaver (Editors), Metal Complexes in Fossil Fuels. ACS Symposium Series, 344, American Chemical Society, Washington, D.C., pp. 308-331.

Quirke, J.M.E., Cuesta, L.L., Yost, R.A., Johnson, J.V., and Britton, E.D. (1989) Studies on high carbon number geoporphyrins by tandem mass spectrometry. Org. Geochem., 14, 43-50.

Quirke, J.M.E., Maxwell, J.R. and Eglinton, G. (1982) Aspects of modern porphyrin geochemistry and the Treibs' hypothesis. In A.A. Prashnowsky (Editor), The Impact of the Treibs Hypothesis on Modern Organic Geochemistry, Gesamtherstellung, Wurtzburg, pp. 37-63.

Sears, L.J., Campbell, J.A., and Grimsrud, E.P. (1987) Ionization dynamics within the high pressure electron capture mass spectrometer; the unusual spectra of derivatized polycyclic aromatic amines and perchlorinated unsaturated hydrocarbons. Biomed. Environ. Mass Spectrom., 14, 401-415.

Shaw, J.G., Eglinton, G., and Quirke, J.M.E. (1981) Analyses of porphyrins by H_2 Chemical Ionisation Mass Spectrometry. Anal. Chem., 32, 2014-2020 (1981).

Sim, P.G., Jamieson, W.D., and Boyd, R.K. (1989) Collision-induced fragmentation reactions of doubly charged ions of polycyclic aromatic hydrocarbons. Org. Mass Spectrom., 24, 327-337.

Smith, K.M. (1972) On the mass spectra of thallium(III) porphyrin chelates. Org. Mass Spectrom., 6, 1401-1402.

Smith, K.M. (1975) Mass spectrometry of porphyrins and metalloporphyrins. In K.M. Smith (Editor), Porphyrins and Metalloporphyrins, Elsevier, Amsterdam, pp. 381-398.

Stemmler, E.A. and Buchanan, M.V. (1989) Negative ions generated by reactions with oxygen in the chemical ionization source I. Characterization of gas-phase and wall-catalyzed reactions of fluorene, anthracene and fluoranthene. Org. Mass Spectrom., 24, 94-104.

Sundararaman, P. (1985) High performance liquid chromatography of vanadyl porphyrins. Anal. Chem., 57, 2204-2206.

Sundararaman, P., Gallegos, E.J., Baker, E.W., Slayback, J.R.B. and Johnston, M.R. (1984) Hydrogen chemical ionization tandem mass spectrometry of metallo-porphyrins. Anal. Chem., 56, 2552-2556.

Sundararaman, P., Gallegos, E.J., Slayback, J.R.B., Johnston, M., and Baker, E.W. (1982) Positive and negative ion hydrogen chemical ionization of porphyrins and metalloporphyrins by quadrupole MS/MS. Abstracts from the 30th Annual Conference on Mass Spectrometry and Allied Topics, Honolulu, Hawaii, June 6-11, 1982, p. 678.

Taylor, L.T. and Dillard, J.G. (1974) Mass spectrometric study of polydentate Schiff base coordination complexes. II. cobalt(II), nickel(II), and copper(II) complexes of N,N'-bis(salicylidene)heptanediamine, N,N'-bis(salicylidene)-3,3'-bis(aminopropyl) amine, N,N'-bis(salicylidene)-3,3'-bis(aminopropyl) ether, and N,N'-bis(salicylidene)-3,3'-bis(aminopropyl) sulfide. Inorg. Chem., 13, 2620-2630.

Thomson, B.A., Iribarne, J.V., and Dziedzic, P.J. (1982) Liquid ion evaporation/mass spectrometry/mass spectrometry for the detection of polar and labile molecules. Anal. Chem., 54, 2219-2224.

Tolf, B., Jiang, X., Wegmann-Szente, A., Kehres, L.A., Bunnenberg, E. and Djerassi, C. (1986) Enhanced structural determination of substituted porphyrins by ammonia desorption chemical ionization mass spectrometry. J. Am. Chem. Soc., 108, 1363-1374.

Treibs, A. (1936) Chlorophyll und Haminderivate in organischen Mineralstoffen. Angew. Chemie, 49, 682-686.

Van Berkel, G.J. and Filby, R.H. (1987) Generation of nickel and vanadyl porphyrins from kerogen during simulated catagenesis. In R.H. Filby and J.F. Branthaver (Editors), Metal Complexes in Fossil Fuels. ACS Symposium Series, 344, American Chemical Society, Washington, D.C., pp. 110-134.

Van Berkel, G.J., Glish, G.L., and McLuckey, S.A. (1988). Mechanism of porphyrin hydrogenation and decomposition in a chemical ionization source. In Proceedings of the 36th ASMS Conference on Mass Spectrometry and Allied Topics, June 5-10, 1988, San Francisco, California, pp. 302-303.

Van Berkel, G.J. Glish, G.L., and McLuckey, S.A. (1989) Geoporphyrin analysis using an ion trap mass spectrometer. Presented at the American Chemical Society 197th National Meeting and Exposition in Dallas, Texas, April 9-14, 1989.

Van Berkel, G.J., Glish, G.L., McLuckey, S.A., and Tuinman, A.A. Mechanism of porphyrin reduction and decomposition in a high pressure chemical ionization plasma. J. Amer. Chem. Soc., in press a.

Van Berkel, G.J., Quirke, J.M.E., and Filby, R.H. The Henryville bed of New Albany shale-I: preliminary characterization of the nickel and vanadyl porphyrins in the bitumen. Org. Geochem., in press b.

Van Berkel, G.J., Quirke, J.M.E., and Filby, R.H. The Henryville bed of New Albany shale-II: comparison of the nickel and vanadyl porphyrins in the bitumen with those generated from the kerogen during simulated catagenesis. Org. Geochem., in press c.

van den Bergh, H. (1986) Light and porphyrins in cancer therapy. Chem. Br., 22, 1986, 430-439.

Verne-Mismer, J., Ocampo, R., Bauder, C., Callot, H.J., and Albrecht, P. (1989) Nickel, copper and vanadyl porphyrins from Moroccan oil shales: compositions, novel structures, biological precursors. Presented at the American Chemical Society 197th National Meeting and Exposition in Dallas, Texas, April 9-14, 1989.

Verne-Mismer, J., Ocampo, R., Callot, H.J., Albrecht, P. (1987) Isolation of a series of vanadyl tetrahydrobenzopetroporphyrins from Timahdit Oil Shale. Structure determination and total synthesis of the major constituent. J. Chem. Soc., Chem. Commun., 1581-1583.

Vouros, P., and Biemann, K. (1969) The structural significance of doubly charged ion spectra: phenylenediamine derivatives. Org. Mass Spectrom., 2, 375-386.

Yost, R.A. and Enke, C.G. (1979) Triple quadrupole mass spectrometry for direct mixture analysis and structure elucidation. Anal. Chem., 51, 1251A-1264A.

BIOGRAPHICAL SKETCH

Brian David Beato was born in Detroit, Michigan, on January 28, 1964. From 1970 until 1982, he lived in Cincinnati, Ohio, where he attended Finneytown High School. Graduating in 1982 as Class Valedictorian, Brian accepted a National Merit Scholarship and an Ohio Academic Scholarship to attend The Ohio State University. During his three years there as an undergraduate, he performed research in inorganic and analytical chemistry under the direction of Dr. Daryle H. Busch. He won an Undergraduate Honors Research Scholarship for this work, and also wrote an Honors Thesis. During each of the three summers before graduate school, Brian worked as an analytical chemist for Procter & Gamble in Cincinnati. The first summer he spent as a technician, but the last two summers he took part in the Summer Analytical Research Program (SARP). Brian graduated from The Ohio State University in June of 1985 with a B.S. in chemistry, and was Phi Beta Kappa. From August of 1985 until August of 1989, he was an analytical chemistry graduate student at the University of Florida, under the direction of Dr. Richard A. Yost. Upon obtaining his Ph.D., Brian will be moving to Lafayette, Indiana, where he will be employed as a Senior Analytical Chemist for Eli Lilly and Company.

I certify that I have read this study and that in my opinion it conforms to acceptible standards of scholarly presentation and is fully adequate, in scope and quality, as a dissertation for the degree of Doctor of Philosophy.

Richard A. Yost, Chairman
Professor of Chemistry

I certify that I have read this study and that in my opinion it conforms to acceptible standards of scholarly presentation and is fully adequate, in scope and quality, as a dissertation for the degree of Doctor of Philosophy.

James D. Winefordner
Graduate Research Professor
of Chemistry

I certify that I have read this study and that in my opinion it conforms to acceptible standards of scholarly presentation and is fully adequate, in scope and quality, as a dissertation for the degree of Doctor of Philosophy.

Willard W. Harrison
Professor of Chemistry

I certify that I have read this study and that in my opinion it conforms to acceptible standards of scholarly presentation and is fully adequate, in scope and quality, as a dissertation for the degree of Doctor of Philosophy.

Russell S. Drago
Graduate Research Professor
of Chemistry

I certify that I have read this study and that in my opinion it conforms to acceptible standards of scholarly presentation and is fully adequate, in scope and quality, as a dissertation for the degree of Doctor of Philosophy.

Anthony F. Randazzo
Professor of Geology

This dissertation was submitted to the Graduate Faculty of the Department of Chemistry in the College of Liberal Arts and Sciences and to the Graduate School and was accepted as partial fulfillment of the requirements for the degree of Doctor of Philosophy.

August, 1989

Dean, Graduate School

UNIVERSITY OF FLORIDA
3 1262 08556 7971